OPENSEES DAYS EUROPE 2017

FIRST EUROPEAN CONFERENCE ON OPENSEES

AN EVENT FROM THE CONFERENCE SERIES OF EOS,
THE EUROPEAN OPENSEES ASSOCIATION

HUMBERTO VARUM
JOSÉ MIGUEL CASTRO
LUÍS MACEDO
NUNO PEREIRA
XAVIER ROMÃO
GIORGIO MONTI ***EDITORS***

OPENSEES DAYS EUROPE 2017

FIRST EUROPEAN CONFERENCE ON OPENSEES

AN EVENT FROM THE CONFERENCE SERIES OF EOS,
THE EUROPEAN OPENSEES ASSOCIATION

JUNE 19 – JUNE 20, 2017
PORTO, PORTUGAL

EDITED BY
HUMBERTO VARUM
FACULTY OF ENGINEERING, UNIVERSITY OF PORTO, PORTUGAL

JOSÉ MIGUEL CASTRO
FACULTY OF ENGINEERING, UNIVERSITY OF PORTO, PORTUGAL

LUÍS MACEDO
FACULTY OF ENGINEERING, UNIVERSITY OF PORTO, PORTUGAL

NUNO PEREIRA
FACULTY OF ENGINEERING, UNIVERSITY OF PORTO, PORTUGAL

XAVIER ROMÃO
FACULTY OF ENGINEERING, UNIVERSITY OF PORTO, PORTUGAL

GIORGIO MONTI
UNIVERSITY OF ROME "LA SAPIENZA", ITALY

ISBN 978-972-752-221-7

Published in 2017 by:

Faculty of Engineering, University of Porto

Rua Dr. Roberto Frias, s/n 4200-465 Porto PORTUGAL

Additional material can be downloaded from http://opensees.fe.up.pt

Preface

The EOSD2017 is the second OpenSees conference held in Porto, Portugal, (after the OpenSees Days Portugal in 2014). This conference appears after a series of successful European events held in Italy (2011, 2015), the U.K. (2014) and Portugal (2014), and is also the official launching event of the European OpenSees Association. It is therefore an honour to host the EOSD2017 conference that coincides with the launch of the European OpenSees Association.

The conference aimed at gathering new users and assembling the OpenSees community in Europe to discuss some of the new features. The Programme included some of the more active OpenSees developers, thus contributing for productive and interesting discussions. The invited speakers included Anastasios Sextos, André Barbosa, Asif Usmani, Dimitrios Lignos, Dimitrios Vamvatsikos, Frank McKenna, Khalid Mosalam, Lu Xinzheng, Pedro Arduino and Theodore Karavasilis.

The invited speakers' presentations addressed topics where OpenSees plays a key role in simulating structural behaviour and geotechnical problems involving different types of structures and hazards such as fire, earthquakes and tsunamis.

The conference programme also included presentations addressing the integration and combination of OpenSees with commercial software, presentations focusing on new software developments and several case study applications. These proceedings compile the extended abstracts of the presentations made during the conference.

The EOSD2017 had approximately 80 participants, originating from 16 different countries. We were therefore pleased to host such an inter-cultural conference and hope that it serves as an opportunity to launch new partnerships.

We would like to thank all the lecturers, authors and participants for their contributions to this event. Finally, we would like to specially thank all who actively contributed to the organization of this event at FEUP, in particular all the funding institutions for their generous contributions and the secretariat of "Instituto da Construção" for their considerable help.

The Organizing Committee of the EOSD2017

Porto, July 2017

Diamond Sponsors

Platinum Sponsors

Gold Sponsors

Supporting Organizations

Contents

OpenSees Days Europe 2017
1st European Conference on OpenSees
Porto, Portugal, 19–20 June 2017

ROBUST AND EFFICIENT NONLINEAR STRUCTURAL ANALYSIS USING THE CENTRAL DIFFERENCE TIME INTEGRATION SCHEME

Reagan Chandramohan[1], Jack W. Baker[2], and Gregory G. Deierlein[3]

[1] Lecturer
University of Canterbury, Christchurch, New Zealand
reagan.c@canterbury.ac.nz

[2] Associate Professor
Stanford University, Stanford, CA, USA
bakerjw@stanford.edu

[3] Professor
Stanford University, Stanford, CA, USA
ggd@stanford.edu

Keywords: explicit scheme; central difference scheme; implicit scheme; Newmark average acceleration scheme; numerical non-convergence; nonlinear structural analysis; collapse simulation; incremental dynamic analysis

Abstract. *The explicit central difference numerical time integration scheme is demonstrated to be a robust and efficient alternative to commonly used implicit schemes like the Newmark average acceleration scheme for nonlinear structural response simulation. Numerical non-convergence issues, which are frequently encountered using the Newmark average acceleration scheme, are shown to introduce conservative biases in the estimated structural capacity and hamper the efficiency of analysis. They are shown to be responsible for the underestimation of the median collapse capacity of a 9-storey steel moment frame building by 10%. Despite requiring shorter analysis time steps, the time taken to conduct an incremental dynamic analysis using the central difference scheme is 73% lower than using the average acceleration scheme.*

1 INTRODUCTION

Nonlinear response history analysis has witnessed increased adoption in seismic design and assessment practice in recent years [1], [2], especially for the design and assessment of tall and important structures. In current research and practice, nonlinear structural response simulations are almost exclusively conducted using implicit numerical time integration schemes, of which, the Newmark average acceleration scheme is the most popular. Implicit schemes are, however, inherently iterative in nature and often fail to converge to a solution when used to simulate the response of structures under intense earthquake ground motions, at or close to their ultimate collapse limit states. The use of implicit schemes, therefore, possesses the potential to introduce conservative biases in the estimated structural capacity. Nevertheless, numerical issues like non-convergence typically receive little attention in comparison to structural modelling and ground motion selection considerations. This study proposes the use of the explicit central difference time integration scheme as a robust and efficient alternative to the Newmark average acceleration scheme for nonlinear structural analysis.

2 NEWMARK AVERAGE ACCELERATION SCHEME

The Newmark average acceleration scheme is the most widely used numerical time integration scheme for response history analysis. The reason for its popularity is its unconditionally stable nature, which permits the use of relatively large analysis time steps. Being an implicit scheme, it enforces equilibrium at the end of each time step which makes it inherently iterative in nature, and convergence of the iterations is not guaranteed. Numerical non-convergence is, in fact, a frequently encountered phenomenon, and the likelihood of encountering non-convergence increases when analysing complex structural models under long and intense ground motions. Upon encountering numerical non-convergence, a series of workarounds is typically employed to overcome it, including trying different solution algorithms and other time integration schemes, decreasing the analysis time step, and raising the convergence tolerance [3]–[5]. These strategies are not always successful, but are computationally intensive and can hamper the efficiency of the analysis if invoked too frequently. If all attempts fail, it is common practice to declare structural collapse, although often incorrectly as demonstrated in this study and others (e.g., [4], [6]).

3 CENTRAL DIFFERENCE SCHEME

The central difference scheme is an explicit scheme since it enforces equilibrium at the beginning of each time step. Being non-iterative in nature, it effectively sidesteps the issue of numerical non-convergence. This makes it a popular choice when conducting simulations that involve large nonlinear deformations like blast and crash simulations [7], [8]. Structural response simulations that involve large nonlinear deformations are, therefore, also expected to benefit from using the central difference scheme, despite the longer duration of earthquake loads when compared to impulse loads like blast and crash loads.

The most commonly cited drawback of the central difference scheme is its conditionally stable nature, which limits the largest analysis time step it can be used with to $\Delta t_{max} = T_{min}/\pi$, where T_{min} is the shortest modal period. This condition precludes the presence of any massless degrees of freedom and extremely stiff elements or penalty constraints in the structural model, which entails some additional effort during model creation. These requirements are, however, not unique to the central difference scheme since they have also been linked to improved convergence performance of implicit schemes [4], [9, Sec. 9.5.2].

The dynamic tangent matrix that needs to be factorised at each time step when using the central difference scheme is a linear combination of just the mass and damping matrices. Since

the mass matrix is typically constant, using a constant damping matrix (like a modal damping matrix) would require the dynamic tangent matrix to be factorised only once during the entire simulation, thereby vastly improving the efficiency of the scheme. When a simulation is conducted in parallel by domain decomposition, this would also significantly minimise the communication overhead between the processors. Since the duration of each analysis is known to be proportional to the length of the accelerogram, it also permits the use of efficient static parallel load balancing techniques when analyzing response under different ground motions on different processors.

4 COMPARISON OF ROBUSTNESS

A concentrated plastic hinge model of the 9-storey steel moment frame building designed as part of the SAC Steel Project [10], was created in OpenSees. The hysteretic behaviour of the plastic hinges was modelled using the Ibarra-Medina-Krawinkler bilinear hysteretic model [11], and the destabilising $P-\Delta$ effect of the adjacent gravity frame was captured using a pin-connected leaning column. The collapse capacity of the frame was estimated separately using the Newmark average acceleration and the central difference time integration schemes by conducting incremental dynamic analysis (IDA) [12] using 44 ground motions from the FEMA P695 [13] far-field record set.

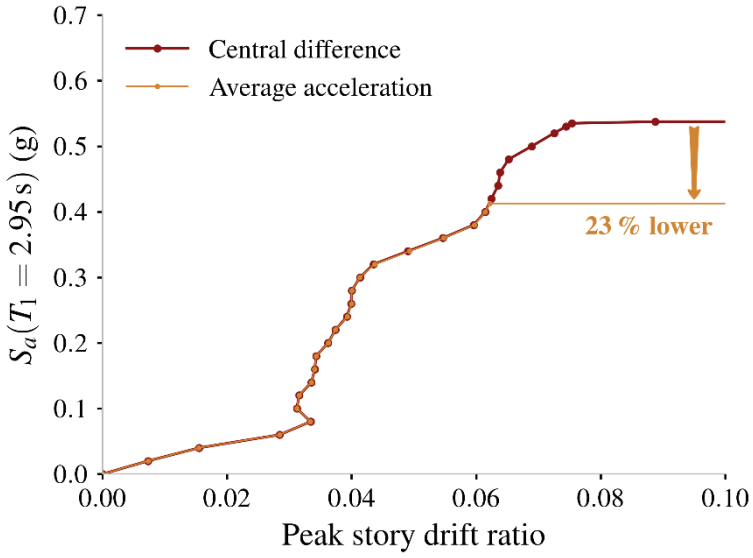

Figure 1: Comparison of the IDA curves computed using the central difference and Newmark average acceleration time integration schemes for one of the 44 ground motions

Upon encountering numerical non-convergence using the average acceleration scheme, the following sequence of efforts were made to overcome it: (i) different solution algorithms were tried; (ii) the analysis time step was sequentially decreased; and (iii) other implicit time-integration schemes (including some with algorithmic damping like the HHT-α scheme) were used. If all efforts failed, structural collapse was declared as per conventional practice. For 12 out of the 44 ground motions, the collapse intensity obtained using the average acceleration scheme was found to be lower than that estimated using the central difference scheme by 10% or more. The IDA curves for one of these ground motions is plotted in Figure 1. The IDA curves computed using the two schemes are seen to be identical until they bifurcate at a certain intensity level. This corresponds to the intensity level at which persistent numerical non-convergence

was encountered using the average acceleration scheme, prompting the premature declaration of structural collapse. The central difference scheme, on the other hand, was able to successfully evaluate the response at that intensity level and a few others above it. The difference between the collapse intensities estimated using the two schemes was lower than 1% for 29 out of the 44 ground motions. The net effect of the premature declaration of collapse for 12 of the 44 ground motions was an underestimation of the median collapse capacity by 10% using the average acceleration scheme. This clearly demonstrate the robust nature of the central difference scheme, which can be attributed to its immunity against numerical non-convergence.

5 COMPARISON OF EFFICIENCY

The simulations were conducted using a time step of 5×10^{-3} s using the average acceleration scheme, and 1.5×10^{-4} s using the central difference scheme. The time taken to analyse the structure under the ground motion recorded during the 1992 Landers earthquake at the Coolwater station using the average acceleration scheme was 1.0 min when it was scaled to a low scale factor where non-convergence was not encountered. The runtime, however, increased to 20.9 min at a higher scale factor where numerical non-convergence compelled the use of computationally intensive strategies to overcome it. The runtime using the central difference scheme was only 3.3 min using a constant damping matrix that required only a single factorisation. Thus we see that although the central difference scheme requires the use of a smaller analysis time step, the system of equations can be solved more efficiently at each time step.

The time taken to conduct the entire IDA in parallel on 160 processors using dynamic load balancing was 118 min using the average acceleration scheme and 32 min using the central difference scheme. The 73% shorter runtime using the central difference scheme can be attributed to the large number of instances where numerical non-convergence was encountered using the average acceleration scheme, forcing the use of computationally intensive steps to overcome it. Thus, the central difference scheme is seen to be a competitive alternative to the Newmark average acceleration scheme, not just in terms of robustness, but also in terms of efficiency. These findings are consistent with other previous studies like [14]–[16].

6 CONCLUSION

The central difference time integration scheme is demonstrated to be a robust and efficient alternative to the Newmark average acceleration scheme for nonlinear structural analysis. Its robustness is attributed to its non-iterative nature, which renders it immune to numerical non-convergence issues. Numerical non-convergence was shown to be responsible for the underestimation of the median collapse capacity of a 9-storey steel moment frame building by 10% when using the average acceleration scheme. The time taken to conduct IDA using 44 ground motions was shown to be 73% lower using the central difference scheme due to the large number of instances numerical non-convergence was encountered using the average acceleration scheme, thereby necessitating the use of computationally intensive workarounds to overcome it.

The only drawback of the central difference scheme is its conditionally stable nature which imposes restrictions on the analysis time step and entails additional effort during model creation to assign mass (or moment of inertia) to all degrees of freedom and avoid the use of stiff elements or penalty constraints.

With the inevitable gradual shift towards more complex structural models and statistically rigorous analysis procedures involving large numbers of ground motions and structural model realisations, it is imperative that adequate attention is paid to the accuracy and efficiency of the numerical solution strategies employed to conduct the simulations.

REFERENCES

[1] Eurocode, "Eurocode 8: Design of structures for earthquake resistance - Part 1: General rules, seismic actions and rules for buildings," European Committee for Standardization, Brussels, Belgium, 2004.

[2] FEMA, "Seismic Performance Assessment of Buildings, Volume 1 - Methodology," Federal Emergency Management Agency, Washington, D.C., 2012.

[3] D. Vamvatsikos and C. A. Cornell, "Applied Incremental Dynamic Analysis," *Earthq. Spectra*, vol. 20, no. 2, pp. 523–553, 2004.

[4] C. B. Haselton, A. B. Liel, and G. G. Deierlein, "Simulating structural collapse due to earthquakes: Model idealization, model calibration, and numerical solution algorithms," in *ECCOMAS Thematic Conference on Computational Methods in Structural Dynamics and Earthquake Engineering (COMPDYN)*, 2009.

[5] A. Hardyniec and F. A. Charney, "A new efficient method for determining the collapse margin ratio using parallel computing," *Comput. Struct.*, vol. 148, pp. 14–25, Feb. 2015.

[6] Y. Araki and K. D. Hjelmstad, "Criteria for assessing dynamic collapse of elastoplastic structural systems," *Earthq. Eng. Struct. Dyn.*, vol. 29, no. 8, pp. 1177–1198, Aug. 2000.

[7] D. Lawver, R. Daddazio, D. Vaughan, M. Stanley, and H. Levine, "Response of AISC Steel Column Sections to Blast Loading," in *ASME Pressure Vessels and Piping Conference*, 2003, pp. 139–148.

[8] G. Dundulis, R. F. Kulak, A. Marchertas, and E. Uspuras, "Structural integrity analysis of an Ignalina nuclear power plant building subjected to an airplane crash," *Nucl. Eng. Des.*, vol. 237, no. 14, pp. 1503–1512, Aug. 2007.

[9] K.-J. Bathe, *Finite Element Procedures*. Upper Saddle River, NJ: Prentice Hall, 1996.

[10] FEMA, "State of the art report on systems performance of steel moment frames subject to earthquake ground shaking," Federal Emergency Management Agency, Stanford, CA, 2000.

[11] L. F. Ibarra, R. A. Medina, and H. Krawinkler, "Hysteretic models that incorporate strength and stiffness deterioration," *Earthq. Eng. Struct. Dyn.*, vol. 34, no. 12, pp. 1489–1511, Oct. 2005.

[12] D. Vamvatsikos and C. A. Cornell, "Incremental dynamic analysis," *Earthq. Eng. Struct. Dyn.*, vol. 31, no. 3, pp. 491–514, Mar. 2002.

[13] FEMA, "Quantification of Building Seismic Performance Factors," Federal Emergency Management Agency, Washington, D.C., 2009.

[14] J. F. McNamara, "Solution Schemes for Problems of Nonlinear Structural Dynamics," *J. Press. Vessel Technol.*, vol. 96, no. 2, p. 96, May 1974.

[15] M. J. Mikkola, M. Tuomala, and H. Sinisalo, "Comparison of numerical integration methods in the analysis of impulsively loaded elasto-plastic and viscoplastic structures," *Comput. Struct.*, vol. 14, no. 5–6, pp. 469–478, Jan. 1981.

[16] Y. M. Xie, "An assessment of time integration schemes for non-linear dynamic equations," *J. Sound Vib.*, vol. 192, no. 1, pp. 321–331, Apr. 1996.

OpenSees Days Europe 2017
1st European Conference on OpenSees
Porto, Portugal, 19–20June 2017

TWO NEW ELEMENTS TO OPENSEES

Pereiro-Barceló, Javier[1], **Fernández-Baños, Manuel**[2]

[1]Cype Ingenieros S.A.
Avda. Eusebio Sempere, 5 – 03003 Alicante, España
e-mail: javier.pereiro@cype.com

[2] Cype Ingenieros S.A.
Avda. Eusebio Sempere, 5 – 03003 Alicante, España
e-mail: manuel.fernandez@cype.com

Keywords: 6-node triangle, Timoshenko, Shape function, structural analysis.

Abstract. *Opensees is a well-known framework to perform non-linear earthquake analysis. Cype has integrated Opensees as calculation engine in its new structural analysis programs (StruBIM). With the purpose of keeping all functionalities of previous calculation engine, two new elements have been developed for Opensees: A one-dimensional elastic 2 node bar and a 6-node triangular shell element. Both support a wide kind of loads, local eccentricities, and stiffness multipliers. One-dimensional element calculates sectional forces and deflections at any inner points of the element without adding new nodes. Shell element supports thick sections and it works for non-linear analysis.*

1 INTRODUCTION

Opensees is a well-known framework to perform linear or non-linear analysis, developed at University of California, Berkeley. Its use is widespread all over the world mainly to simulate seismic behavior in structures.

Cype has integrated Opensees as calculation engine for StruBIM Analysis, StruBIM Design and StruBIM Foundations. These programs are in charge of analyzing, designing and checking structures, including their foundations. To fulfill this, Cype has extended OpenSees in some ways and one of them is creating two new finite elements, which will be explained in the following sections.

2 ONE-DIMENSIONAL ELEMENT

A 2-node one-dimensional elastic finite element has been created for OpenSees (Figure 1.a). It follows Timoshenko's theory. Next, the properties of this element are shown:

2.1 Loads

The element supports point, trapezoidal (even in a portion of the length) and temperature (uniform or gradient) loads. Shear deformability must take into consideration to obtain fixed ends forces. The followed procedure is shown below:

A fully fixed ends beam in considered. It bears a load $P(x)$ which causes two moment reactions M_a and M_b. The bending moment in any position x can be decomposed by the sum of the bending moment in a pinned equivalent isostatic beam due to $P(x)$ (M^P), M_a and M_b. Taking into account Castiglinao's theorem to calculate the rotations at the ends of the isostatic beam and operating, the expressions of reaction moments M_a and $\boldsymbol{M_b}$ are displayed in (1) [1]. The rest of reactions can be obtained by stating equilibrium.

$$M = \frac{1}{\gamma}\left\{m\left[\int_0^L M^P\left(1-\frac{x}{L}\right)\frac{dx}{EI}+\frac{1}{L}\int_0^L Q^c\frac{dx}{GA_v}\right]+n\left[-\int_0^L M^P\frac{x}{L}\frac{dx}{EI}+\frac{1}{L}\int_0^L Q^c\frac{dx}{GA_v}\right]\right\} \quad (1)$$

where:

$$\boldsymbol{\gamma_1} = \int_{\boldsymbol{0}}^{\boldsymbol{L}}\left(\boldsymbol{1}-\frac{\boldsymbol{x}}{\boldsymbol{L}}\right)\frac{\boldsymbol{dx}}{\boldsymbol{EI}}, \boldsymbol{\gamma_2} = \int_{\boldsymbol{0}}^{\boldsymbol{L}}\frac{\boldsymbol{x}}{\boldsymbol{L}}\left(\boldsymbol{1}-\frac{\boldsymbol{x}}{\boldsymbol{L}}\right)\frac{\boldsymbol{dx}}{\boldsymbol{EI}}, \gamma_3 = \int_0^L\left(\frac{x}{L}\right)^3\frac{dx}{EI}, \gamma_4 = \int_0^L\left(\frac{1}{L^2}\right)\frac{dx}{GA_v}$$

$\gamma = (\gamma_1+\gamma_4)(\gamma_3+\gamma_4)-(\gamma_2-\gamma_4)^2$,

$m = (\gamma_3+\gamma_4)$ for M_a and $(\gamma_2-\gamma_4)$ for M_b ; $n = (\gamma_2-\gamma_4)$ for M_a and $(\gamma_1+\gamma_4)$ for M_b

E:Young modulus, G:Shear modulus, $\boldsymbol{A_v}$: Shear area, $\boldsymbol{L}$: Length of the element

2.2 Local eccentricities

A local eccentricity is understood to mean a way to change the relative position of local axis in one-dimensional elements. This allows to model for example, that top or bottom face of a beam coincides with a slab face. Besides, in steel structures allows to model complex joints between bars. Local eccentricities are modeled as multipoint constraints where master DOF are related to slaves ones according to local eccentricities dx, dy and dz [2].

2.3 Sectional forces

Finite elements just get sectional forces at its nodes. If more positions are required, inner nodes must be added. If elements are elastic, this addition can be avoided by stating equilibrium of the element. This way, taking the nodal forces after the analysis, sectional forces are obtained by adding the effect of inner element loads at each longitudinal location where user wants to know the value.

2.4 Deflections

As Timoshenko theory is followed to build this element, displacements and rotations are the sum of two terms: displacements and rotations due to bending moment and ones due to shear.

Deflections are obtained at inner points of element by integrating the following differential equations:

$$EI\frac{d^2y(x)}{dx^2} = M(x) \tag{2}$$

$$GA_v\frac{dy(x)}{dx} = V(x) \tag{3}$$

2.5 Stiffness modifiers

Stiffness modifiers are inputs to reduce stiffness in some elements.

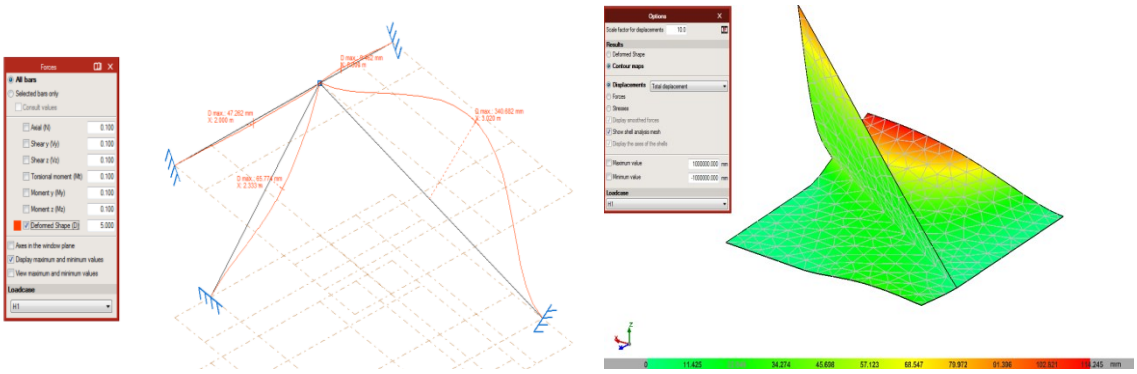

(a) (b)

Figure 1: New elements: (a) One-dimensional element (displacements), (b) Shell element (displacements)

3 SHELL ELEMENT

A 6-node triangular element has been created with membrane and plate behavior (Figure 1.b). Stiffness can be modified in each membrane or plate component. It works for both linear and non-linear analysis. It has quadratic shape functions and supports thick shells [3].

3.1 Loads

Trapezoidal and temperature loads are available in shell element. The equations of these loads are (7-8), which are integrated numerically:

$$\boldsymbol{f}_{trap}^{(e)} = \int\int_{A^{(e)}} \boldsymbol{N}^T \boldsymbol{b} t dA \tag{4}$$

$$\boldsymbol{f}_{temp}^{(e)} = \int\int_{A^{(e)}} \boldsymbol{B}^T \boldsymbol{D}\boldsymbol{\varepsilon}^{\boldsymbol{0}} t dA \tag{5}$$

where:
$\boldsymbol{N}$: Shape function, $\boldsymbol{B}$: Derivative matrix, $\boldsymbol{D}$: Constitutive matrix, $\boldsymbol{b}$: Distributed load in the element area vector, $\boldsymbol{\varepsilon^0}$: Initial strain vector due to temperature, t: shell thickness

3.2 Local eccentricities

As in the case of one-dimensional element, this shell element has local eccentricities as inputs. The explanation is the same as in the previous elements.

3.3 Coplanarity

Shell element has as input parameters if each node is or not coplanar. If node is, a fictitious stiffness is assigned to the rotational DOF (Degree of Freedom) which is perpendicular to the element.

3.4 Linear optimization

Shell element works for both linear and non-linear analysis. However, it is optimized if linear analysis is being performed. This optimization makes that stiffness matrix is just evaluated once in the whole analysis.

3.5 Stiffness modifiers

Stiffness can be modified in each membrane or plate component.

4 CONCLUSIONS

- Two new elements have been created to Opensees: One-dimensional and shell elements.
- One-dimensional element supports a wide variety of loads, local eccentricities, stiffness modifiers, and obtains sectional forces and deflections at inner points of the elements without adding new nodes.
- Shell element is a 6-node triangular element with membrane and plate behavior. It supports linear and non-linear analysis and thick sections. It supports trapezoidal and temperatures loads, local eccentricities and stiffness modifiers. It can manage coplanarity and, if analysis is linear, it is optimized to that effect.
- Elements will be uploaded to OpenSees repository soon.

REFERENCES

[1] J. M. Canet, Resistencia de Materiales y Estructuras, Centro internacional de Métodos Numéricos en Ingeniería, CIMNE, Barcelona, 2012.

[2] C.A. Felippa *Introduction to Finite Element Methods*, Department of Aerospace Engineering Sciences and enter for Aerospace Structures, University of Colorado, USA, 2004.

[3] E. Oñate, *Cálculo de Estructuras por el Método de Elementos Finitos, 1th Edition*, Centro internacional de Métodos Numéricos en Ingeniería, Universitat Politècnica de Catalunya, Barcelona, 1992.

OpenSees Days Europe 2017
1st European Conference on OpenSees
Porto, Portugal, 19–20 June 2017

OPENSEES SOFTWARE ARCHITECTURE FOR SUBSTRUCTURE-BASED SEISMIC SIMULATION METHOD FOR PARTIALLY-NONLINEAR STRUCTURES

Ming Fang[1], Jian Wang[2], and Hui Li[3]

[1] Key Lab of Structures Dynamic Behavior and Control of the Ministry of Education, Harbin Institute of Technology, Harbin 150090, China
E-mail: fangminghit@163.com

[2] Key Lab of Structures Dynamic Behavior and Control of the Ministry of Education, Harbin Institute of Technology, Harbin 150090, China
E-mail: wangjiantx@hit.edu.cn

[3] Key Lab of Structures Dynamic Behavior and Control of the Ministry of Education, Harbin Institute of Technology, Harbin 150090, China
E-mail: lihui@hit.edu.cn

Keywords: Substructure modeling; Model reduction; Partially-nonlinear structure; Hybrid simulation; OpenSees.

Abstract. *The finite-element software framework OpenSees is extended to provide the abilities of model reduction and hybrid numerical analysis in the substructure-based seismic simulation. Based on the Craig-Bampton method, a number of linear and nonlinear substructures are gradually updated according to the varying topology of structural components. The model reduction is only performed for linear substructures by retaining the dominant substructure modes, while the nonlinear substructure remains its original form. At the high level of OpenSees framework, a new transient analysis class is created to implement the substructure generation, mode selection and formation of hybrid coordinate governing equations based on the bridge pattern. At the low level of OpenSees framework, a new abstract layer is created to represent the time-varying substructures based on the adapter pattern.*

1 INTRODUCTION

Normally, reducing or concentrating the damages in the prescribed components or members of the structure is a desirable performance objective in seismic design. As the desirable performance objective requires, the damage is concentrated in weaker members and the main structure remains in elastic or light damaged phase, hence the entire structure can be properly designed to be a partially-nonlinear structure. The weaker members that enter nonlinear phase are difficult to be a priori known due to the randomness of earthquake inputs. Recently, an adaptive modified Craig-Bampton method (AMCB)[1] has been proposed as a substructure-based model order reduction method that can divide the entire structure into the linear and nonlinear substructures. The main idea is to retain a small number of vibration modes to capture the predominant vibrational characteristics of linear substructures in modal space, while nonlinear substructures remain the original form in physical space. Since the AMCB method is able to generate time-varying substructures adaptively, it has the potential to simulate the partially-nonlinear structures with an acceptable computational cost, and it is more feasible to implement such a substructure-based method in the open source software OpenSees. In the last two decades, OpenSees[2] has drawn more attention and becomes one of the most popular software for numerical seismic simulation due to its great flexibility and extensibility. The architecture of OpenSees is designed according to the software design pattern provided by Gamma et al[3]. Based on such a design pattern, the architecture of OpenSees is organized to sustainably integrate the newest research outcomes.

The objective of this study is to implement a substructure-based seismic simulation method for the partially-nonlinear structures in OpenSees. New classes are created to implement the solution of hybrid governing equations and the substructure generation. Some existing classes are modified to merge the new classes with the original software architecture.

2 ADAPTIVE MODIFIED CB METHOD

The Craig-Bampton (CB) method has been modified to make model reduction for an a priori partitioned partially-nonlinear structure in hybrid coordinates by condensing the DOFs of the linear substructures. For the structures subject to earthquake excitation, the nonlinear substructure cannot be a priori known due to the randomness of earthquake risk. Hence the partition of substructures cannot be made before the seismic analysis. In order to overcome such a shortcoming, the AMCB method inserts the modified CB method into each step of the conventional time step integration (TSI) method. At each time step, the distribution of nonlinear components is determined so that the substructure partition can be conducted step by step, thus the modified CB method can perform the model reduction at each time step.

3 IMPLEMENTATION OF AMCB METHOD IN OPENSEES

The implementation of the AMCB method requires important changes at both low level and high level of OpenSees framework. These changes involve the creation of a few new classes and the modification of a few existing classes, as shown in Fig. 1 (new classes are shown in red; modified classes are shown in blue). The SUB_Structure is created as a class that represents a layer of abstraction at the low level of OpenSees framework. To implement the substructure-based AMCB method, the SUB_Structure provides an additional abstraction layer between AnalysisModel and its component objects. Thus, the governing equations for linear and nonlinear substructures in the AMCB method can be formed by calling the methods defined in SUB_Structure. On the other side, the AMCBAnalysis, which is a subclass of Analysis, is cre-

ated as a nonlinear transient analysis at the high level of OpenSees framework. The AMCBAnalysis inherits behaviors from Analysis and incorporates some new numerical procedures, which include substructure generation, mode selection and formation of governing equations in hybrid coordinates. In order to merge the new classes with the original software architecture together, the OpenSees framework is necessarily adapted by modifying a few existing classes.

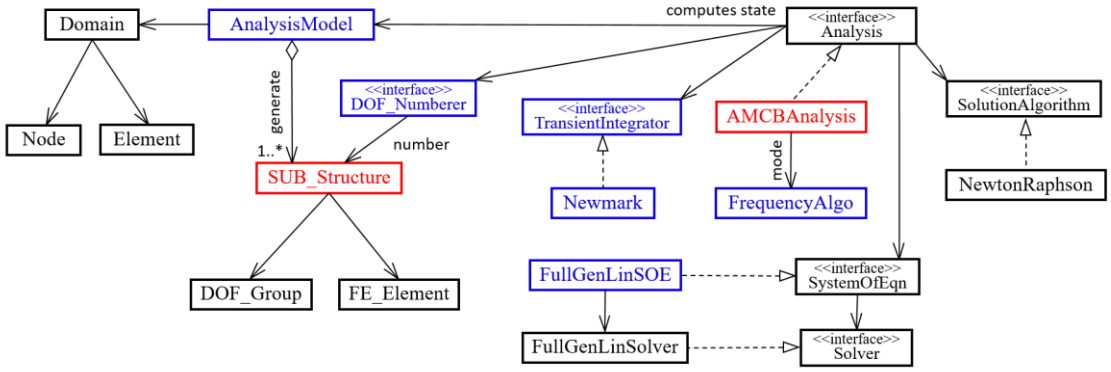

Fig. 1. Class diagram of the AMCB implementation in OpenSees

4 VALIDATION

A 20-story steel high-rise building[4] has been employed to validate the implementation of AMCB in OpenSees. The lateral load-resisting system of the building is comprised of steel-perimeter Moment-Resisting-Frames (MRFs). An in-plane frame in the weak direction of the building with five bays is developed in the OpenSees program. A group of simulation cases are elaborately designed for this steel frame structure. Four strong ground motions, i.e., El Centro, Kobe, Northbridge and Hachinohe, are used as the seismic inputs for the structure along the weak direction. The peak ground acceleration (PGA) is scaled to 310 gal and 620 gal.

To measure the differences in the results between the AMCB scheme and TSI method, the error quantities are defined as the root mean square errors of the differences between the roof displacement curves and the maximum relative error of the envelope of the story-drift ratios. In addition, the errors of simulation results are summarized in Table 1. The maximal error of the roof displacement is approximately 0.72 mm, and the maximal error of the story-drift ratio is approximately 1.22%. As the intensity of the earthquake input increases, the variations in the errors of both the envelope of story-drift ratio and roof displacement are acceptable.

Table 1 Errors of simulation results

Ground motion inputs	PGA (gal)	Roof displacement (mm)	Envelope of story-drift ratio (%)
El Centro	310	0.26	1.22
	620	0.25	0.27
Kobe	310	0.05	0.51
	620	0.45	0.55
Northbridge	310	0.11	0.73
	620	0.40	0.49
Hachinohe	310	0.43	0.65
	620	0.72	0.91

The total number of DOFs in hybrid coordinates for the proposed AMCB scheme is an important index to assess the effect of the model reduction. Fig. 2 describes the variations in the ratio of the hybrid DOFs in the AMCB scheme to the DOFs of the non-reduced model under

the El Centro earthquake with a PGA of 310 gal. The reduction ratios of the DOFs at the last time step for all simulated cases are listed in Table 2. The DOFs of the entire structure are reduced to at least 41% and 72% during the earthquake with PGAs of 310 gal and 620 gal, respectively. The number of DOFs in hybrid coordinates varies following the gradual variation in the nonlinear components, which is presented in physical DOFs, while the variation in the modal DOFs represents the variation in the numbers and types of linear substructures.

Table 2 Ratios of hybrid DOFs to the entire model DOFs

Ground motion inputs	PGA (gal)	Hybrid DOFs	Modal DOFs	Physical DOFs
El Centro	310	0.41	0.11	0.30
	620	0.72	0.11	0.61
Kobe	310	0.42	0.08	0.34
	620	0.72	0.11	0.61
Northbridge	310	0.57	0.16	0.42
	620	0.74	0.10	0.64
Hachinohe	310	0.54	0.12	0.42
	620	0.77	0.09	0.68

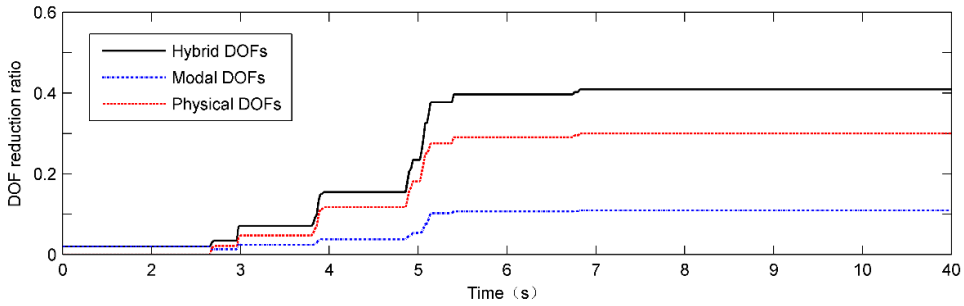

Fig. 2. Variation of reduced DOFs in hybrid coordinates

5 CONCLUSIONS

- The OpenSees is extended to perform the substructure-based simulation with the abilities of the model reduction and hybrid numerical analysis for the partially-nonlinear structures.
- The new classes SUB_Structure and AMCBAnalysis are created to implement the adaptive modified Craig-Bampton method.
- In this study, the calculation error of the story-drift ratio is no more than 1.22%, while the number of DOFs is reduced to approximately 41% under the El Centro earthquake.

6 REFERENCES

[1] M. Fang, J. Wang, H. Li, An adaptive numerical scheme based on Craig-Bampton method for dynamic analysis of tall buildings. *The Structural Design of Tall and Special Buildings,* (In revision).

[2] F. Mckenna, G.L. Fenves, *Open system for earthquake engineering simulation (OpenSees).* Pacific Earthquake Engineering Research Center, University of California, 2013.

[3] E. Gamma, R. Helm, R. Johnson, J. Vlissides, *Design patterns: elements of reusable object-oriented software,* Addison-Wesley, Reading, Mass, 1995.

[4] Y. Ohtori, R.E. Chirstenson, J.B.F. Spencer, Benchmark Control Problems for Seismically Excited Nonlinear Buildings. *Journal of Engineering Mechanics*, **130**:366-85, 2004.

OpenSees Days Europe 2017
1st European Conference on OpenSees
Porto, Portugal, 19–20 June 2017

VIRTUAL HYBRID SIMULATION TESTS ACCOUNTING FOR EXPERIMENTAL ERRORS

Gidewon G. Tekeste[1,2], António A. Correia[1] and Aníbal G. Costa[2]

[1] Laboratório Nacional de Engenharia Civil
Av. do Brasil 101, 1700-066 Lisboa
e-mail: {gtekeste@lnec.pt, aacorreia@lnec.pt},

[2] University of Aveiro
Campus Universitário de Santiago, 3810-193 Aveiro
e-mail: {gidewon.tekeste@ua.pt, agc@ua.pt}

Keywords: OpenFresco, Laboratory errors, ExpSignalFilter class, Shake table model, MATLAB/SIMULINK, Maximum likelihood method

Abstract. *Hybrid simulation (HS) or on-line testing is a technique that involves the partitioning of a test specimen into subdomains. A numerical program solves the equation of motion of a discretized subdomain, while the remaining part of the specimen, more complex or of unknown behavior, is tested in a laboratory using dynamic actuators. Such testing framework requires robust and efficient hardware and a transparent numerical software that can talk to any laboratory control program. To implement this communication, OpenFresco (OF) has been used in many HS tests. The main challenge in real-time HS testing are the errors originating from the laboratory (servo-hydraulic actuator system and data acquisition). The accuracy desired from HS tests can be significantly altered by such errors or they may even lead to instability issues. Currently, LNEC is developing a real-time HS testing facility with the objective of simulating, among other, soil-structure interaction response using both a shake table and an additional actuator. Hence, to mitigate the subsequent effect of such errors, a full computer simulation of HS was performed. This test rehearsal uses OpenSees (OS) and OF along with a MATLAB/SIMULINK model of a shake table. OS was used as a computational driver while the OF was using SimUniaxialMaterials control to mimic the response of the physical element. The ExpSignalFilter class of OF was adopted to model the experimental errors using a White Gaussian Noise (WGN). The parameters of this class were estimated through an offline procedure using the identified shake table dynamics modeled in SIMULINK. The error signal (SIMULINK model output versus OS trial displacements) was fitted to a normal distribution using the Maximum Likelihood (ML). The parameters were then used to generate 50 realizations of virtual hybrid tests. The WGN generated by ExpSignalFilter, in each realization, was computed internally using the Box-Muller transformation. After performing the statistics of the responses, the effect of experimental errors on the responses was assessed. The approach can be easily implemented in a PC without a target machine and the solution to the expected errors using compensation techniques can be studied virtually.*

1 INTRODUCTION

Hybrid simulation is an experimental technique that involves the partitioning of a reference structure into two subdomains: the computational and physical part. The more complex part of the structure is tested in a laboratory while the remaining part is modeled numerically in a finite element software. At the interface boundary of the subdomains, compatibility or equilibrium is enforced – the traditional method being compatibility. Servo-hydraulic actuators are commonly used to impose the displacements (referred as trail displacements hereinafter) solved by the computational driver at the interface nodes. New energy dissipation devices and other complex details in structures can be tested at full scale using this scheme [1].

2 PARAMETRIC SYSTEM IDENTIFICATION OF UNIAXIAL SHAKETABLE

The uniaxial shake table (ST1D) at Laboratório Nacional de Engenharia Civil (LNEC) is driven by a servo-hydraulic actuator capable of applying forces up to 200KN. The shake table is position-controlled by an analog servo-controller using a proportional gain in the inner loop.

The analytical model for the ST1D system can be obtained by combining the mathematical models of the controller, the servo-valve (dynamics and flow characteristics), the hydraulic actuator (continuity and force balance equations), and the platen (mass and friction properties) [2]. The servo-valve model assumes a first-order transfer function. This suffices for the operational frequency range of ST1D [3]. The non-linear general flow equation of the actuator [4] is linearized near its operational point (origin). The schematic diagram of ST1D under a linear SDOF payload condition is shown in Figure 1. A fourth-order transfer function can be derived from the ST1D diagram under no payload condition (4 poles and no zeros).

A Band Limited White Noise (BLWN), in the range of 0-50Hz, was used for parametric system identification of ST1D. The analytical transfer function derived from Figure 1 was modeled parametrically in SIMULINK environment and a constrained non-linear least square solver was implemented to estimate the ST1D parameters. The transfer function computed from the estimated parameters was obtained as:

$$H_{ST1D} = \frac{1.9485e+7}{s^4 + 92.29s^3 + 2.5132e+4\,s^2 + 9.3478e+5s + 1.8746e+7} \tag{1}$$

Equation (1) is the transfer function of the command displacement, at the controller, to the displacement measured at the platen. The entire mass of a rigid reference structure was modeled numerically in this study. Hence, the shake table platen displacement is practically the same as that of the specimen displacement.

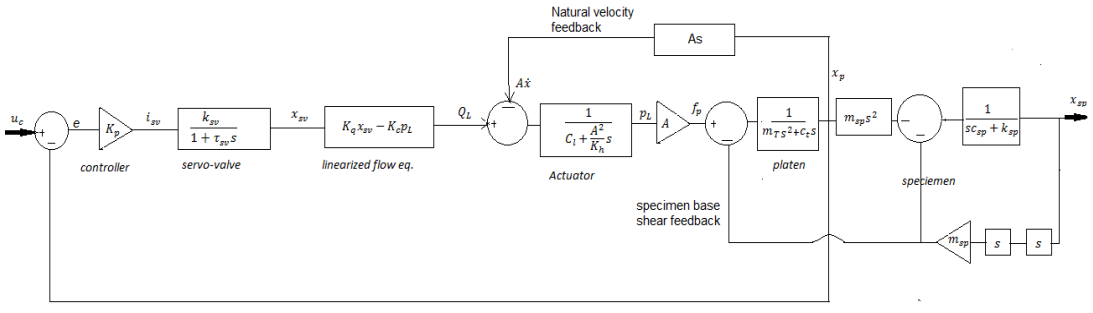

Figure 1 - Schematic diagram of a shake table system

3 VIRTUAL HYBRID SIMULATION USING OPENFRESCO

The Open-source Framework for Experimental Setup and Control (OpenFresco) is an environment-independent software framework that connects finite element models with laboratory control and data acquisition systems. The ExperimentalControl is the one among the four OF abstractions that is responsible for communicating the finite element software with a variety of control and data acquisition systems [5]. The ExperimentalControl class also allows a fully simulated (virtual) HS through SimUniaxialMaterial and SimDomain experimental control objects. In the former control object, a material model simulates the force that the load cell of an actuator would measure for a given set of displacements. On the other hand, the SimDomain control object makes available to OpenFresco all the OpenSees element, material and section libraries [6].

The OpenFresco software framework also offers the ExpSignalFilter (ESF) objects that are used to modify the signals that are going back and forth of the control system. The ESFErrorSimulation filter object is capable of modeling experimental errors through undershoot, overshoot, and a Gaussian white noise. In the latter, a randomly distributed Gaussian error is defined in OpenFresco using a mean value and a standard deviation (referred hereinafter as error parameters). The Box-Muller transformation is used to generate WGN using uniform deviates. The virtual HS performed in this paper assumes a Gaussian white noise error in modeling the experimental errors. This is mainly due to an amplitude-dependent behavior of a servo-hydraulic actuator that arises from its inherent non-linearity combined with a non-linear response of a test specimen.

During the virtual hybrid test, the SimUniaxialMaterial control object was used to simulate the response of the experimental element and the ESFErrorSimRandomGauss filter object was adopted to model the experimental errors. The error parameters that should be defined in OF were estimated using the identified shake table transfer function. The transfer function operates offline, receiving a vector of trial displacements from OS after each complete analysis of the structure. The process started by assigning zero values to the error parameters in OF during the first run. The vector of trial displacements of OS from the previous run were then applied to the SIMULINK model of ST1D as shown in Figure 2. The trial displacements were deducted from the SIMULINK output displacement. The resulting signal was fitted into a normal distribution using the Maximum Likelihood (ML) method and the error parameters were estimated. To ensure the consistency property of ML, its estimates were compared with estimates from the method of moments. The process was followed by performing fifty virtual HS tests using the same estimated error parameters in OF. The statistics, mainly the mean and the standard deviation for each time-step, of the responses was performed. Average of the responses from the fifty realizations were used to define the system responses. These responses were compared with their error-free counterparts to analyze the effects of the modeled error.

The reference structure is a one-bay frame with fixed supports at the base. A truss element connects the two vertical columns (see Figure 3).

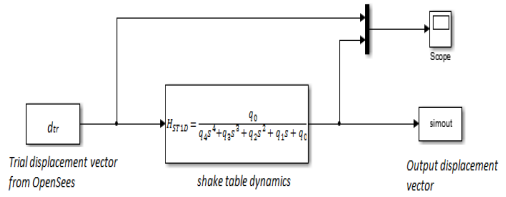

Figure 2 - SIMULINK model of ST1D

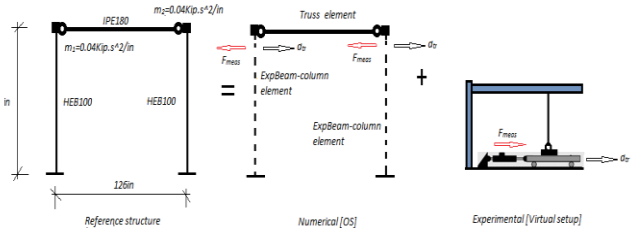

Figure 3 - Partitioning of the test structure during HS

The two columns are experimental elements, while the truss element is a numerical element. Nodes 3 and 4 are free to rotate allowing the experimental control, at the interface boundary, to be a one-actuator control. The structure was subjected to the El Centro ground motion that is scaled to 0.3 g PGA and a time-step of 0.02 sec. An implicit Newmark integration scheme with a fixed number of iterations (five) was adopted during the analysis.

The repeatability of the error model was verified because the same value of standard deviation was attained throughout the test for both forces and displacements, see Figure **4** (top left). It is evident from Figure 4 (bottom left and right) that the ST1D delay introduces a negative damping effect, and hence a smaller dissipation of energy, similarly to the undershoot depicted in the same figure. The outcome is a reasonably good simulation of the system response, which can be further improved by compensation techniques.

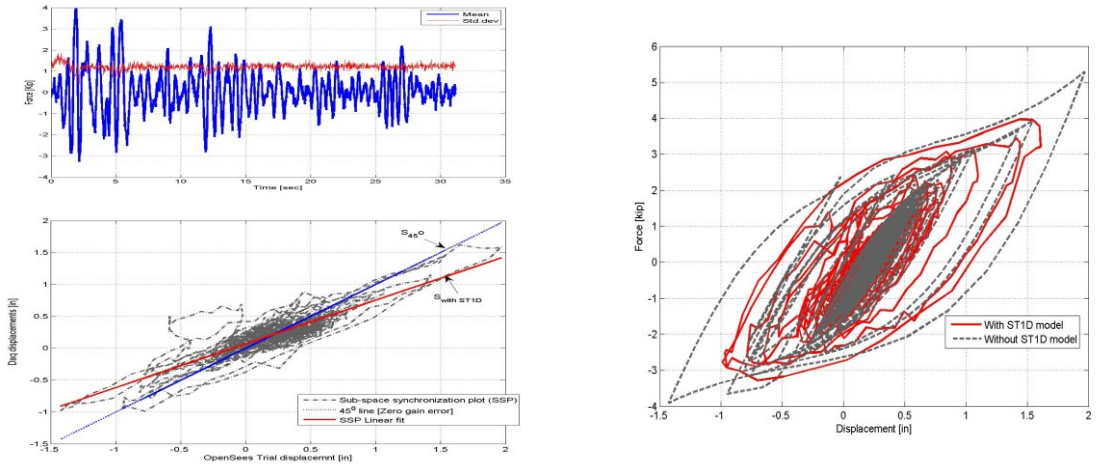

Figure 4 – Coupling force (μ, σ) of the 50 realizations (top left), subspace synchronization plot (bottom left) and top column hysteresis (right)

4 CONLUSIONS

The paper briefly discussed the potential of OS and OF in performing virtual HS using a realistic ST1D model. Results show the coupled effect of delay and gain errors. Although an online procedure was possible, a simple offline method was found to be applicable with fewer resources. Online techniques will be addressed in future developments.

REFERENCES

[1] V. Saouma and M. Sivaselvan, *Hybrid simulation: Theory, Implementation and Applications*. Taylor & Francis, 2008.

[2] J. E. Carrion and B. F. Spencer, Model-based Strategies for Real-time Hybrid Testing. NSEL Report Series. Report No. NSEL-006, lllinois, USA, 2007.

[3] MOOG, Electrohydraulic Valves... A Technical Look - Datasheet, 2002.

[4] H. E. Merrit, *Hydraulic control systems*. John Wiley & Sons, Inc., 1967.

[5] A. H. Schellenberg, S. A. Mahin, and G. L. Fenves, Advanced Implementation of Hybrid Simulation. PEER Report 2009/104, California, USA, 2009.

[6] A. Schellenberg, H. K. Kim, Y. Takahashi, G. L. Fenves, and S. A. Mahin, OpenFresco Command Language Manual: OpenFresco v2.6. Tech. report, California, USA, 2009.

OpenSees Days Europe 2017
1st European Conference on OpenSees
Porto, Portugal, 19–20 June 2017

NUMERICAL MODELLING OF CONCRETE-FILLED STEEL TUBULAR MEMBERS IN OPENSEES

Y. Jiang[1, 2], A. Silva[1, 2], L. Macedo[1], J. M. Castro[1] and R. Monteiro[2]

[1] Department of Civil Engineering, Faculty of Engineering, University of Porto
Rua Dr. Roberto Frias s/n, 4200-465 Porto, PORTUGAL
e-mail: yadong.jiang@fe.up.pt, ajms@fe.up.pt, luis.macedo@fe.up.pt and miguel.castro@fe.up.pt

[2] Istituto Universitario di Studi Superiori di Pavia
Palazzo del Broletto - Piazza della Vittoria n.15, 27100 Pavia, Italy
e-mail: yadong.jiang@umeschool.it

Keywords: OpenSees, Concrete Filled Steel Tube, Concentrated Plasticity Model, Seismic Performance

Abstract. *The research study documented in this document details an accurate and efficient numerical model for concrete-filled steel tubes (CFST) in OpenSees. The feasibility of both Distributed Plasticity (DP) and Concentrated Plasticity (CP) models was assessed based on comparisons with experimental test data. One of the main conclusions obtained pertains the high level of accuracy with the use of the CP model, as it is able to accurately simulate the cyclic response of CFST members. Two moment-resisting framed systems, namely steel and composite frames, were designed in accordance with Eurocode 8 and their seismic performance was evaluated on the basis of the proposed model. The analytical results allowed concluding about the better seismic performance of the composite system in comparison with the steel equivalent, as shown by the results of fragility assessment through Incremental Dynamic Analysis (IDA).*

1 INTRODUCTION

The use of concrete filled steel tube (CFST) member in construction practice has become widespread over recent decades. Confinement effects, that improve both the strength and ductility of the core material, as well as the constraint offered by the core to the encasing steel tube, which minimizes the influence of local buckling, are some of the advantages of these members. As a consequence, the capacity and seismic performance of structures can be improved by the use of CFST members in detriment of reinforced concrete or steel-only solutions. The main purpose of the research study detailed herein is the development of an accurate model for CFST members in OpenSees, and to access the influence of CFST members on the seismic performance of moment-resisting frames.

2 MODELLING OF CFSTS IN OPENSEES

Two types of beam-column elements were considered to model CFST members in OpenSees, namely Distributed Plasticity (DP) and Concentrated Plasticity (CP) models. In order to investigate the bending behaviour of long CFST columns, 16 circular rubberized CFST specimens which, were recently tested [1] at the University of Porto, were used to calibrate the aforementioned models.

2.1 Distributed Plasticity (DP) Model

The DP model is a beam-column model with fibre sections distributed along the element. The modelling of fibre section is made directly, and is compatible with both 2D and 3D frame models. However, composite effects (e.g. confinement effect) and local buckling phenomena are not accurately captured by this model.

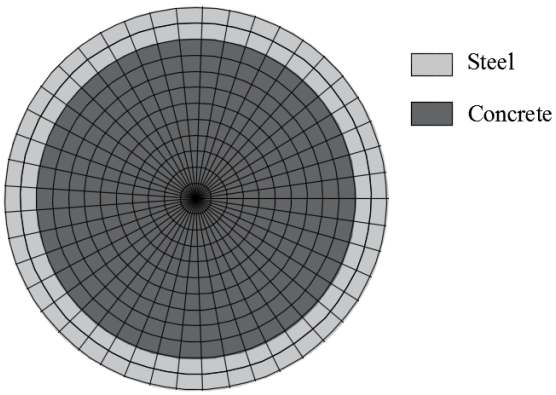

Figure 1: Fibre section mesh details of a circular CFST member

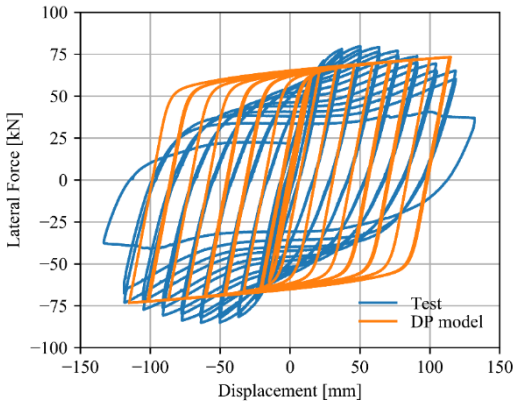

Figure 2: Lateral force-displacement curve comparison between test data and the DP model results

Figure 1 shows the mesh details of the fibre section adopted. The concrete and steel parts were assigned with material models *concrete01* and *Steel01* with uniaxial properties, respectively. Figure 2 shows the comparisons between the numerical results of the DP model and the test data for specimen No.7 [1]. As shown in the figure, by using the uniaxial properties of the materials, the capacity of the CFST members is underestimated by the DP model, as the model does not consider the confinement effects of the concrete. The DP model also fails to predict strength deterioration effects of the CFST member under cyclic loading. Therefore, by using the DP model the ductility of the CFST member under cyclic loading is overestimated, which

will result in inaccurate simulation of the seismic behaviour of a global structural system. Hence, the DP model based on uniaxial material properties is not suitable for modelling CFST members.

2.2 Concentrated Plasticity (CP) Model

The CP model consists of an elastic beam member and two nonlinear springs lumped at the two ends. This approach is often adopted for 2D frame analysis but its extension to 3D analysis is not trivial due to the need to account for interaction effects. The behaviour of the nonlinear springs should be calibrated based on existing data, either from tests or from more accurate models (e.g. detailed 3D finite element model). Thus, the CP model has the ability to represent both concrete confinement effects and the strength degradation of the hysteretic response.

The *ModIMKPeakOriented* material available in OpenSees was adopted as the nonlinear spring of the CP model. The CalTool [2] (Figure 3) framework was used to calibrate the input parameters of the CP model. The target of the calibration was the analytical results of a 3D CFST model in ABAQUS. Figure 4 shows the comparison of the calibrated CP model results with the results of the ABAQUS model. As shown, the CP model is in good agreement with the target in what concerns ultimate capacity, loading/unloading stiffness and strength degradation.

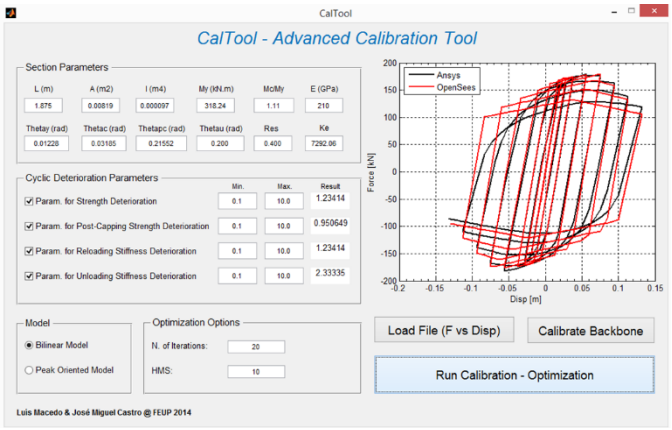

Figure 3: The CalTool

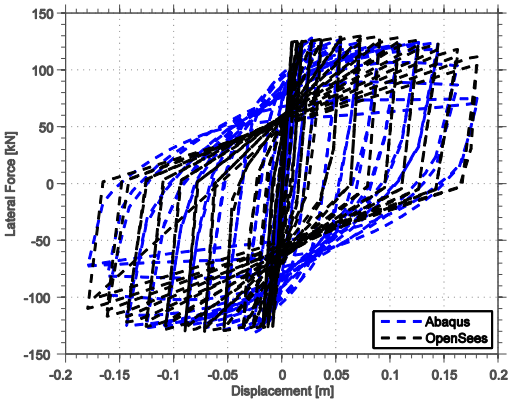

Figure 4: The cyclic behaviour comparison between the CP model in OpenSees and the 3D model from Abaqus

3 SEISMIC PERFORMANCE ASSESSMENT OF A COMPOSITE FRAME

A 5-storey building structure was designed with two frame solutions, namely a composite frame and a steel frame. The composite frame was materialised with CFST columns and IPE beams, whilst the remainder was designed with HEB columns and IPE beams. Both HEB and IPE designate H-shaped and I-shaped European steel open sections, respectively. The design provisions of Eurocode 8 [3] were followed to design the two frames. Besides the CFST members, the IPE and HEB members were also modelled with a CP approach, which were coupled with the *Bilin* material.

The seismic performance assessment of the two frames was conducted using Incremental Dynamic Analysis (IDA). A group of 30 ground motions from real earthquake events were selected and scaled with the SelEQ tool [4] to have a spectra shape compatible with Eurocode 8 spectrum.

Figure 5 shows the fragility curves of the two frames under the limit state of collapse, which was considered as the point where the slope of the IDA curve reduces to 10% of the initial value.

As shown in the figure, the composite moment-resisting frame exhibits a better seismic performance in comparison to the steel frame, with much lower probabilities of exceedance under the same intensive measure level.

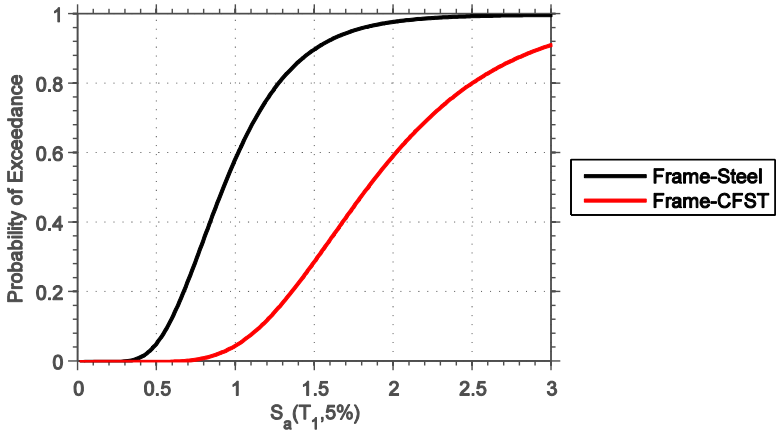

Figure 5: The fragility curve comparison between the steel frame and the composite frame under the collapse limit state

4 CONCLUSIONS

By developing the model for CFST member and evaluating the seismic performance of composite frame in OpenSees, the following conclusions could be drawn:

- The DP model with uniaxial material properties is not suitable for modelling CFST member, as the model is not able to account for concrete confinement effects and local buckling of the steel tube;
- The CP model is able to simulate well the cyclic response of CFST members under flexure, both in terms of member capacity and strength deterioration effects;
- The composite frame studied, materialised with CFST columns instead of equivalent steel member, showed better seismic performance than the steel frame, as shown by the comparison of the collapse fragility curves.

REFERENCES

[1] A. Silva, Y. Jiang, J. M. Castro, N. Silvestre, R. Monteiro. Experimental assessment of the flexural behaviour of circular rubberized concrete-filled steel tubes. *Journal of Constructional Steel Research*, **122**, 557-570, 2016.

[2] L. Macedo. Performance-based seismic design and assessment of steel moment frame buildings. PhD Thesis University of Porto, 2017.

[3] CEN. Eurocode 8: Design of structures for earthquake resistance, part 1: general rules. Seismic actions and rules for buildings, European Committee for Standardization, Brussels, 2004.

[4] L. Macedo and J. M. Castro. SelEQ: An advanced ground motion record selection and scaling framework. *Advances in Engineering Software*, 2017. DOI: 10.1016/j.advengsoft.2017.05.005.

OpenSees Days Europe 2017
1st European Conference on OpenSees
Porto, Portugal, 19–20 June 2017

OPTIMIZED SEISMIC DESIGN OF STEEL FRAMES USING OPENSEES

João Nogueira[1], Luis Macedo[2], and José Miguel Castro[3]

[1] Faculdade de Engenharia da Universidade do Porto
Rua Dr. Roberto Frias, s/n, 4200-465 Porto - Portugal
email: joao.nogueira@fe.up.pt

[2] Faculdade de Engenharia da Universidade do Porto
Rua Dr. Roberto Frias, s/n, 4200-465 Porto - Portugal
email: luis.macedo@fe.up.pt

[3] Faculdade de Engenharia da Universidade do Porto
Rua Dr. Roberto Frias, s/n, 4200-465 Porto - Portugal
email: miguel.castro@fe.up.pt

Keywords: Design, Optimization, Harmony Search Algorithm, Software

Abstract. *This paper describes the concept and development of a software tool that allows the automatic design and optimization of steel frames under the effect of gravitational and seismic loads. The software was developed using Python as a programming language and OpenSees as the structural analysis framework. The design checks are carried out in accordance with Eurocodes 3 and 8. A metaheuristic algorithm was used in order to optimize the design. The results obtained lead to the conclusion that it is possible to obtain economically viable solutions using automated methods.*

1. INTRODUCTION

Civil engineering is an activity of great responsibility, as errors could result on large economical and human losses, as well as a significant impact on the environment and culture. Therefore, it is essential that every decision can be supported by standards and regulations, as thorough as possible. Even though there are dozens of commercial software dedicated to civil engineering, there is still a lack in software that allows not only the design according to eurocodes but also the structural optimization and support research related to the development of new design approaches.

This paper describes the concept and development of a software that allows the automatic and optimal design of steel frames under gravity and seismic loads. This software was developed using Python as a programming language, and OpenSees [1] as the structural analysis framework. The paper ends with a case study that shows a comparison between the solution obtained on this paper and a solution obtained through a conventional design approach.

The analysis of the steel frames was developed in accordance with Eurocode 3, and the seismic analysis in accordance with Eurocode 8. The remaining actions and other basic requirements were defined following Eurocode 0.

2. OPTIMIZATION PROBLEM

2.1 Problem formulation

The objective of this software is to optimize the design of steel frames. Being cost one of the most common criterion in structural design, it was adopted as the objective of the optimization process. In steel structures, cost is mainly a function of the weight of the structure, but also of other factors like fabrication, erection, connections, etc. Since the other factors exceeded the scope of this paper, the objective function was defined as follows:

$$\text{Minimize W} = \sum_{i=1}^{Ne} \gamma_i * L_i * A_i \tag{1}$$

where W is the weight of the structure, N_e is the number of elements, γ_i is the material density of member i, L_i is the length of member i and A_i is the cross-section area of member i. Eurocodes 3 and 8 establish several design criteria, such as maximum values of stress, displacement, etc. Hence, the design process consists of a constrained problem. Pezeshk et al. [2], and later Camp et al. [3], proposed transforming the unconstrained problem into a constrained problem using a penalty function. In this formulation, the constraint violation function was defined to adapt the penalty as a function of the various coefficients

$$C = 5 * \sum_{i=1}^{6} \frac{C_i}{\sum_1^6 C_i} * C_i = \frac{5}{\sum_1^6 C_i} * \sum_{i=1}^{6} C_i^2 \tag{2}$$

where C_i is a penalty coefficient i. These penalty criteria were defined with both the objective of implementing the design checks prescribed in the Eurocodes and to obtain sustainable solutions. The penalty coefficient is obtained as a function of six partial coefficients, each of them corresponding to the ratio of sum of unmet criteria for the total number of design checks. C can vary between 0 and 5. Six penalty ratios were defined: (1) EC8 damage limitation state,

(2) EC8 ultimate limit state, (3) EC8 local ductility condition, (4) EC 3 verifications, (5) cross-section area reduction with height and (6) interstorey drift sensitivity coefficient verification.

2.2 Harmony Search Optimization

The harmony search algorithm (HS) is one of the most recently developed metaheuristic optimization technique, which is based on the concept of music improvisation process involved in search for a better harmony [4]. This algorithm was first developed by Geem et al. [5] with static parameters and later improved by Mahdavi et al. [6] and Kumar et al. [4] who developed expressions to change the main parameters dynamically during the process. Several applications of HS to steel frames can also be found [7-8].

For the development of this software, a variation of the expressions proposed by Mahdavi et al. [6] for the Bandwidth (*BW*) and the expressions proposed by Kumar et al. [4] for the Pitch Adjustment Rate (*PAR*) and Harmony Memory Consideration Rate (*HMCR*) were implemented.

The algorithm was implemented considering two stopping limits. The first one defines the maximum number of iteration during which adaptive parameters are used ($N_{adaptive}$), then the maximum number of iterations (N_{max}) with static parameters. Hence, the parameters evolve as represented in Fig. 1. The second stopping criterion was defined so that it concludes the design if the best structure was not changed for 20% of the maximum number of iterations.

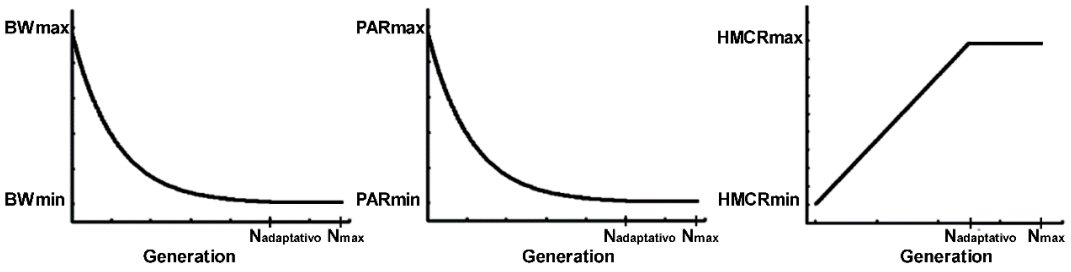

Fig. 1 - Parameters used in this software

BW was set between 1 and 20% of the possible sections' list, *PAR* was set between 0.01 and 0.99, and *HMCR* was set between 0.7 and 0.99. The Harmony memory was set to 2.5 times the number of variables.

3. DESCRIPTION OF THE SOFTWARE

3.1 System architecture

The proposed software for optimized design of steel frames is organized in 4 modules dedicated to: (1) create and manage the data model, (2) interact with Opensees to perform the structural analysis, (3) verify the resistances of the elements and (4) the module that implements the optimization algorithm, which is responsible for controlling the process. The algorithm was developed in Python and the Opensees models are dynamically generated resorting to a template engine available in Python.

3.2 Design of the software

All structural analyses are performed using Opensees and considering P-Δ effects, in accordance with Section 5.2.1 of EC3. Therefore, the geometry of the structure in the Opensees

model is always affected by the imperfections for global analysis defined in Section 5.3.2 of EC3. The results of the forces on the nodes are then parsed in Python and stored in the data model.

The seismic analysis is performed through the lateral force method of analysis. It is worth noting that this approach has limitations that should be taken into account, particularly when dealing with tall frames or frames irregular along the height.

The verification module was conceptualized in a way which not only allowed it to be extended to other structural types (e.g., RC, composite) but also to be used independently from the software.

4. APPLICATION EXAMPLES

In order to demonstrate the efficiency of the software and its synergy with OpenSees, a comparison between optimized design of frames and frames designed in a conventional way [9] will be presented.

The structure designed is a three-bay, five-storey planar steel frame. The structural elements are grouped as shown in Fig. 2 with the objective of ensuring a structure adequate for construction. For this case, a penalty function exponent of 2 was considered and the remaining parameters were obtained via the expressions presented in Section 2.

The following material properties were considered: yield stress, f_y, equal to 275 MPa, Young's modulus, E, equal to 210 GPa, distortion modulus, G, equal to 81 GPa, Poisson coefficient equal to 0.3 and a specific weight, γ, of 77 kN/m^3. Concerning the loads, the structure is subjected to residential loads and a peak ground acceleration of 0.3g, the soil is of type B according to EC8 definition, damping is 5% and the class of importance is II.

European IPE sections were used for the beams and European HEB sections were used for the columns.

The interstorey drift sensitivity coefficient was limited to 0.2 in order to allow a direct comparison with the results obtained by Macedo [9]. The results are presented in Table 1.

Table 1 – Comparison between manual and automated design

		Sections	Weight (ton)
DCM q = 4	Manual [ref]	HEB340, HEB400, HEB280, HEB340, HEB280, HEB340, IPE360, IPE360, IPE330, IPE300, IPE300	14.10
	Automated	HEB240, HEB340, HEB220, HEB280, HEB140, HEB180, IPE400, IPE400, IPE360, IPE300, IPE270	11.12
DCH q = 6.5	Manual [ref]	HEB400, HEB450, HEB340, HEB360, HEB340, HEB360, IPE400, IPE400, IPE400, IPE330, IPE300	16.20
	Automated	HEB280, HEB400, HEB240, HEB360, HEB180, HEB240, IPE500, IPE450, IPE400, IPE300, IPE270	13.59

The software conducted to structures 21.1% and 16.1% lighter than the manual design, resulting in savings of 2.98 and 2.61 tons of steel, respectively.

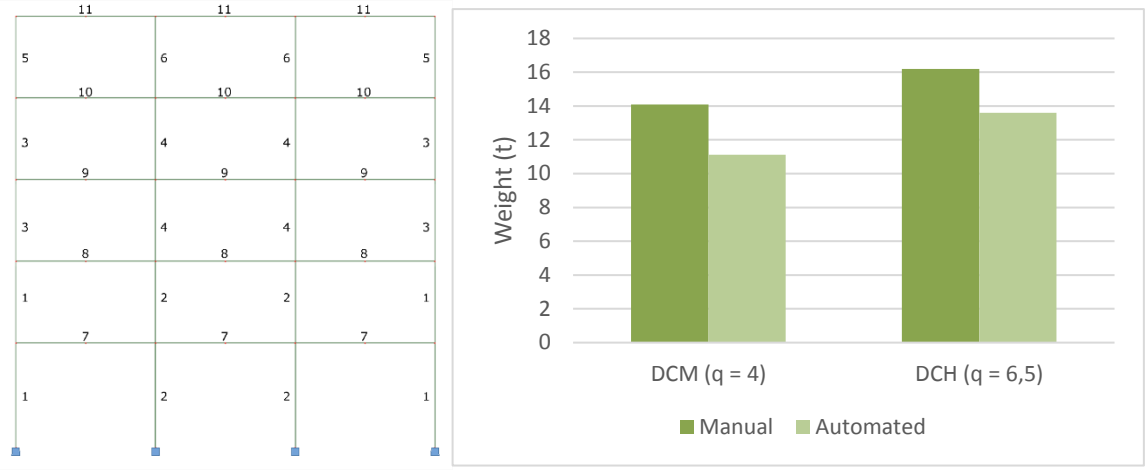

Fig. 2 – Structure geometry and groups of elements (left) and comparison between manual and automated design (right)

5. CONCLUSIONS

This paper presented a new software tool for the optimized design of steel frames. The software is powered by the OpenSees structural analysis framework. The results obtained demonstrate the level of efficiency that can be achieved with the application of optimization algorithms in structural design.

6. REFERENCES

1. PEER, *OpenSEES: Open System for Earthquake Engineering Simulation.* Berkeley,CA, 2006.
2. Pezeshk, S., C. Camp, and D. Chen, *Design of nonlinear framed structures using genetic optimization.* Journal of Structural Engineering, 2000. **126**(3): p. 382-388.
3. Camp, C.V., B.J. Bichon, and S.P. Stovall, *Design of steel frames using ant colony optimization.* Journal of Structural Engineering, 2005. **131**(3): p. 369-379.
4. Kumar, V., J.K. Chhabra, and D. Kumar, *Parameter adaptive harmony search algorithm for unimodal and multimodal optimization problems.* Journal of Computational Science, 2014. **5**(2): p. 144-155.
5. Geem, Z.W., J.H. Kim, and G. Loganathan, *A new heuristic optimization algorithm: harmony search.* Simulation, 2001. **76**(2): p. 60-68.
6. Mahdavi, M., M. Fesanghary, and E. Damangir, *An improved harmony search algorithm for solving optimization problems.* Applied Mathematics and Computation, 2007. **188**(2): p. 1567-1579.
7. Degertekin, S., *Optimum design of steel frames using harmony search algorithm.* Structural and Multidisciplinary Optimization, 2008. **36**(4): p. 393-401.
8. Hasançebi, O., F. Erdal, and M.P. Saka, *Adaptive harmony search method for structural optimization.* Journal of Structural Engineering, 2009. **136**(4): p. 419-431.
9. Macedo, L., *Performance-based seismic design and assessment of steel moment frame buildings*, PhD Thesis University of Porto, 2017.

OpenSees Days Europe 2017
1st European Conference on OpenSees
Porto, Portugal, 19–20 June 2017

AUTOMATIC CALIBRATION OF HYSTERETIC MODELS THROUGH MULTIPLE RESPONSES

Corrado Chisari[1], Gianvittorio Rizzano[2], Claudio Amadio[3], and Massimo Latour[4]

[1] University of Salerno
via Giovanni Paolo II, 132 – 84084 Fisciano (SA) - Italy
e-mail: corrado.chisari@gmail.com

[2] University of Salerno
via Giovanni Paolo II, 132 – 84084 Fisciano (SA) - Italy
g.rizzano@unisa.it

[3] University of Trieste
piazzale Europa, 1 – 34127 Trieste - Italy
amadio@units.it

[4] University of Salerno
via Giovanni Paolo II, 132 – 84084 Fisciano (SA) - Italy
mlatour@unisa.it

Keywords: Genetic Algorithms, Software, Discrepancy, Multi-objective optimization.

Abstract. *This paper describes MultiCal, a software package recently developed by the authors which is able to calibrate parameters of several hysteretic models implemented in OpenSees, by fitting experimental generalized strain-stress curves. The calibration is performed by means of a multi-objective optimization procedure directly interfaced with OpenSees software, in which discrepancy between experimental and numerical responses is minimized. Up to six experimental responses may be utilized to increase robustness of the calibration, and for each one different quantities of interest can be fitted (raw data, energy, envelope). The applicability of the procedure is demonstrated by real-world examples involving steel components.*

1 INTRODUCTION

Material models with different degrees of sophistication are implemented in general structural software codes, and specifically OpenSees [1]. In particular, hysteretic models are able to simulate many phenomena occurring under cyclic loading conditions: stiffness and strength degradation, pinching, crack/gap opening and closing, low-cycle fatigue. These models are called phenomenological because they simulate the phenomenon and not the underlying physics. In this respect, they can be applied to a wide range of structural elements, as they can represent relationships as force-displacement of rods, moment-rotation of beam-to-column joints, base shear-top displacement of buildings, etc. without conceptual differences. Recognizing this, in OpenSees they are all grouped under the *uniaxialMaterial* label.

Even though phenomenological models have great potential for dynamic analyses thanks to low computational cost, they have the important drawback that the parameters involved in the hysteretic behavior often lack physical meaning, and thus their calibration may become problematic. A feasible approach to calibration involves curve fitting of experimental responses, which in turn can be solved with either trial-and-error techniques and expert judgement, or more efficient numerical optimization procedures. In [2], the authors proposed a methodology to perform calibration of the smooth model by Sivaselvan and Reinhorn [3]. Among the main findings of such work, multi-objective calibration accounting for both monotonic and cyclic tests was found to add robustness, since fitting of a single cyclic response may provide incorrect calibration of parameters, due to ill-posedness of the inverse problem.

In this paper, MultiCal, a software package specifically designed to calibrate model parameters for hysteretic models, is described. Some examples are also illustrated to show the potential and the application range of the software.

2 MULTI-OBJECTIVE CALIBRATION

Calibration (or parameter identification) of a numerical model means finding the set of parameters $\tilde{\boldsymbol{p}}$ such that the computed response given by a simulation of a test $\boldsymbol{y_c(p)}$ is as close as possible to the experimental response $\boldsymbol{y_{exp}}$. When N_T calibration tests are performed, this implies solving the optimization problem:

$$\tilde{\boldsymbol{p}} = \arg\min_{\boldsymbol{p}\in\boldsymbol{P}}\{\omega_1(\boldsymbol{p}), \dots, \omega_{N_T}(\boldsymbol{p})\} \tag{1}$$

where $\omega_i(\boldsymbol{p}) = \frac{\|\boldsymbol{y_{exp,i}} - \boldsymbol{y_{c,i}(p)}\|}{\|\boldsymbol{y_{exp}}\|}$ is the discrepancy function measuring the inconsistency between the experimental and computed quantities for the i-th test, and $\boldsymbol{P}$ the set of all possible parameter combinations. The minimization of ω may be accomplished by using different optimization methods. In this work, the solution of (1) is obtained by means of the Non-dominated Sorting Genetic Algorithms II, NSGA-II [4].

In the context of multi-objective optimization, the concept of Pareto optimality replaces the usual notion of optimality. A solution is referred to as Pareto optimal if it is not dominated by any other solution. The ensemble of all Pareto optimal solutions is said Pareto Front $\boldsymbol{PF}$, and it represents the general solution of (1). At the end of the analysis, a unique compromise solution $\boldsymbol{p_{compr}}$ may be extracted from the Pareto Front, according to the rule:

$$\boldsymbol{p_{compr}} = \arg\min_{p\in\boldsymbol{PF}}\left\|\boldsymbol{\omega(p)} - \boldsymbol{\omega_{utopia}}\right\| \tag{2}$$

where $\boldsymbol{\omega(p)} = \left[\omega_1(\boldsymbol{p}), \dots, \omega_{N_T}(\boldsymbol{p})\right]^T$ and $\boldsymbol{\omega_{utopia}}$ is the vector of the minimum discrepancies.

3 STRUCTURE OF THE CODE

The authors developed MultiCal, a software code to solve problem (1), written in C# and directly interfacing with OpenSees. With the aim of facilitating the user, the solver is equipped with a pre-processor able to generate the input files for the optimization, given the curves to fit and the model to calibrate. The software code can be downloaded at www.multical.unisa.it.

3.1 Models implemented

To date, six OpenSees hysteretic models are implemented in the software. Three of them are present in the standard library: *Bilin*, *BoucWen*, *Hysteretic*. Other three are composed of elementary springs in series/parallel: flag-shaped, degrading flag-shape and L-stub models. An additional model [3], for the calibration of which it is necessary to interface with Seismostruct software [5], is also implemented but it will not be discussed here.

3.2 General workflow

After installing the software, the user can optionally run the pre-processor from the command-line with the command:

multical -t -c curve1.csv -c curve2.csv ... -m modelName (3)

where *curve1.csv*, *curve2.csv*, ... are up to six experimental curves to fit, saved in two-column csv file, with standard delimiter ",". The two columns respectively contain generalized strain and stress. The delimiter may be changed to *delim* adding the option "*-d delim*" to the command (3). Command (3) will generate the needed input files in the current directory. They can be modified with a text editor if needed, and afterwards the analysis is launched with the command:

multical -c curve1.csv -c curve2.csv ... -m modelName (4)

where the absence of *-t* option means that the solver is not run in template-generator mode. The *--nozip* argument is optional and can be used to limit the output size.

3.3 Input files

Three input text files are needed for the analysis. They can be created from scratch, or by running the pre-processor as explained in the previous subsection.

- *GA_Parameters.txt* contains the Genetic Algorithms parameters.
- *InputParameters.txt* contains variation ranges for the material parameters to calibrate. They can be defined as constant, variable in a range, or mathematical combination of other parameters.
- *OutputParameters.txt* contains the definition of the objectives. For each curve to fit it is possible to evaluate (and minimize) the error (i) in the generalized stress history, (ii) in the energy history, or (iii) in the envelope curve.

3.4 Output files

The solver will create a folder where all output files are contained. Together with a copy of the input files (useful to keep track of the input for further assessment), they are:

- *ProjectLabel.csv* contains the database of the processed solutions, identified by a numerical ID label. *ProjectLabel* is a specified in *GA_Parameters.txt*. The database contains input and output variables and progressive analysis time. It is updated every GA generation.

- *ParetoFront.csv* is similar to the previous file, but it contains the additional information regarding the domination front of each individual, and thus is generated only at the end of the analysis.
- *Compromise_XY* is a copy of the folder representing the compromise solution chosen per definition (2). It contains OpenSees input and output files as well as the csv files with the computed counterparts of curves *curve1.csv*, etc. mentioned in (4). *XY* is the numerical ID label of the solution during the analysis.

4 EXAMPLES

4.1 Hollow-section steel member

The set of open and hollow cross-section beams investigated experimentally in [6] was used as an experimental database for the calibration of three phenomenological models implemented in OpenSees, namely *Bilin*, *BoucWen*, *Hysteretic*. In particular, the results concerning the 250×250×8 square hollow section will be presented here. A 1865mm-long cantilever beam was tested in pure bending according to monotonic and AISC cyclic protocol. The calibration of the three models was then performed according to the moment-rotation curve for the monotonic test, and energy-time curve for the cyclic test.

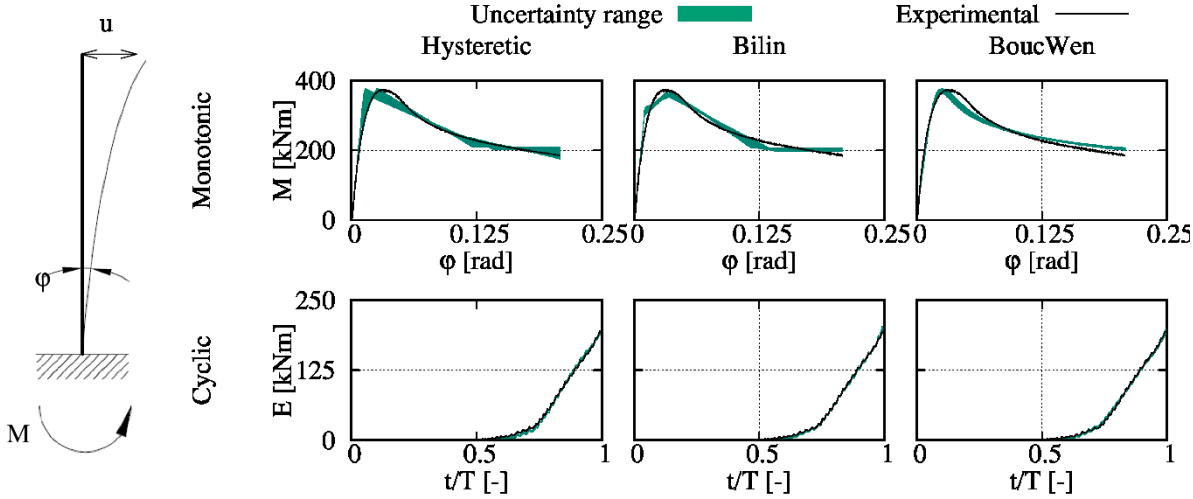

Figure 1. Results of the calibration of a hollow-section profile.

As Genetic Algorithms have a strong stochastic component, it is suggested to repeat the analysis more than once to verify its robustness. The uncertainty range resulting from ten runs of the calibration, together with the experimental results, is displayed in Figure 1. It is possible to notice that all three models fit remarkably well and with low uncertainty both experimental responses.

4.2 Self-centering dissipative base joint

The second example regards the characterization of an innovative dissipative base joint, in which the dissipation is demanded to special friction pads, while the self-centering feature is assigned to a pre-stressed steel bar. A cyclic test according to AISC protocol was performed, with an axial force applied at the top of the column equal to 0.25 times the column plastic capacity. Herein, the simulated response of both flag-shaped and degrading flag-shaped phe-

nomenological models are investigated. The calibration was performed onto the cumulated energy and the envelope of the curve. From Figure 2, it is possible to notice that, unlike the simpler flag-shaped model, the degrading flag-shape is able to capture stiffness degradation and yield point shifting.

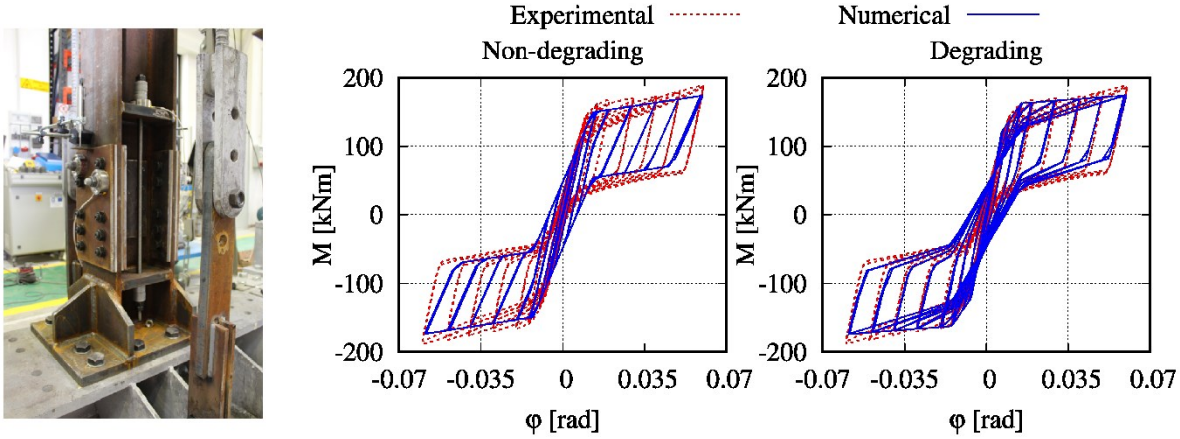

Figure 2. Performance of non-degrading and degrading flag-shaped model in simulating the dissipative joint response.

4.3 L-stub

The last example regards an innovative type of angle to be used in substitution of hold-down in cross-laminated timber panel buildings [7]. The force-displacement response model of the angle has been calibrated onto the data coming from a monotonic and a variable-amplitude cyclic test (Figure 3, top row), and validated against fixed-amplitude cyclic tests (Figure 3, bottom row).

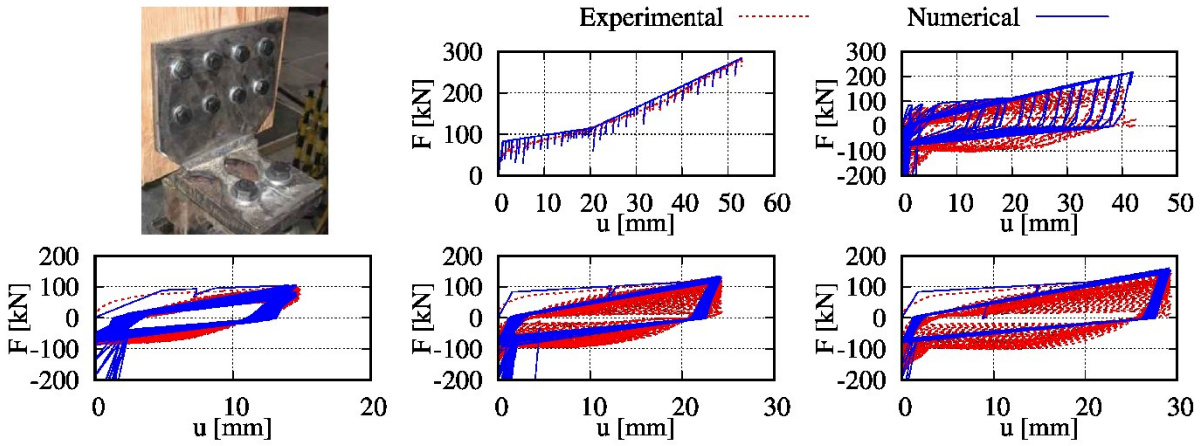

Figure 3. Results of the calibration of the innovative dissipative angle.

5 CONCLUSIONS

In this paper, a software for the automatic calibration of hysteretic uniaxial models implemented in OpenSees by means of multi-objective optimization has been described. The application to several examples regarding steel components has shown the feasibility and generality of the approach. Further extensions will regard the implementation of more numerical models into the software.

REFERENCES

[1] OpenSees, "Open System for Earthquake Engineering Simulation," 2010. [Online]. Available: http://opensees.berkeley.edu/wiki/index.php/Main_Page. [Accessed 12 October 2016].

[2] C. Chisari, A. B. Francavilla, M. Latour, V. Piluso, G. Rizzano and C. Amadio, "Critical issues in parameter calibration of cyclic models for steel members," *Engineering Structures,* vol. 132, pp. 123-138, 2017.

[3] M. V. Sivaselvan and A. M. Reinhorn, "Hysteretic models for deteriorating inelastic structures," *J. Eng. Mech.,* vol. 126, no. 6, pp. 633-640, 2000.

[4] K. Deb, A. Pratap, S. Agarwal and T. Meyarivan, "A Fast and Elitist Multiobjective Genetic Algorithm: NSGA-II," *IEEE Transactions on Evolutionary Computation,* vol. 6, no. 2, pp. 182-197, 2002.

[5] Seismosoft, "SeismoStruct v7.0 – A computer program for static and dynamic nonlinear analysis of framed structures," 2014. [Online]. Available: http://www.seismosoft.com. [Accessed 13 April 2016].

[6] M. D'Aniello, R. Landolfo, V. Piluso and G. Rizzano, "Ultimate behavior of steel beams under non-uniform bending," *Journal of Constructional Steel Research,* vol. 78, pp. 144-158, 2012.

[7] M. Latour and G. Rizzano, "Cyclic behavior and modeling of a dissipative connector for cross-laminated timber panel buildings," *Journal of Earthquake Engineering,* vol. 19, no. 1, pp. 137-171, 2015.

OpenSees Days Europe 2017
1st European Conference on OpenSees
Porto, Portugal, 19–20 June 2017

ADVANTAGES OF USING BAYESIAN INFERENCE FOR MODEL CALIBRATION IN OPENSEES

Ádám Zsarnóczay[1]

[1] Budapest University of Technology and Economics
Kmf. 85. Műegyetem rkp. 3-9. Budapest, 1111
e-mail: zsarnoczay.adam@epito.bme.hu

Keywords: Markov Chain Monte Carlo, uncertainty quantification, posterior distribution, material model, Steel4

Abstract. *Imperfect model calibration is a source of uncertainty rarely quantified in contemporary seismic performance assessment. Calibration using Bayesian inference yields models with random variables as parameters that allow direct consideration of model uncertainty. The paper presents a simple methodology based on the Markov Chain Monte Carlo approach to sample the posterior distribution of model parameters. Two modeling scenarios are presented using numerical models of buckling restrained braces as an example. The influence of empirical data on calibrated parameters and the consideration of uncertainty due to simplified model behavior are briefly discussed. The computational efficiency and flexibility of OpenSees heavily contributes to the simple implementation of the calibration methodology using one of the open-source Bayesian statistical modeling frameworks. Considering the obvious advantages of uncertainty quantification and the simplicity of its application with OpenSees, the author argues that Bayesian inference should be used more often for numerical model calibration in earthquake engineering research.*

1 INTRODUCTION

Numerical models became the primary means of solving problems in structural engineering. Models of various complexity are available for a large range of tasks in several software for numerical analysis. OpenSees is one of many software that use the finite element method (FEM) to formulate and solve structural engineering problems. It stands out with its open-source, community-driven development. That approach makes it a flexible tool that rapidly adapts to the needs of its users. The efficient control of OpenSees using Tcl code is another important feature that becomes especially useful for large-scale parametric studies. This paper presents such a study where OpenSees is controlled by an algorithm developed in Python to gain a better understanding of model uncertainty.

Model uncertainty is the component of result uncertainty caused by imperfect representation of the real behavior in a numerical environment. It might stem from insufficient or erroneous empirical data available for model calibration or a simplified model that is used to describe a complex phenomenon. Model uncertainty is rarely quantified in contemporary seismic performance assessment. Calibration is typically performed with optimization methods that minimize the error between measured, empirical data and simulated results. These methods produce one best set of parameters. Instead of finding a single optimal set of values, we can obtain more information if those parameters are considered random variables and we estimate the likelihood of all of their possible sets of values. This is achieved through Bayesian inference.

This paper briefly demonstrates that information gained through a Bayesian approach can help us answer the following questions on model calibration:

- Does the empirical data describe the investigated structural behavior with sufficient complexity to allow for calibration of every model parameter?
- How to quantify the uncertainty that stems from using a simple model to simulate a more complex behavior?

Numerical material model calibration in OpenSees is used as a vehicle to demonstrate that answering the aforementioned questions is not difficult and seeking those answers can lead to better models and more meaningful results. The numerical simulation of buckling-restrained-brace (BRB) behavior is selected as an example of a complex calibration problem. OpenSees offers several numerical materials for modeling BRB elements. An extended version of *BoucWen* [1], *SteelBRB* [2], and *Steel4* [3] are popular choices in recently published papers. *Steel4* is selected for this paper, because the author has the most experience with that model and can demonstrate the behavior of several fundamentally different materials with it.

2 METHODOLOGY

Results in this study were generated using a simple approach to present a methodology that can easily be adopted by fellow researchers. There are several areas of improvement available. More advanced methods offer improved computational efficiency, but their application provides the same kind of insight.

The objective of a Bayesian approach to model calibration is to describe the likelihood of all possible sets of model parameters ($\boldsymbol{\theta}$) that are consistent with the available empirical data ($\mathbf{X}$). The prior distribution of parameter likelihood $p(\boldsymbol{\theta})$ is available a priori; it is based on previous experience and engineering judgement. When empirical data becomes available through experiments, that new information can be used to update our knowledge about the parameters. The likelihood of the empirical data given a set of model parameters is expressed by the $p(\mathbf{X}|\boldsymbol{\theta})$ conditional distribution. Using this knowledge, the updated probability distribution function of the parameters, the so-called posterior distribution, is calculated with Bayes' Theorem:

$$\mathrm{p}(\boldsymbol{\theta}|\mathbf{X}) = \frac{\mathrm{p}(\mathbf{X}|\boldsymbol{\theta})\mathrm{p}(\boldsymbol{\theta})}{\mathrm{p}(\mathbf{X})} = \frac{\mathrm{p}(\mathbf{X}|\boldsymbol{\theta})\mathrm{p}(\boldsymbol{\theta})}{\int_{\boldsymbol{\theta}} \mathrm{p}(\boldsymbol{\theta})\mathrm{p}(\mathrm{X}|\boldsymbol{\theta})\mathrm{d}\boldsymbol{\theta}} \quad (1)$$

Although its calculation is straightforward, the posterior distribution can be very complex and computationally challenging to sample efficiently. A popular solution to this sampling problem is the application of a Markov Chain that is designed to have a stationary distribution that equals the posterior distribution [4]. After a sufficiently large number of steps, a random walk on such a Markov Chain will produce samples of the posterior distribution. This feature is exploited by the Markov Chain Monte Carlo (MCMC) methods. Markov Chains were created for this research using the Metropolis-Hastings algorithm. More advanced, gradient-based methods are also available in the literature that provide better convergence speed and sample multi-modal distributions more efficiently.

Probabilistic calculations were performed with the PyMC3 module [5] using Python code. OpenSees calculated a set of response quantities (i.e. axial force and nodal displacement) from an SDOF model that corresponds to a given set of material parameters. Those response quantities were used to determine the $\mathrm{p}(\mathbf{X}|\boldsymbol{\theta})$ distribution during every step of the random walk on the Markov Chain. The number of steps required for calibration is in the range of 5000-500000, depending on the number of calibrated parameters. Therefore, the computational efficiency of OpenSees is an important asset for the presented work. Even complex models were calibrated within one hour using a regular PC. An HPC-based approach could reduce this time significantly.

The applied methodology is not limited to material model calibration. It is applicable to the investigation of any parameter of any problem formulated in an OpenSees model. More complex models with large number of degrees of freedom will lead to longer computation times. Besides optimization of the MCMC method, there are other improvements available for such cases (e.g. response surface method) that can make a Bayesian approach feasible.

3 ANALYSES AND DISCUSSION

Material model calibration in the following discussion is performed against numerical results instead of experimental data. The true model that can generate the data used for calibration is called the reference model in the following discussion. Because the reference model is known when reference data is generated numerically, the agreement between calibrated and reference models can be investigated in several loading scenarios. The author believes that this approach provides more insight into the various forms of error and uncertainty in model calibration than a single experimental result would do. Reference results are from a numerical buckling restrained brace element model that had previously been calibrated to an experimental result (C500W-II in [6]). Measurement error is included in the reference data by adding white noise to the simulated force values.

The quality of a numerical model is evaluated through its accuracy and its precision. Accuracy refers to the closeness of the simulated value to the reference result; precision refers to the uncertainty in the simulated values. Because the reference model is not available when calibration is performed against experimental results, it is often difficult to quantify the accuracy of the calibrated model in loading scenarios that differ from the one described by empirical data. Hence, it is recommended to use several different experimental results to improve the accuracy of a numerical model. Model precision can be inferred from the posterior distribution of the calibrated parameters. The scatter of results in the desired analysis can also be directly investigated, because samples from the posterior distribution are readily available.

The questions raised in the Introduction are discussed briefly in the following paragraphs.

3.1 Quality of the empirical data

Model A in Fig. 1 shows an example scenario with low quality empirical data. Although the Steel4 material can model non-symmetric nonlinear kinematic and isotropic hardening, the available data does not provide sufficient information to identify all model parameters. Fig. 1a confirms that the response of the calibrated model is in good agreement with the reference data in spite of the large uncertainty in some of its parameters. The histograms in Fig. 1b illustrate the marginal distributions of six key model parameters based on the posterior distribution function. The red lines indicate the reference values of the parameters. On the one hand, the initial stiffness (E_0), the yield stress (f_y), and the kinematic hardening ratio (b_k) were successfully identified with sufficiently small uncertainty. On the other hand, the ratio of ultimate over yield stress limit (f_u), the saturation point for isotropic hardening (ρ_i), and the initial isotropic hardening ratio (b_i) are neither accurate, nor precise representations of their reference values. Their variance is orders of magnitude beyond the practically acceptable range.

The consequences of such large uncertainty are emphasized by Figs. 1c and 1d. The former shows the response of a large number of models sampled from the posterior distribution against the reference response under a more demanding load history. The stress-strain curves are more saturated where several samples produce identical results. Thus, more saturated points of the curves are more likely representations of the calibrated material. Fig. 1d shows a similar comparison using the strain response of SDOF models to dynamic loading. The X component of the 12012 Northridge ground motion record from the Far Field set of FEMA P695 was used as input motion. Note the scatter of maximum strain values and the even larger uncertainty in the residual strain at the second part of the ground motion.

Model B results in Fig. 2 show that a better designed experiment can provide empirical data that is sufficiently complex to calibrate the numerical model. Comparison of the histograms in Fig. 2b and Fig. 1b highlight the significant reduction in the variance of ρ_i and f_u parameters.

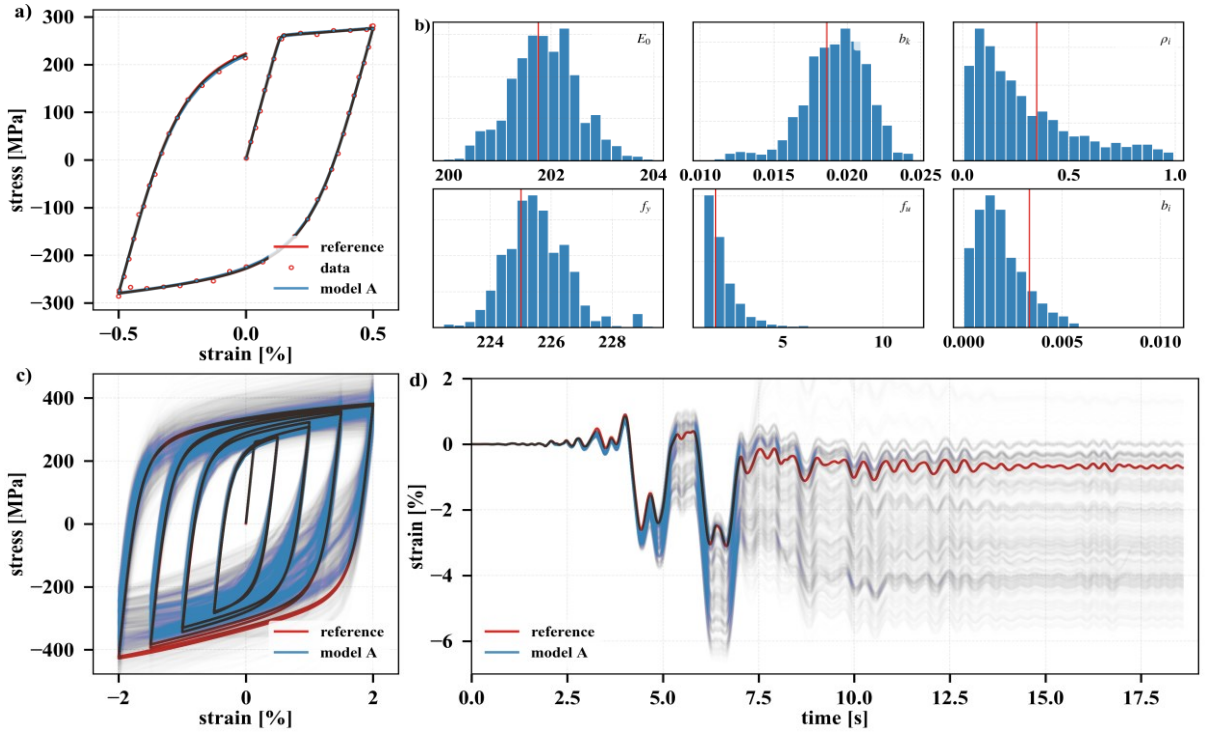

Figure 1: Calibration results for *model A*: stress-strain plots of the model against reference data (a) and a more demanding reference response (c); marginal distributions of key parameters (b); dynamic response of the reference and the calibrated model (d)

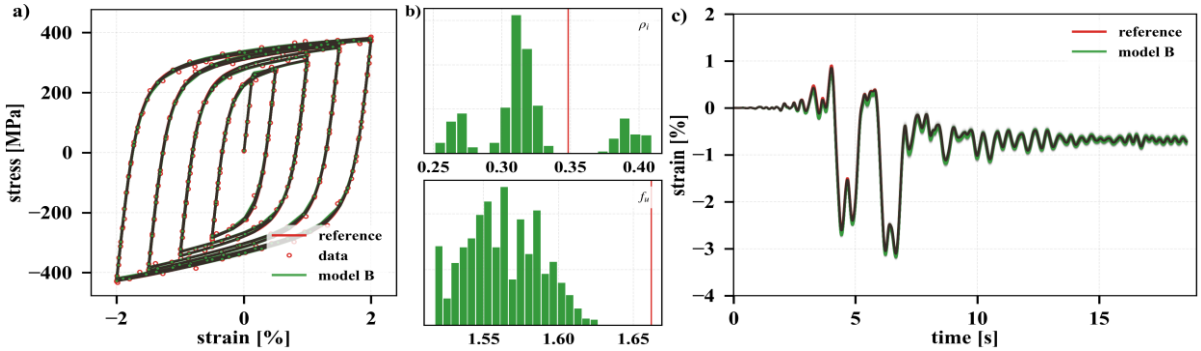

Figure 2: Calibration results for *model B*: stress-strain plots of the model against reference data (a); marginal distributions of key parameters (b); dynamic response of the reference and the calibrated model (c)

Although the calibrated parameters are not perfectly accurate, they are sufficiently close to the reference values to approximate the reference behavior with negligible error in the dynamic analysis (Fig. 2c). Note that the red reference curves in Figs. 1d and 2c are not available when calibration is performed against experimental results. The advantage of knowing the posterior distribution is that we can review the variance of each parameter and the scatter of dynamic results and quantify the precision of the model even without knowing the reference results.

3.2 Complexity of the numerical model

Properly designed experiments can provide sufficiently detailed and high quality empirical data. A more challenging problem that researchers often have to tackle is to describe complex structural behavior with a simplified material model. *Model C* illustrates this case with a material capable only of bilinear behavior through kinematic hardening. Such a simple material cannot accurately follow the nonlinear non-symmetric reference behavior with a single set of parameters. Instead, it can be calibrated to several responses that shall exhaustively demonstrate the important features of the reference behavior that we aim to simulate. Fig. 3 shows an example: besides the familiar load history in Fig. 3a, two additional load histories were used for calibration. The additional protocols contain fewer load cycles with larger displacement amplitudes. Such responses are common in BRB elements under large intensity seismic excitation. The calibrated responses drawn from the combined posterior distribution of the model cover all three sets of reference data with sufficient accuracy at the cost of reduced precision.

Histograms in Fig. 4a confirm that consideration of the three sets of reference data leads to significant uncertainty in the hardening ratio (b_k) of the material. Note that the uncertainty in the initial stiffness (E_0) is not high, because its optimal value is similar for the three load histories. Figs. 4b and 4c show that the reference dynamic analysis result is in good agreement with the numerical simulations corresponding to the posterior distribution. Fig. 4c highlights the

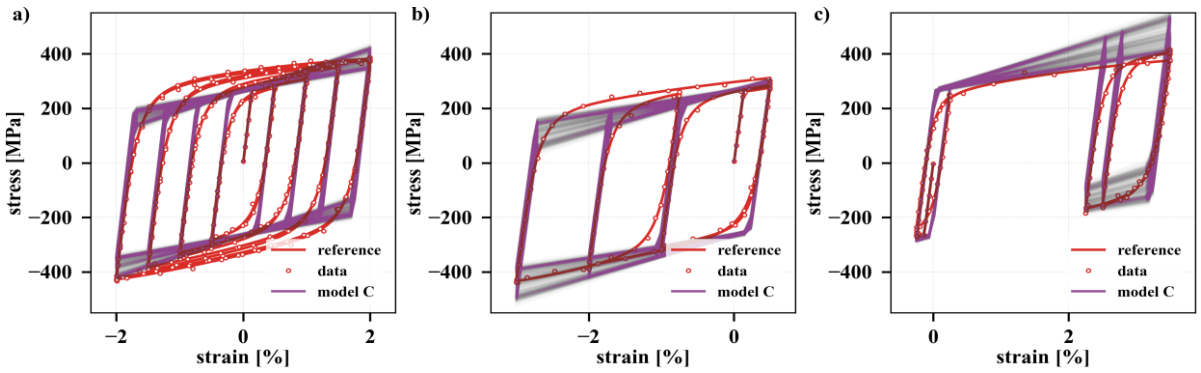

Figure 3: Calibration results for *model C*: stress-strain plots of the model against three sets of reference data

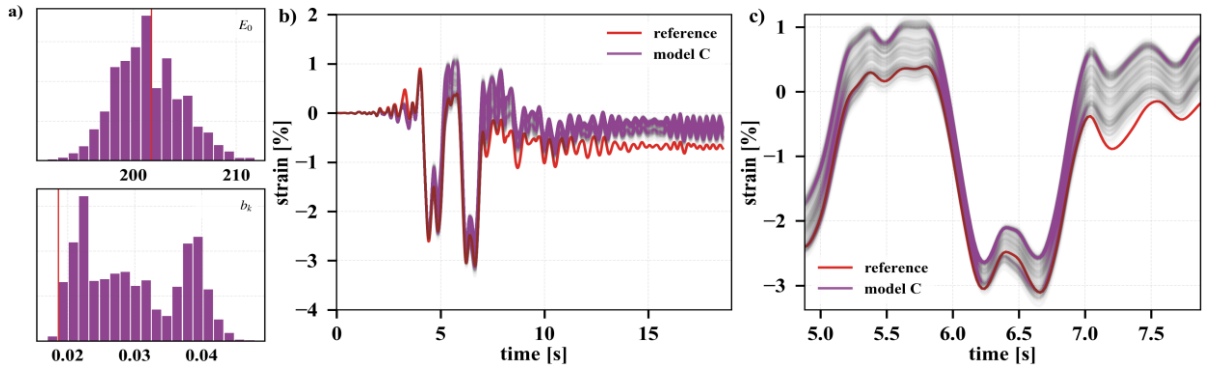

Figure 4: Calibration results for *model C* continued: marginal distributions of key parameters (a); dynamic response of the reference and calibrated model shown for the entire duration (b) and a magnified view in the neighborhood of the maximum strain (c)

accuracy and the precision of the simulated response in the neighborhood of the maximum strain during the ground motion. The simulated model can capture both the maximum and the residual strain with sufficient accuracy. The example of *model C* illustrates that a simple material model might be used to simulate complex behavior if the uncertainty due to simplification is properly considered. The desire to reduce such uncertainty shall be the primary motivation behind using a more advanced material model.

4 CONCLUDING REMARKS

This paper presented a brief overview of two scenarios where a Bayesian approach can provide advantages over conventional parameter calibration methods. Other benefits of using Bayesian inference when working with numerical models (e.g. analysis of correlated parameters, multi-modal parameter distributions, etc.) had to be omitted for brevity. Several frameworks are available for Bayesian statistics that can use external FEM environments for response evaluation. The computational efficiency and flexibility of OpenSees make it an optimal environment for such a task. Considering the obvious advantages of uncertainty quantification and the simplicity of its application with OpenSees, the author argues that Bayesian inference should be used more often for numerical model calibration in earthquake engineering research.

REFERENCES

[1] T.L. Karavasilis, S. Kerawala, E. Hale, Hysteretic model for steel energy dissipation devices and evaluation of a minimal-damage seismic design approach for steel buildings, J. Constr. Steel Res. **70**, 358–367, 2012

[2] A. Zona, A. Dall'Asta, Elastoplastic model for steel buckling-restrained braces, J. Constr. Steel Res. **68**, 118–125, 2012

[3] Á. Zsarnóczay, L.G. Vigh, Eurocode conforming design of BRBF – Part II: Design procedure evaluation, J. Constr. Steel Res. **135**, 253-264, 2017

[4] W.R. Gilks, S. Richardson, D. Spiegelhalter, *Markov Chain Monte Carlo in Practice*, Chapman and Hall/CRC, Taylor & Francis Inc., 1996

[5] J. Salvatier, T.V. Wiecki, C. Fonnesbeck, Probabilistic programming in Python using PyMC3, PeerJ Computer Science **2**, e55 https://doi.org/10.7717/peerj-cs.55, 2016

[6] Á. Zsarnóczay, *Experimental and Numerical Investigation of Buckling Restrained Braced Frames for Eurocode Conform Design Procedure Development*, Ph.D. Dissertation at Budapest University of Technology and Economics, 2013

OpenSees Days Europe 2017
1st European Conference on OpenSees
Porto, Portugal, 19–20 June 2017

RESIDUAL FIRE RESISTANCE OF STEEL FRAMES ASSESSED USING A MULTI-HAZARD ANALYSIS FRAMEWORK IN OPENSEES

Mian. Zhou[1], Liming. Jiang[2], Suwen Chen[3] and Asif.Usmani[2]

[1] Department of Mechanical, Aerospace and Civil Engineering, Brunel University, London, UK

e-mail: mian.zhou@brunel.ac.uk

[2] Department of Building Services Engineering, Hong Kong Polytechnic University, Hong Kong SAR

liming.jiang@polyu.edu.hk, asif.usmani@polyu.edu.hk,

College of Civil Engineering, Tongji University, Shanghai, China

swchen@tongji.edu.cn

Keywords: OpenSees, Multi-hazard, Cementitious passive fire protection, Fire resistance, steel frame structure

Abstract. *Damage to cementitious coatings used for passive fire protection (PFP) may result from seismic loadings. Even moderate earthquakes may pose a major hazard to the structural integrity of a steel frame with potentially severe consequences in the event of fire. The fire may occur immediately after an earthquake or after a considerable period of time has elapsed but the damage to the PFP has remained undiscovered and unrepaired. With an added heat transfer module and thermo-mechanical analysis module, OpenSees now has the capacity to perform the structural analysis for the effects of cascading seismic and fire events in a seamless fashion. This paper presents a case study of assessing the residual fire resistance of multistory steel frames following a moderate earthquake. This work showcases Opensees' capability for multiple hazard analysis, with a practical application of assessing the post-earthquake residual fire resistance of steel frames with cementitious coating as PFP.*

1 INTRODUCTION

The paper presents a case study of residual fire resistance of multistory steel frames following moderate earthquake loading, using two equivalent seismic steel frame designs: a steel moment resisting frame(SMRF); and the other steel concentrically braced frame (SCBF), based on "FEMA P-751, NEHRP Recommended Provisions: Design Examples" [1].

Cementitious fire resistant coatings are a popular PFP for steel frame buildings and are adopted for the two frames. Given these coatings are specifically designed to be lightweight and are naturally fragile, it is a reasonable concern that the fire resistance of such buildings may be compromised after a period in use, especially if this period has included one or more of moderate loading events that may locally damage or remove the coatings (such as windstorms, earthquakes). Due to its unappealing appearance, the PFP is usually covered by architectural finishes allowing little access for integrity inspection which usually is required after moderate earthquakes. Therefore desktop-based assessment using finite element tools, supported by experimental data on material damage mechanism is considered the best engineering solution to evaluate the residual fire resistance of the buildings with such PFP system.

A multi-hazard analysis framework in Opensees can be utilized to fulfill this task. The location and degree of PFP damage were assessed based on the seismic analysis results using a damage index established experimentally [2,3,4]. A 2-D cross-sectional heat transfer analysis was performed to determine the temperature development over time in the fully protected and unprotected steel members subjected to Standard Fire of the duration required by local building regulations. This was followed by a thermo-mechanical analysis to evaluate the residual fire resistance capacity of the frames. All three analyses were performed sequentially using OpenSees. The work represents a vital step towards developing an integrated simulation tool called "SiFBuilder" [5] in that it implements a multi-hazard simulation (restricted to fire following earthquakes) allowing automated multi-hazard analyses with minimal user effort and input.

2 STRUCTURAL DESCRIPTIONS & MODELLINGS

The structural models are designed for a seven-story office building in Los Angeles California [1]. The Canoga Park record of the 1994 Northridge earthquake from OpenSees library was adopted, with a ground motion reduction factor = 0.65 applied to the 0.4g Peak Ground Acceleration (PGA) to achieve the desired moderate earthquake level, which restricted structural behaviour to elastic region in this case study.

3 DAMAGE TO CEMENTITIOUS PFP

The tensile strain was selected as the damage index, with an upper bound=0.198%, a lower bound=0.135%. When the tensile strain at the interface of the structure member and coating exceeds the selected level, the PFP is deemed completely failed.

4 SEISMIC ANALYSIS AND MODELLING SENSITIVITY

Time history analysis was performed. Because the PFP damage relies on the strain results at an element level, the evaluation is sensitive to structure member's relative stiffness ratios. Sensitivity study was carried out on the SMRF with four different types of analytical models to investigate its impact on the damage estimation: 1) Central line to central line model; 2) Panel zone included model; 3) Panel Zone+ Reduced Beam Section; 4) Leaning columns.

The sensitivity study results suggested Model 1 was conservative for its underestimation of connection stiffness. The inclusion of the p-delta effect generated by the inner gravity columns using Leaning Columns showed little impact because structure essentially behaved within the

elastic range in this case. All models suggested PFP damage appear around the beam-column connections at the floors of high inner-story drift ratios, and at columns bases. The model 3 results were adopted for damage evaluation.

For SCBF, high strains were observed in braces however they do not have any bearings on the fire resistance of braced frame, hence SCBF was not included in the following analysis.

5 DAMAGE MAP & SELECT FIRE SCENARIO

A damage map of the cementitious PFP in the SMRF was therefore established. Guided by the map, the ground compartment framed by Pier 2 & 3 was selected as the fire location because bottom column failure would be the most perilous. A two hours fire defined by the Standard fire curve was selected as the fire load because a 2h fire resistance is required for structural elements of office buildings over 30m tall by BS9999:2008, Table 25[6].

Figure 1: Damage Map

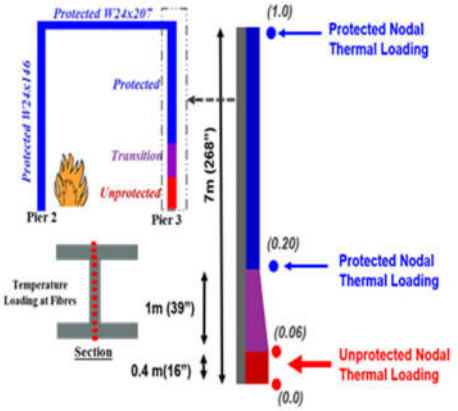

Figure 2: Heat Transfer & Thermal Loading Application

6 HEAT TRANSFER ANALYSIS

Because compartment fire assumes uniform gas temperature, a two dimensional cross section heat transfer analysis for a protected and a fire exposed cross section is sufficient to provide the temperature–time development in the members. The heat transfer analysis was performed using OpenSees heat transfer module, which provides the temperature history of the beams, recorded at each fiber throughout the cross section depth, shown in Figure.2. The thermal properties used for the Cementitious PFP are: λ=0.05W/m/K, ρ=350kg/m^3, c_p=1100J/k/kg.

7 THERMO-MECHANICAL ANALYSIS

7.1 Thermal analysis modelling

The same structural model as developed for seismic analysis was used, with necessary modifications made to facilitate thermo-mechanical analysis. Temperature-dependent steel material SteelECThermal was used which is developed based on the stress-strain curve for steel at elevated temperatures provided in Eurocode 3 [7]. Displacement based element – dispBeamColumn2dThermal was used for all structural members.

No re-segmentation is required for thermal loading application because OpenSees thermal modules offers the Thermal Action Wrapper function. As shown in Figure 2: four nodal thermal loads are applied to the column by defining the application point's position using length ratios. A mixed order interpretation will be applied automatically for the transition area.

7.2 Results

The deformed shapes of the SMRF at 4 different time points are presented in Figure 3. The evolutions of vertical reactions at column bases are plotted in Figure 4. At T=0s, the deformation is due to dead and live load. As heated up to T=1200s, Pier 3 shows clear upward expansion, dragging its connected floor beams with it, which induces uplift tension into the adjacent Piers 2&4. This phenomenon is reflected in the base reactions, where axial loads decrease in Pier 2&4 but increase in Pier 3. The Pier 3's overall stiffness still retains at this stage. At about T=1545s, substantial deformation and curvature are observed in Pier 3.This progression manifests in the base reactions as axial loads starts rising in Pier 2&4 while dropping dramatically in Pier 3. The analysis terminated at T=2300s due to large deformation in Pier 3.

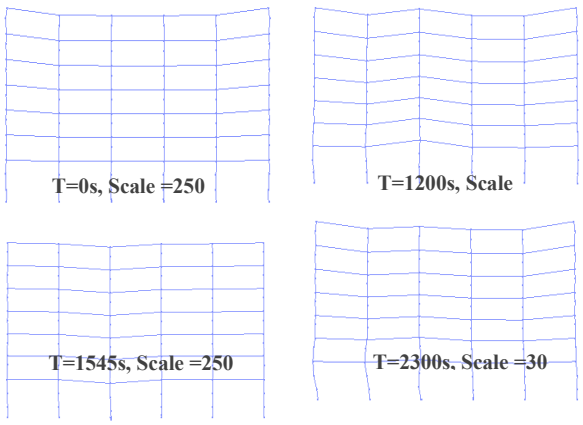

Figure 3: Deformed Shape

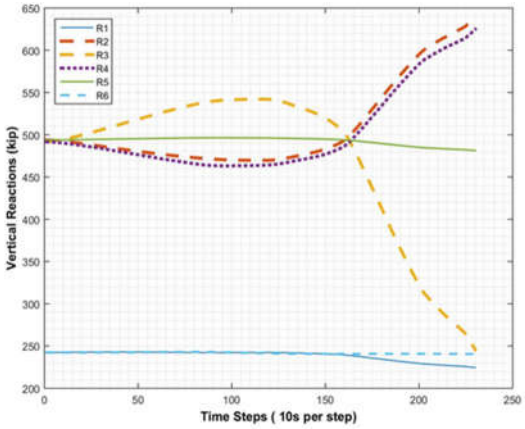

Figure 4: Vertical Base Reaction Development

8 CONCLUSIONS

The analysis results of the selected fire scenario demonstrated the post-earthquake PFP damage can cause significant structural damage in a subsequent fire, which in the worst case may lead to structural collapse due to column failure. Using its native and developed modules, OpenSees capability for simulating structural response under multi-hazards has been demonstrated.

REFERENCES

[1] National Institute of Building Sciences Council and Building Seismic Safety Council, "FEMA P-751: 2009 NEHRP Recommended Seismic Provisions: Design Examples," no. September, p. 916, 2012.

[2] S. Chen, L. Jiang, A. Usmani, G.-Q. Li, and C. Jin, "Damage mechanisms in cementitious coatings on steel members under axial loading," *Constr. Build. Mater.*, vol. 90, pp. 18–35, 2015.

[3] S. Chen, L. Jiang, and A. Usmani, G.-Q. Li ,"Damage mechanisms in cementitious coatings on steel members in bending," *Proc. ICE - Struct. Build.*, vol. 168, no. Volume 168, Issue 5, pp. 351–369(18), 2015.

[4] Y.Wang, Experimental studies on damage mechanisms in cementitious coatings on structural members under complex loadings (MSC thesis). College of Civil Engineering, Tongji University (in chinese); 2016

[5] L. Jiang, X. Dai, A. Usmani and P. Kamath, OpenSees based integrated tool for modelling structures in fire, Proc. of the 1st International Conference on Structural Safety under Fire and Blast, Glasgow, 2-4 Sept. 2015.

[6] Code of Practice for Fire Safety in the Design, Management and use of Buildings. BSI Standards BS9999:2008

[7] *Eurocode 3: Design of Steel Structures. General Rules-Structural Fire Design.* BSI Standards, BS EN 1993-1-2:2005, (2002)

OpenSees Days Europe 2017
1st European Conference on OpenSees
Porto, Portugal, 19–20 June 2017

MODELLING STRUCTUES IN FIRE USING OPENSEES - AN INTEGRATED APPROACH

Liming Jiang and Asif Usmani

Department of Building Services Engineering, The Hong Kong Polytechnic University
Hung Hom, Kowloon, Hong Kong
e-mail: liming.jiang@polyu.edu.hk, asif.usmani@polyu.edu.hk

Keywords: Structure in fire, OpenSees, computational modelling, heat transfer, integrated analysis.

Abstract. *Recent developments in modelling structural response to fires is presented, which includes our ongoing work on thermo-mechanical analysis of frames using beam-column and shell elements, a heat transfer module built in OpenSees, and the 'SIFBuilder' project providing an integrated solution to 'structures in fire' modelling. The class hierarchy has been discussed regarding the thermal action for structural members and the beam-column and shell elements, which is followed by a few examples in order to demonstrate the capabilities added. The heat transfer module is explained in detail with its class structure and the available Tcl commands, which now enable heat transfer analysis for complex fire scenarios. The 'SIFBuilder' project aiming to set up an integrated computational environment for modelling structural response to fire is discussed and demonstrated. An overview is provided of the solution strategy from fire modelling to structural response in an integrated manner and displays the great potential of OpenSees as a research tool and eventually a design tool in the field of fire safety engineering.*

1 INTRODUCTION

In a prescriptive design approach regime, the global behaviour of structures is largely ignored, since the traditional design strategy for structural fire safety was based on Standard Fire tests with respect to the performance of isolated members. Meanwhile, fire models for the design practice in compartmented buildings have been evolving from uniform fire models to non-uniform models as the use of large open-plan compartments becomes common. Moreover, new structural materials and structural sections are gradually implemented in the built environment, which improve the structural performance but also challenge existing design tools. In this context, the need has been identified for a comprehensive simulation tool, which should be able to deal with complex fire scenarios and enable researchers to undertake a range of simulations with the minimum of effort to construct their numerical models. We have chosen OpenSees as a suitable platform to provide the aforementioned capability.

The work was initiated in 2009 at Edinburgh University [1], aiming to enable the whole 'structures in fire' analysis within the "SiFBuilder" framework. As shown in Figure 1, the developed modules include a collection of fire models, a heat transfer module, thermo-mechanical codes distributed into original projects, and the SIFBuilder project to integrate the modules. Further details of the development are provided in the following section and also available on http://openseesforfire.github.io.

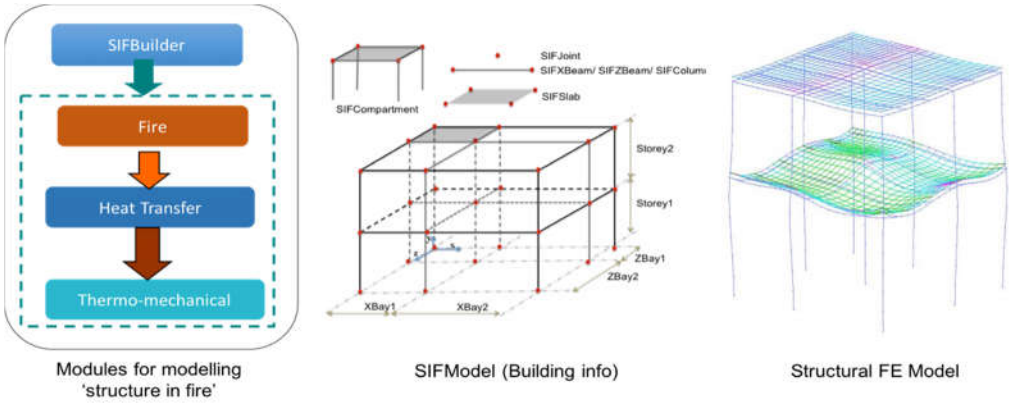

Figue 1. OpenSees development for modelling structure in fire

2 DEVELOPMENTS UNDERTAKEN FOR THERMO-MECHANICAL ANALYSIS

The capability of performing thermo-mechanical analysis within OpenSees is achieved with thermo-mechanical beam-column elements and shell elements, which receive temperature data from the corresponding type of thermal action.

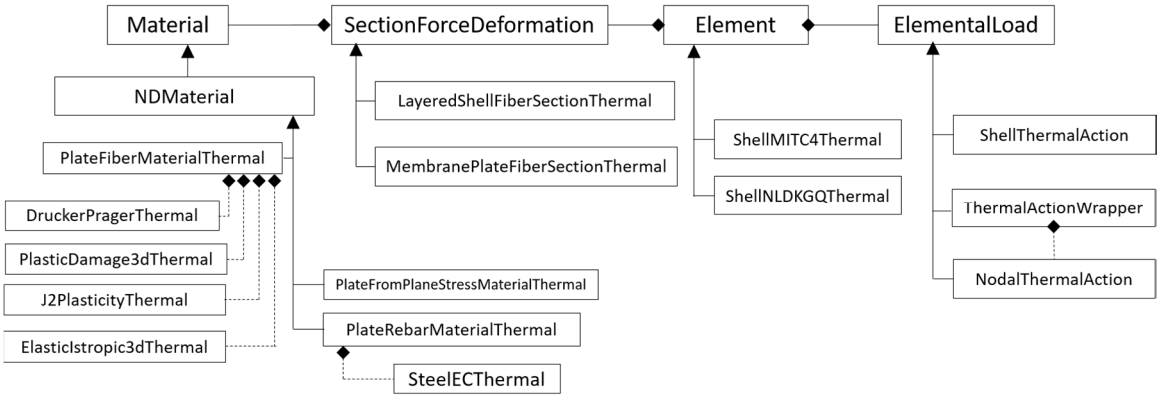

Figure 2. Classes developed for thermo-mechanical analysis using shell elements

Beam-column elements, widely used in modelling steel frames have been extended to account for the thermal loading, which requires modification to the state determination process and the ability to receive temperature data. The development of uniaxial materials and fibre based sections for thermo-mechanical analysis of frames have simultaneously been undertaken. To model reinforced concrete slabs as a part of a composite floor system in fire, thermo-mechanical shell elements can be used, which possesses a class hierarchy as shown in Figure 2. The layered solution is adapted from the code developed by Lu et al. [4] and has been enhanced to include temperature dependent effects. All the thermal action classes have been enhanced by PathTimeSeriesThermal to accept time-dependent temperature variation, and the non-uniform thermal action can be applied to both frame and shell elements.

3 DEVELOPMENTS UNDERTAKEN FOR HEAT TRANSFER ANALYSIS

A variety of well-established fire models are integrated into OpenSees, to provide its users the freedom of using different types of idealised fire scenarios, which include uniform fires in terms of gas temperature distribution such as standard fire (ISO-834), hydro-carbon fire and parametric fire. Compared to uniform fire models, more advanced non-uniform fire models are also included which address the spatial non-uniformity caused by the localised fire [2] or travelling fire [3]. The major part of the C++ code for heat transfer analysis was written by Y.Q. Jiang during his PhD study in Edinburgh University. Further developments were then carried out by the author to implement non-uniform fire models and SIFBuilder tool and providing Tcl commands for users which is facilitated by a mesh package.

The heat transfer classes were written following the basic OpenSees architecture, which uses a HeatTransferDomain to store all the HeatTransferNodes and HeatTransferElements, as well as the HeatFluxBCs to define the heat loss of a structural member to the ambient environment and the heat input resulting from the fire exposure. When defining a heat transfer analysis explicitly with Tcl commands, a meshing tool is employed to define heat transfer entities, fire models, and all the operations upon it. The heat transfer codes can also be implicitly called by the SIFBuilder tool to provide thermal action definition for structural analysis.

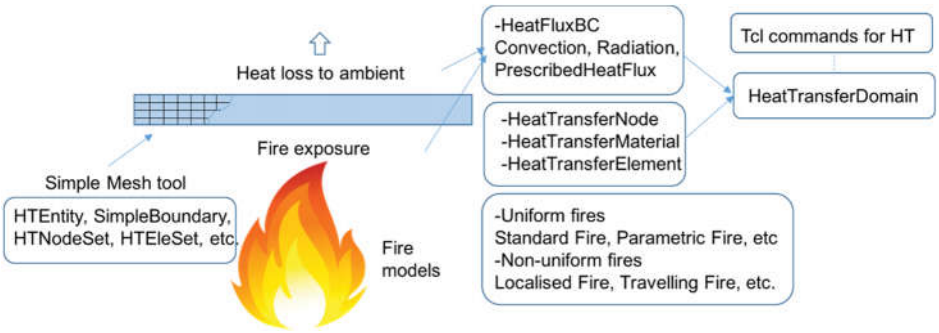

Figure 3. Development for heat transfer analysis in OpenSees

4 DEVELOPMENTS UNDERTAKEN FOR INTEGRATED MODELLING

SIFBuilder can enable analysts to obtain the structural response automatically with the application of the fire load on the structure in the same manner as any other form of load and so provide a performance- based structural fire engineering tool. A script based user input capability based on Tcl provides considerable flexibility and scope due to its programmable nature. Procedural scripts are written to specify geometry, materials, loads, heat transfer parameters, fire type, analysis procedures, solution algorithm and output requirements using Tcl commands. A SIFModel is first created to store the building information, for which the typical

user input script includes: (1) model type definition (2D or 3D); (2) geometry of the structure; (3) cross section and its embedded materials; (4) boundary conditions; (5) structural and fire loadings; (6) mesh control parameters; and (7) output request supported by SIFRecorders. A typical input may be defined as shown in Figure 4. The SIFBuilder tool relies on SIFModel to hold building information in order to sequentially perform analyses for mechanical loads and fire load, which call the heat transfer module to estimate the temperature profile at each step, and automatically define thermal action for the structural finite elements. An example showing a 2×2×2 frame (as plotted in Figure 1) subjected to uniform and non-uniform fires is presented to demonstrate the capability of SIFBuilder.

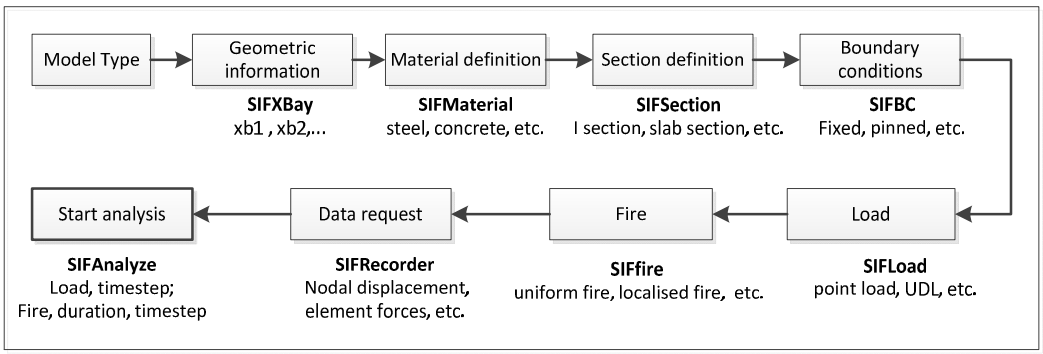

Figure 4. Input sequence for SiFModel

5 CONTINUING WORK

The refinement of SIFBuilder and the addition of new features to it are still ongoing. Hybrid simulation techniques are also being explored with OpenSees and OpenFresco to enable more in-depth simulations of structural response to fires.

6 CONCLUSIONS

- Developments of modelling 'structure in fire' are presented, which include the thermo-mechanical components, the heat transfer module and the integrated tool SIFBuilder .
- Heat transfer analysis can now be performed in OpenSees for various uniform and non-uniform design fire scenarios. Beam-column and shell elements are now available for modelling composite structures in fire. SIFBuilder as an integrated tool facilitates users to model structures in fire with minimal input and enables flexible extension for researchers.

REFERENCES

[1] A. Usmani, J. Zhang, J. Jiang, Y. Jiang, and I. May, Using Opensees for Structures in Fire, *Journal of Structural Fire Engineering.*, **3**(1), 57–70, 2012.

[2] CEN, EN 1991-1-2:2002: Eurocode1: Actions on Structures. General actions-actions on structures exposed to fire, London, UK.

[3] J. Stern-Gottfried and G. Rein, Travelling fires for structural design-Part II: Design methodology, *Fire Safety Journal*, **54**, 96–112, 2012.

[4] X. Lu, L. Xie, H. Guan, Y. Huang, and X. Lu, A shear wall element for nonlinear seismic analysis of super-tall buildings using OpenSees, *Finite Elements in Analysis and Design*, **98**, 14–25, 2015.

OpenSees Days Europe 2017
1st European Conference on OpenSees
Porto, Portugal, 19–20 June 2017

IMPLEMENTATION OF FIRE MODELS IN OPENSEES

Xu Dai[1], Yaqiang Jiang[2], Liming Jiang[3], Stephen Welch[1], and Asif S. Usmani[3]

[1] BRE Centre for Fire Safety Engineering, the University of Edinburgh, UK
emails: x.dai@ed.ac.uk, s.welch@ed.ac.uk

[2] Sichuan Fire Research Institute, Ministry of Public Security, Chengdu, P. R. China
email: yaqiang.jiang@foxmail.com

[2] Department of Building Services Engineering, Hong Kong Polytechnic University, Hong Kong
emails: liming.jiang@polyu.edu.hk, asif.usmani@polyu.edu.hk

Keywords: Structures in Fire, Compartment fires, Realistic Fire Loading, Performance-based Design, OpenSees, Software Architecture.

Abstract. *In the modern routine design of structures, computational modelling of the structural behaviour under natural and man-made hazards has become more and more important. The capabilities of analysing the structural performance under such hazards (e.g. snow, wind, earthquake, impact) have been widely utilized into the mainstream of nonlinear finite element method (NFEM) based software, such as SAP, ANSYS, ABAQUS etc. However, there are very limited software options to characterize fire impact on structures. In general, there are two types of computer programs for simulating structural behaviours in fire: research-oriented and business-oriented. The former such as SAFIR, VULCAN, and ADAPTIC address specific modelling problems, because of a limited number of users and a small team of developers. The latter such as ABAQUS, ANSYS and LS-DYNA are used commercially by researchers and industry across the world. Nevertheless, limited access to source codes, lack of transparency of the computational framework, high cost of purchase and maintenance are major limitations.*

In 2009, OpenSees was adopted at the University of Edinburgh for further development to enable it to perform structural fire analysis. Facilitated by its open-source nature, a large number of thermal capabilities have been added to the framework by Usmani et al. [1]. Significant contributions in terms of heat transfer and fire modules have been made to the framework in developing the 'Thermal' version of OpenSees [2]. After verifying and validating the thermo-mechanical analysis of OpenSees [3], [4], users are able to model structures under extreme thermal actions (such as those resulting from fire conditions) through defining arbitrary non-uniform temperature distributions across and along an element. This paper reviews the existing fire modules in OpenSees, including uniform compartment fire models and localised fire models. The latest development of advanced fire modules, i.e. smoke zone models and travelling fire models are introduced. Finally, a case study using the FIRM zone model in OpenSees is investigated, for validating its results against the original FIRM-QB software package [5], and further exploring the thermal impact from different fire scenarios using OpenSees.

1 A REVIEW OF EXISTING FIRE MODELS IN OPENSEES

Conventional structural fire design codes are based on isolated single structural members with simply-supported boundary conditions under standard fire test exposures, which refers to a heating curve such as ISO-834 standard fire, or ASTM-E119 fire. The standard fire curve along with external fire curve, and hydrocarbon fire curve are categorized as nominal fire curves in Eurocode [6]. This type of fire curve is basically a time-temperature relationship, which stands for the case of a fully developed fire in a compartment (see Fig. 1(a)). All the above-mentioned fire curves are added in the OpenSees fire module as *NominalFireEC1* class [2]. Different from the nominal fire curves, the parametric fire curves [6] which consider fire growth rate, fire load density, and characteristics of the compartment (e.g. thermal boundaries, openings, geometric quantities, etc.) are also added in OpenSees as *ParametricFireEC1* class [2].

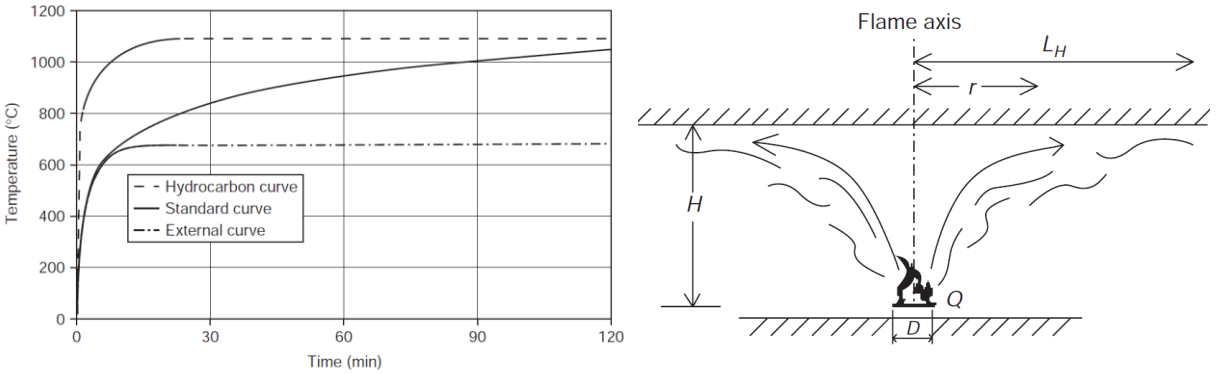

Figure 1(a): Three different nominal fire curves in Eurocode; Figure 1(b): Localised fire model in Eurocode. [7]

Although these fire models are relatively simple, they are still widely used for both research and design purposes in fire safety engineering. A user defined fire curve (*UserDefinedFire* class) [2] is also included in the OpenSees fire module for providing more flexibility. These idealised uniform fire models are all assumed to have the same temperature distribution in the entire compartment at a specific time.

Further, in the case of isolated fuels burning in a large space (e.g. vehicles burning in a car park), localised fire models are regarded to be appropriate for simulating such burning scenarios. The Hasemi localised fire model (adopted in the Eurocode [6], see Fig. 1(b)), Alpert ceiling jet model [8], SFPE handbook-based localised fire model [9], and a user defined idealised local fire model, are added in OpenSees fire module as *LocalizedFireEC1* class, *AlpertCeilingJetModel* class, *LocalizedFireSFPE* class, *Idealised_Local_Fire* class respectively [2], [10]. These localised fire models, in their mathematical nature, are all correlational equations between incidental heat fluxes on the structural surfaces and radial distance from the fire source.

2 ZONE MODELS AND TRAVELLING FIRE MODELS IN OPENSEES

In a prescriptive structural fire design code, the fire exposure is usually constrained by the code with limited room for discussion (e.g. nominal fire curves in Eurocode). In a performance-based structural fire design code, the practitioners have greater flexibility and the fire is usually related to realistic fire loadings (e.g. localised fire models, zone models, and travelling fire models, etc.). The newly added two zone model classes, *ZoneModel_ASET*, *ZoneModel_FIRM*, enable the fire module in OpenSees to simulate the transient generation of a hot smoke layer upon the compartment ceiling. The transient height and temperature of the smoke layer are calculated according to a set of ordinary differential equations (ODEs) based on the mass and energy conservations (see Fig. 2(a)) [5].

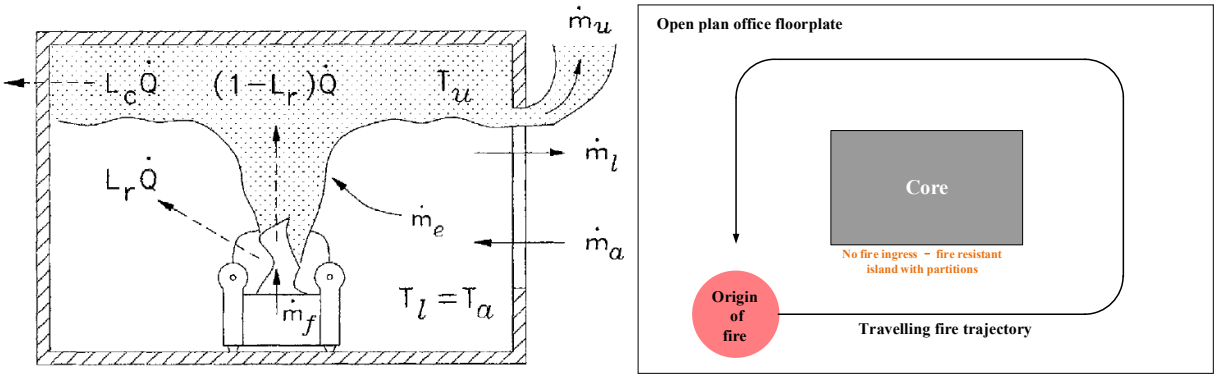

Figure 2(a): Fire problem modelled using FIRM zone model [5]; Figure 2(b): Plan view – extended travelling fire method framework.

The difference between *ZoneModel_ASET* and *ZoneModel_FIRM* is that, *ZoneModel_FIRM* can handle the compartment with vertical natural ventilations, however *ZoneModel_ASET* is basically filling the smoke in a 'box' without considering any significant openings.

More recently, a very active research frontier on performance-based structural fire design named 'travelling fires', is evolving [11]. This type of fire scenario is developed for characterising large compartment fires, which may burn locally and tend to move across entire floor plates over a period of time. An extended travelling fire method (ETFM) framework was developed by Dai et al. [12], and further implemented into OpenSees fire module [13]. This ETFM framework is based on a mobile version of Hasemi's localized fire model combined with a simple smoke layer calculation – the FIRM zone model. The *ETFM_TravellingFire* class is added to the OpenSees fire module to calculate the spatially and temporally non-uniform heat fluxes for different structural elements, produced from the 'summation' of the heat fluxes from the FIRM zone model and Hasemi localised fire model. *TravellingFireFuel* class is included to account for the uniformly distributed meshed fuel cells, and *TravellingFireFuel_Iter* class is introduced for looping over all the meshed fuel cells (i.e. *TravellingFireFuel*) to check if the fuel is currently on fire, or not, at each time step, then aggregating them as the entire burning fuel area.

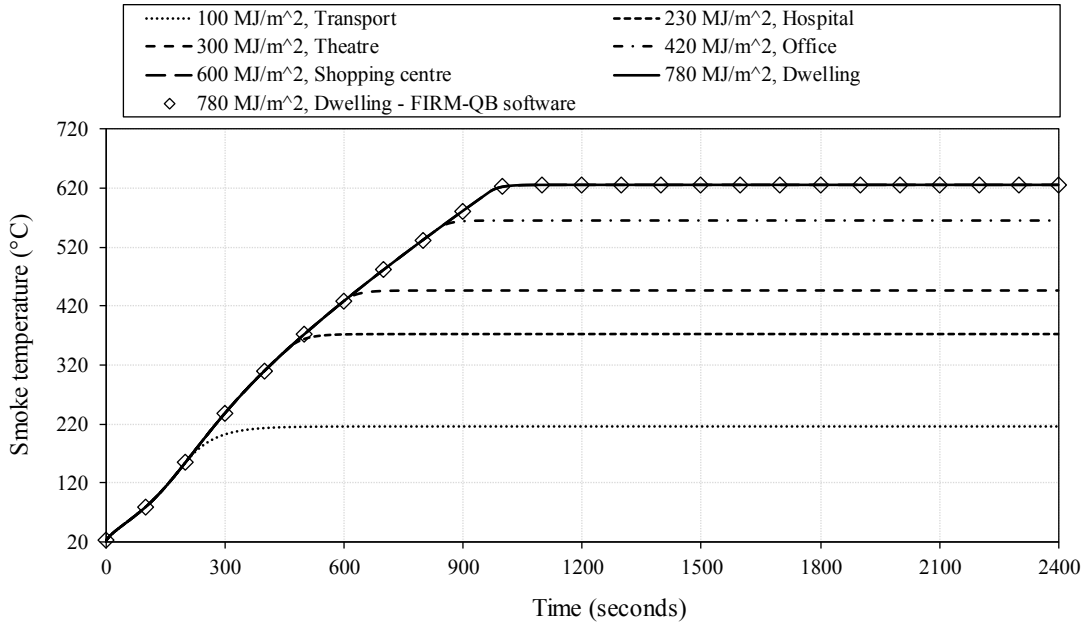

Figure 3: Smoke temperature evolution with various fuel load densities

3 A CASE STUDY USING FIRM ZONE MODEL IN OPENSEES

To validate the results produced from the OpenSees FIRM zone model against the original FIRM-QB software package due to Janssens [5], and to further explore the thermal impact from different fire scenarios, a case study is performed. The investigated compartment floor area is 468m^2, with the clear floor height 3.85m. The total vent widths of this large compartment are 28m. The soffit height and sill height are 3m and 1m respectively. A 'base line scenario' of the fires is assumed with fuel load density ($q_{f,k}$) 570 MJ/m^2, heat release rate per unit area (RHR_f) 500 KW/m^2, and fire spread rate (v) 10 mm/s. Different fire scenarios are generated with changing $q_{f,k}$, (100-780MJ/m^2) but keeping the other two values as constants. Figure 3 shows that the results generated from OpenSees agree well with FIRM-QB software, and illustrates the smoke temperature evolution with various fuel load densities according to Eurocode 1 [6].

4 REFERENCES

[1] A. Usmani, J. Zhang, J. Jiang, Y. Jiang, and I. May, Using OpenSees for structures in fire, *J. Struct. Fire Eng.*, vol. 3, no. 1, pp. 55–70, 2012.

[2] Y. Jiang, Development and application of a thermal analysis framework in OpenSees for structures in fire, PhD Thesis, The University of Edinburgh, 2012.

[3] J. Jiang and A. Usmani, Modeling of steel frame structures in fire using OpenSees, *Comput. Struct.*, vol. 118, pp. 90–99, 2013.

[4] J. Jiang *et al.*, OpenSees software architecture for the analysis of structures in fire, *J. Comput. Civ. Eng.*, vol. 29, no. 1, 2015.

[5] M. L. Janssens, *An Introduction to Mathematical Fire Modeling*, CRC Press, 2000.

[6] Eurocode1: Actions on Structures - Part 1-2: General Actions - Actions on Structures Exposed to Fire. European Standard EN 1991-1-2, CEN, Brussels, 2002.

[7] J. Franssen, V. Kodur, and R. Zaharia, *Designing Steel Structures for Fire Safety*. CRC Press, 2009.

[8] R. L. Alpert, Calculation of response time of ceiling-mounted fire detectors, *Fire Technol.*, vol. 8, no. 3, pp. 181–195, 1972.

[9] B. Y. Lattimer, Heat fluxes from fires to surfaces, in *SFPE Handbook of Fire Protection Engineering*, Third Edit., National Fire Protection Association, 2002.

[10] L. Jiang, Development of an integrated computational tool for modelling structural frames in fire considering local effects, PhD ThesisThe University of Edinburgh, 2016.

[11] X. Dai, S. Welch, and A. Usmani, A critical review of 'travelling fire' scenarios for performance-based structural engineering, *Fire Saf. J.*, no. SI:IAFSS 12th Symposium, 2017.

[12] X. Dai, L. Jiang, J. Maclean, S. Welch, and A. Usmani, A conceptual framework for a design travelling fire for large compartments with fire resistant islands, in *Proceedings of the 14th International Interflam Conference*, 2016, pp. 1039–1050.

[13] X. Dai, L. Jiang, J. Maclean, S. Welch, and A. Usmani, Implementation of a new design travelling fire model for global structural analysis, in *the 9th International Conference on Structures in Fire*, 2016, pp. 959–966.

OpenSees Days Europe 2017
1st European Conference on OpenSees
Porto, Portugal, 19–20 June 2017

TIMBER SHEAR WALLS: NUMERICAL ASSESSMENT OF DAMPING OF SHEATHING-TO-FRAMING CONNECTIONS

G. Di Gangi [1], C. Demartino [3], G. Monti [2,3]

[1] Department of Structural and Geotechnical Engineering,
Sapienza University of Rome, Via Antonio Gramsci, 53, Italy
e-mail: giorgia.digangi@uniroma1.it

[2] Department of Structural and Geotechnical Engineering,
Sapienza University of Rome, Via Antonio Gramsci, 53, Italy
e-mail: giorgio.monti@uniroma1.it

[3] College of Civil Engineering,
Nanjing Tech University, Nanjing 211816, PR China
e-mail: cristoforo.demartino@me.com

Keywords: timber shear walls; sheathing-to-framing connections; plastic behavior of connections; energy dissipation of connections; axial contribution of hold-down devices.

Abstract

The performances related to connections used in timber shear walls are investigated in this paper. Analytical and numerical models developed in the literature have shown that the crucial aspects affecting the overall behavior of shear walls are the connections between timber frame (studs and horizontal joists) and sheathing panel, as well as the base connections. Nonlinear static analysis and cyclic analysis on a parametric numerical model are performed, particularly assessing the energy dissipation ensured by the sheathing-to-framing connections.

1 INTRODUCTION

Timber light-framed constructions are mostly used in North America, New Zealand and Europe. Especially in North America, most housing and commercial structures used wood as main structural material till the 20th century. Historically, for buildings, two types of light-frame have been used: *(i)* balloon and *(ii)* platform framing [1].

In this work, the second type is deeply investigated. Platform framing buildings have discontinuous vertical framing members (studs) connected using plates that support floor joists for each storey, with a shear wall underneath. The dimensions of the frame, usually, are based on the size of the sheathing panel, which is made by different materials like OSB (Oriented Strand Board), plywood, gypsum, GLG (Glued Laminated Guadua) bamboo [2], fiber board and so on. The experimental tests demonstrated that the structural behavior of the shear wall

is mainly influenced by the connections, such as sheathing-to-framing, base and stud-joist joints. Metal fasteners (e.g., nails, screws or staples) are used to connect the timber frame with the sheathing panel, subjected to in-plane shear force. The uplift of the shear wall, due to its rigid rotation, is controlled by hold-downs, while its rigid translation by angle-brackets [3][4].

2 STATE OF ART AND CODE FRAMEWORK

The racking capacity of a shear wall is evaluated when it is subjected to a horizontal force applied at the top. An extensive overview of past research is provided by van De Lindt [5] and Kirkham et al. [6]. An elastic model of a fully anchored shear wall unit was proposed by Källsner and Girhammar [7] to describe its behavior under racking loads (Figure 1, a). Moreover, they proposed also a generalized and extended method for determining the upper and lower bounds of the plastic load-carrying capacity of shear wall [8], providing a simple graphical method to determine the center of rotations of all fasteners belonging to the different edges of the wall (Figure 1, b).

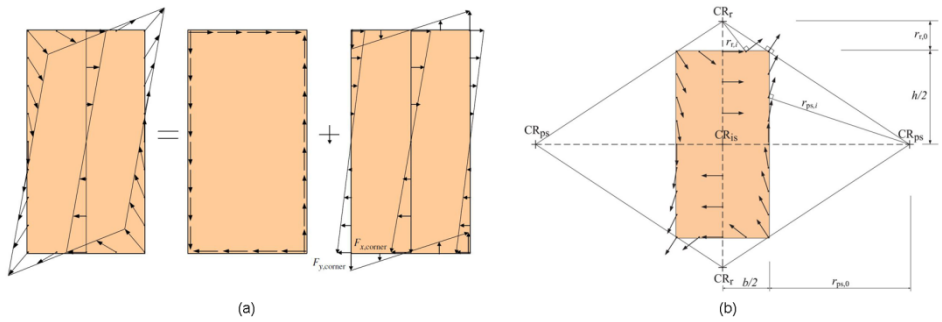

Figure 1 Distribution of the force on the sheet according to: (a) the linear elastic model proposed by Källsner and Girhammar (2009); (b) the plastic upper bound method used in Källsner and Girhammar (2009).

A similar approach, based on the static theorem, is used in the European Standard EN 1995 (Eurocode 5 [9], *§ 9.2.4.2*), where the design load-carrying capacity $F_{v,Rd}$ that represents the design racking resistance, under a horizontal force $F_{v,Ed}$ acting at the top of the cantilevered panel, is determined following a simplified method. The sum of the design racking load-carrying capacity of the different wall panels that make up the wall is considered, assuming a distribution of pure shear flow along the perimeter of the frame and the sheathing panel.

Casagrande et al. (2016) developed a simplified numerical model, called UNITN, to provide a simplified tool to evaluate the elastic response of light timber frame and cross laminated timber shear walls [4]. Starting from the analytical developments of Källsner et al. (2009), they defined the horizontal displacement of a light timber frame wall subjected to a horizontal force as a sum of different contributions and sources, as follows:

$$\Delta = \Delta_{sh} + \Delta_h + \Delta_a + \Delta_p \tag{1}$$

where Δ_{sh} is the contribution given by sheathing-to-framing connections, Δ_h is due to the rigid-body rotation of the shear wall, Δ_a is due to the rigid-body translation and Δ_p is due to the shear deformation of the sheathing-panel. In Gattesco et al. (2016), experimental tests of different configurations of shear walls were performed, to validate their proposed numerical model [10]. The specimen, identified as PLS8, was used as reference to implement the model in OpenSees, taking into account the experimental results of the nailed connections.

3 MODELING OF TIMBER SHEAR WALL

A parametric numerical model, to assess the energy dissipation of sheathing-to-framing connections, was implemented in OpenSees. Thanks to this model, a comparison among the results obtained by different experimental tests already performed in literature, was possible.

3.1 Mechanical model

In the numerical model, the input parameters are length and height of the wall and number of nails (or their spacing), as well as the number of vertical studs.

Once these parameters are assigned, the number of elements (beam, shell, zero-length) used to define the shear wall are automatically updated, allowing a quick assessment of the wall response under the applied horizontal force. In this numerical simulation, the frame elements were modelled using elasticBeamColumn elements. The input data of experimental set up in Gattesco et al. (2016), for the specimen called PLS8, were used. The sheathing panel is represented by stiff plane stress elements (shell), with mesh size varying with the number of nails. The perimeter nodes of the shell are connected by zero-length elements to the nodes of the frame. The bottom nodes at the corners have two different boundary conditions: *(i)* constrained at the base, simulating a rigid connection with the foundation; *(ii)* connected with nodes at ground by zero-length elements, to simulate the presence of hold-downs. The tag of nodes starts with a number that identifies the layer they belong to. Layer number 2 includes the fictitious nodes used to insert internal releases between the end of vertical studs and the horizontal joists elements. This is in agreement with the model proposed by Källsner and Girhammar [7]. Layer number 4 includes the perimeter nodes belonging to the frame, while layer 6 includes nodes belonging to the shell and tag of shell elements. Finally, layer 8 includes the nodes linked to the zero-length elements that represent the hold-downs devices (Figure 2).

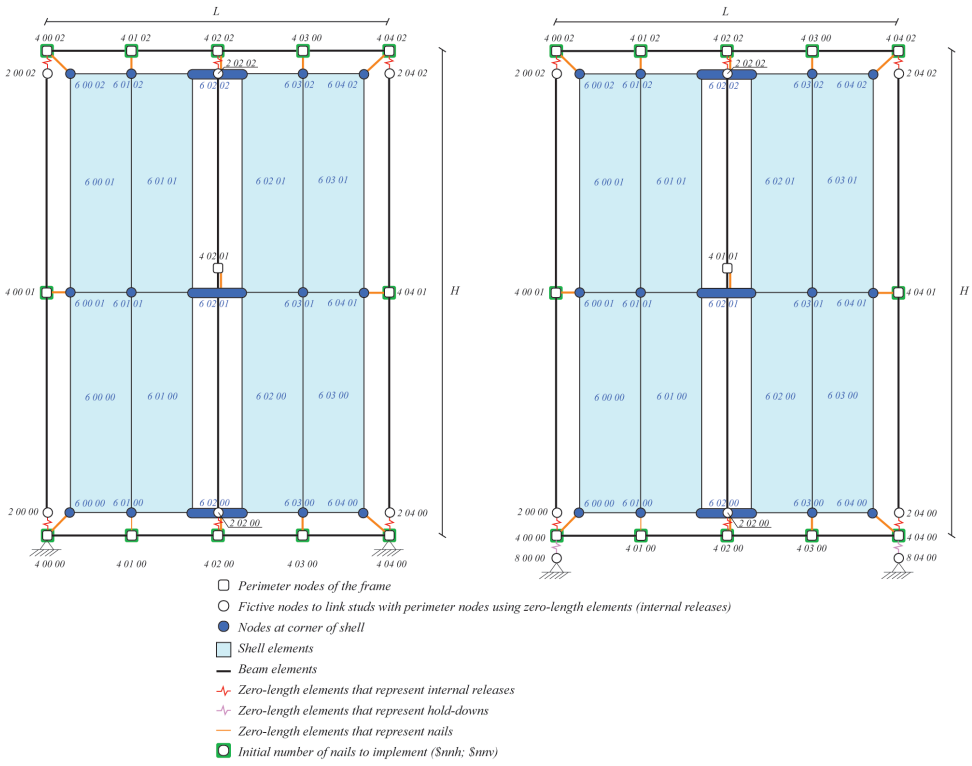

Figure 2 A scheme of the numerical model implemented in OpenSees. On the left, the model without hold-downs; on the right, the model with hold-downs. In this example, L is 1900 mm and H is 2600 mm.

The sheathing-to-framing connections are modelled with non-linear springs, using as constitutive law the SAWS mechanical model developed by Folz and Filiatrault [11]. The calibration of the SAWS parameters is shown in Figure 3.

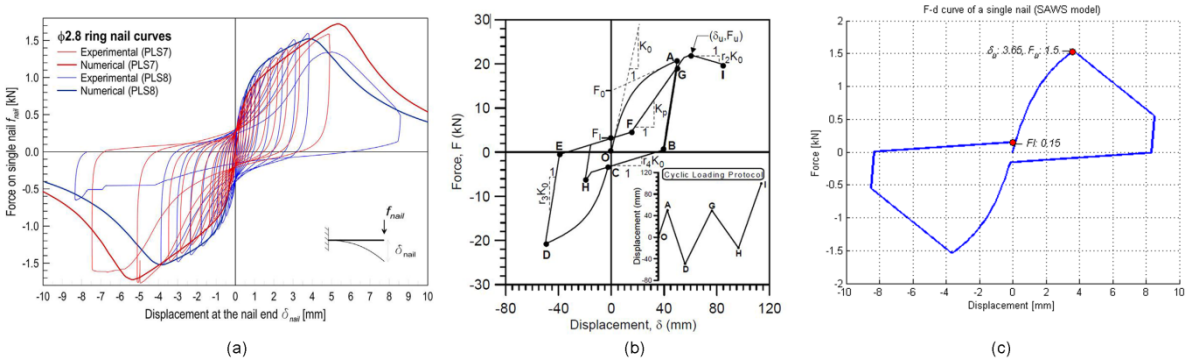

Figure 3 Sheathing-to-framing connections: (a) non-linear behavior of the Φ 2.8 ring nail - comparison between experimental and numerical results (in Gattesco et al. 2016);
(b) the hysteretic mechanical model developed by Filiatrault et al. (2001);
(c) calibration of SAWS parameters for the mechanical model of one nail.

A cyclic load in displacement control was used for the analysis, to evaluate the energy dissipation offered by all nails, taking into account the relative displacement of nodes between shell and frame. Furthermore, a parametric pushover analysis was carried out to assess the different responses of the wall, changing the number of nails.

4 RESULTS AND COMPARISON WITH LITERATURE

Starting from the equation of Equivalent Viscous Damping ratio proposed by Clough and Penzien (1993):

$$\zeta_{eqh} = \frac{E_D}{2\pi \cdot k_{eq} \cdot \Delta_a{}^2} \tag{2}$$

(where E_D is the energy dissipated per cycle, k_{eq} is the overall equivalent secant lateral stiffness, Δ_a the assigned displacement amplitude and Δ_b the building drift in percent), Filiatrault et al. (2003) [12] proposed, in turn, the following range of equivalent viscous damping ratio:

$$\zeta_{eqh} = \begin{Bmatrix} 0.5\Delta_b & 0 \le \Delta_b < 0.36\% \\ 0.18 & 0.36\% \le \Delta_b \end{Bmatrix} \tag{3}$$

correlating its value with an output parameter, Δ_b , related to results of pushover analyses carried out on 24 different building configurations.

Moreover, they proposed another range, considering a nominal damping ratio, ζ_0 , that takes into account the energy dissipation characteristic of other structural and non-structural elements:

$$\zeta_{eq} = \begin{Bmatrix} 0.5\Delta_b + 0.02 & 0 \le \Delta_b < 0.36\% \\ 0.20 & 0.36\% \le \Delta_b \end{Bmatrix} \tag{4}$$

The racking capacity evaluated using the numerical model in OpenSees, slightly underestimates the one obtained in experimental tests performed by Gattesco et al. (2016).

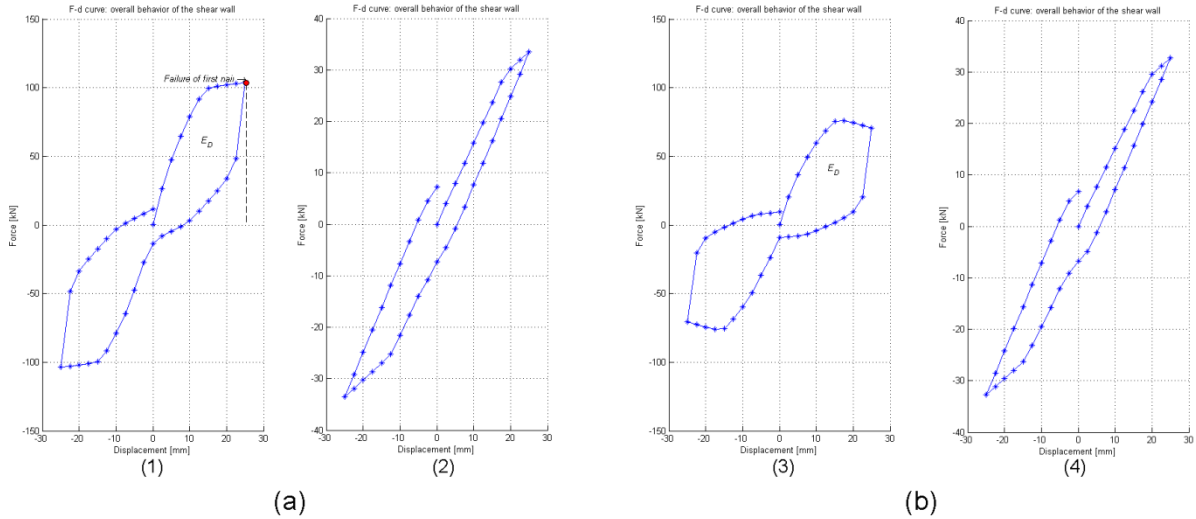

Figure 4 A comparison of the Force-Displacement curves, related to the overall behavior of the timber shear wall: (a) without internal releases; (b) with internal releases; (1,3) without hold-downs; (2,4) with hold-downs.

The value of Equivalent Viscous Damping ratio, considering the absence of hold-downs, is in line with ranges proposed by Filiatrault et al. (2003), but it is worth noting that the overall behavior of the timber shear wall is substantially influenced by the presence of internal releases between the ends of the studs and the horizontal joists, as shown in Figure 4.

Moreover, also the configuration assumed by the loading path of the nails is different (Figure 5), and in correspondence of the most stressed fasteners, placed at the corners, the value of the force is around 2 kN.

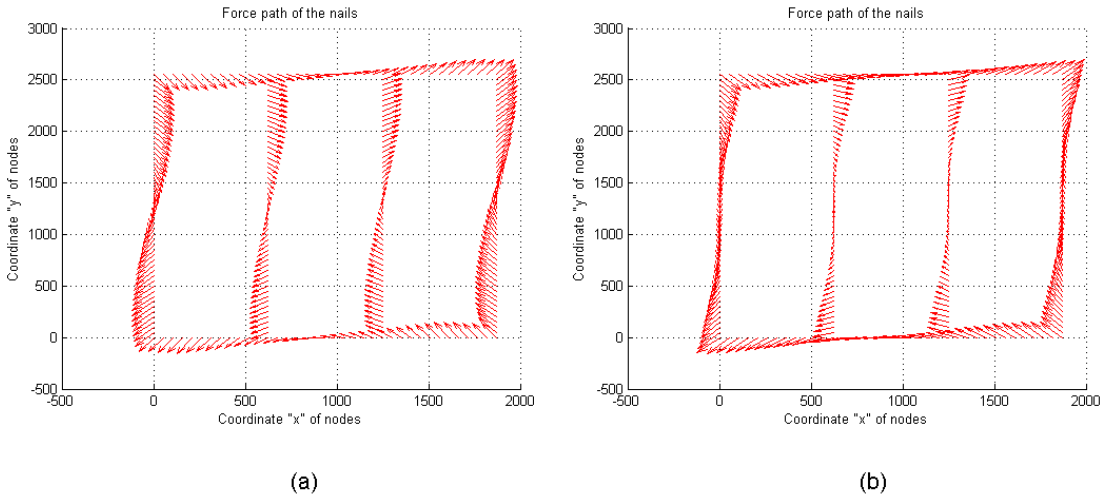

Figure 5 The configuration of the loading path of the nails: (a) considering the model without internal releases; (b) considering the presence of internal releases.

Considering the presence of the hold-downs, the loading path has, in both cases, the same configuration but the value of the force on the fasteners placed at corners is around 1 kN.

5 CONCLUSIONS AND FUTURE DEVELOPMENT

Starting from the assessment of the behavior of the sheathing-to-framing connections, using the parametric numerical model implemented in OpenSees, it was highlighted that the presence of internal releases between the framing elements sensibly affects the overall re-

sponse of the wall in terms of racking capacity and stiffness. The presence of hold-downs at bottom corners also makes the system more flexible, allowing reaching higher values of displacement of the wall, under the applied horizontal force.

The main goal of this work is to correlate the value of the Equivalent Viscous Damping ratio with the input parameters related to the shear wall, using the capacity-design strategy: to avoid failure of sheathing-to-framing connections, which are difficult to replace after an earthquake, by concentrating the energy dissipation on the hold-downs devices.

Moreover, different models considering either the presence of openings, or more than one shear wall per one storey, or more than one storey, will be developed. In this way, a q-factor will be defined for this type of structures, thus obtaining the related design response spectrum.

REFERENCES

[1] J. Wacker, *Use of wood in buildings and bridges*, in Wood Handbook – Wood as an Engineering Material, chapt. 17. Forest Products Laboratory – United States Department of Agriculture Forest Service – Madison, Wisconsin, 2010.

[2] S. Varela, J. Correal, L. Yamin, F. Ramirez, *Cyclic Performance of Glued Laminated Guadua Bamboo-Sheated Shear Walls*, Journal of Structural Engineering, Vol. 139, No. 11, 2028-2037, November 1, 2013.

[3] T. Sartori, R. Tomasi, *Experimental investigation on Sheathing-to-framing connections in wood shear walls*, Engineering Structures 56, 2197-2205, 2013.

[4] D. Casagrande, S. Rossi, T. Sartori, R. Tomasi, *Proposal of an analytical procedure and a simplified numerical model for elastic response of single-storey timber shear-walls,* Construction and Building Materials 102, 1101-1112, 2016.

[5] J. W., van de Lindt, *Evolution of Wood Shear Wall Testing, Modeling, and Reliability Analysis: Bibliography*, in Practice Periodical on Structural Design and Construction, 9, 44-53, 2004.

[6] W. J. Kirkham, R. Gupta, T. H. Miller, *State of the Art: Seismic Behavior of Wood-Frame Residential Structures*, in Journal of Structural Engineering, 2013.

[7] B. Källsner, U. A. Girhammar, *Analysis of fully anchored light-frame timber shear walls-elastic model*, in Materials and Structures 42, 301-320, 2009.

[8] B. Källsner, U. A. Girhammar, *Plastic models for analysis of fully anchored light frame timber shear walls*, in Engineering Structures 31, 2171-2181, 2009.

[9] EN1995-1-1:2004. *Design of timber structures Part 1-1: General-common rules and rules for building,* Brussels, Belgium: CEN, European Committee for Standardization, 2004.

[10] N. Gattesco, I. Boem, *Stress distribution among sheathing-to-frame nails of timber shear walls related to different base connections: Experimental tests and numerical modelling*, in Construction and Building Materials 122, 149-162, 2016.

[11] B. Folz, A. Filiatrault, *Cyclic Analysis of Wood Shear Walls*, in Journal of Structural Engineering 127, 433-441, 2001.

[12] A. Filiatrailt, H. Isoda, B. Folz, *Hysteretic damping of wood framed buildings*, in Engineering Structures 25, 461-471, 2003.

OpenSees Days Europe 2017
1st European Conference on OpenSees
Porto, Portugal, 19–20 June 2017

STUDY OF THE DYNAMIC SOIL-ABUTMENT-SUPERSTRUCTURE INTERACTION FOR A BRIDGE ABUTMENT

Davide Noè Gorini[1] **and Luigi Callisto**[2]

[1] Sapienza University of Rome
Via Eudossiana 18
davideno.gorini@uniroma1.it

[2] Sapienza University of Rome
Via Eudossiana 18
luigi.callisto@uniroma1.it

Keywords: Dynamic Soil-Structure Interaction, OpenSees numerical modelling, parallel computing.

Abstract. *The abutment is the part of a bridge that has a more significant dynamic interaction with the soil; the behaviour of the abutment is also influenced by the interaction with the superstructure, producing a reciprocal time-dependent exchange of inertial forces between them. This note illustrates a finite element description of the coupled dynamic interaction of an abutment with the bridge structure and with the soil, occurring in the occasion of a severe seismic event. The computation procedure was entirely implemented in OpenSees with the aim to investigate the dynamic response of the specific abutment of the Pantano viaduct, which would be used as an accessing facility to the still unbuilt Messina Strait suspension bridge, in Italy. The potentiality and versatility of OpenSees were used to reach an accurate numerical modelling of both the soil and the structure. The mechanical behaviour of the soil was reproduced through the Manzari and Dafalias hardening plasticity constitutive model, that was calibrated in order to reproduce the experimental laboratory data. The abutment was regarded as an elastic structure, while the dynamic interaction of the abutment with the superstructure was studied by means of two approaches of increasing complexity and accuracy. Parallel computing, obtained with the OpenSeesSP interpreter, was needed to optimize the computation time for the non-linear time domain analyses. The strategy solution presented herein is useful in that it enhances the current capability to evaluate the dynamic behavior of bridge structures, implementing a coupled soil-structure interaction analysis that considers explicitly the propagation of seismic waves in the foundation soils ant their interaction with the structure.*

1 INTRODUCTION

The Pantano viaduct was designed as the approaching structure to the Messina Strait suspension bridge (Italy) on the Sicilian side of the bridge. As shown in Figure 1, the Pantano viaduct starts at the terminal structure of the suspension bridge and ends on a massive abutment situated on the Messina side. The subsoil is constituted by a thick deposit of Messina gravels, down to a depth of 245 m from the abutment foundation, followed by Continental Deposits extending down to the bedrock, located at a depth of 445 m. The site of the bridge is characterized by a high seismicity due to the presence of several segmentations of active faults. The viaduct is a girder bridge composed of three curved decks, a central railway and two lateral roadways, supported by five piers, by the terminal structure of the suspension bridge and by the abutment. The bridge was designed to transmit most of the longitudinal seismic forces to the abutment that consequently will be loaded by large seismic forces. In the following, the methodology adopted to investigate the dynamic behaviour of the full soil-abutment-superstructure system will be presented, focusing mainly on the modelling technique of the soil-structure interaction models.

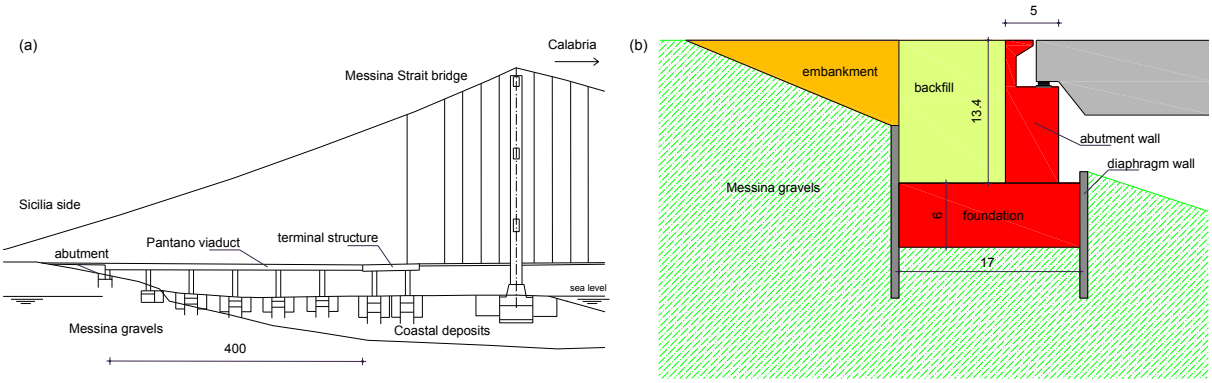

Figure 1: (a) longitudinal section of the Pantano viaduct and of the Messina Strait suspension bridge; (b) geometry of the abutment of the Pantano viaduct.

2 NUMERICAL MODELLING

The system modelling and response computations were performed by using the open source Finite Element analysis framework OpenSees [1] while the mesh of the models was generated and visualized through the pre/postprocessor software GID [2]. The full three-dimensional soil-structure interaction model, depicted in Figure 2, is composed of 400300 elements for a whole extension of 353.5×257.0 m^2 in plan and 128.5 m in depth.

The abutment of the Pantano viaduct, represented in Figure 1, is a massive reinforced concrete structure resting on a foundation slab, that in turn is in contact with the Messina gravels. Because of its large strength compared to the superstructure and the soil, it is reasonable to assume that the abutment exhibits an elastic response under seismic conditions. Hence, every structural member was modelled through the ShellMITC4 element [3] with elastic behaviour, using constitutive parameters relative to a C32/40 strength class concrete in the European standards. A Rayleigh damping was adopted for the elements of the abutment, calibrated in order to consider a damping ratio not greater than 5% for all the significant modes of the abutment.

All the soil domain was discretized through the SSPbrickUP eight node hexahedral elements [4] in which a mixed displacement-pressure formulation is used. The advanced hardening plasticity model developed by Manzari and Dafalias (MD model) [5] was chosen to get an

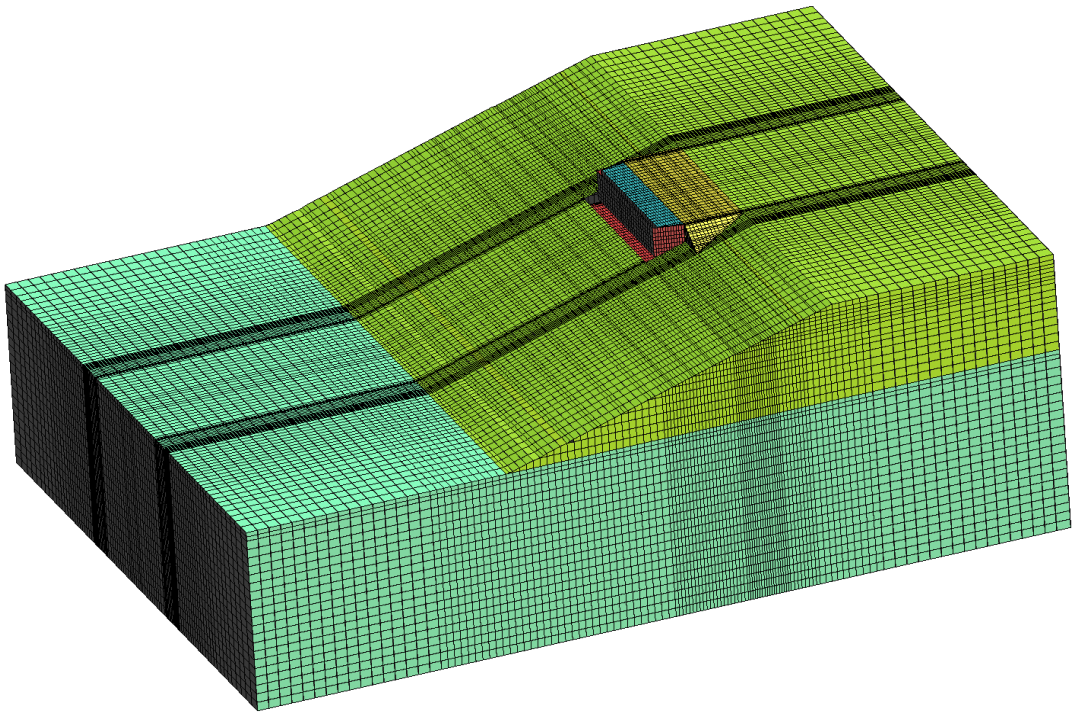

Figure 2: mesh of the three-dimensional soil-structure model

accurate response of the soil under cyclic loading and to predict the development of excess pore water pressures during the earthquake. The parameters of the constitutive model were calibrated against experimental data. It is important to observe that the MD model can reproduce with sufficient accuracy the mechanical behaviour of the soil only in a specific range of strain. More in detail, a calibration based only on monotonic laboratory tests leads to a considerable overestimation of the excess pore water pressure under cyclic conditions and, as a result, an inaccurate prediction of the mechanical response in undrained conditions. To overcome this issue, the calibration was aimed to obtain a good match with the experimental trends under cyclic conditions and, at the same time, to have a reasonable static response in the range of strain of interest for the problem under examination. The MD model is able to reproduce the effective energy dissipation as a function of the strain level, however an additional small damping ratio was introduced using the Rayleigh formulation only to attenuate the effects of spurious high frequencies.

Behind the wall of the abutment two zones can be distinguished: the backfill and the embankment. The former is the part directly in contact with the abutment and is made of a soil-cement mix to have a large stiffness and to avoid the development of significant plastic strains. Therefore the backfill was modelled as an elastic-perfectly plastic material, with a Young's modulus of 10^6 kPa that respects technical provisions on the stiffness, a Poisson's ratio of 0.2, an angle of shearing resistance of 38° and a cohesion equal to 200 kPa. Moreover, the Rayleigh damping model was associated with the elements of the backfill calibrated on the frequency content of the seismic input. Conversely, the embankment is a partially saturated soil, with the presence of negative pore water pressure (suction) providing non-zero stiffness and strength at small stress levels. The mix design for the soil of the embankment was chosen to have a stiffness and a degree of compaction greater than the correspondent limit values imposed by technical provisions. The MD model was adopted to simulate the behaviour of the embankment with an appropriate calibration of the parameters, in which the effect of the suction was modelled as a modest increment of the material stiffness. As done for the soil do-

main, a small Rayleigh damping was added to these elements to stabilized the dynamic time stepping.
The bridge has three curved decks, two lateral roadways designed as continuous steel box girder beams and a central railway composed of a mixed steel-concrete beam for each span, that are supported by five piers with a reinforced concrete box section. All the decks are connected to the abutment by a series of bearings that impede the relative displacements with the abutment. The dynamic interaction between the abutment and the bridge structure was initially modelled by applying equivalent static forces at the top of the abutment. At a successive stage, a more rigorous method was introduced, conceived to reproduce the frequency-dependent transmission of the dynamic interaction forces between the abutment and the superstructure through a transfer tensor, which represents the global effects of the multi-directional dynamic response of the superstructure.
A staged analysis procedure was adopted with gravity loads applied first and followed by the dynamic simulation, in which the use of the parallel computing was needed to get reasonable computation times. During the seismic excitation, the Lysmer and Kuhlemeyer absorbing boundaries [6] were applied along the lateral boundaries of the model, implementing an automatic procedure to set the dashpots with their properties, while the seismic input, applied at the base of the model, resulted from a deconvolution analysis in order to limit the vertical extension of the numerical model. In this way, the seismic actions reaching the abutment derive from the combined effect of the propagation of the seismic waves through the soil and the dynamic interaction of the soil with the structure.

3 CONCLUSIONS AND PERSPECTIVES

The numerical procedure exposed herein is part of an ongoing research on the dynamic response of bridge abutments, starting from the case study of the Pantano viaduct. The purpose of this research is to define useful tools and methods for dealing with the complex soil-abutment-superstructure interaction and to explore the dissipative capabilities deriving from the interaction between the soil and the abutment.

REFERENCES

[1] F.T. McKenna, Object-oriented finite element programming: Frameworks for analysis, algorithms and parallel computing. Ph. D. dissertation, Univ. of California, Berkeley, Calif, 1997.

[2] N.D. Diaz, P.S. Amat, GID the personal pre/postprocessor user's manual, version 5.0. CIMNE, Barcelona, Spain, http://gid.cimne.upc.es, 1999.

[3] E.N. Dvorkin, K.J. Bathe, A continuum mechanics based four node shell element for general nonlinear analysis. *Eng. Comput.*, **1**, 77-88, 1984.

[4] O.C. Zienkiewicz, T. Shiomi, Dynamic behaviour of saturated porous media; the generalised Biot formulation and its numerical solution. *International Journal for Numerical Methods in Geomechanics*, **8**, 71-96, 1984.

[5] Y.F. Dafalias, M.T. Manzari, Simple Plasticity Sand Model Accounting for Fabric Change Effects. *Journal of Engineering Mechanics.* , **130(6)**, 622-634, 2004.

[6] J. Lysmer, R.L. Kuhlemeyer, Finite dynamic model for infinite media. *Journal of Engineering Mechanics Division.* , **95(4)**, 859-877, 1969

OpenSees Days Europe 2017
1st European Conference on OpenSees
Porto, Portugal, 19–20 June 2017

MODELLING OF SOIL-STRUCTURE INTERACTION IN OPENSEES: A PRACTICAL APPROACH FOR PERFORMANCE-BASED ENGINEERING

Smail Kechidi[1], Aires Colaço[2], Mário Marques[2], José M. Castro[2] and Pedro A. Costa [2]

[1] Faculty of Engineering, University of Porto
Rua Dr. Roberto Frias s/n, 4200-465 Porto, Portugal
kechidi@fe.up.pt

[2] Faculty of Engineering, University of Porto
Rua Dr. Roberto Frias s/n, 4200-465 Porto, Portugal
{aires,pacosta,miguel.castro,mariom}@fe.up.pt

Keywords: Soil-structure interaction, Lumped-parameter model, OpenSees, Nonlinear dynamic analysis, Site effect.

Abstract. *In this paper, a numerical tool based on the Monkey-tail fundamental lumped-parameter model is proposed for the simulation of the dynamic soil-structure interaction (SSI). The proposed model has been implemented in the OpenSees finite element environment where the input parameters are merely function of the soil properties. The ease of use, accuracy and versatility of the proposed model is demonstrated in order to encourage its use within, among others, the practicing engineers' community. Furthermore, the influence of the SSI and local soil conditions (i.e., site effect) on the seismic performance of two 5-storey steel moment-resisting frames, has been investigated. Preliminary results shed light on the influence of the geotechnical conditions on the structural seismic response and its dependence on the fundamental period of vibration, seismic intensity level and soil stiffness, which are not taken into account by the current European design codes.*

1 INTRODUCTION

Structures supported by shallow foundations are subjected to inertial loading due to earthquake ground motion and eventually the foundation may undergo sliding, settling and rocking movements. If the capacity of the foundation is mobilised, the soil-foundation interface would dissipate significant amount of vibrational energy, resulting in a reduction in structural force demand. This energy dissipation and force demand reduction may enhance the overall performance of the structure, if potential consequences such as excessive tilting, settlement or bearing failure are accounted for in the formulation of numerical models. Despite these two potential benefits, building codes discourage designs that consider mobilisation of the foundation's capacity. This lack of acceptance to embrace the soil-structure interaction (SSI) may stem from the lack of well-calibrated modeling tools coupled with parameter selection protocols cast in a simplistic manner. In this paper, a practical modelling tool of the SSI for a seismic performance assessment, is presented. The model has been implemented in OpenSees [1] following a simplistic approach where its parameters are related to the soil properties. Subsequently, to provide insights into the impact level of the SSI and site effect on the structural seismic behaviour, the performance of two 5-storey steel moment-resisting frames (MRFs) has been assessed.

2 SOIL-STRUCTURE INTERACTION MODELLING

The model adopted herein represents the frequency dependent SSI of a massless foundation where the ground is simulated by a range of spring and dashpots-masses following a lumped-parameter formulation. The lumped values represent the stiffness, inertial effect and damping generated from the SSI phenomenon. Among the different models available in literature, the present study adopts the "Monkey-tail" fundamental lumped-parameter model [2]. The latter requires five parameters (K, C_0, C_1, M_0 and M_1) to be defined for each degree of freedom as depicted in Figure 1.

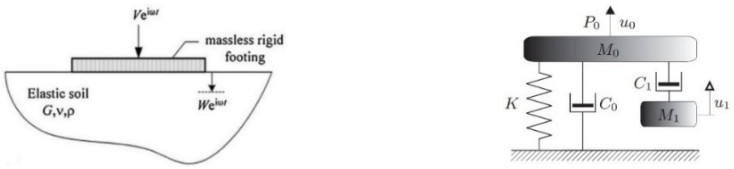

a) b)

Figure 1: Monkey-tail model: a) problem description and b) structural system (adapted from [1]).

2.1 Model implementation in OpenSees software

In this study, OpenSees has been adopted to implement the above described model. In order to check the accuracy of the proposed model and establish a certain reliability for its use in further parametric studies, a validation process should be carried out. For this purpose, two single-degree-of-freedom (SDOF) systems, as shown in Figures 2a and 3a were selected and then analysed considering the SSI effect in their bases using the above described lumped parameter model.

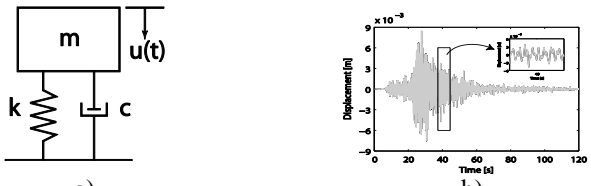

a) b)

Figure 2: a) SDOF (m=94 ton; c=9.3E05 kN.s/m; k=9.3E07 kN/m) and b) comparison of results obtained from OpenSees (black) and the frequency domain analysis using Matlab (grey) for V_{s30}=180.

The time-history response of the mass, produced by a ground motion record selected based on specific soil and structure conditions, can be seen in Figures 2b and 3b. An acceptable correlation rate is observed between the results obtained from the proposed lumped-parameter model and those obtained from analyses carried out in the frequency domain using Matlab software.

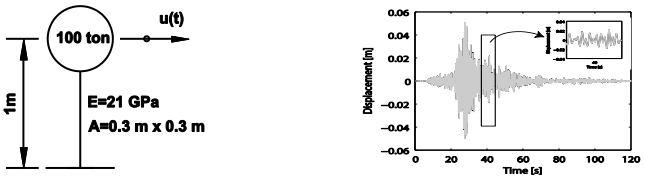

a) b)

Figure 3: a) Oscillator system and b) comparison of results obtained from OpenSees (black) and the frequency domain analysis using Matlab (grey) for V_{s30}=180.

3 CASE STUDY

In this section, the influence of the local soil conditions and SSI on the seismic performance of two steel MRFs, is assessed. The first building, denoted by GB, has been designed to merely resist gravity loads in accordance with the provisions of Eurocode 3 [3]. The second building, designated by SB3, has been seismically designed according to Part 1 of Eurocode 8 [4] considering a behaviour factor "*q*" equal to 4 (Araújo [5]). Three different analysis methodologies which are considered in this study. The first one, identified as approach I, is a typical structural analysis where the SSI is neglected and the site effects are incorporated in the ground motion record selection *i.e.*, through the consideration of the soil factor in the calculation of the response spectrum. The second analysis (approach II) incorporates the SSI and the ground motion records are selected following the same technique adopted in the first analysis. In the last analysis (approach III), along with the incorporation of the SSI, the effect of the local soil conditions is taken into account as well.

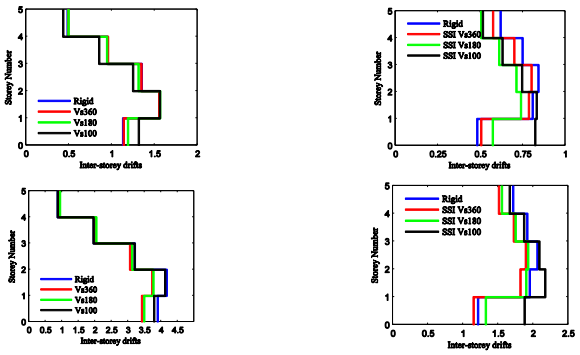

a) b)

Figure 4: a) Interstorey drifts (% of the storey height) for GB and b) SB3 (right) frames considering type I and II approaches and seismic intensity levels associated with T_R=475 years (top) and T_R=2475 years (bottom).

Figure 4a (top) shows a similar trend of deformation for the different analyses where the upper limit corresponds to the curve of the rigid case (approach I) except for the section of the plot corresponding to the lower stories. Moreover, it is found that the maximum values of the interstorey drift are located at the second storey. Comparing now the results obtained for both seismic intensity levels (*i.e.*, 10% and 2% probability of exceedance in 50 years), a similar trend can be seen in Figure 4a (bottom). In fact, there is a low dispersion of the results for the GB

frame (subfigures 4a) and the increase thereof for the SB3 frame, particularly with respect to the case of a low soil stiffness (subfigures 4b). Furthermore, there is a significant increase at the level of deformations, being associated to an increase of the plastic deformations of the frames members coupled with some structural related reasons.

In order to reveal the effect of the local site conditions on the structural response, the results obtained with approach II can now be directly compared with those recorded using approach III, considering the same average soil stiffness. Figure 5 represents the interstorey drift curves obtained for both approaches and for two seismic intensity levels (T_R equal to 475 and 2475 years). As far as approach III is concerned, the two curves are plotted, one corresponding to the homogeneous profile (red) and the other (green) related to the average value of the curves referring to ten geotechnical profiles.

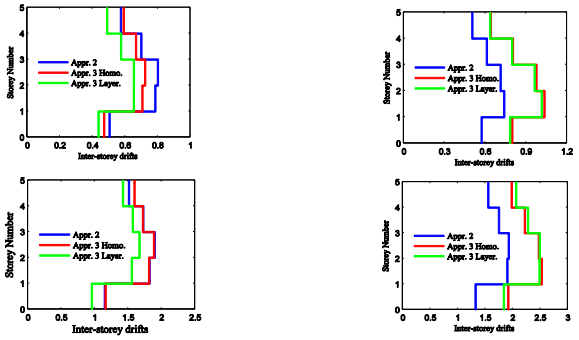

Figure 5: Comparison of the interstorey drift values (% of the storey height) obtained for the SB3 frame considering approach II and III for seismic intensity levels associated with T_R=475 years (top) and T_R=2475 years (bottom) for: a) V_{s30}=360 m/s and b) V_{s30}=180 m/s.

The analysis of Figure 5 indicated that there is a common trend between the two adopted seismic intensity levels, where the main differences stemmed from the soil stiffness. Clear discrepancies are observed between the two different cases of approach III. When considering a value of 360 m/s for the soil stiffness parameter (V_{s30}), approach II gives rise to an outer envelope of the interstorey drift curves excluding the top floor. This finding is no longer valid when the value of V_{s30} is reduced to 180 m/s where the soil amplification plays a crucial role leading to higher interstorey drift curves obtained following approach III than those obtained from approach II.

REFERENCES

[1] PEER. *OpenSees: Open system for earthquake engineering simulation*, Pacific Earthquake Engineering Research Center, University of California, Berkeley, CA, 2006.

[2] L. Ibsen, M. Liingaard, *Lumped-parameter models*. Aalborg University, 2006.

[3] EN 1993-1-1. *Eurocode 3: Design of steel structures - Part 1.1: General rules and rules for buildings*. European Committee for Standardization, Brussels, CEN, 2005.

[4] EN 1998-1, *Eurocode 8. Design of structures for earthquake resistance, Part 1: general rules, seismic actions and rules for buildings*. European Committee for Standardization, Brussels, CEN, 2005.

[5] M. Araújo, *Seismic safety assessment of existing steel buildings*, Civil Engineering Department, Faculty of Engineering, University of Porto, Porto, 2013.

OpenSees Days Europe 2017
1st European Conference on OpenSees
Porto, Portugal, 19–20 June 2017

IMPLEMENTATION AND FINITE-ELEMENT ANALYSIS OF SHELL ELEMENTS CONFINED BY THROUGH-THE-THICKNESS UNIAXIAL DEVICES

Salvatore Sessa[1], **Roberto Serpieri**[2], **and Luciano Rosati**[1]

[1] University of Naples Federico II – Department of Structures for Engineering and Architecture
via Claudio 21, 80125, Napoli, Italia
e-mail: {Salvatore.sessa2, rosati}@unina.it

[2] Università degli Studi del Sannio – Department of Engineering
Piazza Roma 21, 82100, Benevento, Italia
roberto.serpieri@unisannio.it

Keywords: OpenSees, Shell, Through-the-Thickness, Confinement, Jacketing.

Abstract. *This contribution presents the implementation in OpenSees of an integration procedure based on a recently developed theory concerning stress integration along the chords of a shell element reinforced with uniaxial transverse links. Such a model has been developed in order to account for transverse confinement effects induced by through-the-thickness jacketing of masonry and reinforced concrete existing structures. In particular, transverse confinement induces a triaxial stress state in the core material of the shell increasing the stress spherical part and resulting in strength and ductility increments. In order to perform structural analyses with reduced computational costs, the presented tool permits to compute the response of plane elements confined by uniaxial devices. To this end, the implemented object accounts for the mutual interaction of uniaxial reinforcements with a triaxial core by means of equilibrium and compatibility equations involving several object classes of the OpenSees framework. Integration of the triaxial stress state along the thickness of a shell element is therefore performed by numerically solving the equilibrium/compatibility equation system. The adopted implementation strategy is summarized and modeling features are discussed. In conclusion, numerical examples show some possible applications of the proposed tool in common structural design practices.*

1 INTRODUCTION

The use of confinement devices in the retrofit of masonry and reinforced concrete structures has become a very popular approach for its capability of improving structural strength and ductility. More recently, use of confinement retrofit techniques has been extended also to the retrofit of planar structural elements. In particular, masonry panels in existing buildings are also confined by employing Through-the-Thickness reinforcing links connecting external reinforced render layers Jacketing the panel (TTJ) [1].

To model TTJ devices, a formulation of TTJ Shell (TTJS) has been proposed by the authors in a recent research paper [2]. It consists of an Equivalent Single Layer Mindlin First-order Shear Deformation Theory (ESL-FSDT) endowed by enhanced kinematics coupling the stress-strain states of a shell triaxial core material and of uniaxial transverse confining devices.

The present contribution briefly presents the TTJS formulation and illustrates the underlying implementation strategy in OpenSees of an MITC shell element based upon the TTJS theory. Numerical results and validation schemes are also presented.

2 THROUGH-THE-THICKNESS JACKETED SHELL THEORY

The TTJS theory [2] enhances in a simplest possible way an ordinary ESL MITC formulation. Its main idea is to enforce a set of equilibrium and compatibility equations, representing the interaction between the links and the core material over a generic transverse segment of the shell, named *Shell Chord*. For a shell core made of *n* layers these equations are:

$$\text{Compatibility:} \quad \sum_{i=1}^{n} \varepsilon_{33}^{i} t^{i} = \varepsilon_{TT} \sum_{i=1}^{n} t^{i}; \qquad \text{Equilibrium:} \quad \sigma_{33}^{i} + \mu_T \sigma_{TT} = 0; \quad i = 1..n \tag{1}$$

where ε_{33}^{i} and σ_{33}^{i} are the strain and stress components at the *i*-th layer along the direction orthogonal to the shell middle plane, ε_{TT} and σ_{TT} are the uniaxial strain and stress of the confinement devices, t^{i} is the thickness of the *i*-th layer and μ_T is the percentage area of the ties. The i-th layer refers to a specific class of triaxial material providing stress components σ_{jk}^{i} as functions of ε_{jk}^{i} and its derivative.

The compatibility condition in (1) enforces the deformation ε_{TT} to be equal to the transverse stretching of the shell core and the equilibrium condition enforces the core stress component σ_{33}^{i} to be in equilibrium with the term $\mu_T \sigma_{TT}$ representing the uniaxial stress resultants of the ties. In such a way, Eqs. (1) describe the interaction of all layers with the uniaxial ties where the role of transverse confinement is to contrast the transversal stretching of the shell, acting proportionally to the stiffness of the confinement devices.

A set of routines integrating the mechanical state of the Shell Chord according to Equations (1) have been implemented in OpenSees v. 2.5.0 complying with its object-oriented architecture. In brief, the essential steps for the integration of an ESL-FSDT MITC formulation are the following. First, strain components along the shell chord are computed by shape functions. Next, the relevant stress state is evaluated layerwise by the constitutive routines, and, finally, the stress state is integrated in order to obtain generalized forces at the nodes. Solution of compatibility and equilibrium equations in (1) is performed by a Newton-Raphson algorithm. Finally, generalized stress components are computed by summation.

From a computational point of view, integration of generalized stress in performed at each Gauss point of the relevant finite element. The TTJS implementation in OpenSees uses the *ShellMITC4* element, a 4-noded, three-dimensional shell with 6 Degrees Of Freedom (DOFs) per node. Such an element is linked to instances of a *Section* object which defines the layers'

geometry and performs the stress integration. Consistently with the OpenSees philosophy, the TTJS algorithm has been implemented as a subclass of *Section,* as shown in Figure 1: it receives from the parent object the values of the generalized strains and returns the values of the generalized stress and the tangent operator.

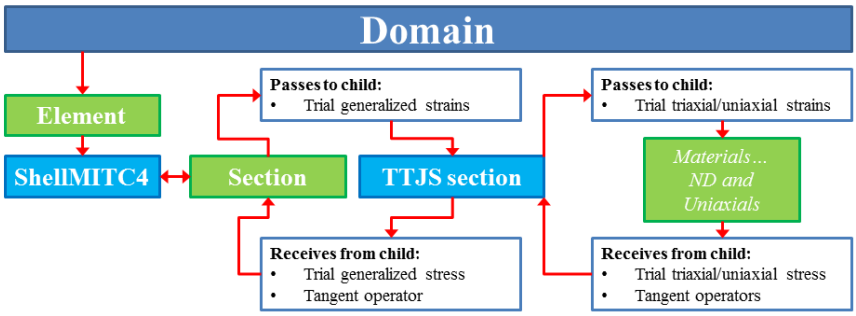

Figure 1 OpenSees parent (green) and child (blue) classes involved in the TTJS analysis

3 NUMERICAL RESULTS

The first numerical example herein reported consists of a reinforced concrete shear wall with steel transverse reinforcements. Core layers are modeled as an elastic – perfectly plastic Drucker Prager material while ties are elastic – perfectly plastic uniaxial rod elements. Results of a second application, the Scordelis Lo roof subject to vertical loads, are also reported showing the behavior of the TTJS in capturing coupling between flexural and membrane behavior.

Global structural responses in the two tests are shown in Figure 1 and Figure 4, respectively, in terms of load-displacement relationships and distributions of the confining stress σ_{TT}.

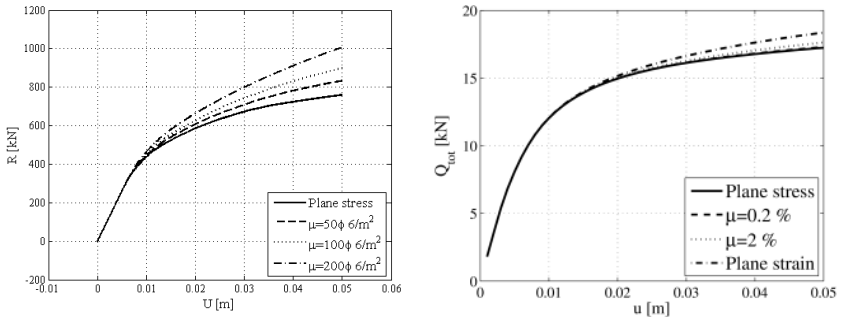

Figure 2 Load-displacement responses of the shear wall test (left) and Scordelis-Lo roof (right).

The load-displacement curves show that increase of the percentage of transverse confinement μ_T results in higher post-elastic stiffness and strength of the structures. Conditions of plane stress and plane strain represent natural boundaries for the responses relevant to all possible confinement ratios, as shown in Figure 2.

The strength increment turns out to be the result of confinement increasing the spherical part of the triaxial stress. As well known, this effect is beneficial in pressure-dependent frictional materials and it is found to be ordinarily captured by the employed Drucker-Prager model, as shown by the family principal stress paths plotted in Figure 3 as function of μ_T.

Figure 4 shows that peak values of the confining stress σ_{TT} are clustered in the compressive regions. This issue highlights the benefits of using shells instead of beam elements for analyzing confined shear walls: a beam accounts for confinement by assuming an average strength increment uniformly distributed among the cross section. On the contrary, Figure 4 clearly shows that distribution of confinement effects depend on geometry and loads.

Results for the Scordelis Lo roof show that, while the confinement effect is less pronounced due to the predominant flexural behavior of this structure, the TTJS-MITC element seems to correctly capture membrane-flexural coupling combined with TTJ coupling.

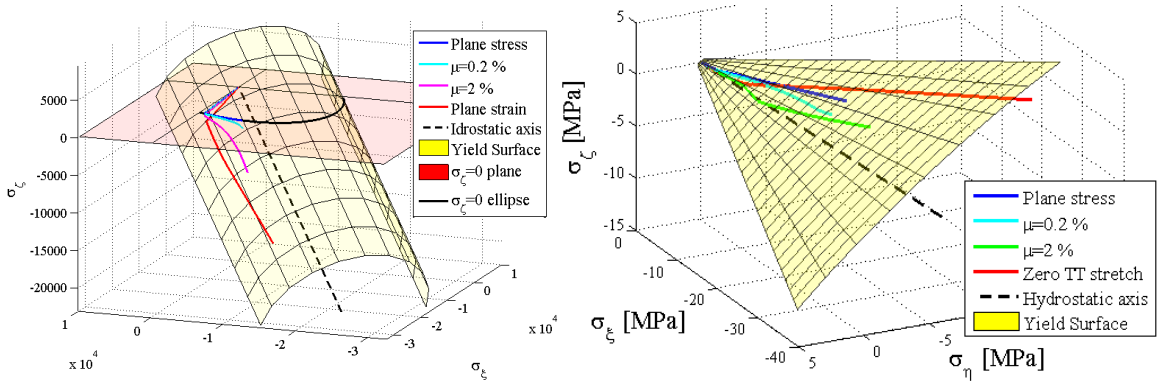

Figure 3 Path of the core principal stress on the Yield surface: Von Mises (left) and Drucker Prager (right).

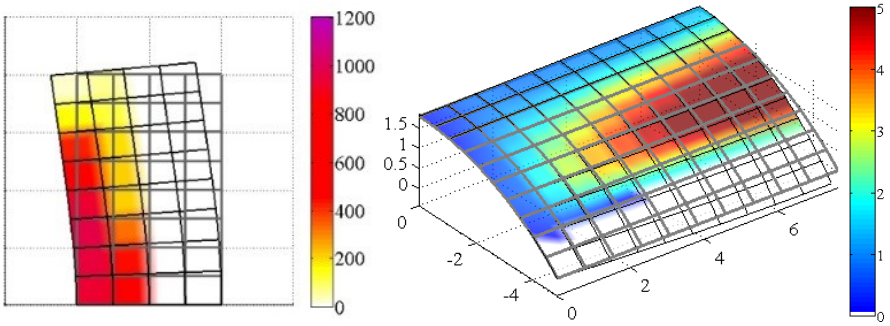

Figure 4 Distributions of confinement stress σ_{TT} of the shear wall test (left)and Scordelis-Lo roof (right).

4 CONCLUSIONS

The TTJS Section object recently implemented in Opensees permits to model the confinement effects induced by transverse reinforcement within a simpler shell FE formulation and to combine structural analysis with the analysis of triaxial stress states. Thanks to the object-oriented philosophy ruling the OpenSees framework, a quite simple implementation of this structural object is possible. The resulting numerical tools are open to be combined with a vast variety of constitutive models for the core material and for transverse reinforcements.

Ongoing research activities are centered on the use of the TTJS formulation in dynamic analyses and in structural reliability applications. Future developments will address the use of TTJS combined with damage-based material models.

REFERENCES

[1] F. S. Pinho, V. J. Lucio, M. F. Baiao, Rubble stone masonry walls strengthened by three-dimensional steel ties and textile reinforced mortar render under compression and shear loads. *International Journal of Architectural Heritage,* **9**(7), 844-858, 2015.

[2] S. Sessa, R. Serpieri, L. Rosati, A continuum theory of through-the-thickness jacketed shells for the elasto-plastic analysis of confined composite structures: theory and numerical assessment. *Composites Part B,* 113, 225-242, 2017.

OpenSees Days Europe 2017
1st European Conference on OpenSees
Porto, Portugal, 19–20June 2017

OPENSEES INTEGRATED IN A BIM WORKFLOW AS CALCULATION ENGINE

Pereiro-Barceló, Javier[1], **Fernández-Baños, Manuel**[2]

[1]Cype Ingenieros S.A.
Avda. Eusebio Sempere, 5 – 03003 Alicante, España
e-mail: javier.pereiro@cype.com

[2] Cype Ingenieros S.A.
Avda. Eusebio Sempere, 5 – 03003 Alicante, España
e-mail: manuel.fernandez@cype.com

Keywords: Open BIM, workflow, Opensees, structural analysis.

Abstract. *Using Open BIM (Building Information Modeling) technology, it is possible to implement a collaborative, multidisciplinary and multiuser workflow that allows for project development in an open, coordinated and simultaneous manner amongst the intervening technical agents. In this workflow, proposed by Cype, the project is solved in an iterative mode by progressively solving its different models. Opensees is integrated in this workflow as calculation engine to perform structural analysis.*

1 INTRODUCTION

Open BIM is a global proposal to achieve user collaboration in the design, execution and maintenance of buildings, based on an exchange of information using standard formats (IFC) and an open workflow.

Using this technology, it is possible to implant a collaborative, multi-disciplinary and multi-user workflow, which allows for projects to be developed in an open, coordinated and simultaneous manner amongst the various technical users or intervening agents, and is completely independent from the applications and platforms used for its development.

Cype has integrated Opensees within Open BIM workflow as calculation engine for StruBIM Analysis, StruBIM Design and StruBIM Foundations.

2 OPEN BIM WORKFLOW

The following table explains the stages of Open BIM workflow:

Stages	Description
Start of the BIM Project	-An IFC format file must be generated based on a 3D model produced by any architectural modeling software.
Specialized applications	-All the applications that are compatible with the Open BIM workflow import the IFC model. All intervening agents receive the same geometry and architecture.
BIM model update	-If any changes are made to the initial model, all the applications can undergo an updating process. This guarantees that no information is lost.
IFC file export	-The applications can also export a file in IFC format. This way, the BIM project is enriched and completed upon accepting all this information.
BIM model consolidation	-The information making up the BIM model increases using IFC files generated by all the applications and defines the complete BIM project.

Table 1: Open BIM workflow

3 STRUCTURAL ANALYSIS AND DESIGN IN OPEN BIM FLOW

The stages to carry out the analysis and design of structures are perfectly delimited:

- Structural model.
- Generation, edition and analysis of analytical model.
- Design and check of structural elements.
- Generation of layouts and reports.

3.1 Structural model

Structural model is made up by structural elements such as beams, columns, ties, shells, etc. In order to perform the Structural analysis and design, it is necessary to gather some initial information from the architectural model. Conventional structural BIM software expects to gather this information from the BIM model. This flow implies that the structural analysis tool is able to read the structural elements and add the information that cannot be described in the modeling tool.

In contrast to this traditional trend, Cype proposes that the structural modeling tools integrated in the Open BIM workflow do not import structural elements but the elements of the BIM model that affect the structure. That is, from the architectural model the software imports

the shape of the building (height between floors and contours of floors, gaps and position of columns…), then the user models the structural elements and its properties.

3.2 Generation, edition and analysis of analytical model

Cype has developed a program to generate, edit and perform structural analysis: StruBIM Analysis. This program forms part of StruBIM suite, which is a group of structural programs, each one related to one stage of structural design.

Sequential version of OpenSees has been used as calculation engine in StruBIM analysis (Figure 1), offering the same functionality that the previous engine. For this purpose several extensions have been implemented in OpenSees: two new finite elements (one-dimensional and shell) [1-3], a new constraints manager, MUMPS (Multifrontal Massively Parallel Sparse Direct Solver) [4], etc. Besides, multiple instances of sequential OpenSees are used to increase parallelism without using MPI.

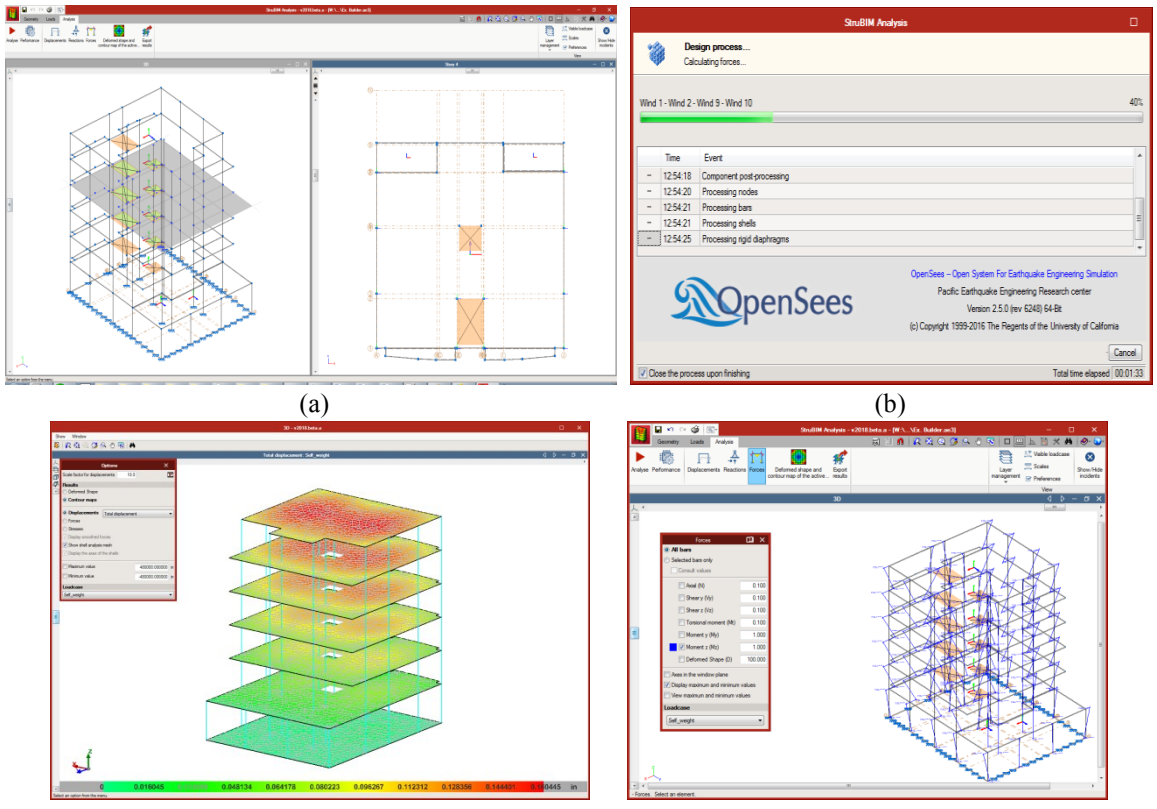

Figure 1: Structural analysis with StruBIM analysis plus OpenSees: (a) Analytical model, (b) Calculating with OpenSees, (c) Deflections results, (d) M_z moments in columns

3.3 Design and check of structural elements

StruBIM Design is responsible of designing and checking columns, beams, slabs and walls according to ACI Codes (Figure 2.a). It imports the analytical model results from StruBIM Analysis or from an xml file with a specific format. Besides, it is able to manage a local analytical model of each floor to design tendons, slabs and beams. It uses OpenSees as calculation engine. Analogously to StruBIM Design, Cype has created StruBIM Foundations to design foundation elements (Figure 2.b).

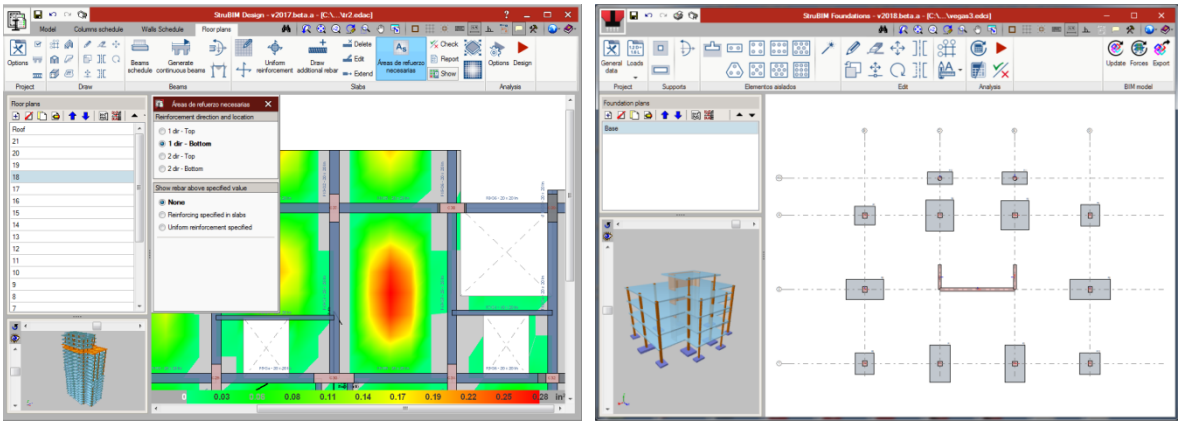

(a) (b)

Figure 2: Design with StruBIM suite plus OpenSees: (a) Slabs design, (b) Foundations design

4 CONCLUSIONS

- Cype proposes that the structural modeling tools integrated in the Open BIM workflow should not import structural elements but the elements of the BIM model that affect the structure, therefore no information is lost.
- OpenSees has been integrated in the Open BIM workflow which is a global proposal to achieve user collaboration in the design, execution and maintenance of buildings, based on an exchange of information using standard formats (IFC). The high performance of OpenSees plus the speed and convenience of BIM models make a powerful combination to deal with structural design.
- OpenSees is integrated in StruBIM suite to carry out the analysis of analytical models of structures. New elements, constraints handler and solver has been added to OpenSees to be able to model every aspect of a building. A new strategy for parallel processing has been implemented.
- OpenSees will soon provide StruBIM with the possibility of performing dynamic and non-linear analysis of complex structures which would became very difficult to model without the capabilities that StruBIM offers.

REFERENCES

[1] E. Oñate, *Cálculo de Estructuras por el Método de Elementos Finitos, 1th Edition*, Centro internacional de Métodos Numéricos en Ingeniería, Universitat Politècnica de Catalunya, Barcelona, 1992.

[2] C.A. Felippa *Introduction to Finite Element Methods*, Department of Aerospace Engineering Sciences and enter for Aerospace Structures, University of Colorado, USA, 2004.

[3] C.A. Felippa *Finite Element Methods in Dynamics*, Department of Aerospace Engineering Sciences and enter for Aerospace Structures, University of Colorado, USA, 2004.

[4] MUltifrontal Massively Parallel Solver (MUMPS), *Users's guide,* March 21, 2017.

OpenSees Days Europe 2017
1st European Conference on OpenSees
Porto, Portugal, 19–20 June 2017

A NEW GRAPHICAL USER INTERFACE FOR OPENSEES

Vassilis K. Papanikolaou[1], **Theocharis Kartalis-Kaounis**[1],
Evangelos Protopapadakis[1], **and Theocharis Papadopoulos**[1]

[1] Lab of R/C and Masonry Structures, School of Civil Engineering,
Aristotle University of Thessaloniki, Greece
P.O. Box 482, Thessaloniki 54124, Greece
e-mail: billy@civil.auth.gr (V.K. Papanikolaou)

Keywords: OpenSees, GiD, Graphical User Interface (GUI), Open Source

Abstract. *The objective of this paper is to present a new graphical user interface that has been recently developed for OpenSees, which seamlessly connects the OpenSees solver with the general pre/post-processor GiD. This interface, available as open-source, is easily installed in the GiD graphical environment and provides an extended set of user dialogs and tools to efficiently create model geometry, assign materials, elements and boundary conditions, select various analysis options and finally invoke the OpenSees solver to execute the analysis. The interface automatically transforms the bulk of numerical results produced by OpenSees to a GiD-compatible format, for the user to take advantage of the versatile GiD graphical postprocessor, which includes a deformed shape viewer with animation capabilities, force/stress/strain vectors and contours, line diagrams and x-y graphs. At the present state of development, all standard and a few advanced modeling capabilities of OpenSees are supported, which renders the interface a promising alternative to the cumbersome code-based modeling, considerably shortening the respective learning curve, especially for new and inexperienced users.*

1 INTRODUCTION

The Open System for Earthquake Engineering Simulation (OpenSees), developed as open-source at the PEER Center [1] is an increasingly popular analysis platform in earthquake engineering research, since it provides a robust solver with numerous standard and advanced constitutive laws, finite element types, boundary conditions and analysis capabilities. It has a large established user base, allowing the end-user not only to take advantage of its advanced features but also actively contribute to its current state of development. However, both the analysis solver and the produced result files are *text-based*, which requires a prior knowledge of TCL coding, even for building simple models. More importantly, the bulk of numeric results, especially when large in size, require the development of ad-hoc postprocessing tools (e.g. in MATLAB or other languages) for easier interpretation via plotting or visualization. The above shortcomings are often a deterring factor for new and inexperienced users to adopt OpenSees in their research, usually resorting to other software packages with graphical capabilities.

Taking the above disadvantage into consideration, the authors have recently developed a new interface (http://gidopensees.rclab.civil.auth.gr) that seamlessly connects the OpenSees solver with the general pre/postprocessor GiD, developed by the International Center for Numerical Methods in Engineering (CIMNE) [2], which not only provides a complete graphical environment for finite element pre/postprocessing, but also a TCL-based scripting language for generating custom input files, compatible with any text solver available. Moreover, by translating the produced result files into a specified format and importing them to the graphical postprocessor, all the standard graphical postprocessing features e.g. deformed shape view, contours and x-y plots are readily available. Similar implementations have been developed for other analysis packages as well (e.g. [3]). It should be stated here that the GiD software is distributed commercially, however its evaluation version has a generous 1010 node limit, which is more than adequate even for large frame models, rendering the full version necessary only for models with a large number of shell or brick elements (e.g. geotechnical and SSI problems).

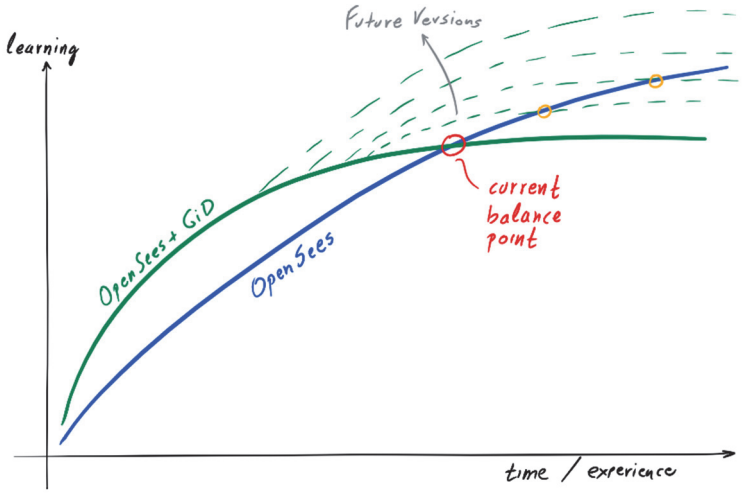

Figure 1: Comparison between OpenSees and GiD+OpenSees learning curves

The advantage of the present interface is depicted in Fig. 1 in a comparison between the learning curve of OpenSees alone and a considerably shorter one using the present interface. At the current state of development there exists a balance point above which the OpenSees user will no longer be benefited from the interface, due to the current limitations in terms of supported materials and elements. However, since the interface is provided as open-source i.e. open to user contributions, it is believed that future versions will contain the complete OpenSees

functionality, shifting this balance point to infinity. Nevertheless, the interface already provides the ability to manually edit the created data file (.tcl) before analysis (e.g. for adding any unsupported commands), execute the analysis and graphically postprocess the results.

2 INTERFACE STRUCTURE

The basic interface structure is depicted in Fig. 2. The model is created in the GiD graphical preprocessor using a standard point'n'click procedure for geometry (points, lines, surfaces, volumes) with the aid of various user dialogs containing the native OpenSees commands for defining and assigning model and analysis properties, together with a robust mesher provided by the preprocessor itself.

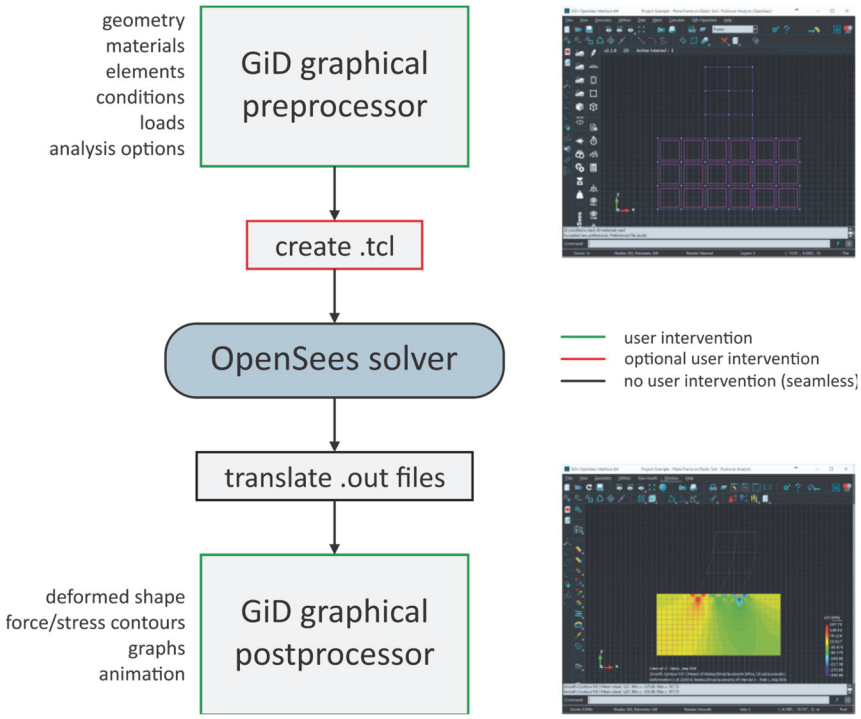

Figure 2: Interface structure

After completing the model, a single button press creates the OpenSees-compatible model data file and invokes the solver for running the analysis. The result output/recorder files (.out) are automatically translated to the required format and automatically imported in the postprocessor. The model is subsequently opened in the postprocessing environment, where all standard visual and graphic tools are available.

3 INTERFACE FEATURES

Table 1 contains a list of all available features at the current state of development (v2.1.0, 15/5/2017). More additions are already planned for upcoming releases. Figure 3 depicts two models created using the present interface, viewed in the GiD postprocessor.

4 CLOSURE

The herein presented GiD+OpenSees interface provides a promising alternative to the native code-based modeling process, making OpenSees accessible to a broader audience of researchers in the field of earthquake engineering. Provided as open-source, it is continually improving to reach even higher levels of functionality in the near future.

Table 1: Interface features (v2.1.0)

<table>
<tr>
<td rowspan="3">Materials
Standard Uniaxial Materials
-Elastic
-Elastic Perfectly Plastic
-Elastic Perfectly Plastic with Gap
Uniaxial Steel Materials
-Steel01
-Reinforcing Steel
Uniaxial Concrete Materials
-Concrete01
-Concrete02
-Concrete04
-Concrete06
Other Uniaxial Materials
-Viscous
Multidimensional (nD) Materials
-Elastic Isotropic
-Elastic Orthotropic
-J2Plasticity
-Damage2p
-PressureIndependMultiYield
-PressureDependMultiYield
Section Force-Deformation
-Fiber
-Plate Fiber
-Elastic Membrane Plate
Combined Materials
-Parallel
-Series
-Section Aggregator</td>
<td>Elements
ZeroLength Elements
Truss
Corotational Truss
Elastic Beam-Column
Elastic Timoshenko Beam-Column
Force-Based Beam-Column
Displacement-Based Beam-Column
Triangular (Tri31)
Quadrilaterals (Quad)
Shell (MITC4)
Standard Brick Element (stdBrick)</td>
<td>Analysis Types
Eigenvalue
Linear Static
Nonlinear Static (Pushover)
- Load control
- Displacement control
- Monotonic or Cyclic
Linear Transient
Nonlinear Transient
- Uniform ground motion excitation
- Uniform sine excitation
- Multi support ground motion excitation
- Multi support sine excitation</td>
</tr>
<tr>
<td>Restraints
On single nodes
On line nodes
On surface nodes

Constraints
Body constraints (equalDOF) on nodes
Body constraints (equalDOF) on line nodes
Rigid diaphragm

Damping
Global Rayleigh damping
Rayleigh damping on specific regions
- On nodes
- On elements</td>
<td>Loads
Forces
- On single nodes
- On line nodes
- On surface nodes
- Uniform forces on frame elements
Displacements
- On single nodes
Ground motion
- Ground motion from record on single nodes
- Sine ground motion

Masses
On single nodes
On line nodes
On surface nodes</td>
</tr>
</table>

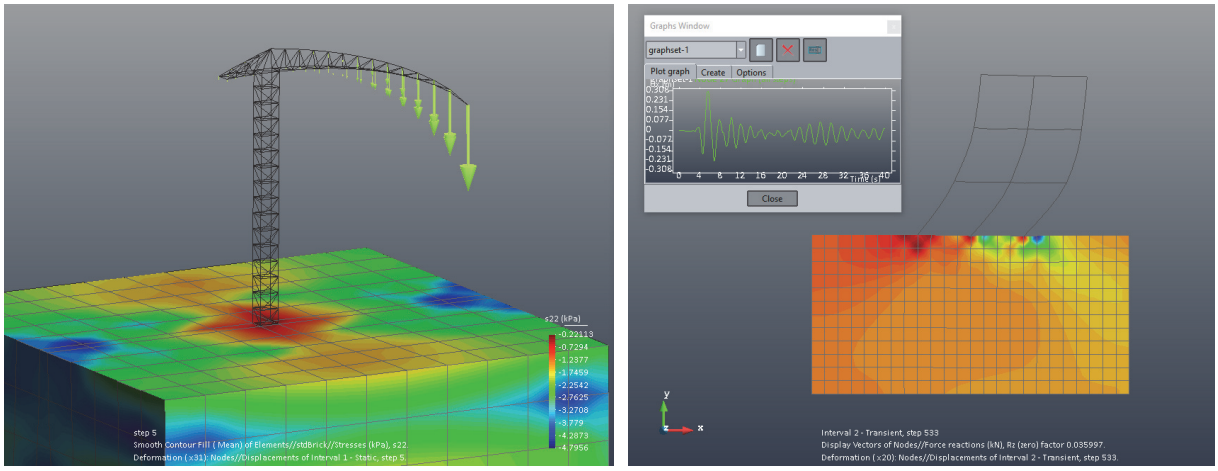

Figure 3: Postprocessor examples (left: 3D elastic analysis of a truss crane on elastic soil, right: 2D dynamic analysis of an inelastic frame on elastic soil – soil-structure interaction)

REFERENCES

[1] F. McKenna, G.L. Fenves, M.H. Scott, Open System for Earthquake Engineering Simulation. *Pacific Earthquake Engineering Research Center*, 2017.

[2] A. Coll, R. Ribó, M. Pasenau, E. Escolano, J.S. Perez, A. Melendo, A. Monros, GiD v.13 Customization Manual, *CIMNE*, 2017.

[3] V. Cervenka, L. Jendele, J. Cervenka., ATENA Program Documentation. Part 1: Theory 2017.

OpenSees Days Europe 2017
1st European Conference on OpenSees
Porto, Portugal, 19–20 June 2017

MODELLING OF A SHEAR REINFORCED FLAT SLAB BUILDING FOR SEISMIC FRAGILITY ANALYSIS

Brisid Isufi[1], Ildi Cismasiu[2], António M. P. Ramos[3] and Válter J. G. Lúcio[4]

[1] PhD Student, Faculdade de Ciências e Tecnologia, Universidade NOVA de Lisboa
Quinta da Torre, Campus Universitário, 2829-516 Caparica
e-mail: b.isufi@campus.fct.unl.pt

[2] UNIC, Faculdade de Ciências e Tecnologia, Universidade NOVA de Lisboa
Quinta da Torre, Campus Universitário, 2829-516 Caparica
e-mail: ildi@fct.unl.pt

[3] CERIS, Faculdade de Ciências e Tecnologia, Universidade NOVA de Lisboa
Quinta da Torre, Campus Universitário, 2829-516 Caparica
e-mail: ampr@fct.unl.pt

[4] CERIS, Faculdade de Ciências e Tecnologia, Universidade NOVA de Lisboa
Quinta da Torre, Campus Universitário, 2829-516 Caparica
e-mail: vjgl@fct.unl.pt

Keywords: flat slab, fragility, OpenSees, shear studs, IDA.

Abstract. *Flat slabs are generally not recommended for buildings in seismic regions, especially due to the risk of punching failures that can lead to progressive collapse if no measures are taken. Nonetheless, they are often used, even in regions with moderate to high seismicity. Shear stud reinforcement has been shown by various researchers to be among the most effective measures to prevent punching failures in flat slabs under vertical and lateral loading. The presented work is part of a research that aims to assess the adequacy of flat slabs reinforced with shear studs for use in a low rise building subjected to seismic actions. Herein, preliminary results from seismic fragility assessment are presented. The nonlinear behavior of the building is modelled in the OpenSees platform with special consideration of the slab-column connections, including the degradation due to cyclic loading and loss of unbalanced moment transfer capacity due to punching failure. The hysteretic model of the connections is calibrated using laboratory test results obtained on a specimen subjected to constant gravity loads and reversed lateral cyclic loading. Fragility curves are derived using Incremental Dynamic Analysis (IDA) for a set of synthetic ground motions. A simple local damage index is used to estimate damage in each connection and a global index, corresponding specifically to damage in the flat slabs, is evaluated. Concrete compressive strength, steel yield strength and the gravity loads are considered as random variables to account for the structural capacity uncertainties. The preliminary results showed that punching failures were avoided and the shear reinforcement was effective in reducing damage to the flat slabs for the considered building.*

1 INTRODUCTION

Fragility analysis is used in this research to assess the adequacy of shear stud reinforcement for use in a low rise flat slab building in which the slabs and the connections are part of the lateral force resisting system. The *OpenSees* [1] platform was chosen to perform a total of 1920 dynamic nonlinear time history analyses under a set of 64 Eurocode 8 [2] spectrum compatible accelerograms. Eight peak ground acceleration levels, starting from 0.05g up to 0.40g with a 0.05g step were considered. For each ground acceleration level, 8 synthetic accelerograms were generated using *SeismoArtif* [3]. Thirty nonlinear dynamic time history analyses were performed for each of the 64 accelerograms. The concrete strength, reinforcement yield strength and gravity loading were considered as random variables with prescribed probability distribution functions. Variables were sampled using the *Latin Hypercube* technique. *OpenSees* proved to be a suitable platform for the fragility analysis because it allowed automation in the modelling process, in sampling of the variables and in post-processing.

Two main issues need to be addressed in the structural modelling of flat slabs for fragility analysis when dynamic nonlinear history analyses are involved. First, the model should be able to capture the punching failure mode of flat slabs. Secondly, the model should adequately represent the load-deformation relationship of slab-column connections, which typically exhibit significant pinching. In order to adequately represent the loss of unbalanced moment transfer in the slab-column connection, the available *Joint2D* element [4] was used in combination with the *Pinching4* [5] uniaxial material to model the joints as rotational springs. Previous research related to fragility analysis of flat slabs includes [6], [7] and [8].

2 MODELLING AND ANALYSIS

A 2D frame of a three story flat slab building with five bays is considered (Figure 1). The building corresponds to the prototype building used for the reversed lateral cyclic loading test of a flat slab-column connection at *Faculdade de Ciências e Tecnologia, Universidade NOVA de Lisboa* in Portugal. The gravity load applied to the specimen was approximately equal to 50% of the concentric punching shear resistance of the specimen without shear reinforcement and it was kept constant throughout the test. The laboratory specimen was able to attain a 4.0% drift ratio before a sudden punching failure caused an immediate drop in the unbalanced moment transferred through the connection. Integrity reinforcement was provided to the specimen and it is assumed that the building also has integrity reinforcement that prevents progressive collapse once a punching failure occurs.

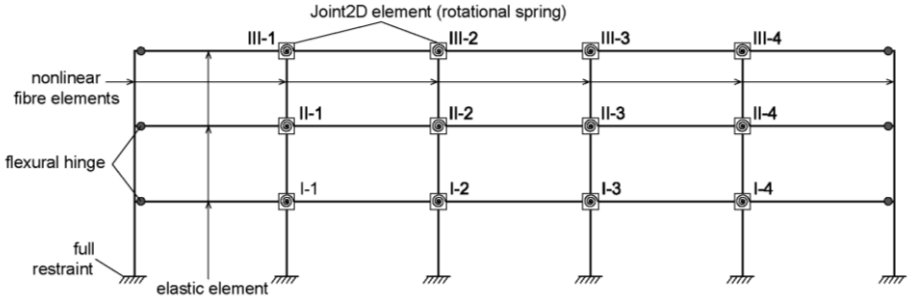

Figure 1: *OpenSees* model of the frame

It is assumed that punching shear failure at the exterior connections cannot occur, due to the presence of a beam and larger column dimensions. However, flexural failures are possible at the exterior connections and a plastic hinge is modelled at the end of the slab element (Figure 1). As a result of concentrating the nonlinearity to the joints, the slabs itself are modelled as elastic elements with cross section dimensions equal to those of the tested speci-

men (width 1850mm and depth 150mm). Nonlinear fiber elements are used to model the columns.

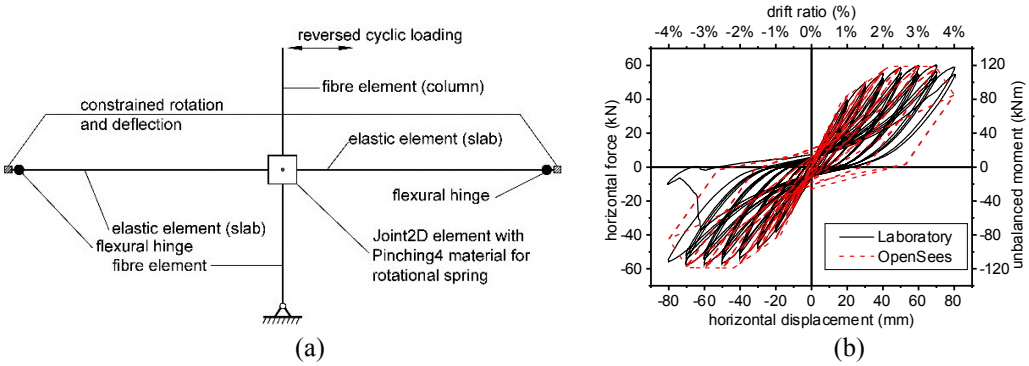

(a) (b)

Figure 2: a) Model used for calibration; b) comparison of experimental and numerical results

The interior slab-column joints are calibrated using the model shown in Figure 2-a, which adequately simulates the boundary conditions imposed by the test setup described in detail in [9]. From Figure 2-b it can be observed that the model is able to capture important aspects of the behavior of the tested specimen, such as pinching behavior, the backbone response and a close fit to the actual unloading response for low to medium range drift ratios.

3 RESULTS

The results of the simulation were processed in terms of maximum roof displacements and damage indices versus ground accelerations. The first were used as estimators of global collapse of the building, based on reference values from a pushover analysis. Local damage indices were defined as the ratio between the maximum joint rotation during the analysis and the ultimate rotation of the flat slab-column connection limited by punching failure. The overall damage indices were then estimated based on a weighting process on the basis of energy dissipation, similarly to the procedure described in [10] for the overall Park and Ang Damage Index. Four damage states specific for the flat slabs under consideration were defined based on the damage observed in the laboratory specimen for various slab-column joint rotation levels.

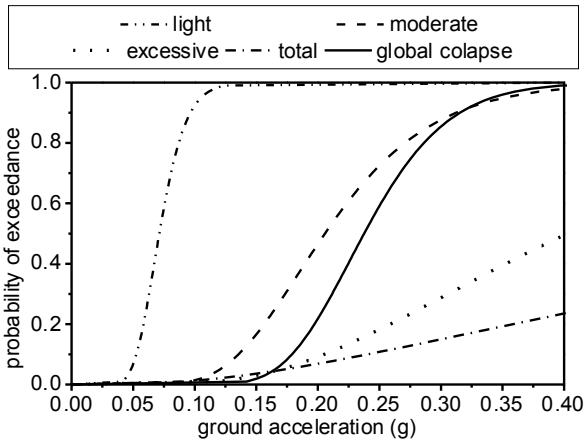

Figure 3: Fragility curves referring to damage in the flat slabs and an indicative global collapse curve

An estimate of the probability of exceedance for each damage state is evaluated for each ground acceleration level, based on the results of the IDA. The fragility curves are then represented by the lognormal cumulative distribution functions that best fit to the point estimates of

the same damage level by means of the “least squares”. Similarly, an indicative curve corresponding to global collapse of the building is derived based on maximum roof displacements observed during the IDA. It is plotted in Figure 3 alongside the flat slab fragility curves in order to compare the damage state of the flat slabs in relation to the probability of global collapse (governed by the failure of the columns).

4 CONCLUSIONS

Analytical model-based fragility curves were developed for a three story building with flat slabs calibrated using the reversed lateral cyclic loading test of a flat slab-column connection. *OpenSees* was used to perform modelling, sampling of input variables, nonlinear time history analyses and part of the post-processing of results. For the building under consideration, it was shown that the global structural behavior is not governed by punching of the flat slabs. Due to the presence of shear reinforcement, punching failures occurred at large drifts, in which the capacity of the vertical elements was exhausted. For the analyzed building, the punching shear reinforcement with shear studs was not only effective in the prevention of brittle punching failures, but it also contributed in the limitation of damage to the flat slabs.

REFERENCES

[1] "OpenSees," Pacific Earthquake Engineering Research Center, [Online]. Available: http://opensees.berkeley.edu. [Accessed 12 January 2017].

[2] CEN, *EN 1998-1, Eurocode 8: Design of structures for earthquake resistance - Part 1: General rules, seismic actions and rules for buildings,* CEN, 2004.

[3] SeismoSoft, "SeismoArtif," SeismoSoft, [Online]. Available: http://www.seismosoft.com/seismoartif. [Accessed 20 02 2017].

[4] A. Altoontash, Simulation and damage models for performance assessment of reinforced concrete beam-column joints (PhD thesis), Standfort, California, USA: Stanford University, 2004.

[5] L. N. Lowes, N. Mitra and A. Altoontash, "A Beam-Column Joint Model for Simulating the Earthquake Response of Reinforced Concrete Frames, PEER Report 2003/10," Pacific Earthquake Engineering Research Center, Berkeley, California, USA, 2004.

[6] M. A. Erberik and A. S. Elnashai, "Fragility analysis of flat-slab structures," *Engineering Structures,* vol. 26, p. 937–948, 2004.

[7] M. B. D. Hueste and J.-W. Bai, "Seismic retrofit of a reinforced concrete flat-slab structure: Part II — seismic fragility analysis," *Engineering Structures,* vol. 29, p. 1178–1188, 2007.

[8] H. Aslani and E. Miranda, "Fragility assessment of slab-column connections in existing non-ductile reinforced concrete buildings," *Journal of Earthquake Engineering,* vol. 9, no. 6, pp. 777-804, 2005.

[9] A. F. O. Almeida, M. M. Inácio, V. J. Lúcio and A. Pinho Ramos, "Punching behaviour of RC flat slabs under reversed horizontal cyclic loading," *Engineering Structures,* vol. 117, no. June, p. 204–219, 2016.

[10] Y. J. Park, A. H.-S. Ang and Y. K. Wen, "Damage-Limiting Aseismic Design of Buildings," *Earthquake Spectra,* vol. 3, no. 1, pp. 1-26, 1987.

OpenSees Days Europe 2017
1st European Conference on OpenSees
Porto, Portugal, 19–20 June 2017

NON-LINEAR DYNAMIC ANALYSES OF A 60'S RC BUILDING COLLAPSED DURING L'AQUILA 2009 EARTHQUAKE

Maria Gabriella Mulas[1] **and Paolo Martinelli**[1]

[1] Politecnico di Milano, Department of Civil and Environmental Engineering
Piazza Leonardo da Vinci 32, 20133, Milano, Italy
e-mail: {mariagabriella.mulas,paolo.martinelli}@polimi.it

Keywords: seismic collapse, RC non-ductile frame, obsolete code, shear failure, OpenSees platform, 3D nonlinear model.

Abstract. *This study presents the numerical simulation of the partial seismic collapse of a building during 2009 L'Aquila earthquake (Italy). The 7-story building was designed in the early '60s and is characterized by a reinforced concrete frame structure. In elevation, above a first basement and a ground floor, three wings rise. The collapse affected the North wing, where three separate collapse mechanisms were identified. All the columns at ground story failed with a weak-story mechanism in North-South direction. Three columns, located near the interface with the other wings, failed on the full height. In the same area, subjected to strong distortions due to the difference in vertical displacements following the weak-story mechanism, a third collapse mechanism involved (at stories 1-4) a beam supporting a non-structural wall inserted in recent renovation works. Previous investigations explained why the collapse was confined to the North Wing, providing the knowledge of the building to the date of the earthquake in terms of geometry, material properties, gravity loads and seismic input to the site. The building structural response during the earthquake as well as the sequence of the different mechanisms and their possible interdependence are investigated here. Nonlinear dynamic analyses on OpenSees adopt a refined 3D nonlinear FE model with beam-columns fiber elements and the components of the ground motion at site. Results up to the collapse onset satisfactorily simulate the identified collapse mechanisms clarifying the interaction and the likely sequence among the different mechanisms and the role played by the three wings during the earthquake.*

1 INTRODUCTION

During the April 6th 2009 earthquake of L'Aquila (Italy), a partial collapse causing a high death toll took place on a reinforced concrete (RC) building hosting an University dorm, 6 km away from the epicenter. This is one of the cases of failure of RC buildings in the urban area of L'Aquila (EERI Special Report 2009 [1]). The 7-story building including two underground stories had an irregular T-shaped plan composed of three nearly rectangular "wings" connected through a common stairwell (Fig. 1a). The building was designed in 1965, adopting the equivalent lateral forces approach of the Italian codes of 1937 and 1962. The collapse is connected to a complex building history involving several changes of property and intended use. The original design of the structural frame system was affected by an error that was brought to the light neither in the two changes of property nor in the design phase of the refurbishment intervention of 1999-2001.

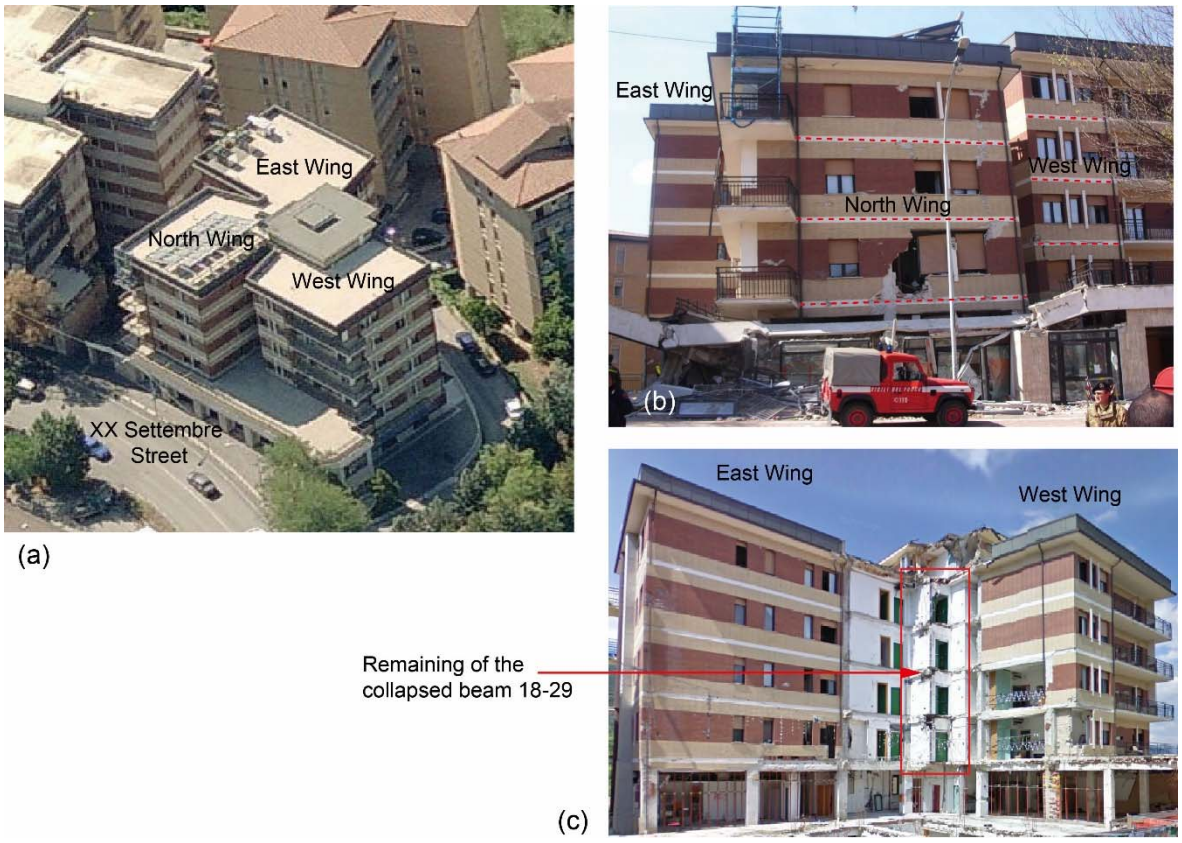

Figure 1: The student dorm building: (a) aerial view before the earthquake; (b) view before demolition of the collapsed North wing and (c) front view from XX Settembre Street after the removal of unsafe elements.

The partial collapse was limited to the North wing facing XX Settembre Street (Fig. 1a). Previous studies conducted for legal reasons [2], pinpointed the existence of multiple mechanisms in this wing. First, the failure of all ground floor columns, which triggered a weak/soft story mechanism in the North-South (N-S) direction (Fig. 1b). Then, at the interface with the other wings, failure of three columns along the whole height of the building and mid-span failure at floors 1-4 of the beam connecting columns 18 and 29 (see Fig. 1c). The beam was affected by the insertion of a non-structural wall during the renovation works. The lack of flexural strength of ground story columns was detected as the main cause of the collapse.

Given the availability of material properties, acting loads and geometric data on both the structure and the steel reinforcement, the collapse sequence is investigated through non-linear

dynamic analyses on a 3D numerical model of the whole building. The analyses have been performed with the OpenSees platform [3], using the accelerograms at the site. In [4] the collapse sequence of the North wing was simulated, and the role of the non-structural wall was examined. This paper summarizes the main findings obtained in [4] and [5].

2 NUMERICAL MODELLING OF THE BUILDING

The simulation of the seismic collapse is performed with the open–source platform OpenSees [3]. The beam–column fiber element with distributed inelasticity and force formulation, based on the Navier–Bernoulli's hypothesis, is selected for the FE model [6]. The geometric nonlinearity is included through a P–Δ formulation. Uniaxial material laws describe the hysteretic response of the materials. The modified Kent–Park model describes the response of the concrete fibers in compression. For concrete in tension, a linear elastic branch is followed by a linear softening branch up to zero stress to include the effect of tension stiffening. The well-known nonlinear model of Menegotto and Pinto is used for the steel fibers.

A comprehensive 3D model reproduces the building configuration of April 6th 2009 in terms of geometry, masses and stiffness of structural elements. One nonlinear fiber beam–column element is used for both columns and beams of the main resisting frames in each wing (denoted with solid lines in Figure 2b). Floors are modeled as rigid diaphragms. The FE model has 1835 nodes and 805 elements. Among them, 449 are nonlinear beam elements. Figure 2a presents a schematic view of the nodes and elements layout. The average values of material properties coming from on-site and laboratory tests are used for the unconfined concrete. The low amount of stirrups in both columns and beams and the lack of longitudinal reinforcement along the long sides of the rectangular cross-sections limit the confinement effect.

3 RESULTS AND CONCLUSIONS

The building first mode (T_1=0.99 s) mainly involves a translation along the N-S direction with a small torsional component. The second (T_2=0.95 s) and fourth (T_4=0.93 s) mode combine a translation of the floors in the N–S direction and a predominant torsional component. The third mode (T_3=0.38 s) involves a translation of the floors in both the E–W and N–S directions without torsional component. The response to the ground motion is analyzed first in terms of nodal displacements in Figure 2b. The orbits of the displacements at the top floor in the X-Z plane are analyzed for the corner nodes and for those corresponding to the two interior columns collapsed over the entire height of the building (within a red circle in Figure 2b). The prevailing displacement component is directed along the Z axis (N-S direction). This is the direction both of the North wing frames, the only ones to resist significantly to horizontal forces in this direction, and of the first mode shape. Due to the rigid diaphragm assumption, the corner nodes of the three wings move in a similar way. In spite of the displacement magnitude, columns in the East and West wings have not suffered significant damage, since their reinforcement layout is designed to withstand moments about the Z-axis and their weak axis is aligned on the strongest earthquake direction (Z-axis in Fig. 2b). Consequently, these columns are not highly stressed despite high displacement values detected at the top floor. A not negligible torsional effect is also visible in Figure 2b.

To evaluate the structural response, internal forces are compared to the corresponding resistances. The variable truss model proposed in the Italian code is adopted to assess the shear capacity. For the ground story columns of the North Wing, the shear demand exceeds the capacity in closely spaced time instants, indicating their almost simultaneous failure. Moreover, the analysis of shear force and bending moment time histories has pointed out that the ultimate shear capacity is reached before the complete development of flexural resistance. The numerical

analyses have highlighted a weak-story mechanism, which caused the crushing of columns at ground story. This result, as the pattern of displacements along the N-S direction (the strong direction of the main frames of the North Wing), is in excellent agreement with the situation observed immediately after the earthquake. The numerical results indicate that the building developed a bidirectional resistance, but the demand was not distributed as the masses in each wing. The East and West wings attract around 80% of the total base shear V_x along the E-W direction. A completely different trend was observed along the N-S direction, where the North wing attracts more than 50% of the total shear actions V_z.

It is concluded that the time-histories analyses have simulated successfully the collapse mechanisms. The result is remarkable because no model updating or tuning of the parameters was pursued. Further studies should address the simulation of the incremental collapse, taking into account the large relative displacements arising at the interior edge of the North wing.

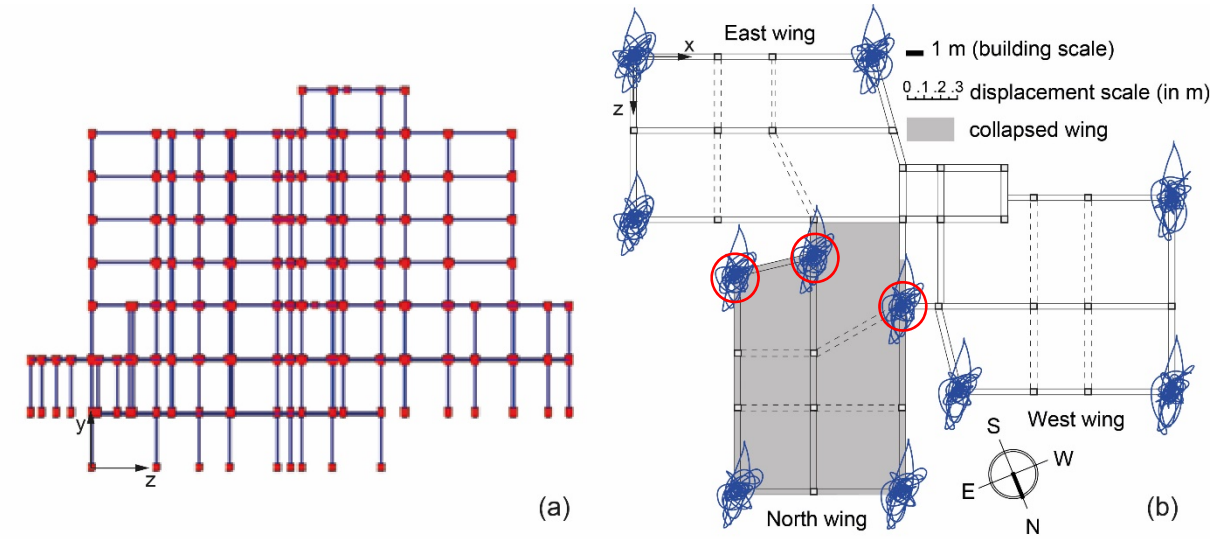

Figure 2: (a) FE model for the whole structure: view in the Z-Y plan, North (right) and East (left) wings; (b) representation of the displacement orbits at the top floor. Columns collapsed along the height within red circles.

REFERENCES

[1] EERI Special Earthquake Report. *Learning from Earthquakes. The M_w 6.3 Abruzzo, Italy, Earthquake of April 6, 2009*. June 2009.

[2] M.G. Mulas, F. Perotti, D. Coronelli, L. Martinelli, R. Paolucci. The partial collapse of "Casa dello Studente" during L'Aquila 2009 earthquake. *Engng Fail Analysis*, 2013(34): 566-584.

[3] F. McKenna, G.L. Fenves, M.H. Scott. Open system for earthquake engineering simulation. Univ. of California, Berkeley, Calif.; 2000. <http://opensees.berkeley.edu> [25.11.16].

[4] M.G. Mulas, P. Martinelli. Numerical simulation of the partial seismic collapse of a 60's RC building. Submitted for possible publication to *J. Perf. Constr Fac*, ASCE, Jan. 2017.

[5] M.G. Mulas, P. Martinelli, S. Capriotti. Non-linear dynamic analyses of a RC frame building collapsed during L'Aquila 2009 earthquake, Compdyn 2017, accepted.

[6] E. Spacone, F.C. Filippou, F.F.Taucer. Fibre beam–column model for non-linear analysis of R/C frames. Part I: formulation. *Earthq Eng Struct Dyn* 1996a; 25 (7): 711–25.

OpenSees Days Europe 2017
1st European Conference on OpenSees
Porto, Portugal, 19–20 June 2017

A GENETIC ALGORITHM AIMED AT OPTIMISING SEISMIC RETROFITTING OF EXISTING RC FRAMES

C. Faella, R. Falcone, C. Lima, E. Martinelli

Department of Civil Engineering, University of Salerno
Via Giovanni Paolo II, 132 – Fisciano (SA), Italy
e-mail: c.faella@unisa.it; rfalcone@unisa.it; clima@unisa.it; e.martinelli@unisa.it

Keywords: Seismic retrofitting, Optimisation, RC frames, Steel bracings, Confinement

Abstract. *This paper presents a novel numerical procedure based on a dedicated genetic algorithm aimed at selecting the "optimal" retrofitting solution among the technically feasible ones obtained by combining structure- and member-level techniques. Specifically, both steel bracing systems, considered as structure-level intervention, and FRP-confinement of under-designed RC members, thought-out as member-level technique, are taken into account for achieving the retrofitting objectives within the conceptual framework of a multi-level Performance-Based approach. OpenSEES is one of the main "characters" of the numerical procedure, as it is intensively utilised for running the analyses that are needed for determining the seismic performance of the RC frame under consideration strengthened by means of a set of structure- and member-level interventions representing the generic "individual" of the current "generation" of the genetic algorithm. The paper focusses on describing the interactions between OpenSEES and the aforementioned genetic algorithm implemented by the Authors in Matlab. Specifically, the main data structures and subroutines are outlined with the aim to show how input and output operations in/from OpenSEES are handled. Particularly, the paper describes how basic mechanisms inspired to the well-known Theory of Evolution by Charles Darwin are transposed to the problem under consideration. It is worth highlighting that executing the Non Linear Static (NLS) analyses requested for assessing the actual effect of seismic strengthening interventions represents the most computationally demanding and time consuming operation in the whole numerical procedure. Therefore, the paper gives some details about some specific measures taken in implementing the numerical procedure with the aim to enhance computational efficiency without affecting simulation accuracy.*

1 INTRODUCTION

Seismic retrofitting of existing RC structures can be achieved by means of either member- or structure-level techniques. The former aims at increasing capacity in under-designed members (i.e. FRP confinement of columns), the latter are rather intended at introducing new substructures (i.e. steel bracings systems) intended at reducing seismic demand on the existing frame. In principle, those techniques may be also combined with the aim to obtain a synergy in reaching the target performance objectives [1]. However, no well-established rules are currently available for choosing their "optimal" combination, as the solution of this complex optimization problem would require meta-heuristic numerical methods. The general procedure proposed herein is based on a genetic algorithm [2] inspired to the Darwin's "evolution of species" concept [3]. It is developed in Matlab and OpenSEES [4] is employed in performing the NonLinear Static Analyses (NSA) needed for quantifying the values of the objective function for each combination of member- and structure-level techniques. The present paper focuses on the role of OpenSEES within the present numerical procedure and the influence of alternative modelling choices on the resulting computational effort.

2 OVERVIEW OF THE GENETIC ALGORITHM

The optimal retrofitting solution $\boldsymbol{x}_{opt}$ is obtained by combining member- and structure-level techniques by solving the following constrained problem:

$$\boldsymbol{x}_{opt} = \arg\min\left[C_{tot}\left(\boldsymbol{x}\right) + \Phi_{pen}\left(\boldsymbol{x}\right)\right] \tag{1}$$

subjected to the respect of the Limit State function $g_{LS,i}$

$$g_{LS,i}\left(\boldsymbol{x}\right) = C_{LS,i}\left(\boldsymbol{x}\right) - D_{LS,i}\left(\boldsymbol{x}\right) \geq 0 \quad \forall i = 1...n_{LS}\,, \tag{2}$$

where $C_{LS,i}$ and $D_{LS,i}$ are, respectively, the capacity and the demand at the i-th relevant Limit State under consideration. Moreover, $C_{tot}(\mathbf{x})$ represents the total cost of intervention and Φ_{pen} is the penalty function intended at increasing the nominal cost of those technical solutions that do not respect the retrofitting objective (Eq. 2). The main steps of the proposed meta-heuristic strategy are shown in the conceptual flow-chart of Figure 1.

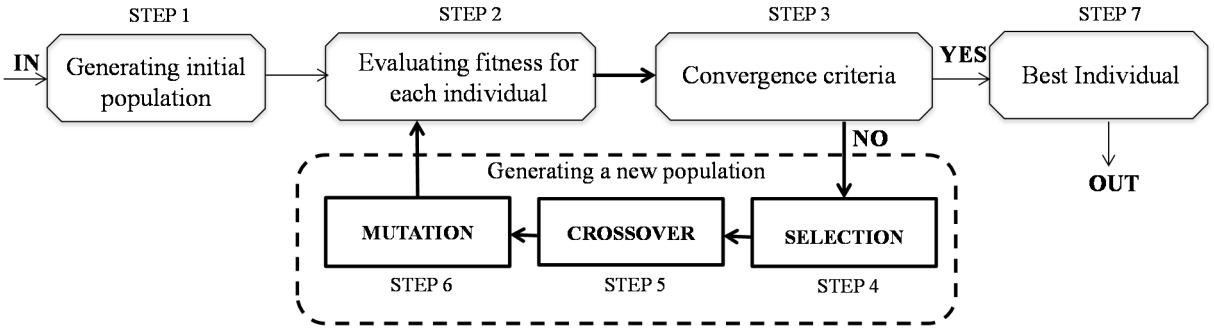

Figure 1: Flow-chart of the optimization procedure

The vector **x** collects the design variables: it consists of both FRP confinement of RC columns (member-level technique) and concentric X-shape steel bracings (structure-level technique). Fig. 2 describes a generic array of bits corresponding to the codified version of a generic combination of member- and structure-level techniques under consideration.

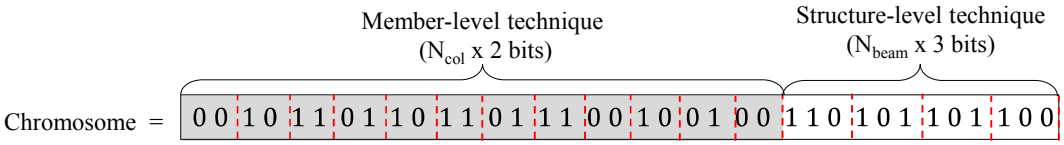

Figure 2: Example of binary genotype describing a retrofitting intervention

An initial "population" of n individuals $\boldsymbol{x}$ is randomly generated at the beginning of the procedure. Nonlinear Static Analyses (NSA) are performed on the models obtained by merging the existing RC frame and the intervention described by each one of the aforementioned individuals. The analysis results are elaborated with the aim to determine a "fitness function" measuring the capability of each individual to achieve the target performance objectives. This function is used for obtaining the next generation individuals by means of selecting three fundamental operators, namely selection, crossover and mutation, intended at reproducing the key evolutionary mechanisms. Specifically, the "selection" operator selects "parents" based on the "survival of the fittest" principle: individuals with higher fitness function values have higher probability of surviving and reproducing their features in the next generation. Then, "crossover" combines segments of the selected individuals into new "offspring" solutions by commuting their genetic information. Finally, "mutation" randomly changes the value of single bits (from 0 to 1 or *vice versa*). Once the second generation of individuals is created the procedure goes on iteratively, until convergence is achieved. It is worth highlighting that parallel computing is adopted for carrying out the NSA requested for quantifying fitness functions across the current generation.

3 FIRST RESULTS ON THE COMPUTATIONAL EFFICIENCY

Two different approaches can be used for simulating mechanical nonlinearity of frame elements: concentrated plasticity and spread plasticity models. In concentrate plasticity models, inelastic resources are concentrated at the end element in the so-called "plastic-hinges" region, while the central part of the beam is simulated by a linear elastic element (Fig. 3,a). Otherwise, a fiber approach is used in distributed plasticity models. In this case, the structural element is discretized into a number fibers which account for material nonlinear behaviour and sectional integration is performed at the Gauss quadrature integration points (Fig. 3,b). OpenSEES allows to simulate distributed plasticity elements by means of both force- and displacement-based formulation related to the different approach used for solving the static problem. In this paper only force-based distributed plasticity elements (namely "nonlinearbeamcolumn") with five Gauss points are taken into account and the results are compared with the ones obtained by modelling RC elements with plastic-hinges approach (namely "beamWithHinges" command).

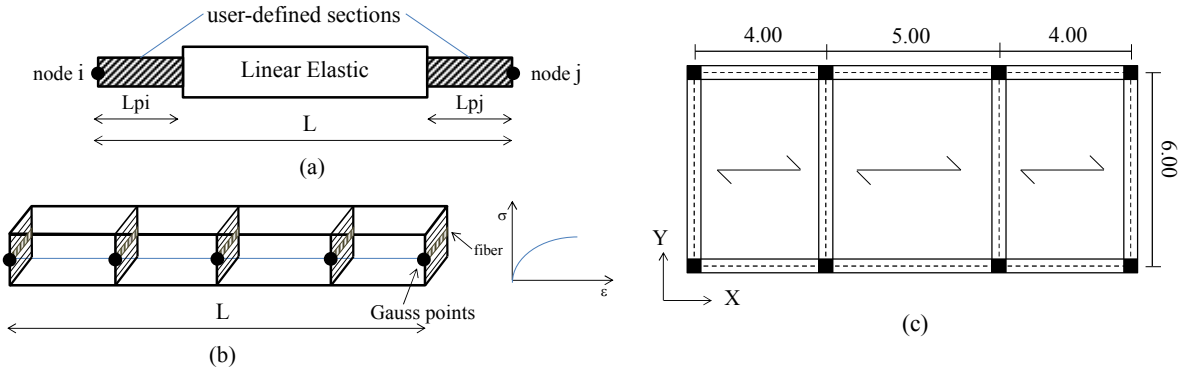

Figure 3. "Plastic-hinges" (a) and "fiber" models (b); in plane configuration of the analyzed structure (c)

A simple 3D three-storey RC frame (Fig. 3,c) is considered as a preliminary case-of-study. The two aforementioned models are analyzed and the computation time needed to execute NSA is compared (Fig. 4). Both stiffness and post-elastic branch obtained by means of the two models are significantly different. The slope of hardening branch and the maximum strength are higher in the fiber model (Fig. 4,a). However, the computational effort needed by the spread plasticity model (Fig. 4,b) is 40 % higher than the corresponding time required for carrying out the same non-linear static analysis on the plastic-hinges model.

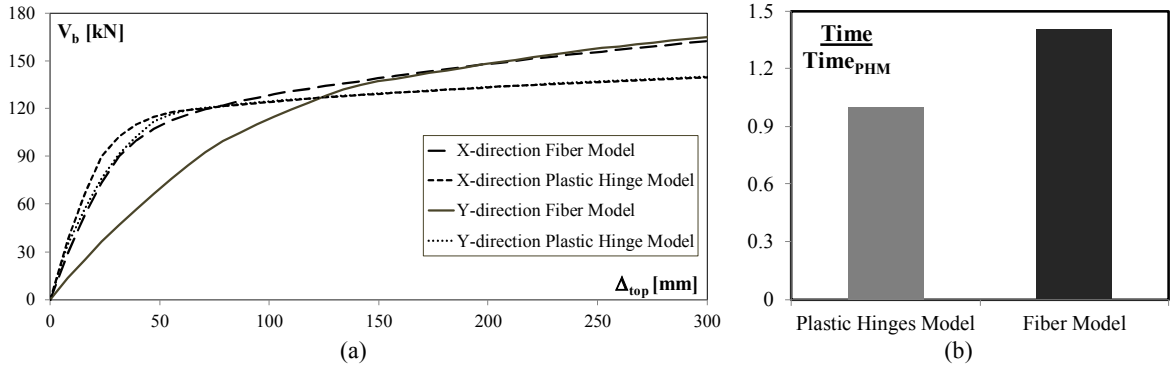

Figure 4. Pushover curves (a) and comparison of the computational time (b)

4 CONCLUSION

A rational procedure intended at optimizing seismic retrofitting of existing structures by combining member- and structure-level techniques is being developed by the authors. Despites the limitations of the current state of development it is a promising tool for approaching a subject of high relevance. Current research is devoted at enhancing the computational efficiency of the programming code. In fact, almost 94% of the total computational time of the procedure is taken by seismic analysis in OpenSEES, whereas the 6% only refers to pre- and post-processing operations handled by the genetic algorithm. Different modelling strategies are actually under investigation by considering various approaches in simulating nonlinearity of RC members, steel bracings, floor diaphragms and so on. The first results herein outlined about the nonlinear simulation of beam and column elements encourage the authors at using concentrated plasticity elements.

REFERENCES

[1] E. Martinelli, C. Lima, C. Faella, Towards a rational strategy for seismic retrofitting of RC frames by combining member- and structure-level techniques. *SMAR2015 – Third Conference on Smart Monitoring, Assessment and Rehabilitation of Civil Structures*, Antalya (Turkey), September 6-9, 2015.

[2] J.H. Holland, *Adaptation in natural and artificial systems*. Ann Arbor, University of Michigan Press, Michigan 1975.

[3] C. Darwin, *On the Origin of Species by means of Natural Selection or the Preservation of Favored Races in the Struggle for Life (The Origin of Species)*. Murray, London 1859.

[4] S. Mazzoni, F. McKenna, M.H. Scott, G.L. Fenves, et al., *OpenSEES command language manual*. Pacific Earthquake Engineering Research (PEER), 2006.

OpenSees Days Europe 2017
1st European Conference on OpenSees
Porto, Portugal, 19–20 June 2017

NUMERICAL MODELLING OF RC COLUMNS WITH PLAIN REINFORCING BARS

J. Melo[1], H. Varum[1], and T. Rossetto[2]

[1] Civil Engineering Department, Faculty of Engineering, University of Porto, Porto, Portugal
{josemelo, hvarum}@fe.up.pt

[2] EPICENTRE, Department of Civil, Environmental & Geomatic Eng., University College of London, UK
t.rossetto@ucl.ac.uk

Keywords: RC columns, plain reinforcing bars, bond-slip, numerical modelling.

Abstract. *The earthquakes induce cyclic loading on the existing reinforced concrete (RC) structures that may lead to bond degradation and significant bar slippage. The bond-slip mechanism is reported to be one of the most common causes of damage and even collapse of existing (RC) structures subjected to earthquake loading. RC structures with plain reinforcing bars, designed and built prior to the enforcement of the modern seismic-oriented design philosophies, are particularly sensitive to bond degradation. However, currently perfect bond conditions are typically assumed in the numerical analysis of RC structures.*

This paper describes the numerical modelling of the cyclic response of two RC columns, one built with deformed reinforcing bars and another with plain bars, both with structural detailing similar to that typically adopted in pre-1970s structures. The numerical models were developed on the OpenSees framework and calibrated with the available tests results. The bond-slip effects were included in the models developed resorting to a simple modelling strategy. Several linear fiber elements were used and the numerical results were compared to the experimental results.

1 INTRODUCTION

In the analysis of RC structures, perfect bond is usually assumed, i.e. considering compatibility between concrete and reinforcement strains at each structural member point. However, this assumption is only correct for early loading stages and low strain levels. For large loads, cracking and bond failure will occur and bar slippage takes place in the structural elements [1]. Considering the assumption of perfect bond conditions may lead to predicted lateral deformation significantly smaller than the real element deformation or to predicted lateral stiffness larger than the existing element stiffness [2]. Bond-slip effects should therefore be included in the numerical models of structural analysis to represent more accurately the elements response as stated [3].

The numerical modelling of the cyclic response of two analogous RC columns is here presented. One with deformed reinforcing bars and another with plain bars, both with structural detailing similar to that typically found in RC structures designed and built before the 1970s (that is, without specific details for seismic demands). For each column, different models and linear elements were used in the OpenSees numerical models. Attention was given to the effects of bar slippage, which were incorporated in the OpenSees models resorting to a simple modelling strategy. The results of the cyclic tests previously conducted on the columns were used to calibrate the adopted models. After describing the models, comparisons are established between the numerical and experimental results to conclude about their adequacy to simulate the columns response, and about the importance of including the effects of bar slippage.

2 SPECIMENS DETAILING AND NUMERICAL MODELS

2.1 Specimens detailing and material properties

The specimen detailing and material properties can be found in [4]. Specimen CPA-3 and specimen CD were built with plain and deformed reinforcing bars, respectively. Both specimens have the same geometry dimensions and amount of steel reinforcement and were built in full-scale. The imposed loading conditions and the lateral displacement history (d_c) are shown in Figure 1. The lateral displacements were imposed at 1.7m from the column base (see Figure 1a). The axial load (N) was kept constant during the tests and equal to 305kN. The axial load imposed by the testing setup is centered at the column' base and consequently P-delta effects are not considered.

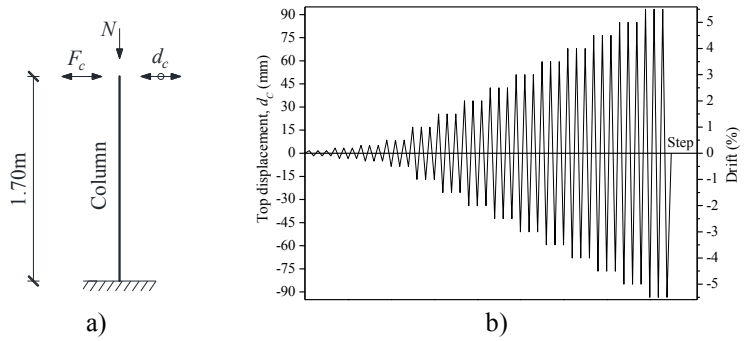

a) b)

Figure 1. a) Support and loading conditions idealized; b) imposed lateral displacement history.

2.2 Numerical modelling with OpenSees

For each column specimen, four nonlinear models were developed, namely: i) with *nonlinearBeamColumn element*, i.e. with distributed plasticity; ii) with *BeamWithHinges element*, in which the plasticity is concentrated over specified hinge lengths at the element ends; iii) with

nonlinearBeamColumn element and *zero-length section element*; and, iv) with *BeamWithHinges element* and *zero-length section element*. The *zero-length section element* was incorporated to simulate the bar slippage effects associated with the strain penetration and the bond-slip mechanism.

In the numerical models, the *Concrete02* model and *Steel02* model were adopted for the concrete and steel reinforcement, respectively. It should be noted that the elastic part of the *BeamWithHinges element* was modelled using an elastic material with the same elastic modulus of the concrete. The *Concrete02* model was also assigned to the concrete fibres of the *zero-length section element*. All model parameters can be found in [4].

3 NUMERICAL RESULTS

3.1 Numerical results of the specimen with plain reinforcing bars

The comparison of the experimental force-drift diagrams for the column with plain reinforcing bars with those obtained from the numerical models under investigation is shown in Figure 2. The best-fit to the experimental results was obtained by the OpenSees model with concentrated plasticity (*BeamWithHinges element*) and considering bar slippage (*zero-length section element*).

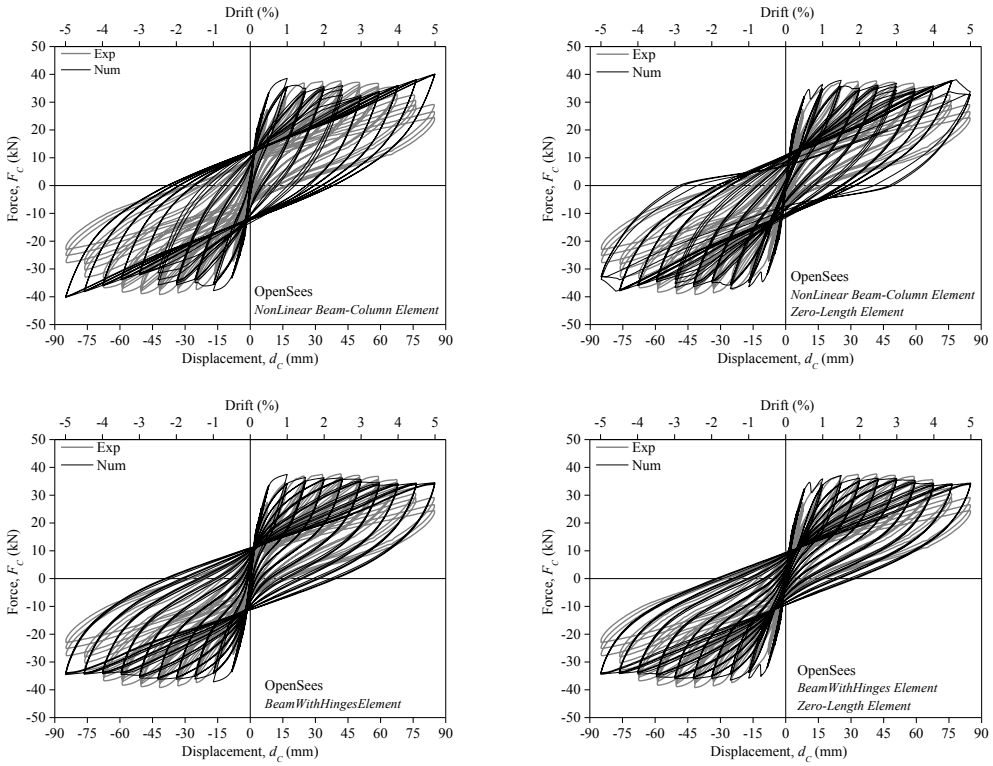

Figure 2: Comparison between the experimental and numerical force-drift diagrams of specimen CPA-3

3.2 Numerical results of the specimen with deformed reinforcing bars

Figure 3 compares the experimental force-drift diagrams with those obtained from the numerical models under investigation. As concluded for the specimen with plain bars, the best-fit to the experimental force-drift response was obtained with *BeamWithHinges element* and *zero-length section element*.

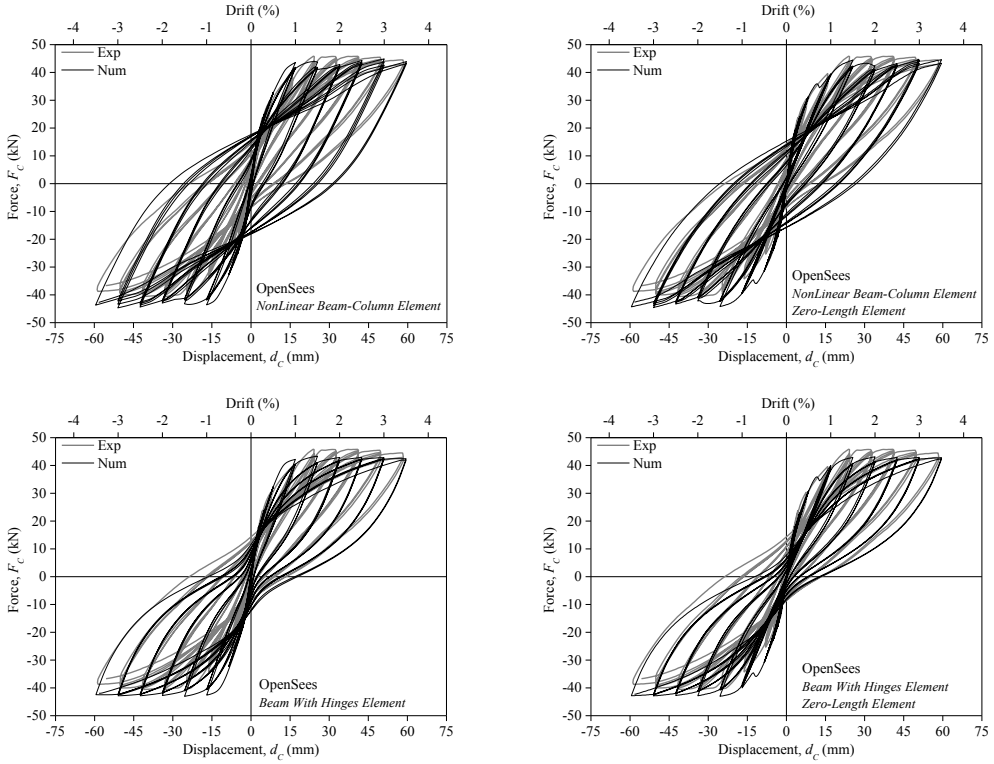

Figure 3: Comparison between the experimental and numerical force-drift diagrams of specimen CD

4 CONCLUSIONS

- All developed models, generally, provided a satisfactory simulation of the experimental force-drift diagrams. However, any of the models could properly capture the strength degradation, nor the stiffness of the reloading branches, nor the pinching effect.
- For both column specimens, a better agreement between the numerical and experimental results (in terms of force, stiffness and energy dissipation) was obtained considering the non-linearity concentrated in the plastic hinge regions. This was particularly relevant for the column with plain reinforcing bars, namely in terms of stiffness evolution and energy dissipation.

REFERENCES

[1] G. Monti, E. Spacone, Reinforced concrete fiber beam element with bond-slip. *Journal of Structural Engineering*, **126**, 6:654-661, 2000.

[2] H.G. Kwak, Improved numerical approach for the bond-slip behavior under cyclic loads. *Structural Engineering and Mechanic,* **5**, 5:663-677, 1997.

[3] J. Melo, C. Fernandes, H. Varum, H. Rodrigues, A.G. Costa, A. Arêde, Numerical modelling of the cyclic behaviour of RC elements built with plain reinforcing bars. *Engineering Structures,* **33**, 2:273-286, 2011.

[4] Melo J. Characterization of the cyclic behaviour of reinforced concrete elements with plain bars. PhD thesis, Aveiro University, Portugal, 2014.

OpenSees Days Europe 2017
1st European Conference on OpenSees
Porto, Portugal, 19–20 June 2017

IMPROVED DRIFT ASSESSMENT APPROACH FOR STEEL MOMENT FRAMES UNDER REALISTIC EARTHQUAKE LOADING

Borjan S. Petreski[1], **Mihail A. Garevski**[1*]

[1] Institute of Earthquake Engineering and Engineering Seismology
Todor Aleksandrov Str., 165, P.O. Box 101, 1000 Skopje, Republic of Macedonia
e-mail: borjan@pluto.iziis.ukim.edu.mk
[*]e-mail: garevski@pluto.iziis.ukim.edu.mk

Keywords: steel structures, MRFs, concentrated plasticity, OpenSees, stiffness deterioration, performance based assessment.

Abstract. *This research studies an improved performance based assessment method of steel moment resisting frames (MRFs) through alternative modelling of the structure subjected to realistic earthquake loading. The improvement is evaluated through a comparison of two different modelling approaches for design and assessment of the MRFs. The initial approach for modelling of the steel frame is the distributed plasticity approach using fibre discretization of nonlinear beam - column elements. On the other hand, the improved method is represented via the lumped plasticity modelling characterized by elastic beam - column elements ending with plastic hinges. For the distributed plasticity approach a bilinear steel material is used while for the plastic hinges of the concentrated plasticity approach, a stiffness deterioration model is applied by means of the OpenSees software framework. To simulate the realistic earthquake loading two sets of seven far-field ground motion records scaled to match the Eurocode 8 (EC8) design spectra are used, representing both the medium seismicity and the high seismicity scenarios. Both sets are used in three separate analyses denoting three different performance targets to control the level of drift at design level earthquake, near collapse and collapse level earthquake. The structure investigated is a three bay, six story steel moment frame designed following the Eurocode 8 provisions. For the sake of complying with the Eurocode 8 requirements for the limitation of the inter-story drifts, the frame subjected to the high-hazard scenarios is slightly modified. The performance evaluation presented focuses on the use of the floor drifts as the basic parameters for performance assessment. The story drift is the only parameter used in this discussion as the intent is to evaluate the performance of the structures according to current guidelines and procedures. Alternatively, in order to obtain more information about the behaviour of the structure and to compare the new findings with already existing work in the field, some other structural characteristics are being recorded in the analyses performed such as the floor accelerations and beam rotations. In the end, the focus is set on the relations, similarities and deviations between the recorded inter-story drifts (maximum and residual), and the existing requirements and recommendations in the European and American codes of practice.*

1 INTRODUCTION

There are plenty of research findings on the evaluation of the realistic drifts of the steel MRFs and their comparison with the existing codes of practice. It is shown that EC8 requirements regarding the drift are a lot more rigorous than the provisions in other earthquake design codes, specifically characterized by the stability factor (θ). This factor, as a result of the strict drift and stability constraints and the sensitivity of the moment resisting frames to the lateral deformation effects, can often govern the design, resulting in over-strength which reduces the ductility demand of the structure and affects the loads acting on it, especially if a high ductility factor is adopted [1]. Other research investigating the structural behaviour of steel moment resisting frames also observed that EC8 provisions are highly conservative while the US provisions seem to under-predict the global and maximum drift modification factors. It also points out the oversimplified nature of drift demand criteria adopted in the design codes, particularly in the European codes of practice [2].

In this research paper an improved approach for evaluating the steel moment frames' behaviour is implemented in order to tackle the deficiency in the assessment of this type of structures. Using the finite element program OpenSees, a six story – three bay moment resisting frame is modelled and analyzed.

2 DEFINITION OF MODELS AND ANALYSIS PROCEDURES

2.1 Distributed plasticity model

Firstly, the modelling is performed using the nonlinear beam - column elements with distributed plasticity and a bilinear steel material from the OpenSees database [3] for both the beams and the columns. These elements permit the spread of plasticity along the element using pre-defined number of Gauss points and are quite useful for capturing the axial force-moment interaction. On the other hand, their main characteristic is the fibre discretization which is very sensitive and needs pre-calculations.

2.2 Concentrated/Lumped plasticity model

Consequently, the same frame model is constructed using the elastic beam - column elements ending with zero-length plastic hinges modelled by a stiffness deteriorating steel material. The deterioration model used [4] presents the breakthrough of the use of the deteriorating stiffness models in the field of earthquake engineering. This model which is afterwards improved to refer to the asymmetric element hysteretic performance, incorporating varying rates of cyclic deterioration in the two separate loading directions is shown in Fig. 1.

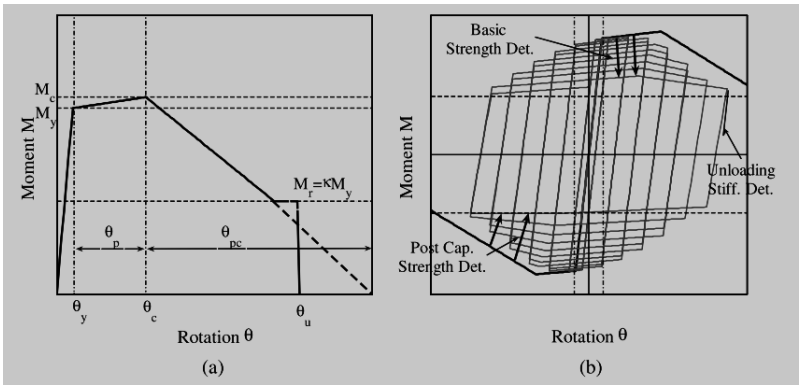

Figure 1. – IK deterioration model: (a) monotonic curve; (b) basic modes of cyclic deterioration and associated definitions [5]

The stiffness deteriorating springs in the concentrated plasticity model are placed only at the ends of the beams as the intention is to limit the occurrence of plastic hinges during realistic earthquake loading in the beams of the structure (weak beam – strong column rule).

2.3 Scenario and intensity based performance assessment

According to the scenario based performance assessment, two sets of seven acceleration records are chosen as realistic earthquake loading to represent the medium seismicity (MH) and high seismicity (HH) scenarios. They are extracted from the database and scaled to match the EC8 elastic spectra for the two hazard scenarios with PGA = 0.25g and PGA = 0.35g.

Regarding the intensity levels, three levels of transient dynamic loading are considered. In EC8 the levels of the seismic action on structures are defined as the design earthquake scenario considering 100% intensity of the ground motion and near collapse scenario represented with 175% of the ground motion intensity. Additionally, collapse level subjecting the structure to 350% increased realistic ground motion is performed.

3 MATERIAL STIFFNESS DETERIORATION EFFECT

It is not satisfactory to state that the comparison of the two frames is only due to the different plasticity modelling of the structural elements. Another essential segment of the full image about the study is the stiffness and strength deterioration material property assigned to the hinge elements of the concentrated plasticity approach. In order to clarify the differences that the deterioration model generates in the steel moment frame response evaluation, a simple pushover analysis is performed. The results of the analysis are shown in Fig. 2.

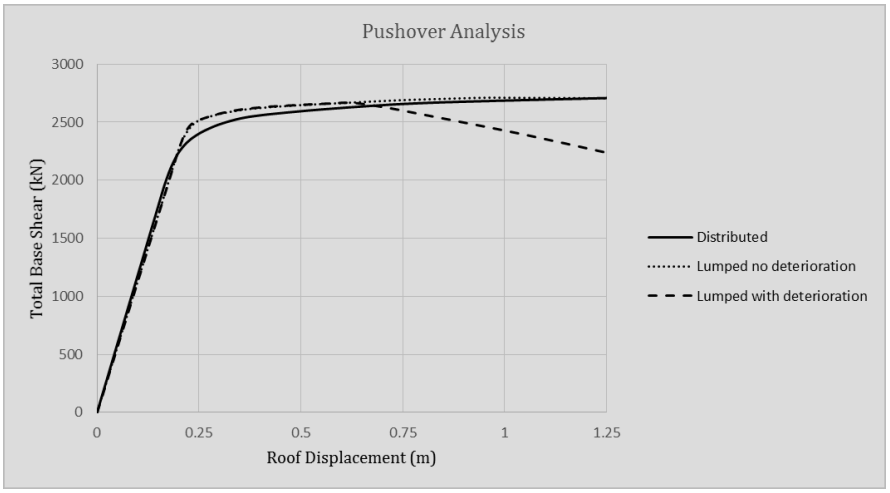

Figure 2. Pushover analysis curves

The general contrast between the approaches compared in the study can be observed from the graph above. Until the roof displacement measures about 3% of the total building height (0.66 m), the three frames behave similarly, but after that displacement limit the strength and stiffness deterioration of the material in the lumped plasticity model starts influencing the push-over curve and the base shear capacity of the investigated frame starts decreasing.

4 CONCLUDING REMARKS

Eventually, the lumped and distributed plasticity models' drift demands vary differently at different performance levels investigated. In general, the lumped plasticity model experiences greater drift demand which might be negligible within the lower loading intensity degrees. The

main difference between the models is evaluated to occur at greater levels of inelasticity represented with more intense seismic loads and total drift value of around 3% shown in Fig. 3. That value presents the global frame's stiffness degradation zone when the strength and stiffness deterioration property of the lumped plasticity hinge regions occurs.

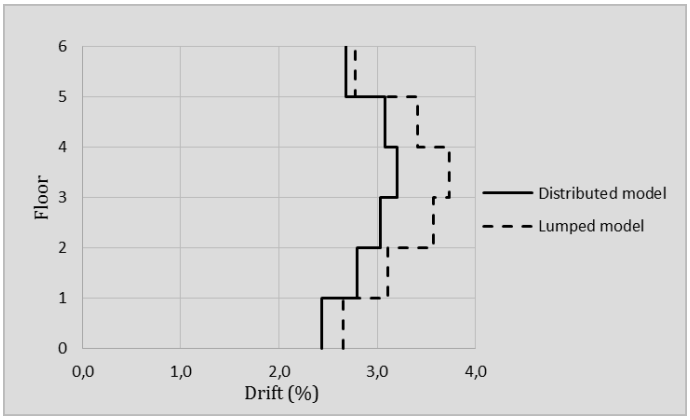

Figure 3. Comparison of floor drift distribution along the height at 350% intensity level (MH)

Model	Total frame drift (%)	Total frame displacement (m)
Distributed	2.71226000	0.597
Lumped	3.02523857	0.666

Table 1. Comparison of total frame drift at 350% intensity level (MH)

In the end, general compliance of the models with previous study parameters and design codes provisions is observed. The elastic behaviour of the structure satisfies the European code limitations which it is being designed for. Also, based on FEMA 273 recommendations [6] the MH and HH frames fit in the same performance level classes for the equivalent intensity level transient analyses according to the maximum and residual drift limit indicators.

REFERENCES

[1] A. Elghazouli, Assessment of European seismic design procedures for steel framed structures. *Bulletin of Earthquake Engineering*. 8 (1), 65-89, 2010.

[2] M. Kumar, P. Stafford, A. Elghazouli, Influence of ground motion characteristics on drift demands in steel moment frames designed to Eurocode 8. *Engineering Structures*. 52, 502-517, 2013.

[3] OpenSees – OpenSees Version 2.4.3., http://opensees.berkeley.edu/index.php, 2015.

[4] L. F. Ibarra, R. A. Medina, H. Krawinkler, Hysteretic models that incorporate strength and stiffness deterioration. *Earthquake Engineering and Structural Dynamics*. 34 (12), 1489-1512, 2005.

[5] D. G. Lignos, H. Krawinkler. Deterioration modeling of steel components in support of collapse prediction of steel moment frames under earthquake loading. *Journal of Structural Engineering* 137.11: 1291-1302, 2010.

[6] ATC. Seismic Performance Assessment of Buildings, 90% Draft. ATC-58-1, *Applied Technology Council edition*. Redwood City, California, 2011.

OpenSees Days Europe 2017
1st European Conference on OpenSees
Porto, Portugal, 19–20 June 2017

ASSESSMENT OF THE SEISMIC PERFORMANCE OF STEEL FRAMES USING OPENSEES

Sara Oliveira[1], Filippo Gentili[1], Ashkan Shahbazian[1], Hugo Augusto[1], Ricardo Costa[1], Carlos Rebelo[1], Yukihiro Harada[2] and Luís Simões da Silva[1]

[1] ISISE, Department of Civil Engineering, University of Coimbra, Portugal
Rua Luís Reis Santos - Pólo II, Coimbra, Portugal
e-mail: saradiogodeoliveira@gmail.com
{filippo.gentili, shahbazian}@uc.pt
{hugo.augusto, rjcosta, crebelo, luisss}@dec.uc.pt

[2] Department of Architecture, Chiba University, Japan
1-33 Yayoi, Inage, Chiba, Japan
e-mail: yharada@faculty.chiba-u.jp

Keywords: steel structures, beam-to-column joints, component method, macro-elements, dual concentrically braced frames, OpenSees.

Abstract. *The prediction of the behavior of beam-to-column steel joints is an important task in order to achieve economical and sustainable structures. The steel joints play a crucial role in the overall seismic behavior of steel frame structures, since the deformations in the panel zone of the beam-to-column joint region significantly affect the seismic behavior of steel joints. Therefore, an accurate modelling of the beam-to-column joint is essential. This paper aims at assessing the seismic performance of Dual Concentrically Braced Frames (D-CBF) through static and incremental dynamic nonlinear analyses. The parametric study was carried out on ten D-CBF where structural properties as number of stores, number of bays and the length span were varied. The analyses were implemented in OpenSEES using appropriate models for the nodal zones.*

1 INTRODUCTION

The RFCS project EQUALJOINTS (European Commission Directorate General for Research and Innovation) has been carried out research on the seismic behavior of steel beam-to-column joints at European level, aimed at predicting deformation capacity and cyclic performance of certain connections typologies commonly used in Europe. The dual concentrically braced frames (D-CBF) are one of the typical frames selected to study and estimate the seismic demand of the semi-rigid partial strength joints in the European project and presented in this paper.

This paper briefly describes the estimation of the seismic demand of the semi-rigid partial strength joint in typical D-CBF on bases of non-linear static analysis (pushover analysis) and nonlinear time history analysis. Numerical models were created by Gentili et al. [1] in order to perform the analysis using Open System for Earthquake Engineering Simulation (OpenSees) [2]. This paper presents the modelling alternative in which the internal node joints are represented by a "scissor"-type model.

2 SIMPLIFIED NUMERICAL MODELS

2.1 Parametric study on D-CBF

A parametric study was carried out only considering the scissor model (see right side of Figure 1) for ten D-CBF studied to cover various structural configuration with different number of stories and bays and length of spans (presented in Table 1). The D-CBF were designed within the scope of the EQUALJOINTS projects with the following aspects considered in the design: (i) an inverted "V" (Chevron) configuration was chosen, (ii) the dual frame was designed using a behavior factor q=2.5 and (iii) square hollow sections were selected for the braces. Also, according to EN 1993-1-1 [3], member strength and stability verifications were performed for the seismic action effects defined in EN 1998-1 [4].

The D-CBF (see left side of Figure 1) were designed with braces located at the central bay of each frame for both the 3-bay and the 5-bay frame configurations. For each configuration, the following joint typologies were considered: (i) EH-S: Full-strength with strong panel zone, (ii) ES-B-E: Equal-strength with balanced panel zone, (iii) E-B-P(0.6): Partial-strength with balanced panel zone, and (iv) E-B-P(0.8): Partial-strength with weak panel zone.

Frame Name	Structural Configuration
D-CBF-6-3-6-MH-a	D-CBF, 6-storey, 3-bay, 6m span, PGA=0.25g
D-CBF-6-3-6-HH-a	D-CBF, 6-storey, 3-bay, 6m span, PGA=0.35g
D-CBF-6-3-8-MH-a	D-CBF, 6-storey, 3-bay, 8m span, PGA=0.25g
D-CBF-6-3-8-HH-a	D-CBF, 6-storey, 3-bay, 8m span, PGA=0.35g
D-CBF-6-5-6-HH-a	D-CBF, 6-storey, 5-bay, 6m span, PGA=0.35g
D-CBF-12-3-6-MH-a	D-CBF, 12-storey, 3-bay, 6m span, PGA=0.25g
D-CBF-12-3-6-HH-a	D-CBF, 12-storey, 3-bay, 6m span, PGA=0.35g
D-CBF-12-3-8-MH-a	D-CBF, 12-storey, 3-bay, 8m span, PGA=0.25g
D-CBF-12-3-8-HH-a	D-CBF, 12-storey, 3-bay, 8m span, PGA=0.35g
D-CBF-12-5-6-HH-a	D-CBF, 12-storey, 5-bay, 6m span, PGA=0.35g

Table 1: Designed dual concentrically-braced frames (D-CBF) [1].

The connection springs representing the connection were assumed to have with an elastic-plastic behavior with 1% post-yield hardening. The plastic rotation capacity of the connection component pre-capping was assumed to be 18 mrad (ASCE 21-13, Table 9-6, yield bolts, 2014). In OpenSees the connection behavior was implemented by assigning a Bilin material (modified

Ibarra-Medina Krawinkler model) to the rotational DOF of the spring and the spring for the column web panel zone was modelled according to the tri-linear model by Krawinkler [1].

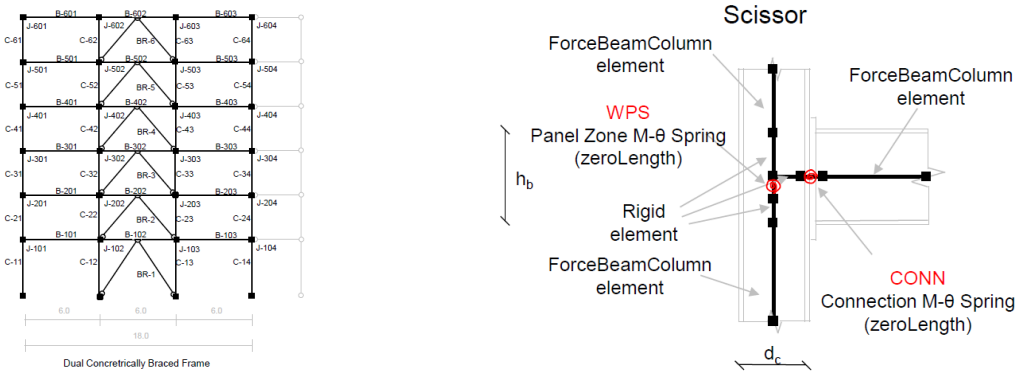

Figure 1: (a) D-CBF and (b) Scissor model [1].

2.2 Modal analysis

In the modal analysis, in order to calculate the modes and the eigen periods, seismic masses were assigned to the joint nodes at each floor. The 1st, 2nd and 3rd period of the frames can be consulted in [1]. In general, frames with shorter span are stiffer than the ones with longer span, while the 5-bay frame shows the smallest stiffness.

2.3 Non-linear static pushover analysis

The pushover analysis was performed with uniform and modal distribution of lateral forces along the height of the building, according to EN 1998-1 [4] (section 4.3.3.4.2). The structure was pushed to its target top displacement (horizontal displacement of the last floor) to obtain the pushover curves. Base shear force, V, is normalized by design base shear, V_b, where V_b was calculated according to EN 1998-1 [4].

The pushover curves clearly show that after the first plastic event a sudden reduction in the lateral resistance of the frame occurs, which can be explained due to the buckling phenomena on the brace in compression. Following this decrease, and increase of lateral stiffness is experienced. As an example, Figure 2 depicts the normalized pushover curves (modal distribution) for two structural configurations (D-CBF-6-5-6-HH and D-CBF-12-5-6-HH).

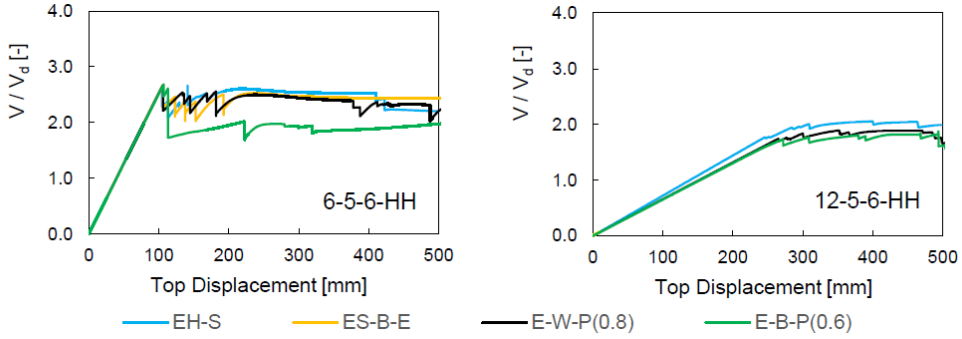

Figure 2: Normalized pushover curves – Modal distribution [1].

When comparing the pushover curves for the different frames configurations is concluded that: (i) sudden decrease in lateral stiffness influences more frames with larger span, while 5-bay frames are not significantly affected by this behavior, (ii) 12 story frames have larger V/V_d ratio than the 6-storey frames and (iii) V/V_d ratio is slightly higher for frames with shorter span.

2.4 Incremental dynamic analysis

In order to evaluate the inelastic behavior the frames, an incremental dynamic analysis (IDA) was carried out for two sets of 7 acceleration records. The acceleration records were extracted from PEER NGA database, from European and Middle East events. The first set of 7 records represents medium seismic hazard (MH) using the following criteria: magnitude M from 5.0 to 6.5, distance fault 10 to 100 km and target spectrum with PGA0=0.25 g. The second set of 7 records represents a high seismic hazard (HH) using the following criteria: magnitude M higher than 6.5, distance fault from 20 to 100 km target spectrum with PGA0=0.35 g. for both cases was considered a shear wave velocity from 180 to 800 m/s, EN 1998-1 Type 1 Soil C and minimization of DRMS over a period range from 0.2 to 2.0 s. Verifications were carried out for the three limit states: Damage Limitation, Significant Limitation and Near Collapse intensity.

The local behavior of DCBFs is analyzed in terms of maximum (i) connection rotation, (ii) panel rotation and (iii) beam rotation. The values are compared with threshold proposed in ASCE 41-13 in each limit state, which revealed that although the observed beam rotation satisfies always the criteria, the seismic demand for the connections is too high for many frames with 12 stories. As an example, the IDA curves for interstory drift ratio vs. ground motion intensity level are presented, in Figure 3, for two structural configurations (D-CBF-6-5-6-HH and D-CBF-12-5-6-HH).

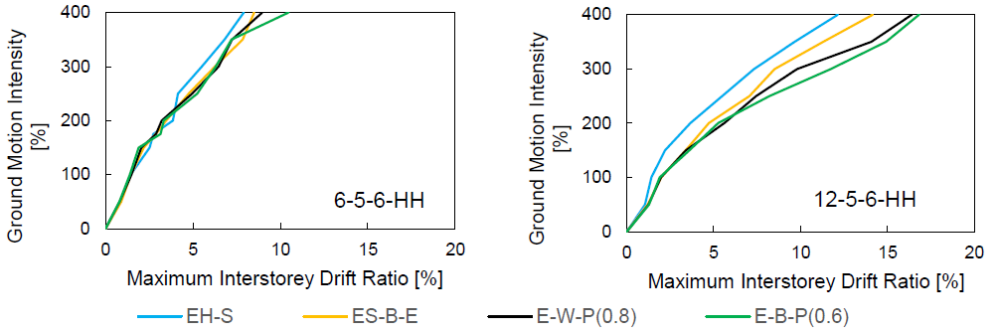

Figure 3: IDA curves in terms of max interstory drift ration for D-CBF [1].

3 CONCLUSIONS

In this paper, s parametric study was carried out aimed to assess the behavior and the seismic demand on beam-to-column steel joints of typical frame typologies, the D-CBF. Ten D-CBF with different values of selected parameters, such as, the level of seismic hazard, building height, span length and number of bays. The parametric study was performed through a pushover and dynamic analysis.

REFERENCES

[1] F. Gentili, A. Shahbazian, C. Rebelo L. Simões da Silva, The role of joint modelling on the seismic performance of steel frames. *Journal of Constructional Steel Research*, (submitted in 11.10.2016).

[2] F. McKenn, G Fenves, M Scott, B. Jeremic, Open System for Earthquake Engineering Simulation (OpenSees). *Pacific Earthquake Engineering Research Center*, UCA, 2000.

[3] CEN, EN 1993-1-8. Eurocode 3: Design of steel structures, Part 1-8. Design of joints. *European Committee for Standardisation*, Brussels: 133, 2005.

[4] CEN, EN 1998-1. Eurocode 8 – Design of structures for earthquake resistance. Part 1: General rules, seismic actions and rules for buildings. *European Committee for Standardisation*, Brussels, 2004.

OpenSees Days Europe 2017
1st European Conference on OpenSees
Porto, Portugal, 19–20 June 2017

DEVELOPMENT OF AN OPENSEES MODEL FOR COLLAPSE RISK ASSESSMENT OF ITALIAN-CODE-CONFORMING STEEL SINGLE-STOREY BUILDINGS

F. Scozzese[1], A. Zona[1], A. Dall'Asta[1]

[1] University of Camerino
School of Architecture and Design, Viale della Rimembranza, 63100 Ascoli Piceno, Italy
{fabrizio.scozzese, alessandro.zona, andrea.dallasta}@unicam.it

Keywords: Steel Structures, Nonlinear Static and Dynamic Analyses, Concentric Brace Models, Buckling Modelling, Second Order Effects, Seismic Risk.

Abstract. This paper aims at evaluating the risk of collapse in single-storey steel buildings designed according to the current Italian Seismic Design Code. A set of case studies made by buildings having different geometries and located in sites having different seismic hazard is modelled and subsequently analysed within the OpenSees software framework. An accurate structural model is developed and an insight into the main modelling aspects is given, in order to share with the OpenSees community the main modelling strategies adopted. The model developed here accounts for both mechanical and geometrical nonlinearities: the former by adopting a distributed plasticity model for beams, columns, and concentric braces; the latter by using a corotational coordinates transformation for all the elements. The out-of-plane buckling phenomenon on compressed lateral bracing systems is simulated by assigning proper local imperfections (i.e., initial curvature) to the braces and including the gusset plates deformability and relevant post-elastic behaviour. Since the seismic design follows capacity design principles, hysteretic behaviour of the joints is not considered as joints are no-dissipative elements. In addition, due to the geometry of beams, columns and braces, yielding in shear is excluded and a linear elastic behaviour in shear is used in the model. Push-Over analyses are used for a preliminary evaluation of the nonlinear behaviour under increasing horizontal loads. Afterwards, multi-record incremental dynamic analyses are performed for 10 increasing seismic intensities.

1 INTRODUCTION

The structural systems consist in three-dimensional single-storey steel buildings, designed according to the criteria of the current 2008 Italian code [2]. The structures have different resistant mechanisms for the two in-plane directions: moment-resisting portal frames in the transversal direction (direction X) and concentrically braced frames [3] in the longitudinal one (direction Y). A total number of 24 case studies has been analysed with different geometry (Lx = 20/30 m, Ly = 6/8 m), site (L'Aquila, Milano, Napoli) and soil category (A and C). Figure 1 shows a qualitative scheme of the finite element model. The structural models of the non-residential single-storey steel buildings investigated in this study and developed in the OpenSees software [4], account for both geometric and material nonlinearities. Multi-stripe analysis at 10 Intensity Measure (IM) levels are carried out, by using a set of 20 X-Y-Z pairs of ground motions for each IM level. Push-over analyses are also carried out for comparison and preliminary investigation purposes.

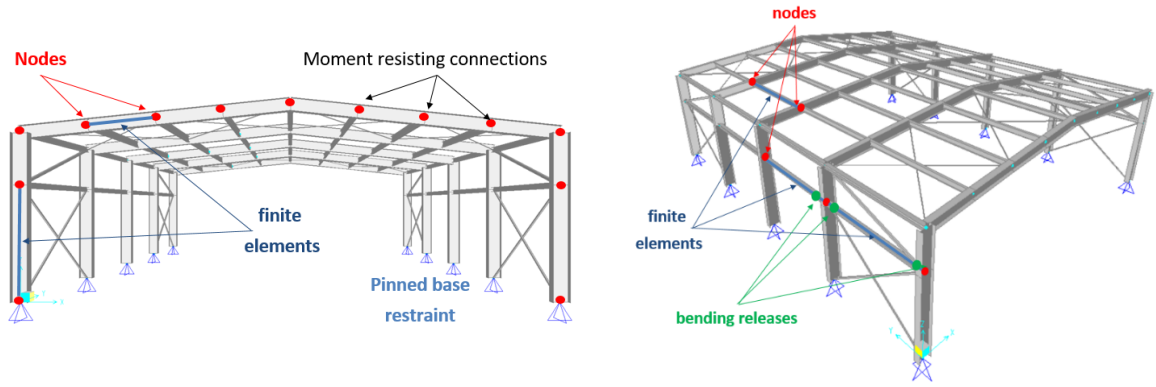

Figure 1: Finite Element Model

2 MODELLING ISSUES AND STRATEGIES

All columns are hinged at their bases. The pinned-end connections in longitudinal direction are modelled by generating a pair of nodes (one master and one slave) having the same spatial coordinates and by linking them with a proper *equalDOF* constraint. In particular, the equalDOF's properties are such that the slave node inherits all the master node's degrees of freedom except for the rotational ones around the global X and Z directions. All the elements have been modelled as Force-Based *nonlinearBeamColumn* elements and a variable Number of Integration Points (NIPs) is adopted depending on the length of the elements themselves: the longer the element, the higher the NIPs in order to improve the accuracy of the solution. The steel nonlinear behaviour is modelled by assigning to each section's fibre the uniaxialMaterial Steel02 constitutive law (Giuffre-Menegotto-Pinto steel material object with isotropic strain hardening). The distributed plasticity approach allows an accurate description of the yielding processes occurring along the element; the number of sections' fibres has been defined with the aim of providing a trade-off between the convergence improvement and a not excessive rise of the computational burden during the analysis. The torsional stiffness (J_tG_s) is introduced by adding this contribution (in series) to that of the fibre section, by means of the *section Aggregator*. For what concerns the lateral braces there are two main modelling aspects requiring particular care: accounting for the buckling phenomenon in compression and a proper modelling of the gusset plate connections, that in real structures are neither pinned nor fixed joints. The method followed for modelling the bracing systems is the one proposed by Hsiao [5, 6, 7] and

consist in simulating the nonlinear out-of-plane rotational behaviour of the gusset plate connections by means of a rotational nonlinear spring located at the physical end of the brace. The nonlinear spring is modelled in OpenSees through a zero-length element having the out-of-plane rotational degree of freedom represented by a Steel02 material with properly calibrated properties. In order to simulate the buckling of the lateral braces during the compression phases, each brace is discretized into a certain number of nonlinear (with distributed plasticity) sub-elements and a sinusoidal curvature is assigned by modifying parametrically the coordinates of the nodes of the intermediate sub-elements (see Figure 2). This initial curvature, representing the local imperfection of the diagonal brace, has the role of triggering the buckling by furnishing a preferential buckling shape to the element. The value of the initial imperfection is chosen in such a way to furnish a buckling axial force consistent with the ultimate value $N_{b,Rd}$ provided by the Italian code of practice [1, 2] (i.e., $N_{b,Rd} = \frac{\chi \cdot A \cdot f_y}{\gamma_{M1}}$)

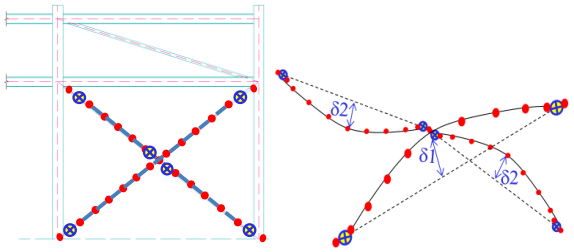

Figure 2: X brace NL springs and sub-elements and initial imperfections

3 NONLINEAR ANALYSIS: MAIN RESULTS

3.1 Push-Over analysis

A preliminary investigation of the nonlinear lateral behaviour of the structure is carried out by means of nonlinear static analysis (push-over). As shown in Figure 3, the model developed in OpenSees experiences both wide excursions in the steel post yielding range and buckling with significant global post-elastic stiffness reduction.

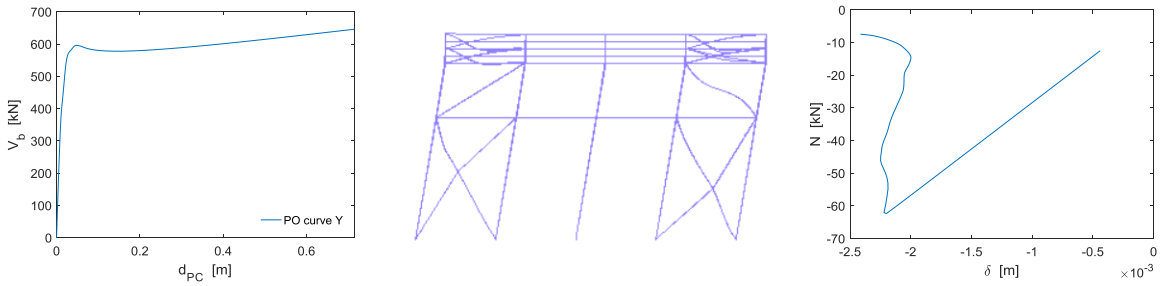

Capacity curve Push-Over Y Deformed configuration: lateral view N-δ curve for X-cut-brace

Figure 3: system deformation and N-δ curve for the compressed X-cut-brace for the case of analysis PO Y.

3.2 Incremental Dynamic Analysis

The results of the incremental dynamic analysis confirm the significant excursions in the nonlinear range as for example shown in Figure 4, where the two results are related to an IM=8 seismic event: cyclic response for a cut X-brace and the corresponding gusset plate Moment-Rotation plot. The fact that the gusset plate undergoes plastic deformations is in witness of the need of its inclusion in the model in order to properly account for both buckling and second order effects.

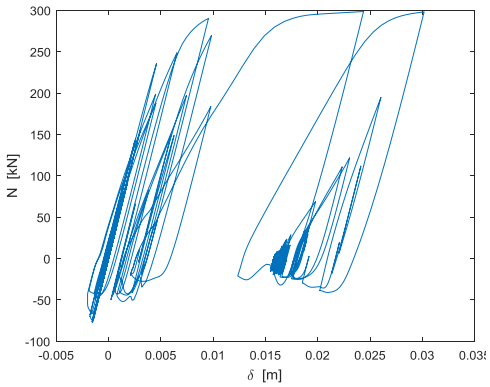

N-δ cyclic response for Cut X-brace

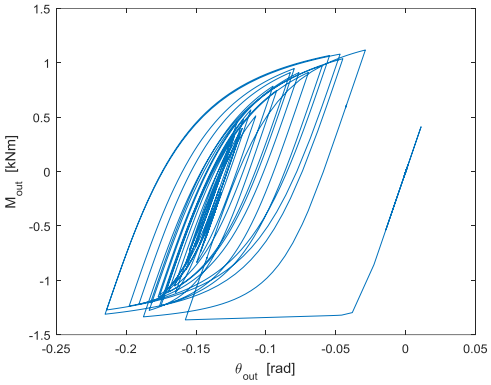

M–θ cyclic response for Gusset Plate

Figure 4: N-δ and M–θ cyclic responses (IM=8 seismic records) for Cut X-brace (sx) and gusset plates (dx)

REFERENCES

[1] Circolare 02/02/2009 n. 617 (2009). "Istruzioni per l'applicazione delle "Nuove norme tecniche per le costruzioni" di cui al D.M. 14 gennaio 2008." M. d. I. e. d. Trasporti, ed. Gazzetta Ufficiale n. 47 del 26 febbraio 2009.

[2] D. M. 14/01/2008 (2008). "Norme Tecniche per le Costruzioni (in Italian) ", G.U. n. 29 4 febbraio 2008.

[3] Mazzoni S, McKenna F, Scott MH, Fenves GL. (2006). Open system for earthquake engineering simulation, user command-language manual. Pacific Earthquake Engineering Research Center, Berkeley (CA).

[4] Tremblay R, Archambault M-H, Filiatrault A. (2003). Seismic response of concentrically braced steel frames made with rectangular hollow bracing members. Journal of Structural Engineering129(12):1626-1636.

[5] Hsiao, P. C., Lehman, D. E., Roeder, C. W. (2012). Improved analytical model for special concentrically braced frames. Journal of Constructional Steel Research, 73, 80-94.

[6] Hsiao, P. C., Lehman, D. E., Roeder, C. W. (2013). Evaluation of the response modification coefficient and collapse potential of special concentrically braced frames. Earthquake Engineering & Structural Dynamics, 42(10), 1547-1564.

[7] Tirca, L., Chen, L., Tremblay, R. (2015) Assessing collapse safety of CBF buildings subjected to crustal and subduction earthquakes, Journal of Constructional Steel Research 115(1):47-61

OpenSees Days Europe 2017
1st European Conference on OpenSees
Porto, Portugal, 19–20 June 2017

Evaluating the use of OpenSees for Lifetime Seismic Performance Assessment of Steel Frame Structures

John Hickey[1], Brian Broderick[2], and Terence Ryan[3]

[1] Department of Civil, Structural& Environmental Engineering, Trinity College Dublin
e-mail: hickeyj2@tcd.ie

[2] Department of Civil, Structural& Environmental Engineering, Trinity College Dublin
Brian.Broderick@tcd.ie

[3] Department of Civil Engineering and Materials Science, University of Limerick
terence.ryan@ul.ie

Keywords: Concentrically Braced Frame, Lifetime Seismic Performance Assessment, Behaviour Factor, Model Validation

Abstract. *The overall aim of this work is to examine the influence of structural design procedure on the lifetime seismic performance of steel Concentrically Braced Frames (CBFs). Under dissipative seismic design principles, bracing members are allowed to behave inelastically under infrequent, high-intensity earthquakes; in Eurocode 8 based design the extent of this inelasticity is effectively controlled by the behaviour factor, q. Increasing the behaviour factor results in greater ductility demand and structural damage, however doing so allows for reduced member sizes and consequently lower initial costs. As CBFs designed in accordance with modern codes are unlikely to collapse but may experience significant damage at various hazard levels, a comprehensive lifetime seismic performance assessment procedure is required to compare the full costs of different frame designs. This paper focuses on the structural analysis section of this procedure, in particular the ability of OpenSees to capture the complex cyclic response of CBFs. The modelling assumptions made are assessed using results from a series of shake table tests on a full-scale model CBF. The impact of these modelling assumptions, and the resulting inaccuracies, on the performance assessment procedure is then investigated. Finally, the lifetime seismic performances of a set of case study CBFs designed to Eurocode 8 using various behaviour factors are evaluated. It is shown that expected repair costs and downtime increase with the design value of the behaviour factor.*

1 INTRODUCTION

The overall aim of this work is to examine how the behaviour factor used in design affects the life cost of a facility. This is done using a lifetime performance assessment procedure, carried out using the PACT tool [1]. Structural analysis to obtain the probability of Engineering Demand Parameter (EDP) values, namely peak inter-storey drift and floor acceleration, being exceeded is a key element of the procedure. These analyses need to be accurate, and any inherent inaccuracy needs to be understood in the context of the overall lifetime seismic assessment. This can be done by validating the numerical model and performance assessment procedure using experimental results. Once this is achieved, performance assessment of case study buildings can be carried out with a reasonable level of confidence.

2 PROCEDURE

A site in Oakland, California was selected as a case study site. A series of two, five and ten storey perimeter CBFs were designed in accordance with Eurocode 8 using behaviour factors between 1 and 5. The frames were modelled in OpenSees [2] using the modelling procedures discussed below. Ground motions records for nonlinear time history analysis (NLTHA) were selected from the PEER database [3] to match the conditional spectrum for the site.

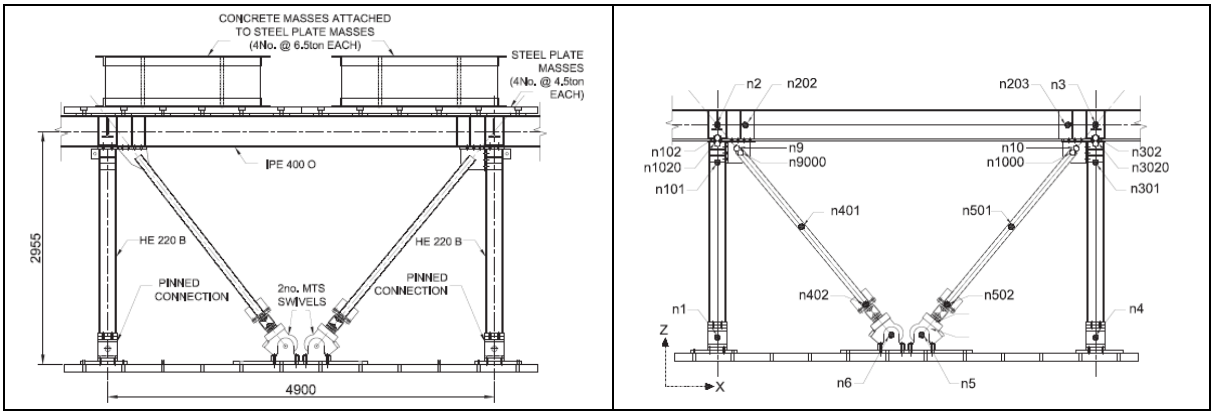

Figure 1. The BRACED test frame and illustration of the OpenSees model employed

Following the recommendations of Uriz et al., [4], the brace elements were modelled using two force based nonlinearBeamColumn elements with 3 integration points per element and an initial camber displacement of 0.1% of the brace length. Gusset plate connections were modelled using nonlinear rotational springs, as proposed by Hsiao et al. [5]. The beams and columns were modelled using force based nonlinearBeamColumn elements with 3 integration points and discretized fiber sections. The Steel02 material, which represents the Giuffre-Menegotto-Pinto model, was used for all components. For all analysis 5% Raleigh damping proportional to the mass and tangent stiffness matrix at the first and third modes was applied.

The validity of these modelling assumptions was assessed using experimental results from the BRACED test program [6]. Shake table tests were performed for a series of single storey CBFs, illustrated in Figure 1, at ground motion intensity levels approximately corresponding to 2%, 10% and 50% probability of exceedance in 50 years for a site in Los Angeles. OpenSees models of the test frame were developed and NLTHA performed using the recorded shake table accelerations. The peak displacement and acceleration calculated were compared to the experimental results. The results are summarized in Figure 2.

The impact of these modelling inaccuracies on lifetime performance assessment was then examined. Using PACT, performance assessment was carried out for a single-storey building with the BRACED test frame as the seismic resisting element. This was done using EDPs obtained from the experimental testing program and from the OpenSees NLTHA. It was demonstrated that the use of the numerically-calculated EDPs led to expected repair and downtime costs being underestimated relative to the costs obtained using the experimental EDPs. In PACT, a factor, β_m, can be included to account for uncertainty in structural modelling. Put simply, this works by increasing the standard deviation of the distribution used in the PEER equation to assess the performance. When the recommended β_m value of 0.5 is included in the assessment for the numerical EDPs, the performance metrics estimated using the numerical and experimental EDPs are similar, as illustrated in Table 1.

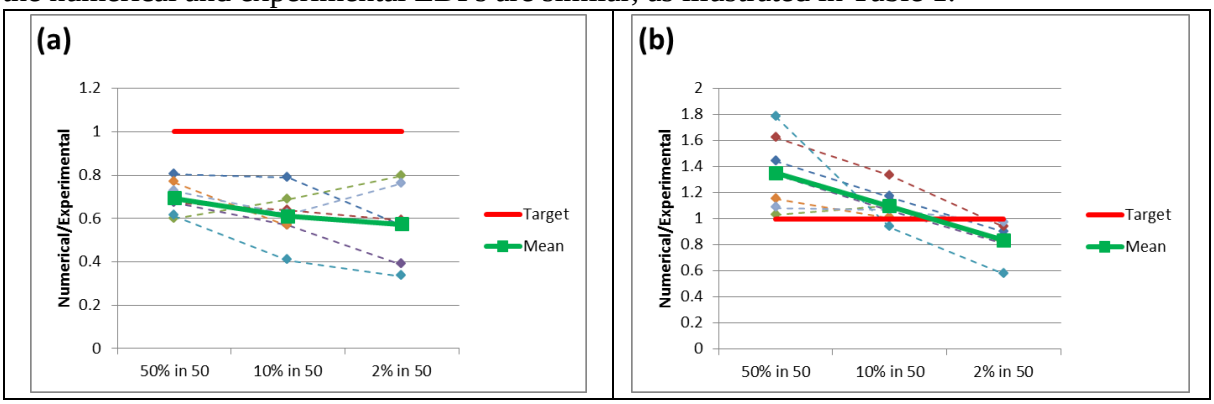

Figure 2. Ratio of numerically calculated EDPs from OpenSEES to experimental EDPs for seven shake table tests from the BRACED project: (a) peak drift, (b) peak acceleration

Input EDPs	Modelling Uncertainty Factor: β_m	Annualized Repair Cost ($/ft^2)	Annualized Downtime (Days)
Numerical	0	0.823	0.93
Numerical	0.5	0.907	1.08
Experimental	0	0.938	1.13

Table 1: Performance assessment results for the BRACED test frame obtained from PACT

3 SUMMARY OF RESULTS

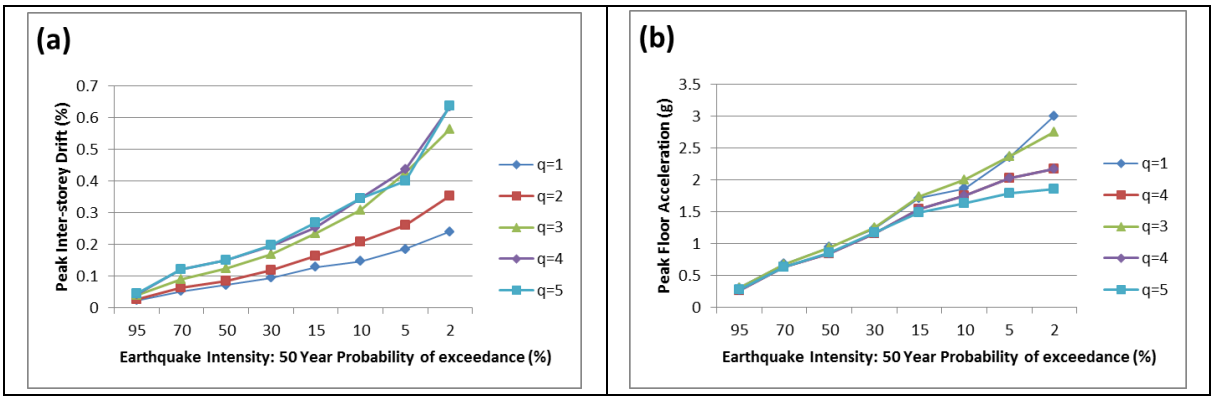

Figure 3. Median values of (a) Peak Inter-storey Drift, (b) Peak Floor Acceleration, for 5 storey CBFs at each intensity level recorded from time history analysis.

NLTHA was performed for the two, five and ten storey CBFs designed using different behaviour factors. Figure 3 presents a selection of the results for the 5-storey CBFs.

The EDPs obtained from these NLTHAs were used as the inputs to a PACT model to perform lifetime performance assessment. Financial losses and business downtime were the two performance metrics used to assess the performance of the structures examined. Figure 4 presents an example of the results obtained for 2 and 5 storey CBFs. As expected, the losses incurred are lowest for the q=1 frames and increase as the behaviour factor is increased.

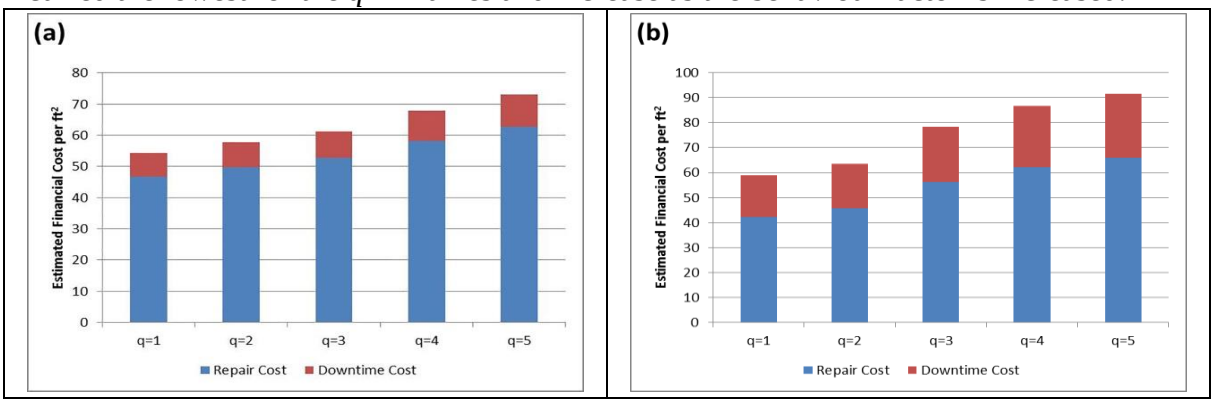

Figure 4. Estimated 50 Year Losses (repair and downtime costs) for (a) 2 Storey CBFs, (b) 5 Storey CBFs

4 CONCLUSIONS

The study examined the influence of the behaviour factor on the lifetime performance of CBFs designed to Eurocode 8. Experimental results were used to evaluate the OpenSees modelling procedures employed to calculate EDPs; it was shown that while some biases exist in the numerically-calculated EDPs compared to experimentally-obtained values, these are in line with the expected influence of model uncertainty in the PACT model. On a general level, the study demonstrates how performance assessment can be employed to improve and optimise design. It can be concluded that the maximum behaviour factor value allowed by Eurocode 8 does not necessarily lead to the most economical design solution.

REFERENCES

[1] Applied Technology Council (ATC), *Performance Assessment Computation Tool (PACT)*, Applied Technology Council, Redwood City, CA, 2012

[2] McKenna, F., OpenSees: a framework for earthquake engineering simulation. *Computing in Science & Engineering, 2011*. **13**(4): p. 58-66.

[3] Chiou, B., et al., NGA Project Strong-Motion Database. *Earthquake Spectra*, 2008. 24(1): p. 23-44.

[4] Uriz, P., F.C. Filippou, and S.A. Mahin, Model for cyclic inelastic buckling of steel braces. *Journal of Structural Engineering*, 2008. 134(4): p. 619-628.

[5] Hsiao, P.-C., Lehman, D.E. & Roeder, C.W., Improved analytical model for special concentrically braced frames. *Journal of Constructional Steel Research*, 2012. 73: 80-94.

[6] Broderick, B. M. et al., *Assessment of the Seismic Response of Concentrically-Braced Steel Frames*. Experimental Results in Earthquake Engineering 2015 Springer Intl Publishing. 35: 327-344

OpenSees Days Europe 2017
1st European Conference on OpenSees
Porto, Portugal, 19–20 June 2017

BLIND TEST PREDICITON OF AN INFILLED RC BUILDING WITH OPENSEES

Hugo Rodrigues[1], André Furtado[2A], António Arêde[2B]and Humberto Varum[2C], Marin Grubnisic[3A] and Tanja Sipos[3B]

[1] RISCO – School of Management and Technology, Polytechnique Institute of Leiria
Leiria, Portugal
hugo.f.rodrigues@ipleiria.pt

[2] CONSTRUCT-LESE, Faculty of Engineering of University of Porto
Porto, Portugal
e-mail: A: afurtado@fe.up.pt; B: aarede@fe.up.pt; C: hvarum@fe.up.pt

[3] University of Osijek, Faculty of Civil Engineering Osijek,
Osijek, Croatia
e-mail: A: marin.grubisic@gfos.hr; B: tanja.kalman.sipos@gmail.com

Keywords: Blind Prediction, infilled RC structures, Seismic behaviour, Numerical modelling.

Abstract. *Over the last years the seismic behaviour of infilled reinforced concrete (RC) structures have been focus of innumerous experimental and numerical studies. A big effort is being made by the scientific community with the aim of increase the knowledge regarding the seismic response of these type of structures and improve the numerical modelling accuracy to predict their expected behaviour. In 2015, a blind prediction contest was organized by the Faculty of Civil Engineering Osijek with main goal of invite the technical and scientific community to predict the nonlinear seismic behaviour of a 1:2.5 scaled 3D building structure. The three-storey infilled RC structure was subjected to ten incremental earthquake sequence on a shake table test. The blind numerical analyses were performed knowing only the specimen geometry, reinforcement detailing, material characteristics and the actual ground motions recorded during the testing. In this context and, in view of the author's participation success, the present paper mainly aims at presenting the key aspects of the adopted numerical methodology (and related difficulties) which proved to yield good results, while also providing some insight regarding key problems in numerical simulations of infilled RC structures seismic behaviour.*

1 INTRODUCTION

In the context of seismic scientific testing works developed in the last years and in particular resorting to shaking tables, which usually happens with the objective of providing additional information not available from simpler experimental tests. In 2015, the FRAmed–Masonry Composites for Modeling and Standardization (FRAMA) Blind Prediction Contest 2014 [1] pretended to evaluate different modelling strategies proposed by different international teams/experts that were challenged to predict the experimental response of a scaled three storey infilled RC structure that will be subjected to ten increased and scaled ground motions where the authors team became in the first position. This paper aims at describing the modelling strategy adopted by the authors namely in terms of the RC structure and infill masonry walls modelling. Along the manuscript it will be discussed the aspects which are both critical and difficult to evaluate, regarding a three storey RC structure seismic behaviour. Along the present manuscript, the global teams' blind prediction results will be presented.

2 EXPERIMENTAL CAMPAIGN

2.1 Specimen description

The experimental program associated with the FRAMA Blind Prediction Contest [10] initiative was performed in DYNLAB at IZIIS shaking table with the support of University of Osijek (Croatia) and is briefly described in this chapter. It basically involved of a 1:2.5 scaled infilled RC structure (Figure 1) under uniaxial ground motions with increasing intensity. The shake-table test specimen was a 1:2.5 scale model that contains two parallel connected planar frames, with two bays and three storeys, making the structure of the gross dimensions of 4.6 m in length, 2.8 m in width and 3.9 m in height. The RC structured is filled with masonry walls with openings in certain bays. The structure has been designed for medium ductility levels according to the EC8 provisions

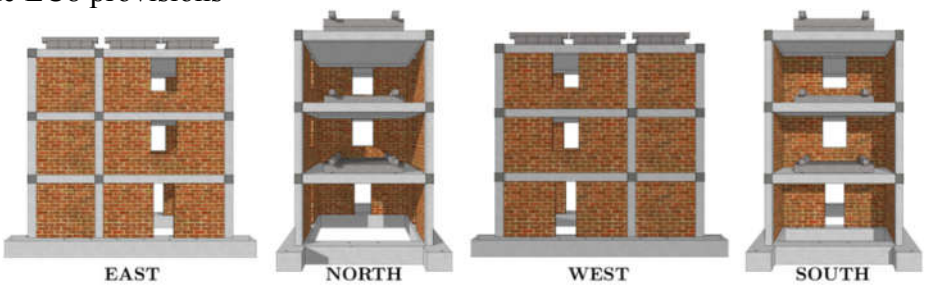

Figure 1 – 3 storey masonry-infilled RC frame and reinforcement details Lateral views.

Thick slabs were added at the floor and roof levels to reproduce the correct gravity mass of the specimen. These slabs were attached with hinge connections to the transverse beams protruding from the plane frame, so that they would not introduce unrealistic moment restraints to the RC frame. Three sets of additional masses will be placed on top of the slab at each floor. Each set contains four steel ingots with overall dimensions of 23.5×14×150 cm. The specimen was built from beginning of June till the end of July 2015. The mock–up was cast in–situ in five distinct phases. First, the foundations were concreted and afterwards columns, beams and slabs at each floor in fazes two through four. Finally RC frames were filled with hollow clay masonry units. Concrete reinforcing steel, mortar and masonry samples were taken to characterize their mechanical behaviour.

2.2 Ground motion and test sequences

The specimen was subjected to ten different one-directional ground-motions recorded at the Herceg Novi station during the April 15th, 1979 Montenegro earthquake. The earthquake had a moment magnitude of 6.9 and a hypocentral depth of 12 km. To account for the fact that the structure is constructed at 1:2.5 scale, the record was scaled in time by reducing the duration by a factor $1/\sqrt{2.5}$. The record was base line corrected and then scaled to match the different levels of peak ground acceleration (0.05g, 0.10g, 0.20g, 0.30g, 0.40g, 0.60g, 0.70g, 0.80g, 1g, 1.2g) that was used as input signals for the shake table test.

3 MODELLING STRATEGY AND NUMERICAL RESULTS

The authors participated in the FRAMA contest by carrying out an numerical modelling prediction by using the OpenSees software [2]. Three specific issues were assumed by the authors as important to consider in the numerical modelling process i) consideration of the openings effect in the infills strength and stiffness reduction; b) consideration of the infills out-of-plane behaviour for the panels distributed in the central alignment along the direction Y-Y; c) taking into account past numerical and experimental studies carried out by different authors, it was assumed for the RC a viscous damping of ξ=2%. For the numerical modelling of the RC elements lumped-plasticity model was applied (with plastic-hinge length equal to the larger dimension of the elements section). Fiber discretization was assumed to represent the behaviour at the section level, where each fiber was associated with a uniaxial stress-strain hysteretic behaviour. Regarding the infill masonry walls numerical modelling it was adopted the Furtado et al. proposal [3] as illustrated in Figure 2.

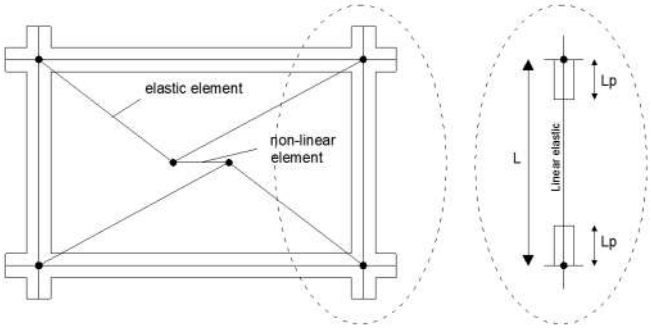

a) b)

Figure 2 – Numerical modelling strategy to represent: (a) infill masonry wall through equivalent double-diagonal strut element (b) RC element modelling using lumped-plasticity element approach.

The prediction of the RC structural elements under an earthquake requires the consideration of the nonlinearity of the material, namely the uniaxial material stress-strain hysteretic response. For this contest, the authors adopted the uniaxial material model Concrete 02 available on the OpenSees library. The uniaxial model steel 02 was adopted for the steel reinforcement. For the numerical simulation of the non-linear behaviour of infill masonry Furtado *et al* [3] model was adopted, which is an equivalent double-strut model that is able to represent the in-plane behaviour of the infill panels with and without openings and the interaction with the out-of-plane behaviour through a removal algorithm. Regarding the infills numerical modelling the authors considered the infills openings by applying a reduction factor of the infills strength capacity and initial stiffness. The authors decided to apply a reduction factor given by the ratio between the openings area and the infill panel area that will reduce the parameters cracking force F_c,

yielding force F_y, maximum strength F_{max}, and initial stiffness K_1. The cracking drift (d_c) was reduced for 0.05%, yielding drift (d_y) for 0.12% and maximum drift d_{max} to 0.25%. The remaining infill panels numerical parameters were determined as suggested by Furtado *et al* [3] without reduction factors. Eighty-one percent of the infill panel mass was considered concentrated in the two central nodes of the numerical model and bending stiffness values were considered. In Figure 3a it is illustrated the comparison between the experimental and numerical relative displacements of the storey 2 subjected to a ground motion with pga=1g with a good match. From the ten different intensity levels (0.05g, 0.1g, 0.2g, 0.3g, 0.4g, 0.6g, 0.7g, 0.8g, 1g and 1.2g) simulated, it can be observed in Figure 3b that the error obtained on 5 different levels was lower than 10 and only for pga=1.2g the error was higher than 30. It is observed that the error is progressively increasing with the increasing pga demand, however for pga=0.4g the error is slightly above of those observed before which reach an $Error_{E\text{-}RMS}$=11.86. From the analysis of the error obtained for each displacement in each storey (Figure 3c) it can be observed that the error obtained in the prediction of the 3rd storey displacement is around 2-2.5 times higher than the obtained for the 1st storey and 1.25-1.5 times the ones achieved for the 2nd storey.

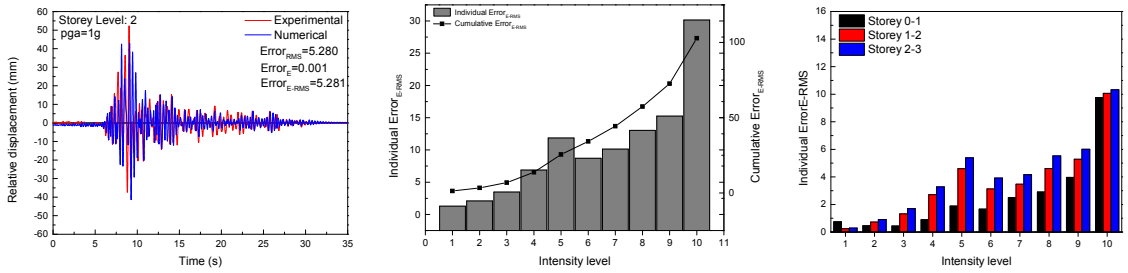

a) b) c)

Figure 3 – Numerical modelling strategy to represent: (a) infill masonry wall through equivalent double-diagonal strut element (b) RC element modelling using lumped-plasticity element approach.

4 CONCLUSIONS

A blind prediction contest of the seismic response of a three storey scaled infilled RC structure that was subjected to ten scaled and progressively increased ground motions was carried out. From this manuscript, it can be concluded that the three different aspects must be given on this type of structures: a) the infills masonry walls contribution in terms of stiffness and strength must be considered; b) consideration of the infill panels openings through the reduction of the infills strength properties and the reduction of the drift parameters in the hysteretic behaviour; c) the viscous damping made an important role in the seismic response of the specimen.

REFERENCES

[1] V. Sigmund, P. Brana, D. Dzakic, M. Galic, G. Gazic, M. Grubisic, *et al.*, "FRAmed–MAsonry Composites for Modeling and Standardization, FRAMA, International Benchmark within Research Project, Faculty of Civil Engineering Osijek, Josip Juraj Strossmayer University of Osijek, Croatia,," 2014.

[2] F. Mckenna, G. Fenves, M. Scott, and B. Jeremic, "Open System for Earthquake Engineering Simulation (OpenSees)," ed. Berkley, CA, 2000.

[3] A. Furtado, H. Rodrigues, A. Arêde, and H. Varum, "Simplified macro-model for infill masonry walls considering the out-of-plane behaviour," *Earthquake Engineering & Structural Dynamics,* vol. 45, pp. 507-524, 2016.

OpenSees Days Europe 2017
1st European Conference on OpenSees
Porto, Portugal, 19–20 June 2017

MODELLING IN-PLANE AND OUT-OF-PLANE RESPONSE OF INFILLED FRAMES THROUGH A FIBER MACRO-MODEL

F. Di Trapani[1], **P.B. Shing**[2] and **L. Cavaleri**[3]

[1]Politecnico di Torino
Department of Structural, Geotechnical and Building Engineering
fabio.ditrapani@polito.it

[2]University of California, San Diego
Department of Structural Engineering
pshing@ucsd.edu

[3]University of Palermo
Dipartimento di Ingegneria Civile, Ambientale, Aerospaziale, dei Materiali
liborio.cavaleri@unipa.it

Keywords: Masonry infills, in-plane, out-of-plane, arching action, macro-model.

Abstract. *A new fiber macro-model for the simulation of combined in-plane and out-of plane response of infilled frames subjected to seismic actions is presented in the paper. The model consists of 4 pinned struts (two diagonals, one horizontal and one vertical) modeled with the nonlinear beam/column fiber-section elements available in OpenSees. The model is particularly suitable to predict the out-of-plane response as fiber-section elements can account for the coupling between axial load and bending moment occurring because of the arching mechanism developed by the infills beyond the first cracking. Moreover the model can account for the effect of the reciprocal damaging accumulated both in-plane and out-of-plane during shakings. The procedure for the identification of the struts is presented in the paper and is validated with experimental test data from different authors. The proposed model may be used as a computationally-light and effective tool for the assessment of the response of 3D structures subjected to ground motions acting in arbitrary directions.*

1 INTRODUCTION

Infill-frame interaction under in-plane (IP) and out-of-plane (OOP) seismic loads is still a debated issue. Different approaches and theories have been proposed to account the presence of infills in structural models. One of the most effective ways is the use of one (or more) equivalent diagonal struts, reproducing stiffening and strengthening action (e.g. [1-3]). Research on this topic has been mainly addressed to the evaluation of the in plane response of infilled frames, while the issue of the assessment of the out-of-plane response and its reciprocal dependence on the in-plane damage is currently not solved in a satisfactory way.

Theoretical and experimental studies [4-6] have shown that masonry infills have significant out-of-plane resistance because of the arching mechanism, which develops because of the confining action exerted by the boundary frames. From the aforementioned and other studies one can conclude that OOP resistance: depends on the compressive strength of masonry rather than tensile strength; decreases with the square of the slenderness ratio of the infills; depends on a 2-way arching effect. Moreover in-plane and out-of-plane responses are mutually influenced as a function the damaging occurred in each direction. In consideration of this most of the analytical expressions proposed to predict the OOP maximum load (q_a) of the infill refer to the following proportionality law:

$$q_a \propto \frac{f_m}{\left(\frac{h}{t}\right)^2} \tag{1}$$

where f_m is the compressive strength of masonry and h/t the slenderness ratio of the infill.

On the other hand, only a few recent modelling approaches (e.g. [7,8]) have been proposed in order to define an integrated IP-OOP macro-model to use for 3D simulations.

The aforementioned modelling approaches have however the limit of using fictitious expedients to simulate the arching mechanism. In the current paper is proposed the use of fiber-section elements as equivalent struts. An integrated four-strut macro-model is proposed to simultaneously account for in-plane and out-of-plane response of infilled frames. Fiber section elements can account directly the arching mechanism as the can model the coupling between axial-load and bending moment occurring at the cracked stage of the cross-section. Validation tests with experimental data are finally presented.

2 PROPOSED MACRO-MODEL

The proposed model consists of 4 pinned fiber-section beam-column elements (each one divided in two parts). A scheme of the model is illustrated in Fig. 1. Concrete type (Concrete02) stress-strain laws are used for the struts. Since the struts have no tension, cracking occur after the elastic stage. Fiber-section elements can account for the coupling between axial force and bending moment occurring at the cracked stage and hence for the arching mechanism. The diagonal struts are thought to provide the whole in-plane response of the infill and a significant portion of the OOP capacity. The horizontal and vertical struts do not influence the in-plane response but provide a complementary OOP contribution which simulates the 2-way generation of the arching mechanism. The struts do not have a common mid-span node (four different mid-span nodes are defined). Relative displacements are free to occur in *x-z* plane but all the mid-span nodes are constrained to the same displacement along *z* direction in such a way that each strut can provide its contribution to the OOP response. The identification of the struts is carried out starting from the definition of the diagonals, which are initially dimensioned by fixing their width (w_d) as 1/3 of the internal diagonal length (a) and their thickness as the actual thickness (t). An equivalent stress-strain relationship is instead assigned to the fibers by converting the force-displacement curve resulting for the infilled frame and defined as in [9].

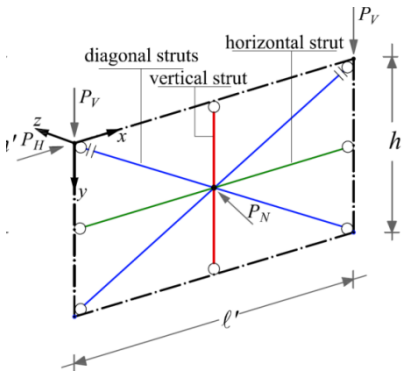

Figure 1: The proposed four-strut macro-model.

In this identification process the peak strength f_{md0} of the diagonal strut results generally lower than the actual compressive strength of masonry f_{m0}. This would reduce the OOP strength capacity of the diagonals, since OOP resistance depends on the actual compressive strength. This is compensated by defining the fictitious dimensions $\tilde{w}_d$ (surrogate width) and $\tilde{t}$ (surrogate thickness) as:

$$\tilde{t} = \frac{f_{m0}}{f_{md0}} t; \quad \tilde{w}_d = \frac{t}{\tilde{t}} w_d \tag{2}$$

with the specification that the resulting area of the cross-section remains unchanged.

The horizontal and vertical struts, which provide the residual OOP, have the actual thickness t of the infill and the actual strength f_{m0} of the masonry. The widths of the two struts are obtained as the difference of the height and the length of the panel and the horizontal and vertical projections of the diagonals initial width on the infill perimeter.

$$w_h = h - \frac{w_d}{\cos\theta}; \quad w_v = \ell - \frac{w_d}{\sin\theta} \tag{3}$$

The four-strut model defined according to the aforementioned procedure can account simultaneously IP and OOP response and explicitly considers arching mechanism. Moreover reciprocal in-plane/out-of-plane damage can be simulated.

3 VALIDATION TESTS

Validation tests were carried out comparing numerical prediction with experimental test results from different authors. The simulation of the experimental tests was made in OpenSees [10] after implementing the model with the proposed procedure. A first comparison regarded tests by Angel (1994) [4] who investigated full-scale, single-story, single-bay reinforced concrete frames infilled with different typologies of infills. Specimens were firstly subjected to in-plane cycles up to first cracking, then an air-bag was used to apply an out-of-plane monotonic pressure. Other validation tests were made with experimental data by Dawe and Seah (1989) [5] and Flanagan and Bennett (1999) [6] who investigated steel infilled frames. In [4] no prior in-plane damaging was applied, while in [5] the OOP load was applied cyclically.

For all the tests the comparison between experimental results and OpenSees simulation have shown the capacity of the model to predict out-of-plane stiffness, ultimate load and displacement capacity. Moreover the proposed model has proved to adequately account also mutual in-plane / out-of-plane damaging effects.

Further tests of the model have also shown that prior in-plane damage delays the capacity of the infill to gain out-of-plane stiffness, while the out-of-plane maximum load is not substantially reduced.

4 CONCLUSIONS

The paper presented a new simplified macro-model for the evaluation of in plane and out-of-plane responses of infilled frames in seismic simulations. The model consisted of four fiber-section struts (two diagonals, one horizontal, one vertical) opportunely defined. Nonlinear beam-column elements are able to account for the arching mechanism actually developed by the infills. Validation tests were carried out comparing numerical predictions with the results of several experimental tests on reinforced concrete and steel infilled frames. The model has proved to be a suitable tool, predicting with sufficient accuracy the OOP response of masonry infills both in terms of stiffness, ultimate load and displacement capacity. The model has also shown to be particularly accurate in predicting the effect of in-plane damaging to the out-of-plane response. Results have shown that if in-plane damage occurs previously or simultaneously, the stiffening capacity of the panel is delayed but the out-of-maximum resistance is not significantly reduced.

REFERENCES

[1] R.J. Mainstone, Supplementary note on the stiffness and strength of infilled frames, *Building Research Station*, Current Paper CP 13/74, UK.

[2] P.G. Asteris, L. Cavaleri, F. Di Trapani, V. Sarhosis, A macro-modelling approach for the analysis of infilled frame structures considering the effects of openings and vertical loads, *Structure and Infrastructure Engineering,* **12**(5), 551-566, 2016.

[3] L. Cavaleri, F. Di Trapani, Cyclic response of masonry infilled RC frames: Experimental results and simplified modeling, *Soil Dyn. and Earthquake Eng.,* **65**, 224–242, 2014.

[4] R. Angel, Behavior of reinforced concrete frames with masonry infill walls. PhD thesis. University Illinois at Urbana-Champaingn, Illinois, 1994.

[5] J.L. Dawe, C.K. Seah, Out-of-plane resistance of concrete masonry infilled panels, *Can. J. Civ. Eng* **16**(6), 854-864, 1989.

[6] R.D. Flanagan, R.M. Bennet, Bidirectional behavior of structural clay tile infilled frames. *J. Struct. Eng. (ASCE)*, **125**(3), 236-244, 1999

[7] S.A. Hashemi, K.M. Mosalam, Seismic Evaluation of Reinforced Concrete Buildings Including Effects of Infill Masonry Walls. Pacific Earthquake Engineering Research Center, PEER 2007/100, 2007

[8] S. Kadysiewski, K.M. Mosalam, Modeling of Unreinforced Masonry Infill Walls Considering In-plane and Out-of-Plane Interaction, Pacific Earthquake Engineering Research Center, PEER 2008/102, 2009

[9] P.B. Shing, A.Stavridis, Analysis of Seismic Response of Masonry- Infilled RC Frames through Collapse, *ACI Structural Journal*, **297**(7), 1-20, 2014.

[10] F. McKenna, G.L. Fenves, M.H. Scott, *Open system for earthquake engineering simulation*, University of California, Berkeley, CA, 2000.

OpenSees Days Europe 2017
1st European Conference on OpenSees
Porto, Portugal, 19–20 June 2017

EVALUATION OF SEISMIC FRAGILITY OF INFILLED REINFORCED CONCRETE FRAMES SUBJECT TO AFTERSHOCKS

F. Di Trapani[1], **M. Malavisi**[1], **G. Bertagnoli**[1] and **V.I. Carbone**[1]

[1]Politecnico di Torino
Department of Structural, Geotechnical and Building Engineering
Corso Duca degli Abruzzi 24 - Torino
fabio.ditrapani@polito.it, marzia.malavisi@polito.it, gabriele.bertagnoli@polito.it

Keywords: OpenSees, Incremental Dynamic Analysis, Fragility Curves, Infilled Frames, Reinforced concrete

Abstract. *Masonry infills strongly interact with primary framed structures in presence of seismic loads. Depending on the regularity of the distribution in plan and over the height, and on the geometrical and mechanical properties of the infill/frame system they can reduce or amplify structural damage due to mainshocks and aftershocks. The paper presents an assessment framework to determine fragility curves of reinforced concrete bare and infilled frames subject previous earthquake induced damage. Mainshock ground motions are defined using spectrum-compatible accelerograms having return period associated with different limit states. Aftershocks are defined as spectrum compatible signals and are scaled in amplitude to different intensity levels. Incremental dynamic analysis (IDA) is carried out in OpenSees using signals composed of a fixed part (mainshock) and a variable part (aftershock). Aftershocks are varied in amplitude in order to assess the response of the pre-damaged structure to earthquakes having different intensity levels. Fragility curves are derived for bare and infilled framed structures, considering the cases of no pre-damaging, low pre-damaging, and high pre-damaging. Results show that the response of infilled frames to the aftershocks significantly depends on the damage experienced during the mainshock. For the cases of low pre-damaging (low-intensity mainshock) seismic response has resulted less sensitive to further shakings. Conversely, infilled frames severely damaged by mainshock achieved collapse in correspondence of intensity levels f the aftershocks significantly lower than those of the mainshock.*

1 INTRODUCTION

Masonry infills are typically used as partition walls in reinforced concrete and steel structures. Although they are usually not included in structural models, it has been observed that they radically change structural response to lateral loads induced by seismic events. Depending on the regularity of their distribution in plan an over the height, the contribution of masonry infill can be beneficial or not to the overall response. On the one hand if infills are regularly distributed in plan and over the height, they can effectively reduce structural damage to primary structures and dissipate energy from seismic input. On the other hand, irregular distributions are often the cause of additional inelastic demand, as the case of soft-storey mechanism. In the case of strong infills associated with non-seismically designed frames, the interaction between infills and frames may also lead to local brittle failures. This is the case of shear failure of joints and column ends. Different methods can be used to model the presence of infills in structural models. Among these the use of equivalent struts replacing infills [1-3] has been widely adopted in seismic simulations, as it allows accurately accounting inelastic response of infills with relatively low computational costs. In most cases the influence of masonry infills has been assessed using nonlinear static analysis [4] or dynamic analysis [5] referring to an initial undamaged state of the structure. However, severe earthquakes are generally followed by a sequence of shakings which can reach also considerable intensities. Another case is that of structures which have been slightly damaged by previous weak earthquakes and undergo severe shaking in a second time. In both cases masonry infills influence the response to the aftershocks differently from how they have influenced the response to the mainshock. This is due to the fact that the damage state induced by the first earthquake has changed their stiffness and residual strength capacity. In consideration of this, this paper investigates the influence of masonry infills in the seismic fragility of reinforced concrete structures which have undergone previous seismic damage of different entity. The assessment framework proposed provides using incremental dynamic analysis (IDA) with ground motion signals composed of a reference fixed mainshock, and a variable aftershock scaled in amplitude. A prototype 4-storey reinforced concrete frame actually tested by other authors [6], has been used as reference structure to perform numerical simulations. Results were provided in terms of fragility curves, which have been obtained for bare and infilled frames. In particular the evaluation of the fragility curves was carried out for the intact state and for a damaged state resulting from mainshocks having different intensities.

2 THE CASE STUDY

The case study considered is a real scale prototype building subjected to pseudo dynamic tests in the ELSA laboratory [6]. The specimen is a four-storey three-bay RC infilled frame, designed without seismic details to be representative of typical RC buildings realized from 1960s to the 1980s in Southern Europe. The bare frame and the infilled frame configurations have been considered (Fig. 1). Design details can be found in [4,6]

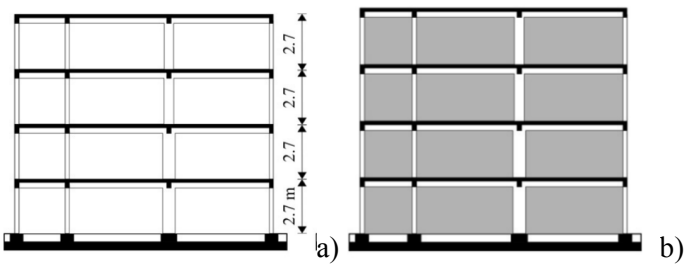

Figure 1: Prototype case study: a) bare frame; b) infilled frame. Image from [4].

3 OPENSEES MODELLING

The model of the prototype structure has been realized in OpenSees [7]. Beam and column elements were modeled with force-based nonlinear beam-column elements. The fiber cross-section of RC elements considered different stress-strain relationships for confined core concrete, unconfined cover concrete and steel rebars. Infills were modeled as compression only trusses with a concrete type (Concrete02) law. The identification of the geometry of the struts has been performed according to [2], while the definition of the stress-strain parameters, identifying the nonlinear response followed the correlation rules proposed in [8].

4 DEFINITION OF THE INPUT

For the aftershocks, a set of 30 artificial ground motion records have been defined to match spectrum-compatibility criteria of the target spectrum associated with seismic hazard of the city of L'Aquila (Italy). The return period was 1950 years. Two different levels of mainshock ground motions were used as initial part of the signal. The latter were obtained by scaling a further artificial spectrum-compatible record to the return periods of 50 and 475 years. Incremental dynamic analyses were carried subjecting the reference structural models (bare and infilled) to input signals defined to account for the three following conditions. Condition A (no pre-damaging) was defined by simply subjecting the structural models to the aforementioned 30 accelerograms scaled to 10 different scale factors. Condition B (low pre-damaging) consisted in subjecting the models to the aforementioned 30 signals modified by placing the 50 years return period mainshock before the aftershocks (Fig. 2a). Only the aftershock portion of the signal was scaled to perform IDA. Condition C (high pre-damaging) was the same of B, but the 475 years return period mainshock was used instead (Fig. 2b).

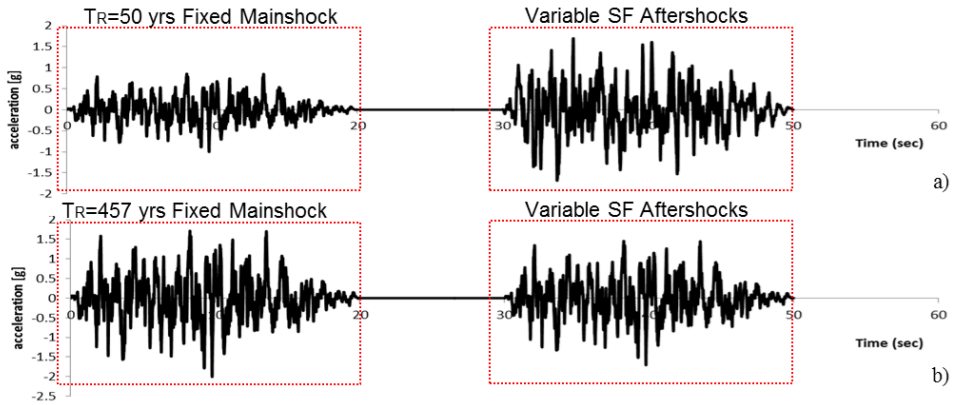

Figure 2: Definition of input signals: a) Condition B signals; b) Condition C signals.

5 FRAGILITY ASSESSMENT AND RESULTS

IDA curves were defined using the peak ground acceleration (PGA) as intensity measure (IM) and the maximum interstorey drift at the first floor as damage measure (DM). The definition of fragility curves was carried out by evaluating the distribution of peak ground accelerations achieved at an interstorey drift of 2%, considered as collapse limit state (as also suggested by FEMA technical code).

Results have shown that if local failure of RC frame does not occur because of an excess of shear demand, the presence of infill reduces the probability of collapse. In particular, considering the results of intact (bare and infilled frame) structures (Condition A), it can be observed that infills significantly limit structural damage to primary structures at the lowest intensities, and reduce inelastic demand at of the largest intensities. Results of mainshock/aftershock

analyses have highlighted that low pre-damaging (Condition B) is entirely absorbed by the infills. This will induce a pre-damaged infilled frame structure to be less sensitive to the subsequent aftershocks (probably because of the period elongation due to cracking) with respect to the undamaged structure. Conversely if severe damage is achieved during the mainshock (Condition C), collapse occurs at very rapidly when as the intensity level tends to that of the mainshock.

6 CONCLUSIONS

The presence of masonry infills in reinforced concrete structures may reduce seismic vulnerability if the latter are regularly distributed and local shear failure is inhibited. IDA based fragility assessment of intact and pre-damaged bare and infilled structures have highlighted that the ability to resist to aftershock events depends on the level of damage achieved during the mainshock. If the level of pre-damage is low, the structure shows a lower sensitivity even to strong aftershocks. Conversely if pre-damage level is significant, the structure is less sensitive to aftershocks of medium to low intensity but rapidly reaches collapse if a given intensity threshold is exceeded. The post-earthquake observation of the level of damage of infilled frame structures plays a key role in defining priorities in emergency conditions especially in presence of aftershock following a major seismic event.

REFERENCES

[1] R.J. Mainstone, Supplementary note on the stiffness and strength of infilled frames, *Building Research Station*, Current Paper CP 13/74, UK.

[2] P.G. Asteris, L. Cavaleri, F. Di Trapani, V. Sarhosis, A macro-modelling approach for the analysis of infilled frame structures considering the effects of openings and vertical loads, *Structure and Infrastructure Engineering,* **12**(5), 551-566, 2016.

[3] L. Cavaleri, F. Di Trapani, Cyclic response of masonry infilled RC frames: Experimental results and simplified modeling, *Soil Dyn. and Earthquake Eng.,* **65**, 224–242, 2014.

[4] M. Dolšek, P. Fajfar, The effect of masonry infills on the seismic response of four storey reinforced concrete frame - a deterministic assessment, *Eng. Structures*, **30**, No. 7, 1991-2001, 2008.

[5] P.B. Shing, A.Stavridis, Analysis of Seismic Response of Masonry- Infilled RC Frames through Collapse, *ACI Structural Journal*, **297**(7), 1-20, 2014.

[6] E.C. Carvalho, E. Coelho, Seismic assessment, strengthening and repair of structures. radECOEST2- ICONS report no. 2, European Commission—Training and Mobility of Researchers Programme, 2001.

[7] F. McKenna, G.L. Fenves, M.H. Scott, *Open system for earthquake engineering simulation*, University of California, Berkeley, CA, 2000.

[8] F. Di Trapani, L. Cavaleri, G. Bertagnoli, G. Mancini, D. Gino, M. Malavisi, Definition of a fiber macro-model for nonlinear analysis of infilled frames. *6th International Conference on Computational Methods in Structural Dynamics and Earthquake Engineering,* Rhodes, Greece, June 15-17, 2017.

OpenSees Days Europe 2017
1st European Conference on OpenSees
Porto, Portugal, 19–20 June 2017

SIMPLIFIED MACRO-MODELLING APPROACH FOR INFILL MASONRY WALL IN-PLANE AND OUT-OF-PLANE BEHAVIOUR USING OPENSEES

André Furtado[1A], Hugo Rodrigues[2], António Arêde[1B]and Humberto Varum[1C]

[1] CONSTRUCT-LESE, Faculty of Engineering of University of Porto
Porto, Portugal
e-mail: A: afurtado@fe.up.pt; B: aarede@fe.up.pt; C: hvarum@fe.up.pt

[2] RISCO – School of Management and Technology, Polytechnique Institute of Leiria
Leiria, Portugal
hugo.f.rodrigues@ipleiria.pt

Keywords: Infill Masonry Walls, Seismic Behaviour, In-Plane, Out-Of-Plane, Numerical modelling

Abstract. *Over the last years the seismic behaviour of infilled reinforced concrete (RC) structures have been focus of innumerous experimental and numerical studies. A big effort is being made by the scientific community with the aim of increase the knowledge of the seismic response of this type of structures and improve the numerical modelling accuracy to predict their expected behaviour. One of the main challenges in earthquake risk mitigation is the assessment of existing buildings not designed according to modern codes and the development of effective techniques to strengthen these structures. Particular attention should be given to RC frame structures with masonry infill panels, as demonstrated by their poor performance in recent earthquakes in Europe. Understanding the seismic behaviour of masonry-infilled RC frames presents one of the most difficult problems in structural engineering. Analytical tools to evaluate infill–frame interaction and the failure mechanisms need to be further studied. This research intends to present a simplified macro-model that takes into account the combined in-plane and out-of-plane behaviour of the infill panels when subjected to seismic loadings that can be used in the software OpenSees. Detailed considerations regarding this numerical modelling approach will be presented along the manuscript.*

1 INTRODUCTION

Understanding the seismic performance of constructions, in general, has been a concern of the scientific community for quite long. Recent earthquakes demonstrated the importance and influence of the infill masonry (IM) walls in the seismic behaviour of reinforced concrete (RC) structures. Recently, some experimental studies have been carried out in order to characterize the infills seismic behaviour and it was observed that the out-of-plane (OOP) capacity of the IM walls is reduced with the increasing in-plane (IP) demands, which allow to conclude that this combined IP-OOP behaviour in the numerical modelling of such elements must be taken into account [1]. Aiming at providing ever more insight to this particular area, several methodologies and techniques were developed. Different techniques are available in the literature to simulate the response of infilled frames, from refined micro-models to simplified macro-models. The macro-models are simpler than the micro-models insofar as they require a smaller number of variables, such as the interaction between brick and mortar. They allow us to represent the global behaviour of the IM and its influence in the structural response of the buildings when subjected to earthquakes in a much smaller period of time, and furthermore they reduce the computational demand.

In the present research paper a simplified macro-model that considers the IP and OOP behaviour of the IM walls is presented for the computer software OpenSees [2]. This numerical model takes into account also an element removal algorithm that allows the removal of elements during an earthquake simulation, including the interaction of IP and OOP behaviour.

2 DESCRIPTION OF THE PROPOSED MASONRY INFILL WALL NUMERICAL MODEL APPROACH

In the light of field observations, it is intended that the numerical models are a fundamental tool to understand the IM behaviour when subjected to horizontal cyclic loadings. The macro-model presented here, to be used in the software framework OpenSees [2], is based on the Rodrigues et al. [24] proposal, which is an improvement of the commonly used equivalent bi-diagonal strut model. In this model, each masonry infill wall is simulated by four diagonal struts with rigid behaviour, and a central element where the non-linearity hysteresis is concentrated (Figure 1), and the two central nodes with panel mass. The numerical model can be defined with the available elements and materials in the OpenSees library [3], namely the five elements adopted can be BeamWithHinges elements or alternatively four elastic BeamColumns for the diagonal struts and one non-linear BeamColumn for the central element. This numerical model is designed to represent the IM wall's non-linear behaviour when subjected to biaxial cyclic loading, such as in-plane and out-of-plane. These two components are modelled independently although when subjected to this biaxial cyclic action they interact through an element removal algorithm that is implemented, as will be described in the next section.

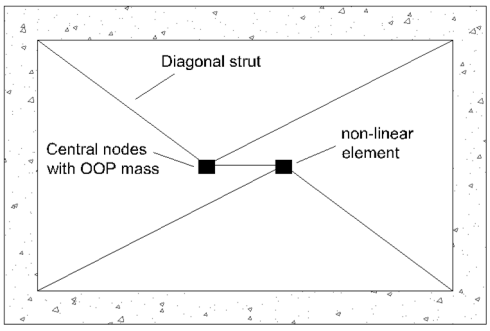

Figure 1 – Masonry infill wall proposed simplified macro-model.

2.1 Numerical simulation of the IM walls' in-plane behaviour

The in-plane behaviour of the infill panel is considered through a central element with non-linear axial behaviour, which is characterized by a multi-linear curve that represents the IM in-plane behaviour, defined by eight parameters (Figure 2), representing: (i) cracking (cracking force Fc and cracking dc); (ii) yielding (yielding force Fy and yielding displacement dy); (iii) maximum strength, corresponding to the beginning of crushing (Fcr and corresponding displacement dcr); (iv) residual strength (Fu) and corresponding displacement (du). The hysteretic rules calibrated for infill models are controlled by three additional parameters: stiffness degradation—α, pinching effect—β and strength degradation—γ.

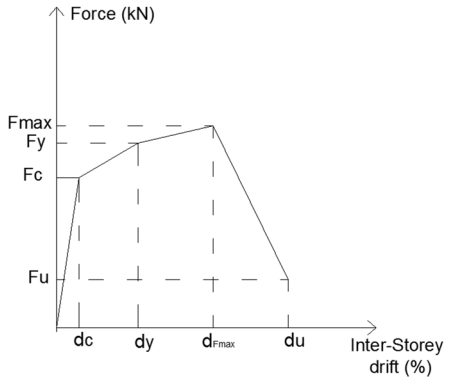

Figure 2 – Hysteretic material in-plane behaviour of the central element.

The Pinching4 uniaxial material model was used to represent the hysteretic behavior of the infill panel and was attributed for the central element. This uniaxial material is used to construct a material that represents a 'pinched' load-deformation response and exhibits degradation under cyclic loading. Cyclic degradation of strength and stiffness occurs in three ways: unloading stiffness degradation, reloading stiffness degradation, strength degradation. Furtado *et al.* [4]I proposed a calibration procedure for the in-plane hysteretic curve of the central element.

This numerical modelling approach proposed to represent the in-plane infill walls behaviour is ideally conceived to represent a combination of failure modes, namely diagonal cracking, sliding and corner crushing. As reported by Rodrigues et al [5], this in-plane numerical modelling approach can be adapted for which failure mode as it is pretended, since the non-linearity of the central element can be adjusted, and be more representative of one type of failure mode specifically.

2.2 Numerical simulation of the IM walls' out-of-plane behaviour

The modelling of this particular type of behaviour through simplified macro-models is difficult, so there is not much information about experimental studies relating to the out-of-plane behaviour of IM walls, considering all the relevant parameters, and about the in-plane and out-of-plane interaction. The following considerations were satisfied to represent the out-of-plane behaviour of IM walls:

- The IM walls' out-of-plane behaviour is considered as following a linear elastic hysteretic curve;
- The numerical representation of this behaviour was implemented through the application of mass at the central nodes, which can be calculated as 0.81 M, where M is the total mass of the infill panel and is divided by two (equal value for each node of

0.405 M). Assuming that the model has the same natural period as the original infill wall, the OOP mass and bending stiffness values were determined as suggested by Furtado et al. [6]

In order to obtain a realistic representation of the behavior of the infill in the panels when subjected to biaxial loadings, a masonry walls element removal algorithm. The IM walls are considered as collapsed if they reach the in-plane and out-of-plane interaction drift limits. After that, the algorithm removes the five elements and the corresponding central nodes and respective masses. The modelling strategy layout scheme for the implementation of the IM wall in OpenSees and the respective function of the element removal algorithm are illustrated in Figure 3.

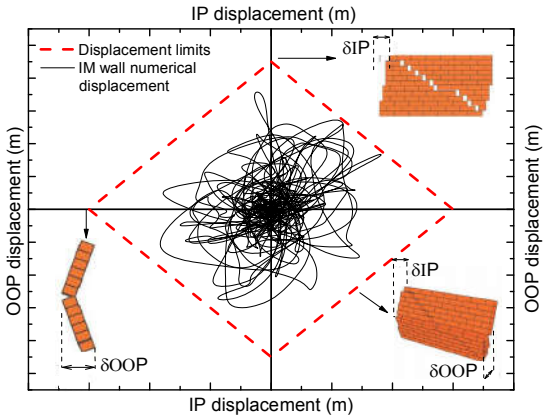

Figure 3 – IM wall displacement interaction law – element removal implementation.

3 CONCLUSIONS

This research paper presents a simplified macro-model that simulates the IP and OOP behaviour of IM walls when subjected to seismic loadings. This model is adapted from the typical bi-diagonal strut model which considers the interaction between the infill and the surrounding RC frames. The numerical model was developed in order to associate the IP and OOP behaviour in the response of the IM walls during an earthquake. When the numerical model reaches the drift limits, the IM walls are removed through an element removal algorithm.

REFERENCES

[1] A. Furtado, H. Rodrigues, A. Arêde, and H. Varum, "Experimental evaluation of out-of-plane capacity of masonry infill walls," *Engineering Structures,* vol. 111, pp. 48-63, 2016.

[2] F. Mckenna, G. Fenves, M. Scott, and B. Jeremic, "Open System for Earthquake Engineering Simulation (OpenSees)," ed. Berkley, CA, 2000.

[3] *Pre-standard and commentary for the seismic rehabilitation of buildings* F. E. M. Agency, 2000.

[4] A. Furtado, H. Rodrigues, and A. Arêde, "Modelling of masonry infill walls participation in the seismic behaviour of RC buildings using OpenSees," *International Journal of Advanced Structural Engineering (IJASE),* vol. 7, pp. 117-127, 2015.

[5] H. Rodrigues, H. Varum, and A. Costa, "Simplified Macro-Model for Infill Masonry Panels " *Journal of Earthquake Engineering,* vol. 14, pp. 390 - 416, 2010.

[6] A. Furtado, H. Rodrigues, A. Arêde, and H. Varum, "Simplified macro-model for infill masonry walls considering the out-of-plane behaviour," *Earthquake Engineering & Structural Dynamics,* vol. 45, pp. 507-524, 2016.

OpenSees Days Europe 2017
1st European Conference on OpenSees
Porto, Portugal, 19–20 June 2017

MODELLING THE OUT-OF-PLANE BEHAVIOUR OF URM INFILLS AND THE IN-PLANE/OUT-OF-PLANE INTERACTION EFFECTS

Paolo Ricci[1], **Mariano Di Domenico**[1], **and Gerardo M. Verderame**[1]

[1] University of Naples Federico II
Department of Structures for Engineering and Architecture
Via Claudio 21 – 80125 – Naples - Italy
(paolo.ricci, mariano.didomenico, verderam)@unina.it

Keywords: URM infills, out-of-plane, in-plane/out-of-plane interaction, macro-model

Abstract. *Unreinforced masonry infills are non-structural elements subjected, during seismic action, to in-plane and out-of-plane displacement and acceleration demands. In-plane and out-of-plane seismic responses of such elements are not independent as in-plane damaging reduces out-of-plane capacity and vice-versa. This phenomenon is called in-plane/out-of-plane interaction. In this paper, a macro-modelling strategy aimed at accounting for both in-plane both out-of-plane behaviour of unreinforced masonry infill walls is presented. Out-of-plane strength reduction due to in-plane damaging is modelled. Out-of-plane stiffness reduction due to in-plane displacement demand and vice-versa is also considered, in order to correctly estimate acceleration demand during seismic motion. A routine aimed at removing infills from the structural model during non-linear time-history analyses at the attainment of the in-plane or of the out-of-plane collapse condition is defined. The proposed modelling strategy has been implemented in OpenSees in order to allow users to model the in-plane and out-of-plane behaviour of infills, as well as their degrading rules, adopting any material model. The effect of taking into account or neglecting in-plane/out-of-plane interaction phenomena on the results of non-linear time-history analyses by applying the proposed model is shown through the seismic assessment of an example RC frame in a non-linear dynamic framework.*

1 INTRODUCTION

In the Mediterranean area, Reinforced Concrete (RC) buildings are usually provided of Unreinforced Masonry (URM) infill wall panels. When subjected to the seismic action, these non-structural elements are sensitive to the displacements produced in the In Plane (IP) direction and to the acceleration in the Out Of Plane (OOP) direction. IP displacements can damage infill walls with significant effects in terms of repairing costs for RC buildings after earthquakes. OOP acceleration can produce infills' collapse by their overturning, which is a great risk for life safety as well as an obstacle to escape/rescue operations during seismic emergency [1]. IP and OOP responses of infills are not independent as in-plane damaging reduces out-of-plane capacity and vice-versa. This phenomenon is called IP/OOP interaction. Modelling strategies for the OOP behaviour of URM infills and the IP-OOP interaction were proposed by Hashemi and Mosalam [2], Kadysiewski and Mosalam [3], Furtado et al., [4], Longo et al. [5], Shing et al. [6], Oliaee and Magenes [7].

In this work, a new infill macro-model accounting for IP-OOP interaction is proposed and applied through Incremental Dynamic Analyses on a simple example frame, in order to show the effects of IP-OOP interaction in the seismic capacity assessment of RC frames.

2 PROPOSED MODELLING STRATEGY

The proposed empirical-based model has been implemented in OpenSEES. First, the OOP force-displacement behaviour relationship should be defined, for example, through the semi-empirical approach proposed by the Authors in [8]. Hereafter, the above-defined OOP behaviour relationship will be mentioned as the IDR=0 backbone. Then, n IDRs (IDR_i, with i=1, …, n) should be set as discrete IP damage thresholds. Through degradation-modelling relationships, as the ones proposed by the Authors in [8], it is possible to define n OOP backbones, corresponding to the n IDRs: each one of these curves, which will be mentioned hereafter as $IDR=IDR_i$ backbone, represents the OOP behaviour that the infill will exhibit from the moment the IP IDR demand exceeds the damage threshold represented by IDR_i (see Figure 1).

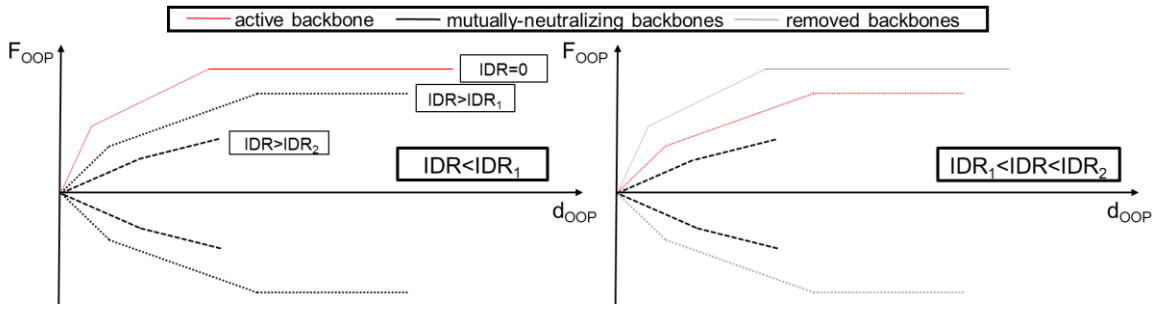

(a) (b)

Figure 1. Proposed modelling strategy of the IP-OOP interaction. Active and mutually-neutralizing OOP backbones for $IDR<IDR_1$ (a); active, mutually-neutralizing and removed backbones for IDR between IDR_1 and IDR_2 (b).

As shown in Figure 2, each infill should be represented by a diagonal element representing the IP behaviour of the infill. Each of these elements is connected through a pinned joint to the surrounding frame and is provided of a central node connected to a second central node in which the mass participating to the first OOP vibration mode of the infill is lumped: generally, it can be assumed equal to the 81% of the panel total mass [3]. The connection between these central nodes is ensured by $2n$+1 plastic hinges. First, a plastic hinge carrying the IDR=0 backbone must be defined (in the following example, a Hysteretic Material is used to this aim). Then, for

each IDR=IDR_i backbone, a couple of plastic hinges must be defined: the first one, which will be called "*i*-th real plastic hinge", models the OOP behaviour defined by the considered IDR_i backbone; the second one, which will be called "*i*-th auxiliary plastic hinge", behaves according to the force-displacement relationship defined by the IDR=IDR_i backbone mirrored with respect to the displacements axis. This goal can be achieved in OpenSEES by defining the "auxiliary" backbones through a Parallel Material that is referred, with scale factor equal to -1, to the constitutive relationship used to define the corresponding "real" backbone. This means that the OOP force for a given OOP displacement in the *i*-th real plastic hinge is always equal and opposite to the OOP force at the same displacement in the *i*-th auxiliary plastic hinge. This also means that as long as all plastic hinges are part of the infill model, the panel OOP behaviour is the one defined by the IDR=0 backbone, while the effects of the other plastic hinges are mutually neutralizing.

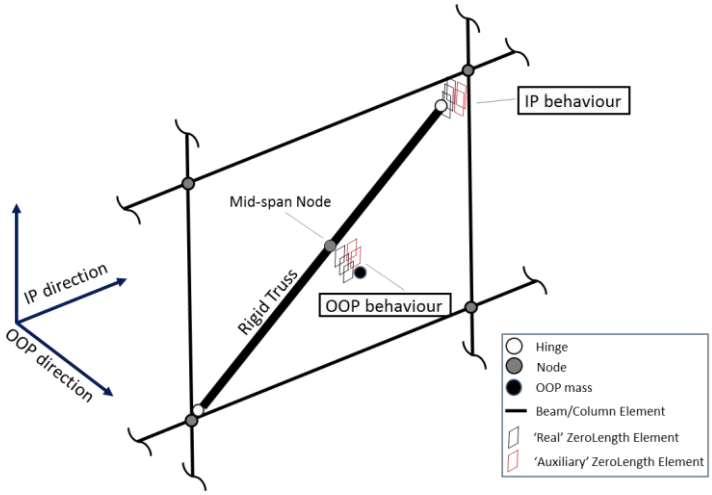

Figure 2. Graphical representation of the proposed modelling strategy.

Integral part of the proposed model is a routine that removes from the structural model the IDR_{i-1} real plastic hinge and the IDR_i auxiliary plastic hinge when the IP IDR exceeds the previously defined damage threshold represented by IDR_i. In this way, as soon as the IDR exceeds IDR_i and as long as the IDR is lower than the successive IP damage threshold IDR_{i+1}, the panel OOP behaviour is defined by the IDR=IDR_i backbone "contained" in the *i*th real plastic hinge, while the effects of the remaining plastic hinges are still mutually neutralizing. Moreover, if the OOP displacement exceeds the ultimate displacement associated to the IDR=IDR_i backbone, all the elements representative of the infill wall are removed from the structural model. An explanatory version of the removal routine is shown in Figure 3.

The IP strength and stiffness can be modelled, together with the whole infill removal due to the attainment of the IP ultimate displacement, through a procedure very similar the one explained in the previous lines for the modelling of the infill OOP behaviour.

3 EXAMPLE APPLICATION

The proposed model is applied to a one-leaf URM infill of a simple one-bay one-storey RC frame. Example applications carried out on multi-bays multi-storeys RC frames are shown in [9]. The example infill is 2.8 m high, 3.6 m wide, 0.10 m thick. Masonry compressive and tensile strength and elastic modulus were assumed equal to 2.4, 0.30 and 2500 N/mm^2, respectively. The infill IP behaviour was modelled according to Panagiotakos and Fardis [10], The OOP behaviour was modelled accordingly to [8]. OpenSEES code has been used to carry out Incremental Dynamic Analyses (IDAs) on a model accounting for IP/OOP interaction (W/

Model) and on a model in which the interaction was not active (W/O model). The frame was subjected to the 22 bidirectional records of the ATC-63 Far-field Ground Motion Set [12].

PRIOR TO THE STRUCTURAL ANALYSIS

```
for each Infill Wall modelled
    set CF1, a control flag for the element removal, to 0
    for each ZeroLength element (ZL) carrying a "real" OOP backbone
        set IPLD, the value of the IP displacement at which the ZL must be removed
        set CF2, a control flag for the ZL removal, to 0
        set OOPUD, the value of the ultimate OOP displacement associated to the ZL
    end
end
```

DURING THE STRUCTURAL ANALYSIS, AT EACH STEP CONVERGED

```
for each Infill Wall modelled
    set IPD to the current in-plane displacement
    set OOPD to the current out-of-plane displacement
    if (element not already removed, i.e., CF1==0)
        if OOPD>OOPUD
            remove the whole infill wall
            set CF1 to 1
        else
            for i that skims each ZL carrying a "real" OOP backbone
                if (the i-th ZL not already removed, i.e., CF2==0)
                    if IPD>IPLD
                        remove the i-th ZL carrying the "real" OOP backbone
                        remove the ZL carrying the i+1-th "auxiliary" OOP backbone
                        set CF2 to 1
                    end
                end
            end
        end
    end
end
```

Figure 3. Removal routine simplified schema.

The IDA curves for all records and for W/ and W/O Models are shown in Figure 4 together with median IDA curves.

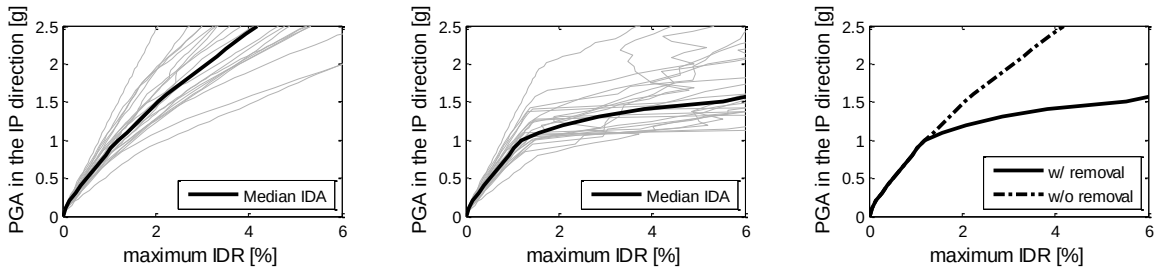

Figure 4. IDA curves for W/O (a), W/ (b) models with median IDA curves for both models (c).

Now, let us consider a specific ground motion (Ground Motion 14 of the ATC-63 set) and the corresponding IDA curves obtained for W/ and W/O Models (Figure 5). At "check point" A, for a PGA in the IP direction equal to 0.30 g, the displacement demands in both the IP and the OOP direction caused no interaction phenomena. At "check point" B, for a PGA in the IP direction equal to 1.60 g, the displacement demands in both the IP both the OOP direction produced the infill's strength and stiffness degradation, but not the infill collapse and removal from the structural model. The maximum IDR demand passed from about 1.8% for W/O Model to about 2.7% for W/ Model. At "check point" C, for a PGA in the IP direction equal to 2.10 g, the displacement demands in both the IP and the OOP direction produced the infill's strength and stiffness degradation and then the infill collapse and removal from the structural model. The infill removal produced a significant variation in the IP displacement time history: the maximum IDR demand passed from about 2.9% for W/O Model to about 5.9% for W/ Model.

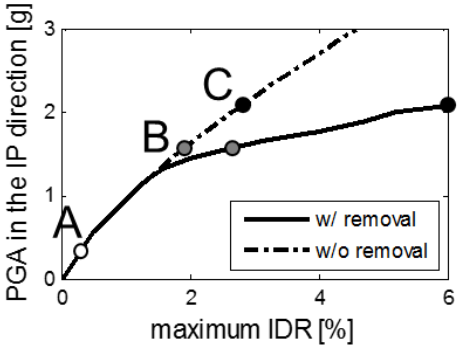

Figure 5. IDA curves for Ground Motion 14.

4 CONCLUSIONS

This work is focused on the OOP behaviour of URM infills and on the effects of IP damage on it and vice-versa, i.e., on the IP/OOP interaction.

A new macro-modelling strategy based on the proposed empirical relationships is presented. Details on the model implementation in OpenSEES are reported. The proposed model is applied on a case-study one-bay one-storey RC infilled frame in a non-linear incremental framework. At increasing seismic excitation level, accounting for infills' capacity degradation due to IP/OOP interaction seems to be unavoidable in order to estimate correctly the expected displacement demand.

REFERENCES

[1] S. Taghavi, E. Miranda, Seismic performance and loss assessment of nonstructural building components. *Proceedings of 7th National Conference on Earthquake Engineering*, Boston, United Stated of America, July 21-25, 2002.

[2] S.A. Hashemi, K.M. Mosalam, *Seismic evaluation of reinforced concrete buildings including effects of infill masonry walls*. PEER Center, 2007.

[3] S. Kadysiewski, K.M. Mosalam, *Modelling of unreinforced masonry infill walls considering in-plane and out-of-plane interaction*. PEER Center, 2009.

[4] A. Furtado, H. Rodrigues, A. Arede, H. Varum, Simplified macro-model for infill masonry walls considering the out-of-plane behaviour. *Earthquake Engineering & Structural Dynamics*, **45.4**, 507-524, 2015. DOI: 10.1002/eqe.2663.

[5] F. Longo, G. Granello, G. Tecchio, F. da Porto, C. Modena, A masonry infill wall model with in-plane out-of-plane interaction applied to pushover analysis of RC frames. *Proceedings of the 16th IBMAC*, Padua, Italy, June 26-30, 2016.

[6] P.B. Shing, L. Cavaleri, F. Di Trapani, Prediction of the out-of-plane response of infilled frames under seismic loads by a new fiber-section macro-model. *Proceedings of the 16th IBMAC*, Padua, Italy, June 26-30, 2016.

[7] M. Oliaee, G. Magenes, In-plane out-of-plane interaction in the seismic response of masonry infills in RC frames. *Proceedings of the 16th IBMAC*, Padua, Italy, June 26-30, 2016.

[8] M. Di Domenico, P. Ricci, G.M. Verderame, Empirical unreinforced masonry infill macro-model accounting for in-plane/out-of-plane interaction. *COMPDYN 2017*, Rhodes Island, Greece, June 15-17, 2017.

[9] P. Ricci, M. Di Domenico, G.M. Verderame, Empirical-based infill model accounting for in-plane/out-of-plane interaction applied for the seismic assessment of EC8-designed RC frames. *COMPDYN 2017*, Rhodes Island, Greece, June 15-17, 2017.

[10] T.B. Panagiotakos, M.N. Fardis, Seismic response of infilled RC frames structures. *11th World Conference on Earthquake Engineering*, Acapulco, Mexico, June 23-28, 1996.

[11] Federal Emergency Management Agency. Quantification of building seismic performance factors. Applied Technology Council ATC-63 Project Report, FEMA P695, Washington DC, USA, 2009.

OpenSees Days Europe 2017
1st European Conference on OpenSees
Porto, Portugal, 19–20 June 2017

NONLINEAR COMBINATION OF INTENSITY MEASURES FOR RESPONSE PREDICTION OF RC BUILDINGS

Alessandra Fiore[1], Fabrizio Mollaioli[2], Giuseppe Quaranta[3], and Giuseppe C. Marano[4,1]

[1] Department of Science of Civil Engineering and Architecture, Technical University of Bari
Via Orabona 4, 70125 Bari, Italy
{alessandra.fiore, giuseppecarlo.marano}@poliba.it

[2] Department of Structural and Geotechnical Engineering, Sapienza University of Rome
Via Gramsci 53, 00197 Rome, Italy
fabrizio.mollaioli@uniroma1.it

[3] Department of Structural and Geotechnical Engineering, Sapienza University of Rome
Via Eudossiana 18, 00184 Rome, Italy
giuseppe.quaranta@uniroma1.it

[4] College of Civil Engineering, Fuzhou University
Xue Yuan Road, Fuzhou 350108, China
marano@fzu.edu.cn

Keywords: Engineering demand parameter, Evolutionary Polynomial Regression, Intensity measure, Reinforced concrete building, Seismic assessment.

Abstract. *Estimating the seismic demand as function of the earthquake intensity is a critical issue in performance-based assessment of structures and infrastructures. This requires proper functional relationships between intensity measures (i.e., parameters that characterizes the severity of the seismic ground motion) and engineering demand parameters (i.e., parameters that quantify the expected damage and losses in structural or non-structural systems). Existing models have been obtained by performing conventional linear regressions over data carried out from numerical simulations. Conversely, this work proposes a set of new nonlinear models obtained by combining multiple intensity measures, in order to enhance the prediction of the seismic response of fixed base or base-isolated reinforced concrete buildings subjected to ordinary and pulse-like earthquakes. Numerical data were first generated by means of nonlinear dynamic analyses performed using OpenSees. The data-driven calibration of the final nonlinear regression models has been performed using the Evolutionary Polynomial Regression technique.*

1 INTRODUCTION

The present study illustrates new formulations able to correlate engineering demand parameters (EDPs) with given intensity measures (IMs) for reinforced concrete (RC) buildings. In this perspective, two multi-storey RC buildings are considered, namely a fixed-base building and a base-isolated building. The seismic response is calculated through non-linear dynamic analyses, taking into account ordinary and pulse-like seismic records. Nonlinear data-driven models able to correlate the selected IMs and the considered EDPs are obtained by means of an advanced regression method, namely the Evolutionary Polynomial Regression technique (EPR) [1][2].

2 STRUCTURAL MODELS AND SEISMIC INPUT

The selected case-study is a six-storey, three-bay framed RC building with a fixed base or retrofitted with a base-isolation system. The superstructure is representative of existing buildings located in a high seismic zone. The inter-storey high is 3.5 m while the span length of the beams is 6 m. The periods of the first three modes of vibration of the fixed-base structure are equal to 1.17 s, 0.4 s and 0.24 s. A non-degrading stiffness model has been implemented to simulate the constitutive law used for representing the cyclic response of the isolation system. In this regards, the elastic strength F_d is set equal to 0.03 times the seismic weight W of the structure. The elastic limit displacement D_y is assumed equal to 0 mm (as for friction pendulum isolators) whereas four values of the post-elastic stiffness K_d are considered. They are calculated in such a way to obtain isolation periods T equal to 3.0, 3.5, 4.0 and 4.5 s. A total of 139 seismic ground motion (GM) records is selected from the Next Generation of Attenuation Project Database of the PEER dating back to 2005. These accelerograms are used as input dynamic loading for non-linear dynamic analyses. This database is divided into two groups, i.e. ordinary GMs (80 records) and pulse-like near-fault GMs (59 records). The structural response is evaluated by means of OpenSees 2.2.2.

3 INTENSITY MEASURES AND ENGINEERING DEMAND PARAMETERS

3.1 Engineering demand parameters

The EDPs considered in this study are the following:

- Maximum Inter-story Drift Ratio (MIDR), i.e. the maximum value of the peak inter-story drift ratio (drift normalized by the story height) over all the stories;
- Maximum Floor Acceleration (MFA), i.e. the maximum value of the peak floor absolute acceleration over all stories of the superstructure.

The MIDR is a dimensionless quantity whereas the unit used for MFA is [m/s^2].

3.2 Intensity measures

The IMs explored in this study are classified into two groups. The first group includes non-structure-specific IMs calculated directly from ground motion time-histories. It is divided into three sub-groups: i) acceleration-related (i.e., peak ground acceleration PGA, Arias intensity AI, cumulative absolute velocity CAV, compound acceleration-related IM I_a), ii) velocity-related (i.e., peak ground velocity PGV, compound velocity-related IM I_v, cumulative absolute displacement CAD, incremental velocity IV, specific energy density SED), iii) displacement-related (i.e., peak ground displacement PGD, compound displacement-related IM I_d, incremental displacement ID) non-structure-specific IMs. The second group includes structure-specific IMs obtained from response spectra of ground motion time-histories depending

on the period of the structure. Structure-specific IMs are divided into two groups: i) IMs obtained from the response spectral ordinate at certain periods (i.e., spectral acceleration at isolation period S_a, relative input energy at isolation period E_{Ir}, absolute input energy at isolation period E_{Ia}) and ii) IMs carried out from the integration of response spectra over a defined period range (i.e., acceleration spectrum intensity ASI, velocity spectrum intensity VSI, Housner intensity I_H, relative input equivalent velocity spectrum intensity $V_{EIr}SI$, absolute input equivalent velocity spectrum intensity $V_{EIa}SI$, modified ASI MASI, modified VSI MVSI, modified I_H MI_H, modified $V_{EIr}SI$ $MV_{EIr}SI$, modified $V_{EIa}SI$ $MV_{EIa}SI$). Length and time units used for the IMs are [cm] and [s], respectively. The interested reader can found further details about the adopted IMs elsewhere, e.g. Refs. [3][4] and the reported literature.

4 RESPONSE PREDICTION BASED ON NONLINEAR MODELS

4.1 Prediction of Maximum Inter-story Drift Ratio

Nonlinear formulations of the MIDR as function of multiple IMs have been calibrated by means of the EPR technique. A very good compromise between complexity and accuracy is achieved by means of the formulations listed hereafter.

- Fixed-base building, ordinary GMs (COD=94.36%):

$$\mathrm{MIDR} = 0.014728 \cdot \mathrm{IV}^{0.33} \cdot \sqrt{\mathrm{S_a}} + 6.6417 \cdot 10^{-7} \cdot \mathrm{PGA}^3 \cdot \mathrm{VSI}^2 \cdot \sqrt{\mathrm{AI}} \tag{1}$$

- Fixed-base building, pulse-like GMs (COD=88.28%):

$$\mathrm{MIDR} = 4.789 \cdot 10^{-8} \cdot \mathrm{CAD}^{0.33} \cdot \sqrt{\mathrm{VSI}} \cdot \mathrm{MVSI} \cdot \mathrm{MV_{EIr}SI} \cdot \ln\left(\frac{\sqrt{\mathrm{V_{EIa}SI}}}{\mathrm{S_a}}\right) + \\ + 0.00041743 \cdot \mathrm{VSI} \cdot \sqrt{\mathrm{S_a}} \tag{2}$$

- Base-isolated building, ordinary GMs (COD=83.26%):

$$\mathrm{MIDR} = 2.3688 \cdot 10^{-6} \cdot \sqrt{\mathrm{SED} \cdot \mathrm{MASI}} \cdot \ln\left(\frac{1}{\mathrm{SED}^3}\right) + \\ + 9.2246 \cdot 10^{-6} \cdot \sqrt{\mathrm{I_v}} \cdot \mathrm{E_{Ia}}^{0.33} \cdot \mathrm{I_H} + 0.062274 \cdot \ln\left(\mathrm{AI}^{0.33} \cdot \sqrt{\mathrm{VSI}}\right) \tag{3}$$

- Base-isolated building, pulse-like GMs (COD=92.11%):

$$\mathrm{MIDR} = 1.9566 \cdot 10^{-5} \cdot \frac{\mathrm{PGD}^{0.33}\mathrm{S_a}^2}{\sqrt{\mathrm{CAV}}} + 0.010218 \cdot \sqrt{\mathrm{VSI}} + 0.0016844 \cdot \mathrm{PGA}^{0.33} \tag{4}$$

4.2 Prediction of Maximum Floor Acceleration

Moreover, suitable nonlinear formulations of the MFA as function of multiple IMs have been calibrated using the EPR technique. The best compromise between complexity and accuracy is obtained by means of the formulations listed hereafter.

- Fixed-base building, ordinary GMs (COD=92.82%):

$$\mathrm{MFA} = 0.0099258 \cdot \mathrm{ASI} + 0.12824 \cdot \sqrt{\mathrm{S_a}} \cdot \ln\left(\mathrm{I_H}^{0.33}\right) + \\ + 0.080633 \cdot \mathrm{PGA}^3 \cdot \mathrm{S_a} \cdot \ln\left(\mathrm{PGA}^{0.33}\right) \tag{5}$$

- Fixed-base building, pulse-like GMs (COD=85.95%):

$$\mathrm{MFA} = 0.44302 \cdot \ln\left(\frac{\mathrm{PGA}^2 \cdot \mathrm{AI} \cdot \mathrm{I_a} \cdot \mathrm{MVSI}^3}{\mathrm{CAD}^2}\right) + 0.001986 \cdot \mathrm{PGV} \cdot \sqrt{\mathrm{IV}} + \\ + 3.5837 \cdot 10^{-5} \cdot \mathrm{PGA} \cdot \mathrm{V_{EIa}SI}^2 \cdot \ln\left(\mathrm{PGA}^{0.33}\right) \tag{6}$$

- Base-isolated building, ordinary GMs (COD=59.55%):

$$\mathrm{MFA} = 0.0035592 \cdot \frac{\sqrt{\mathrm{E_{Ir}} \cdot \mathrm{I_a}} \cdot \mathrm{PGV}^3 \cdot \mathrm{MVSI}}{\mathrm{CAV} \cdot \mathrm{IV}^3} + 0.69413 \cdot \mathrm{VSI}^{0.33} + \\ + 0.001581 \cdot \sqrt{\mathrm{PGA}} \tag{7}$$

- Base-isolated building, pulse-like GMs (COD=62.79%):

$$\mathrm{MFA} = 0.0025771 \cdot \sqrt{\mathrm{I_v}} \cdot \left(\mathrm{S_a} \cdot \mathrm{MASI}\right)^{0.33} \cdot \ln\left(\frac{\mathrm{IV} \cdot \mathrm{E_{Ia}}^{0.33}}{\mathrm{PGA}}\right) + \\ + 0.0077503 \cdot \mathrm{PGA}^{0.33} \cdot \ln\left(\mathrm{VSI}\right) + \\ + 0.47974 \cdot \frac{\mathrm{CAV}^{0.33} \cdot \mathrm{MI_H}}{\mathrm{MASI}} \cdot \ln\left(\mathrm{AI} \cdot \mathrm{I_v}\right)^{0.33} \tag{8}$$

5 CONCLUSIONS

The main goal of this work was the calibration of suitable models able to estimate the seismic demand for fixed-based and base-isolated RC buildings under ordinary or pulse-like near-fault ground motions using most common IMs. The proposed nonlinear models obtained by combining multiple IMs have a very good predictive capability. In some cases, it is significantly larger than the accuracy level that can be achieved by means of existing linear models.

6 ACKNOWLEDGMENTS

Fabrizio Mollaioli and Giuseppe Quaranta acknowledge the support from Sapienza University of Rome through the project “Smart solutions for the assessment of structures in seismic areas”. Their work is also framed within the research project DPC-ReLUIS 2017.

REFERENCES

[1] O. Giustolisi, D.A. Savic, Advances in data-driven analyses and modelling using EPR-MOGA. *Journal of Hydroinformatics*, **11**, 225-236, 2009.

[2] A. Fiore, G. Quaranta, G.C. Marano, G. Monti, Evolutionary Polynomial Regression-based statistical determination of the shear capacity equation for reinforced concrete beams without stirrups. *Journal of Computing in Civil Engineering*, **30**(1), 04014111, 2016.

[3] F. Mollaioli, A. Lucchini, Y. Cheng , G. Monti, Intensity measures for the seismic response prediction of base-isolated buildings. *Bulletin of Earthquake Engineering*, **11**, 1841-1866, 2013.

[4] H. Ebrahimian, F. Jalayer, A. Lucchini, F. Mollaioli, G. Manfredi, Preliminary ranking of alternative scalar and vector intensity measures of ground shaking. *Bulletin of Earthquake Engineering*, **13**(10), 2805-2840, 2015.

OpenSees Days Europe 2017
1st European Conference on OpenSees
Porto, Portugal, 19–20 June 2017

NUMERICAL INVESTIGATIO ON THE SEISMIC BEHAVIOR OF REPAIRED AND RETROFITTED CHINESE BRIDGE PIERS USING OPENSEES

Davide Lavorato[1], Alessandro V. Bergami[1], Camillo Nuti[1], Bruno Briseghella[2], Junqing Xue[2], Angelo M. Tarantino[3], Giuseppe C. Marano[2], Silvia Santini[1]

[1] Dept. of Architecture, University of Roma Tre
Largo G.B. Marzi 10, Rome, Italy
{davide.lavorato, alessandro.bergami, camillo.nuti, silvia.santini}@uniroma3.it

[2] College of Civil Engineering, Fuzhou University
Fuzhou, Fujian 350108
{Bruno_junqing.xue, marano}@fzu.edu.cn

[3]Dept. of Engineering,
University of Modena and Reggio
Via Università 4, 41121 Modena
angelomarcello.tarantino@unimore.it

Keywords: repair, retrofitting, existing RC bridge, OpenSees, numerical simulation, UHPFRC, FRP, SCC

Abstract. *Numerical investigations were carried out to study the seismic behavior of Chinese RC (Reinforced Concrete) bridge piers with seismic deficiencies repaired and retrofitted by rapid interventions after seismic damage. Some 1:6 scaled pier specimens designed on the base of Chinese codes [1]-[3] were repaired and retrofitted using two different procedures and then tested by cyclic tests in the lab of Fuzhou University ([4]-[12]). The first procedure uses a self-compacting concrete (SCC) jacket to restore the damaged concrete parts, new longitudinal rebar parts to the partial substitution of the damaged rebars and a carbon Fiber Reinforced Polymer (CFRP) wrapping to assure the seismic improvements. The second procedure uses an ultra-high performance fiber reinforced concrete (UHPFRC) with steel or polymeric fibers to restore the damaged concrete parts and to improve the seismic pier capacity and new longitudinal rebar parts to the partial substitution of the damaged rebars allowing time and cost saving. Numerical finite element models of the 1:6 scaled piers repaired and retrofitted by the two procedures were built in OpenSees [13] to investigate the seismic behavior of these specimens. These numerical results were compared with the experimental ones to understand better the experimental behavior observed.*

REFERENCES

[1] JTG D60-2004 Chinese code. General code for design of highway bridges and culverts.

[2] JTG D62-2004 Chinese code. Code for design of highway reinforced concrete and pre-stressed concrete bridge and culverts.

[3] JTG/T B02-01-2008 Chinese code. Guidelines for seismic design of highway bridges.

[4] Albanesi T, Lavorato D, Nuti C, Santini S. Experimental program for pseudodynamic tests on repaired and retrofitted bridge piers. European Journal of Environmental and Civil Engineestrip, Paris: Lavoisier,Vol. 13 - No. 6/2009; 2009, 671-683.

[5] Lavorato D., Nuti C. Pseudo-dynamic tests on reinforced concrete bridges repaired and retrofitted after seismic damage. Engineering Structures,94, 2015, 96-112.

[6] Albanesi T., Lavorato D., Nuti C., Santini S. Experimental tests on repaired and retrofitted bridge piers. In Proceedings of the International FIB Symposium, 2008, 673-678.

[7] Lavorato D., Nuti C. Seismic response of repaired bridges by pseudo dynamic tests. Bridge Maintenance, Safety, Management and Life-Cycle Optimization - Proceedings of the 5th International Conference on Bridge Maintenance, Safety and Management. Pennsylvania, USA, 11-15 July 2010.

[8] Lavorato D., Nuti C., Santini S. Experimental Investigation of the Seismic Response of Repaired R.C. Bridges by Means of Pseudodynamic Tests. IABSE Symposium, Large Structures and Infrastructures for Environmentally Constrained and Urbanised Areas, Venice, 22-24 September 2010.

[9] Lavorato D., Nuti C. Pseudo-dynamic testing of repaired and retrofitted r.c. bridges, Proceedings of Fib Symposium Concrete Engineering for Excellence and Efficiency, Czech Republic, Prague, 8-10 June 2011.

[10] Lavorato D., Bergami AV., Nuti C., Briseghella B., Tarantino AM., Santini S., Huang Y., Xue J. Seismic damaged Chinese rc bridges repaired and retrofitted by rapid intervention to improve plastic dissipation and shear strength. Proceedings of 16WCEE 2017, Santiago Chile, January 9th to 13th 2017.

[11] Lavorato D., Nuti C., Briseghella B., Santini S., Xue J A repair and retrofitting intervention to improve plastic dissipation and shear strength of Chinese rc bridges. Proceedings of IABSE Conference – Structural Engineering: Providing Solutions to Global Challenges September 23-25 2015, Geneva, Switzerland

[12] Lavorato D., Nuti C., Briseghella B., Santini S., Xue J. A rapid repair technique to improve plastic dissipation of existing Chinese RC bridges. Proceedings of ACE 2015 Advances in Civil and infrastructure Engineering, International Symposium Vietri sul Mare, Italy, 12-13 June 2015

[13] McKenna F., Fenves G.L., Filippou F.C. OpenSees: Open System for Earthquake Engineering Simulation. Pacific Earthquake Engineering Research Center. USA; 2002.

OpenSees Days Europe 2017
1st European Conference on OpenSees
Porto, Portugal, 19–20 June 2017

AN OPENSEES MATERIAL MODEL FOR THE CYCLIC BEHAVIOUR OF CORRODED STEEL BAR IN RC STRUCTURES

Davide Lavorato[1], Riccardo Tartaro[2], Alessandro V. Bergami[1], Camillo Nuti[1]

[1] Dept. of Architecture, University of Roma Tre
Largo G.B. Marzi 10, Rome, Italy
{davide.lavorato, alessandro.bergami, camillo.nuti}@uniroma3.it; riccardo.tartaro@gmail.com

Keywords: rebar, corrosion, buckling, material model, existing RC structures, OpenSees

Abstract. *A nonlinear uniaxial material model for steel bars was developed and implemented in OpenSees to model the nonlinear behavior of reinforced concrete (RC) columns damaged by corrosion and subject to cyclic loading. The corrosion of longitudinal and transversal steel reinforcements in RC column is detrimental to the seismic response of structural elements as: (i) the mechanical characteristics of the longitudinal rebars (maximum and yielding strengths, maximum available steel deformation) are smaller than the ones of the uncorroded rebar; (ii) the longitudinal rebar shows different behaviors in tension or in compression; (iii) the corrosion of transversal reinforcement can change the slenderness of the longitudinal rebar and so the rebar buckling in compression can be more detrimental. The proposed model can include these effects of corrosion by the proper definition of the input characteristics for corroded rebars. The model can be used to investigate the impact of a corroded rebar on the inelastic response of existing RC columns damaged by corrosion. The results of this model were verified by comparison among numerical and experimental behaviors of corroded reinforcement in RC sections.*

REFERENCES

[1] Albanesi T, Lavorato D, Nuti C, Santini S. Experimental program for pseudodynamic tests on repaired and retrofitted bridge piers. European Journal of Environmental and Civil Engineestrip, Paris: Lavoisier,Vol. 13 - No. 6/2009; 2009, 671-683.

[2] Lavorato D., Nuti C. Pseudo-dynamic tests on reinforced concrete bridges repaired and retrofitted after seismic damage. Engineering Structures,94, 2015, 96-112.

[3] Albanesi T, Lavorato D, Nuti C. Prove sperimentali monotone e cicliche su barre di acciaio inox. Proceedings of National Conference Sperimentazione su materiali e strutture. Venezia, Italy; 2006, p. 357-366 [in Italian].

[4] Lavorato D., Nuti C. Seismic response of repaired bridges by pseudo dynamic tests. Bridge Maintenance, Safety, Management and Life-Cycle Optimization - Proceedings of the 5th International Conference on Bridge Maintenance, Safety and Management. Pennsylvania, USA, 11-15 July 2010.

[5] McKenna F., Fenves G.L., Filippou F.C. OpenSees: Open System for Earthquake Engineering Simulation. Pacific Earthquake Engineering Research Center. USA; 2002.

[6] Zhou Z., Lavorato D., Nuti C., Marano G.C. A model for carbon and stainless steel reinforcing bars including inelastic buckling for evaluation of capacity of existing structures COMPDYN 2015 - 5th ECCOMAS Thematic Conference on Computational Methods in Structural Dynamics and Earthquake Engineering

[7] Zhou Z., Nuti C., Lavorato D. Modified Monti-Nuti model for different types of reinforcing bars including inelastic buckling. Proceedings of Opensees days Italy 10-11 and ACE 2015 Advances in Civil and infrastructure Engineering, International Symposium Vietri sul Mare, Italy, 12-13 June 2015.

[8] Zhou Z., Lavorato D., Nuti C. Modeling of the mechanical behavior of stainless reinforcing steel, Proceedings of the 10th fib International PhD Symposium in Civil Engineering. UNIVERSITÉ LAVAL, CANADA, July21–23, 2014. ISBN 978-2-9806762-2-2

OpenSees Days Europe 2017
1st European Conference on OpenSees
Porto, Portugal, 19–20 June 2017

MODELING WITH FIBER BEAM ELEMENTS FOR LOAD CAPACITY ASSESMENT OF EXISTING MASONRY ARCH BRIDGES

M. Laterza[1], M. D'Amato[2], V. M. Casamassima[2] and M. Signorelli[2]

[1] University of Basilicata - DICEM
Via Lazazzera, 75100 Matera, Italy
e-mail: michelangelo.laterza@unibas.it

[2] University of Basilicata - DICEM
Via Lazazzera, 75100 Matera, Italy
e-mail: michele.damato@unibas.it, vito.casamassima@unibas.it, michele.signorelli@unibas.it

Keywords: Non linear fiber beam, OpenSees, Masonry arch bridge, Pushover.

Abstract. *In this work non-linear beam elements with fibre cross-section approach has been adopted for modelling the multi-span masonry arch bridges and evaluating the ultimate capacity. This numerical model approach is validated by some recent experiments on masonry prisms under eccentric compression, where it has been demonstrated that the classical hypothesis that plane sections remain plane after deformation is still valid also in the non-linear range, when cracks initiation occurs. This approach is then applied for modelling the main arch of the Italian ancient brick masonry arch bridge. Then, it is also discussed the effect on the ultimate of the C-FRP reinforcement on the ultimate capacity.*

1 INTRODUCTION

The conservation and safety assessment of old masonry arch bridges represent nowadays a research field of considerable interest. When handling with these structures, which have been designed with empirical rules and have been subjected in time to an increase in service loading, there is a definite need of simple tools to be used for assessment and determination of the load-carrying capacity. To date it is more copious the bibliography concerning the theoretical aspects for dimensioning and modelling the brick arches. Rankine, Stephenson, and Baker (Heyman, 1982) [1] proposed empirical methods for calculating the arch thickness, the intermediate piers and many other dimensions. In order to determine the load capacity several numerical assessment packages and computer-based applications have been proposed as, for example, RING (1992) [2]. In literature also works based on yield design of masonry arches (Heyman, 1982) [1] have been published, such as the contributions of Gilbert and Melbourne (1994) [3]. With this approach, it is assumed a plastic behavior of the material, although the masonry, as demonstrated during laboratory tests, shows a softening branch after the peak strength with a limited ductility. Nevertheless, this method is still largely applied when the possible failure due to the material crushing is also taking into account, since it represents the simplest assumption for avoiding solution convergence problems. The influence of the limited ductility on the load carrying capacity of masonry arch bridges may be found, for example, in de Felice (2007) [4]. While a complete and more refined bridge simulation should be preferable, a general modelling may reveal excessively time-consuming from a computational point of view, especially when many spans are present. The aim of this paper is to propose an approach for preliminary assessment of multi-span masonry arch bridges that makes use of non-linear incremental analysis, using beam elements. This modelling approach is validated by some recent experiments on masonry prisms under eccentric compression, where it has been demonstrated that the classical hypothesis that plane sections remain plane after deformation is still valid also in the non-linear range, when cracks initiation occurs, de Felice 2007 [4]. The use of beams with fibre cross-section has become current for the analysis of reinforced concrete structures, but, as far as the author knows, has never been used for structural analysis of masonry arches.

2 FIBER BEAM ELEMENTS MODEL AND NUMERICAL RESULTS

The numerical model has been implemented into OpenSees (2009) [5], by using rectilinear fibers beams having the unit width section reported in Figure 1.

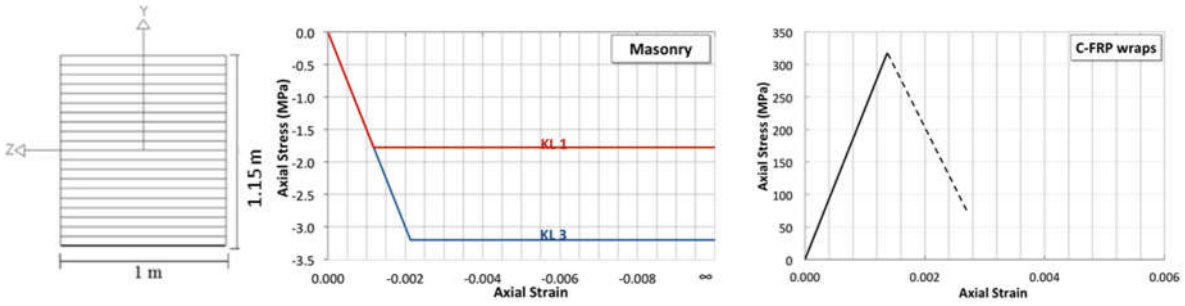

Figure 1: Fiber section of the arch and uniaxial stress-strain relationships assigned to the fibers of masonry and CFRP.

Analyses methods based on plane section assumption may be found also in Chen (2002) [6], and CNR-DT 200/R1 (2013) [7]. The backfill passive pressure is as well taken into account

with the classical assumption that the magnitude of the horizontal backfill pressure is proportional to the vertical weight pressure exerted by the backfill material, in according to the work of Gelfi (2002) [8].The masonry material has been modelled with an uniaxial elastic-perfectly plastic relationship having strength only in compression Figure 1, with infinite ductility for avoiding solution convergence problems during the numerical simulations. On the other hand, the infinite ductility will permit of evaluating, in the case of main arch typology, the ultimate carrying load although this assumption may lead, as demonstrated in de Felice, (2009) [9], to an overestimation of the actual arch capacity. However, for the aim of this work this assumption is considered acceptable. The CFRP wraps are supposed to be completely bonded with resin and continuously applied along the width and the longitudinal length of the arch, starting from the impost. They have a Young's modulus of 230000 MPa, a rupture tensile strength of 4800 MPa and, in this study, a total thickness of 0.33 mm (two layers of CFRP). The reinforcement has been modelled as an additional layer with an elastic uniaxial stress-strain law only in tension, having an axial strength fdd evaluated in accordance with CNR-DT 200/R1 (2013) [7], and corresponding to the debonding failure from the masonry support. In this study, the fdd strength is equal to 316 MPa. After reaching the maximum strength fdd the CFRP material law suddenly reduces (Figure 1), for simulating the fibers detachment invalidating the plane section assumption. As regards as the masonry compressive strength is concerned, the following values are assumed for the two simulated knowledge levels: Limited Knowledge Level (KL1) and Full Knowledge Level (KL) with compressive strength equal to 2.40 MPa and 3.20 MPa rispectivley and confidence factor CF 1.35 for KL1 and 1 for KL3. The investigations are performed by varying the debonding strength between the CFRP wraps and the masonry support as shown in Figure 2. The numerical simulations are conducted by imposing an increasing monotonic displacement in correspondence of the key and haunch sections, until the arch failure.

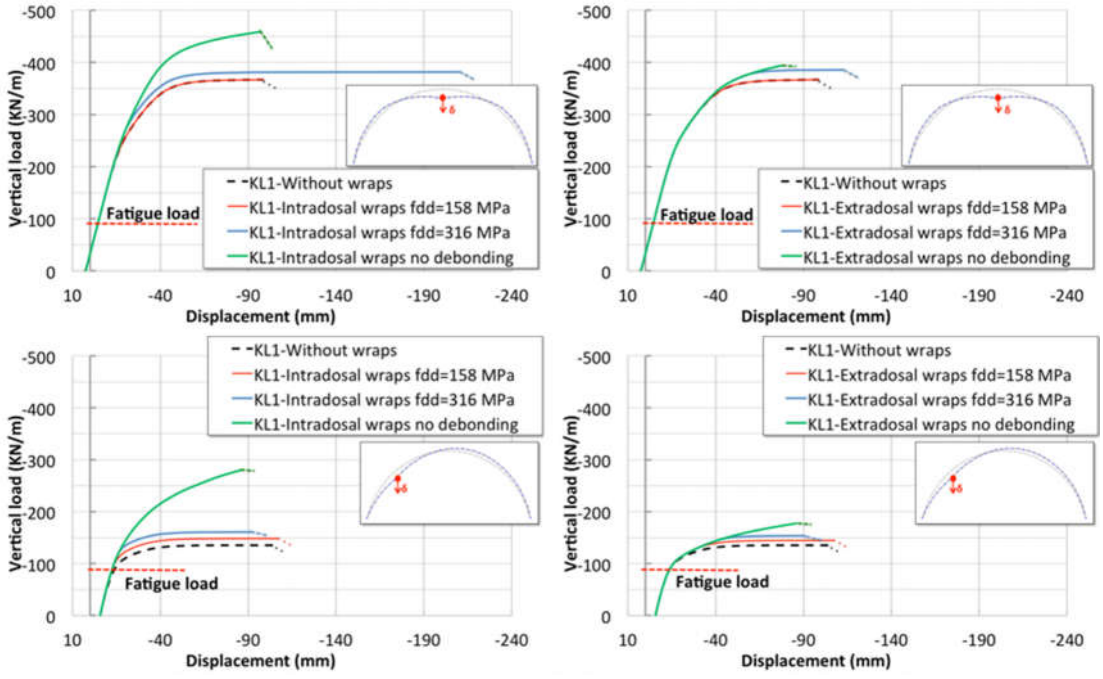

Figure 2: Vertical carrying capacity evaluated with respect to the haunch and key section

The obtained results are shown in Figure 2, where the ultimate carrying capacity without any reinforcement is also plotted (indicated with a dashed line). The analyses are conducted by

applying at first all the weights along the arch, and then by imposing an increasing vertical force at the monitored section.

3 CONCLUSIONS

An approach for a preliminary estimate of the load-carrying capacity of masonry arch bridges that takes is presented and applied to an ancient italian masonry arch bridge.The results clearly show that all the diagrams have a linear branch, confirming that the CFRP wraps modify only the main arch ultimate capacity. In particular, the higher the debonding strength the higher the ultimate carrying capacity. One of the advantages of the proposed approach is that it makes use of available general-purpose engineering software, having recourse to analysis methods accepted and widely used in other fields of structural engineering and consistent with the philosophy of modern design and assessment codes. In conclusion, the paper makes a contribution towards the development of analysis tools for assessing and preserving existing masonry arch bridge.

REFERENCES

[1] Heyman J., 1982. The masonry arch. Ellis Horwood Ltd., Chichester, England. ienkiewicz, R.C. Taylor, *The finite element method, Vol. I, 4th Edition*. McGraw Hill, 1989.

[2] RING, 1992. Masonry arch bridge analysis software: Theory & Modelling Guide. Limitstate Ltd, http://www.limitstate.com/ring.

[3] Gilbert M., Melbourne C., 1994. Rigid-block analysis of masonry structures. The Structural Engineer, Vol. 72, pp. 356–361.

[4] de Felice G., 2007. *Load-carrying capacity of multi-span masonry arch bridges having limited ductility*, in Proceedings of ARCH'07, 5th International Conference on Arch Bridges, Madeira, Portugal.

[5] OpenSees, 2009. Open System for Earthquake Engineering Simulation, http:// opensees.berkeley.edu.

[6] Chen J. F., 2002. Load-bearing capacity of masonry arch bridges strengthened with fibre reinforced polymer composites, Advances in Structural Engineering, Vol. 5(1), pp. 37-44.

[7] CNR-DT 200 R1/2013. Istruzioni per la Progettazione, l'Esecuzione ed il Controllo di Interventi di Consolidamento Statico mediante l'utilizzo di Compositi Fibrorinforzati, Materiali, strutture di c.a. e di c.a.p., strutture murarie. (In italian).

[8] Gelfi P., 2002. Role of Horizontal Backfill Passive Pressure on the Stability of Masonry Vaults, International Journal for Restoration of Buildings, Aedificatio Verlag, Freiburg, Vol. 8(6), pp. 573-589.

[9] de Felice G., 2009. Assessment of the load-carrying capacity of multi-span masonry arch bridges using fibre beam elements, Engineering Structures, Vol. 31, pp. 1634–1647.

OpenSees Days Europe 2017
1st European Conference on OpenSees
Porto, Portugal, 19–20 June 2017

A NEW FEM APPROACH FOR FRP-STRENGTHENED RC FRAMES

M. Rezaee Hajidehi[1], **G. Minafò**[1], **and G. Giambanco**[1]

[1] Università degli Studi di Palermo, Dipartimento di Ingegneria Civile, Ambientale, Aerospaziale, dei Materiali (DICAM)
Viale delle Scienze, Ed.8, Palermo, Italy
{mohsen.rezaeehajidehi, giovanni.minafo, giuseppe.giambanco}@unipa.it

Keywords: RC frame, FRP sheet, FEM procedure, OpenSess modelling.

Abstract. *Owing special mechanical properties has made Fiber Reinforced Polymer (FRP) as one of the best strengthening materials for Reinforced Concrete (RC) structures. The effect of externally applied FRP sheets on RC elements has been the topic of many experimental investigations. On the other hand, simulating the behavior of RC structures strengthened by means of externally bonded FRP sheets is yet to be scrutinized. In this work, a new Finite Element (FE) procedure for inelastic analysis of RC structures has been enriched to account the presence of externally bonded FRP sheets on RC sections. The proposed FE procedure works in the framework of lumped plasticity. It is able to identify the exact location of plastic hinges and imposes rotational discontinuities in the position of plastic hinges. The yield domain of the FRP-strengthened sections is constructed based on the hypothesis of strain linearity and taking into account the debonding failure between FRP sheet and concrete substrate. Numerical applications are presented for unstrengthened and strengthened RC frames. Pushover analysis has been carried out on numerical applications and the results are compared to each other. In order to verify the results of the numerical applications, the same models are built and analyzed in OpenSees, which proves the integrity of the FE procedure and its applicability for FRP-strengthened RC frames.*

1 INTRODUCTION

So far, many strengthening techniques have been invented to repair or structurally improve the behavior of reinforced concrete (RC) structures. Thanks to their unique features such as high strength-to-weight ratio, long term durability, high corrosion resistance and ease of installation, FRP sheets have gained wide applicability in many engineering areas specially structural engineering that many research studies are devoted to better understand the various applications of FRP sheets and its effectiveness on the performance of RC structures.

Literature survey has shown that, up to date, many experimental and theoretical studies have been performed to investigate the behavior of FRP-strengthened RC structures. Studying the effect of CFRP and GFRP on the flexural and shear behavior of RC beam elements [1], strengthening full-scale structures [2], and investigating the role of FRP sheets on the ductility enhancement of brittle RC structures [3] are some of these experimental studies. However, in spite of tremendous theoretical studies that have been carried out and have mainly focused on the structural analysis of FRP-strengthened RC structures, and aspects related to the bonding behavior between FRP sheet and concrete substrate, still exist some modelling issues that need to be dealt with such as simulating the behavior of RC structures strengthened by means of FRP sheets. Performing nonlinear static analysis on RC structures with FRP-retrofitted joints considering lumped plasticity method [4], and modelling an eight-story RC frame with flexural strengthening [5] are some modelling cases.

The weak beam-strong column principle is the basis of any strengthening method that makes the structure adequately ductile by evolving the plastic hinges in the beam elements. To fulfil the above aspect in the numerical procedure adopted for nonlinear static analysis of FRP-strengthened frames, distributed plasticity models can be implemented. However, high computational cost has made these models less efficient. On the other hand, lumped plasticity models with low computational effort thanks to the employment of elasticity in the mid-span of the elements and concentrating the nonlinearity in the extreme segments has gained applicability. However, the model is less appropriate for the structures in which the position of the plastic hinges cannot be anticipated.

An application of a recently proposed FE procedure [6] is presented here. The proposed FE procedure runs nonlinear static analysis on RC frames. It works on the framework of lumped plasticity and is able to find the exact position of plastic hinges along the beam/column elements. In this work, the FE procedure is updated to account the FRP-strengthening on RC sections. The analysis of the strengthened sections is carried out based on the Italian Guidelines [7]. Numerical applications are presented to test the efficiency of the FE procedure for strengthened RC frame and the results are verified by OpenSees code [8].

2 MODELLING EXAMPLE

A two-floor one-bay RC frame, which was modelled by Rezaee Hajidehi et al. [6] is strengthened by means of externally bonded CFRP sheets. For the purpose of validation, the identical FRP-strengthened frame is modelled in OpenSees using elements with distributed plasticity framework, Force-Based (FBE) and Displacement-Based (DBE) elements. The cross sections of the elements are meshed using 20 X 20 elements and Concrete02, Steel02 and Elastic materials are assigned. The full detail of the model is presented in figure 1. The results of the push-over analysis for strengthened model are presented in figure 2 and compared with the results of OpenSees. As it is shown in figure 2, for the Opensees model with DBE, at least 16 sub-elements are needed to produce acceptable results, while by only assigning 3 integration points the error of the FBE Opensees model will be negligible.

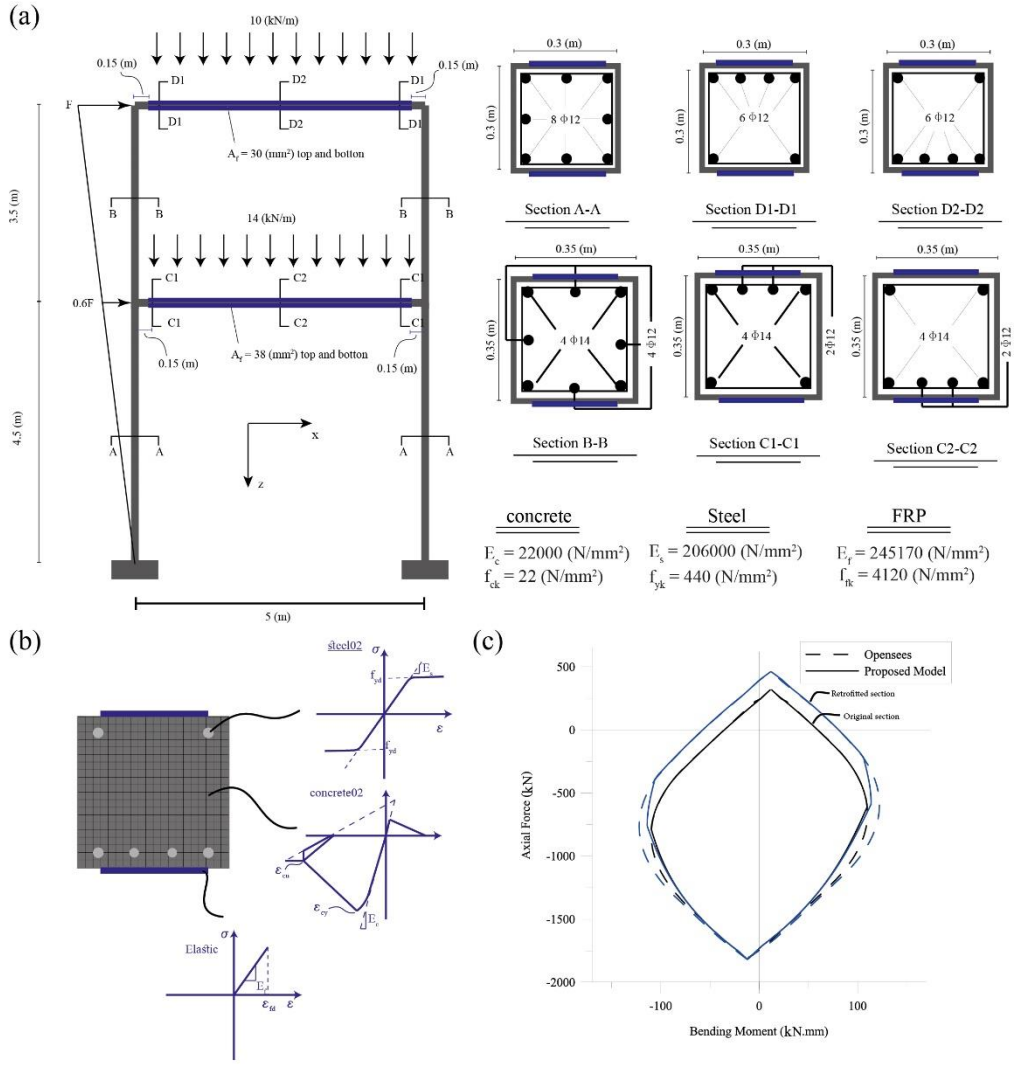

Figure 1: (a) The full description of the model, (b) details of the fiber section in OpenSees and (c) comparison of the N-M interaction domain for unstrengthened (black) and strengthened (blue) domains.

3 CONCLUSION REMARKS

An application of the FE procedure proposed by Rezaee Hajidehi et al. [6] is presented in this work. Based on the results of the numerical application and the results of Opensees code, the following conclusions are drawn:

1. As shown in figure 1c, the interaction domain, which was built according to CNR-DT200, is in good correlation with the domain generated using fiber section in Opensees. This proves the efficiency of the procedure for taking into account the FRP-strengthening in RC sections.
2. Comparing the results of the pushover analysis demonstrates the capability of the proposed FE procedure for FRP –strengthened RC frames.
3. DBE models are computationally more expensive compared to FBE models. In order to obtain reasonable results using DBE elements, 16 sub-elements are implemented that progressively increases the computational time.

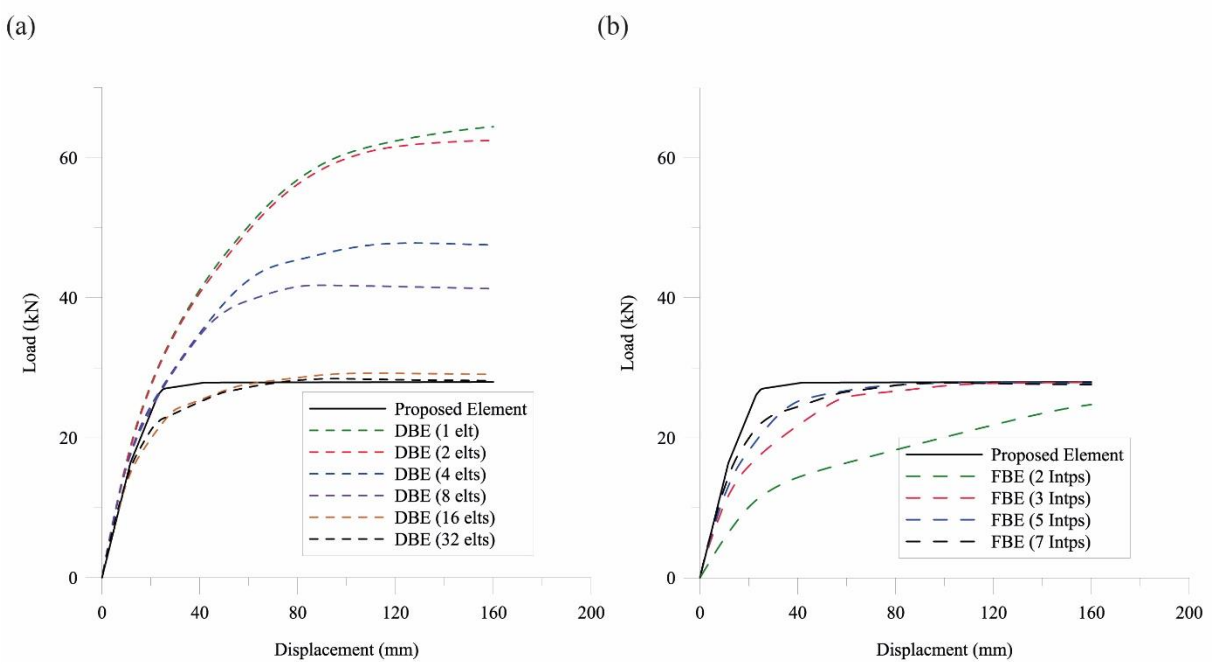

Figure 2: Comparison of the pushover load vs. top displacement curves for (a) DBE models with different number of elements and (b) FBE models with different number of integration points.

REFERENCES

[1] D. Kachlakev, D. McCurry, Behaviour of full-scale reinforced concrete beams retrofitted for shear and flexural with FRP laminates. *Composites Part B: Engineering*, **31(6)**, 445-452, 2000.

[2] U. Meier, Strengthening of structures using carbon fiber/epoxy composites. *Construction and Building Materials*, **9(6)**, 341-351, 1995.

[3] S. Mahini, H. Ronagh, A new method for improving ductility in existing RC ordinary moment resisting frames using FRPs. *Asian Journal of Civil Engineering (Building and Housing)*, **8(6)**, 581-595, 2007.

[4] A. Niroomandi, A. Maheri, MR. Maheri, S. Mahini, Seismic performance of ordinary RC frames retrofitted at joints by FRP sheets. *Engineering structures*, **32(8)**, 2326-2336, 2010.

[5] HR. Ronagh, A. Eslami, Flexural retrofitting of RC buildings using GFRP/CFRP – A comparative study. *Composites Part B: Engineering*, **46**, 188-196, 2013.

[6] M. Rezaee Hajidehi, A. Spada, G. Giambanco, The multiple slope discontinuity beam element for nonlinear analysis of RC framed structures. *Submitted to Meccanica*, May 2017.

[7] Research Council of Italy, Guide for the Design and Construction of Externally Bonded FRP Systems for Strengthening Existing Structures-CNR-DT200R1-2013. Advisory Committee on Technical Regulations for Constructions, Rome, 2013.

[8] S. Mazzoni, F. McKenna, MH. Scott, GL. Fenves, et al., Opensees command language manual. Pacific Earthquake Engineering Research (PEER) center, 2006.

OpenSees Days Europe 2017
1st European Conference on OpenSees
Porto, Portugal, 19–20 June 2017

USE OF OPENSEES FOR THE VALIDATION OF A SIMPLIFED PROCEDURE FOR THE SEISMIC ASSESSMENT AND RETROFIT OF STEEL CONCENTRIC BRACED FRAMES

Alessandro Rasulo[1] and Ernesto Grande[2]

[2] University of Cassino and Southern Lazio, Dept. Civil and Mechanical Engineering, Italy
via G. Di Biasio 43, 03043 – Cassino (FR)
e-mail: a.rasulo@unicas.it

[2] University "Guglielmo Marconi", Dept. of Sustainability Engineering, Italy
via Plinio 44, 00193 - Roma
e-mail: e.grande@unimarconi.it

Keywords: Fiber Section; Corotational Transformation; Dynamic non-linear analysis; CBFs; Seismic Assessment; Seismic Retrofit; Displacement Based Design.

Abstract. *Concentric braced frames (CBFs) is one of the most used structural typology for steel buildings. Indeed, the truss mechanism, which activates in presence of lateral forces due to wind or earthquake loads, leads to levels of lateral stiffness significant higher in comparison to other structural typologies such as moment resisting frames (MRFs). On the other hand, the possible occurrence of buckling phenomena in the members of CBFs, which are prevalently subjected to axial forces, can lead to either fragile global failure mechanisms, when buckling occurs in beams, columns and local failures affects the connections, or to a significant reduction of the global ductility and energy dissipation of CBFs, when buckling only involves diagonal members. For these reasons, for a long time CBFs were not included among structural typologies of steel buildings to be used in seismic prone area. Design codes followed elastic concepts, principally assuring that the strength of each CBFs' member was adequate to resist the external loads neglecting the contribution of diagonal in compression. Only in recent years, CBFs have been considered as a seismic resistant structural typology. In particular the capacity design approach inspiring the modern codes suggests provisions aimed to assure to CBFs a ductile ultimate mechanism, characterized by the yielding (reasonably distributed along the building height) of diagonals, whilst the buckling of beams and columns is prevented.*

In the present extended abstract, in continuity with the previous studies performed by the Authors, in which a retrofit procedure for CBFs is developed and applied to some cases of study, OpenSEES (Open System for Earthquake Engineering Simulation) is used for the non-linear time-history of some CBFs in order to demonstrate the ability of the proposed procedure to carry out suitable retrofitting interventions.

1 INTRODUCTION

Recent studies together with experimental evidences have pointed out criticisms and potentialities of steel concentric braced frames (CBF) in seismic areas. In particular, it has been observed that plastic mechanisms characterized by the yielding of diagonals while preventing the yielding/buckling of beams and columns and the failure of connections, lead to good performances of CBFs in terms of ductility and energy dissipation. The Authors in previous papers ([1], [2]) have illustrated an assessment and retrofit procedure for CBFs. In the retrofit procedure different strategies are considered, all based on the substitution of diagonals with new standard profiles able to improve the global seismic performance in terms of lateral stiffness, damping and energy dissipation. The reliability of the proposed approach has been evaluated considering some realistic X-braced frames. In particular non-linear time-history (NLTH) analyses have been applied to obtain the seismic response of both the non-retrofitted and retrofitted braced frames.

2 CASE STUDY STRUCTURES

The case study structures are three and five-story buildings with a structural resistant system composed of four X-braced frames arranged along each principal direction of the plan (Figure 1). The case studies are characterized by the same plan (dimensions 27x11 m with six bays along x-direction and two bays along y-direction) and by equal story height dimension equal to 3.5 m. All the buildings have been designed according to [3], an old Italian code which does not provide specific regulations for CBFs, by considering an intermediate seismicity level equivalent to a peak ground acceleration a_g=0.07g. The columns and the beams are characterized by wide flange sections (HE and IPE European profiles) and the diagonals are composed of two coupled L profiles. A steel grade S235 (f_y=235MPa) characterizes all members.

3 NUMERICAL APPLICATIONS

The braced frames have been analyzed by performing non linear time history (NLTH) analyses through the OpenSEES computer program [4]. In particular, the diagonals composing the frames are modeled following Uriz et al. [5]. Each diagonal is schematized through two (or more) force-based non-linear beam-column elements with spread plasticity and fiber formulation. The geometrical configuration of the elements composing the brace provides a displacement for the middle joint devoted to account the initial camber (see figure 2 for reference). The analysis have been performed averaging the NLTH results obtained by using seven real accelerograms selected from the PEER NGA-Database [6]. Their selection was guided in order to assure the matching, without scaling, in average, with the EC8 [7] Type 1 elastic response spectrum for ground Type A with peak ground acceleration (PGA) equal to 0.30 g (eve if they were subsequently scaled to comply with regulatory prescriptions).
The main results obtained from NLTH analyses are presented (figure 3) in terms of inter-story drift profiles. They are derived for each accelerogram by selecting at each story the maximum value of the inter-story drift (grey thin lines). In the same plots are also reported the average inter-story drift profile (continuous black thick line) and the inter-story drift corresponding to the attainment of the maximum plastic deformation of diagonals at the selected limit state ($\delta_y/h=9\varepsilon_y$ L/cos(θ)/h; dash-dot line) and the inter-story drift corresponding to the yielding of diagonals ($\delta_y/h=\varepsilon_y$ L/cos(θ)/h; dotted line). By examining the plots, it is possible to observe that both for three and five story frames the proposed procedure allows to obtain structural solution which satisfies the requirements corresponding selected limit state, that is the maximum plastic elongation of diagonals.

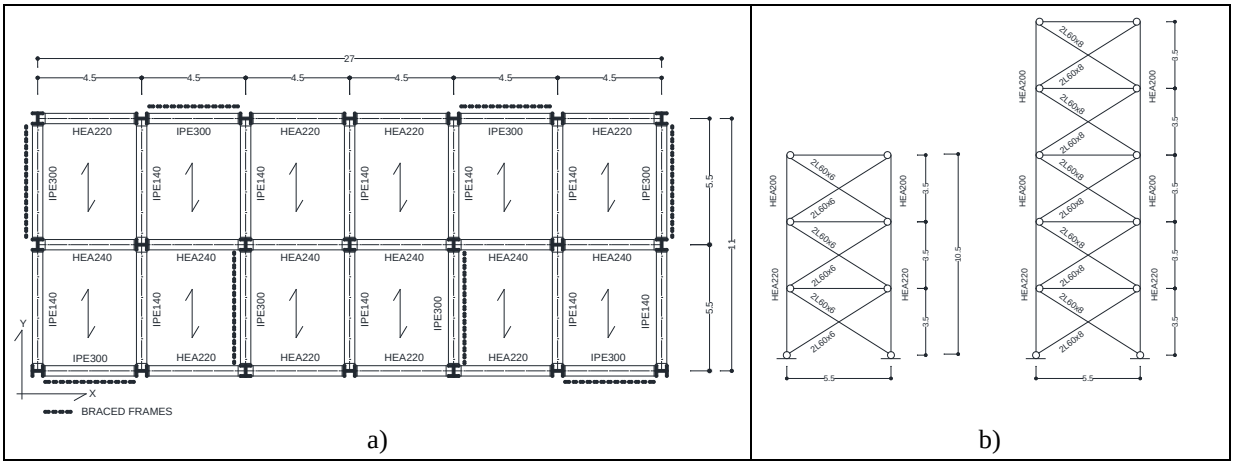

Figure 1: a) plan; b) braced frames

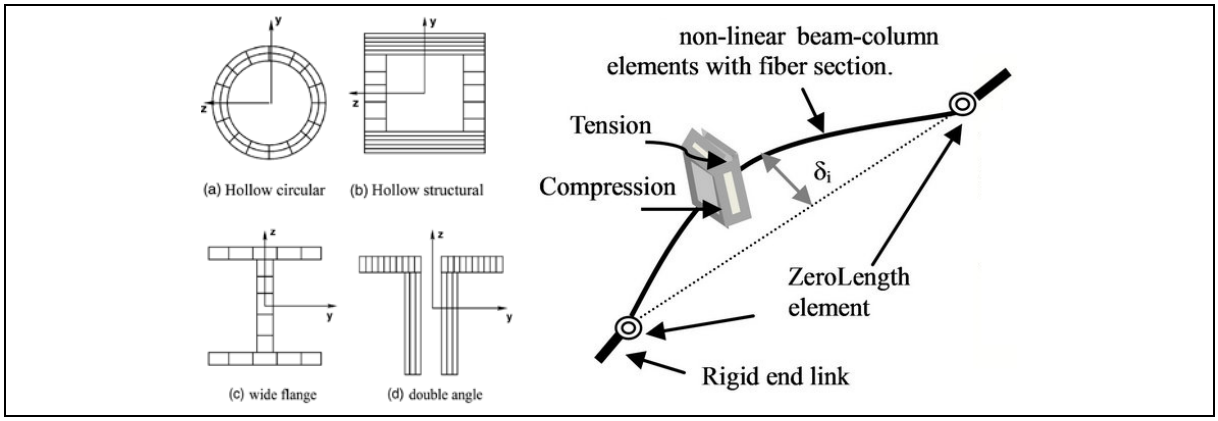

Figure 2: Schematic representation of the FEM model for diagonal braces.
Left: Fiber model sections, Right: Element arrangement with middle point displacement.

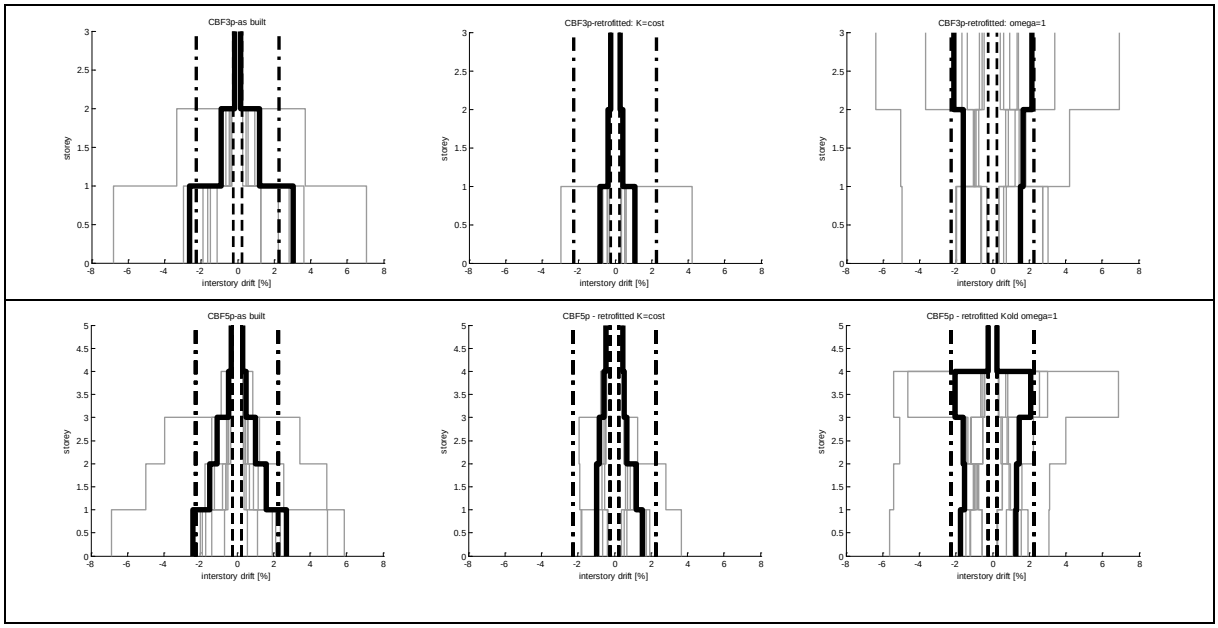

Figure 3: Results derived from NTH analyses. Above: 3-story; Below: 5-story-CBF.

4 CONCLUSIONS

The approach proposed in this paper aims at to provide a fine element validation of a simple procedure for the retrofit of CBFs. Indeed the retrofit procedure has been validated on several case studies (with different story numbers) through non-linear time history analyses with a set of spectrum compatible accelerograms.
The examined cases have shown the following aspects:

- the preliminary phase of assessment is particularly effective in recognizing the potential deficiencies of CBFs, to examine the efficacy of the retrofit intervention and to analyze the level of optimization of the obtained retrofitting solution through an iterative process;
- the propose approach allows to examine different retrofitting solutions for improving the seismic response of CBFs taking into account the relevant design parameters affecting the structural response;
- the performed FE analyses have shown the capability of the proposed approach in furnishing reliable retrofitted solutions for CBFs both in terms of limitations corresponding to the selected limit states and in terms of prediction of the seismic response;
- merging the fiber section model and the corotational transformation, both available in OPENSEES, it has been possible to model the post-buckling cyclic behavior of steel diagonals and, then, to account for this important phenomenon in the developed NLTH analyses.

ACKNOWLEDGEMENTS

The first Author wishes to acknowledge the contribution by the EU funded project LIQUEFACT "Assessment and mitigation of liquefaction potential across Europe: a holistic approach to protect structures / infrastructures for improved resilience to earthquake-induced liquefaction disasters" (Project ID: 700748, Funded under: H2020-EU.3.7. "Secure societies - Protecting freedom and security of Europe and its citizens").

REFERENCES

[1] E. Grande, A. Rasulo, 2013. "Seismic Assessment of Concentric X-Braced Steel Frames". *Engineering Structures*, vol. 49, pp. 983-995.

[2] E. Grande, A. Rasulo , 2015. "A simple approach for seismic retrofit of low-rise concentric X-braced steel frames". *Journal of Constructional Steel Research*, vol. 107C, pp. 162-172,

[3] Ministero dei Lavori Pubblici – Decreto Ministeriale del 16 gennaio 1996. Norme tecniche per le costruzioni in zone sismiche; 1996 [in Italian].

[4] OpenSees - Open system for earthquake engineering simulation. Pacific Earthquake Engineering Research Center, University of California, Berkeley 2006.

[5] P. Uriz,, F.C. Filippou, S.A. Mahin, 2008. "Model for cyclic inelastic buckling for steel member". *Journal of Structural Engeenering,* ASCE Vol. 134(4), pp. 619–628.

[6] European Committee for Standardization – Eurocode 8. Design of structures for earthquake resistance. Part 1: General rules. EN1998-1-2004. CEN, Brussels: Seismic Actions and Rules for Buildings.

[7] PEER - NGA Database 2010. http://peer.berkeley.edu/nga/earthquakes.html

U.PORTO
FEUP FACULDADE DE ENGENHARIA
UNIVERSIDADE DO PORTO

EOS
EUROPEAN OPENSEES